

**TECHNOLOGY NEEDS FOR UNDERWATER
UXO SEARCH AND DISCRIMINATION**

**Final Report
SERDP Project UX-1322**

**Jim R. McDonald
AETC Incorporated**



120 Quade Drive
Cary, North Carolina 27513

| Report Documentation Page | | | Form Approved OMB No. 0704-0188 | | |
|--|------------------------------------|-------------------------------------|--|---|------------------------------------|
| Public reporting burden for the collection of information is estimated to average 1 hour per response, including the time for reviewing instructions, searching existing data sources, gathering and maintaining the data needed, and completing and reviewing the collection of information. Send comments regarding this burden estimate or any other aspect of this collection of information, including suggestions for reducing this burden, to Washington Headquarters Services, Directorate for Information Operations and Reports, 1215 Jefferson Davis Highway, Suite 1204, Arlington VA 22202-4302. Respondents should be aware that notwithstanding any other provision of law, no person shall be subject to a penalty for failing to comply with a collection of information if it does not display a currently valid OMB control number. | | | | | |
| 1. REPORT DATE OCT 2003 | | 2. REPORT TYPE | | 3. DATES COVERED 00-00-2003 to 00-00-2003 | |
| 4. TITLE AND SUBTITLE Technology Needs for Underwater UXO Search and Discrimination | | | 5a. CONTRACT NUMBER | | |
| | | | 5b. GRANT NUMBER | | |
| | | | 5c. PROGRAM ELEMENT NUMBER | | |
| 6. AUTHOR(S) | | | 5d. PROJECT NUMBER | | |
| | | | 5e. TASK NUMBER | | |
| | | | 5f. WORK UNIT NUMBER | | |
| 7. PERFORMING ORGANIZATION NAME(S) AND ADDRESS(ES) AETC Incorporated,120 Quade Drive,Cary,NC,27513 | | | 8. PERFORMING ORGANIZATION REPORT NUMBER | | |
| 9. SPONSORING/MONITORING AGENCY NAME(S) AND ADDRESS(ES) | | | 10. SPONSOR/MONITOR'S ACRONYM(S) | | |
| | | | 11. SPONSOR/MONITOR'S REPORT NUMBER(S) | | |
| 12. DISTRIBUTION/AVAILABILITY STATEMENT Approved for public release; distribution unlimited | | | | | |
| 13. SUPPLEMENTARY NOTES | | | | | |
| 14. ABSTRACT | | | | | |
| 15. SUBJECT TERMS | | | | | |
| 16. SECURITY CLASSIFICATION OF: | | | 17. LIMITATION OF ABSTRACT Same as Report (SAR) | 18. NUMBER OF PAGES 194 | 19a. NAME OF RESPONSIBLE PERSON |
| a. REPORT unclassified | b. ABSTRACT unclassified | c. THIS PAGE unclassified | | | |

TABLE OF CONTENTS

| | |
|--|----|
| List of Figures | iv |
| List of Tables | v |
| 1. Project Title | 1 |
| 2. Performing Organization | 1 |
| 3. Project Background | 1 |
| 4. Program Objective | 2 |
| 5. Technical Approach | 2 |
| 5.1 The Magnetometer Array..... | 3 |
| 5.2 The EM Array | 3 |
| 5.3 The Program Plan and Milestones | 4 |
| 6. Summary | 5 |
| 7. Project Accomplishments | 5 |
| 7.1 The Sensor Platform | 5 |
| 7.1.1 <i>Platform Design Concepts</i> | 5 |
| 7.1.2 <i>Static Platform Modeling</i> | 10 |
| 7.1.3 <i>Dynamic Platform Modeling</i> | 10 |
| 7.1.4 <i>Remaining Platform Issues</i> | 11 |
| 7.2 EMI Sensor Response in Seawater | 13 |
| 7.2.1 <i>The Modeling Approach</i> | 13 |
| 7.2.2 <i>Time Domain Instruments</i> | 13 |
| 7.3 The EMI Array Design | 15 |
| 7.3.1 <i>Coil Designs</i> | 15 |
| 7.3.2 <i>Signal Distortion Effects</i> | 15 |
| 7.3.3 <i>Testing Breadboard Arrays</i> | 16 |
| 7.3.4 <i>The EMI Array</i> | 16 |
| 7.4 Marine Sonars | 17 |

| | |
|---|--------|
| 8. Conclusions..... | 19 |
| 9. Transition Plan..... | 20 |
| 10. References..... | 20 |
| 11. Appendices..... | 21 |
| Appendix A – Program Documents..... | CD Rom |
| Appendix B – Program Design Review..... | CD Rom |
| Appendix C – Interim Reports..... | CD Rom |

FIGURES

| | |
|--|----|
| 1. Sensor platform design concept feasibility study | 6 |
| 2. Preliminary concept design for the sensor platform | 6 |
| 3. Concept diagram for the sensor platform and the tow vessel showing the identities of the positioning sensors | 8 |
| 4. Wire frame and perspective renderings of the sensor platforms; 10-meter at the top, 4-meter in the center, and 2-meter at the bottom | 9 |
| 5. Static hydrodynamic modeling predictions for the 4-meter sensor platform | 10 |
| 6. Four meter platform depth keeping response at 2 and 5 knots | 11 |
| 7. Frequency components from the boat contributing to the sensor platform tow point motion | 11 |
| 8. Four meter platform tow point depth response to heave and surge input | 12 |
| 9. Response fields (inphase and quadrature) as a function of frequency for a 20-cm ferrous target | 13 |
| 10. Time domain comparison of air and seawater sensor returns | 14 |
| 11. Receiver response as a function of depth below the coils for several different coil combinations | 15 |
| 12. Distortion of the receiver signal due to the turn-off effect | 16 |
| 13. Test setup to evaluate a 4-meter transmitter with a small receive coil | 16 |
| 14. Signal response for two ordnance items in the test rig. Each is shown in both vertical and horizontal orientations. The 105-mm is shown at two “depths” below the coil | 17 |
| 15. Final concept layout for the EM array | 17 |
| 16. A specially developed sonar mounting system is shown in the left panel. The right panel shows the adjustment feature of the mounting system | 18 |

TABLES

| | |
|--|----|
| 1. Program plan for the Marine MTADS system development | 4 |
| 2. Marine MTADS survey platform, requirements and design decisions..... | 7 |
| 3. Comparison of the features of the 2-meter, 4-meter, and 10-meter sensor platforms | 8 |
| 4. Platform response to a seaway surge surveying at 4 knots at a depth of 4-ft | 12 |

1. **Project Title** Technology Needs for Underwater UXO Search and Discrimination
2. **Performing Organization** AETC Incorporated
3. **Project Background**

During the 1990s, largely with SERDP, ESTCP, and Army R&D support, the UXO R&D community is increasingly fielding more modern search technologies employing automated arrays of more sophisticated passive and active metal detectors. These detectors are often coupled with state-of-the-art GPS systems to provide more accurate real-time localization capability.^{1,2} Digital geophysical mapping has become the goal, if not the standard, in UXO search technologies. The improved detection technologies have been coupled by different groups with data analysis systems of varying sophistication that allow either interactive or automated analysis capability. In some cases the use of multiple sensors has shown promise in “data fusion” approaches to provide some documented discrimination capability.³⁻⁶ In all but very complex mixed-use ranges, detection efficiencies can approach 100% (with false alarm rates varying with site complexity).^{7,8} With few exceptions,^{9,10} commercially-deployed (vehicular or man-portable) systems show direct applicability only for dry-land operation in areas that can be routinely traversed. The MUDSS system, developed and demonstrated by the Naval Coastal Systems Command (NCSC) and partners, is an exception. This system incorporates optical, sonar, and magnetic sensors on a tow fish behind a powered vessel for marine searches. This system is primarily designed for deeper search applications.

The bulk of DoD 6.2-6.4 UXO R&D funds currently support refinements of hardware, deployment strategies, and data management/processing techniques to improve target classification ability using high resolution survey data. Shallow underwater UXO search approaches are in a much more primitive stage, as demonstrated by the failures in deployment of some of the commercial sensors at Mare Island and by the rudimentary strategies employed even by the better performers in this demonstration.¹⁰ Recognizing these limitations and the unique dangers associated with UXO in very shallow water, ESTCP issued a call (UXSON-02-04) for proposals to address technologies for water depths of 0-15 ft. The nature of these shallow water environments offers both opportunities and unique challenges that are very different from deeper water search techniques. A potential advantage of working in limited water depths is that it will likely be possible to employ GPS location technologies to precisely map the sensor readings. This information is critical to success in the use of modern target analysis and discrimination algorithms. Typically, shallow water environments are very turbid, limiting the use of optical visualization techniques. Additionally, application of high resolution sonar imaging is more difficult in shallow water and in near shore environments.

To field a robust and versatile underwater UXO search system requires: (1) an improved understanding of the performance of active EMI sensors in the marine environment, resulting in the design of a sensor appropriate for an extended array, which will provide a useable target classification capability, (2) a comprehensive engineering approach to fielding and operating shallow water sensor arrays, (3) inclusion of “visualizing” acoustic and optical sensors for additional identification/discrimination by taking advantage of the marine environment and its typical shallow-buried threats and finally, (4) refining our data analysis capabilities to incorporate newly-designed EMI sensors, and developing data analysis approaches to merge acoustic image data with the magnetic dipole data to build a target classification/discrimination capability for underwater UXO searches. We deferred addressing task 4 in this project; it was incorporated into the follow-on ESTCP program (UX200324). We feel the effort required for this task will allow us to effectively complete it in parallel with the prototype advanced development effort, which will also include extended system integration and shakedown phases.

Because there were several legitimate research issues associated with the design and deployment of underwater sensor arrays and with the operation and design of EMI sensors in a marine environment, the scope of this program was limited to addressing these issues, rather than acquiring, testing, and integrating hardware. Once the EMI modeling studies and the system engineering design studies were completed, a GO/NO GO decision was to be made relevant to proceeding with the full-scale development of the underwater system and its demonstration at appropriate UXO sites.

4. Program Objective

In this project we have addressed the development of new sensor array platforms and new deployment techniques and that will support integrated magnetometer/EM search technologies in a robust and versatile underwater search system to both detect and discriminate shallow-buried UXO. The combined sensor approach maximizes detection capability, and coupled with the *MTADS* Data Analysis System (DAS), will ultimately create a strong discrimination capability. Our goal for detection limits for single isolated targets were 60-mm mortars (or their equivalents) if they are buried shallow in the bottom sediments. Our current predictions are that 60-mm mortars may be just beyond the practical size limits for reliable detection. More information on system detection capabilities will become available during our shakedown studies.

On land, surface clearances are typically done before UXO surveys; because they are not practical underwater, this project has also addressed the design and incorporation of a precisely-cued visualization system in order to minimize unnecessary target recovery costs. In addition to the metal detecting sensors, we will incorporate a high-frequency (>1 MHz) acoustic imaging system for bottom mapping and object imaging, which will aid in target classification.

5. Technical Approach

This project involved the extension of current technologies from both the land UXO and marine underwater (countermine) search arenas for specific application to the shallow water UXO problem. We adopted the premise that the combined use of both passive and active magnetic sensor arrays are required. In addition, we have chosen to add a high-resolution acoustic imaging sensor. The combined use of these sensors is designed to provide data that will allow both improved detection and discrimination capabilities.

In developing the Marine UXO detection system we are leveraging many techniques and technologies from the vehicular, man-portable, and airborne *MTADS* platforms that were previously developed with SERDP and ESTCP support. Specifically, we are drawing on the most recent Airborne *MTADS* component developments, directly incorporating or adapting:

- The data acquisition and pilot guidance systems,
- The Cesium vapor magnetometer sensors,
- Time-domain EMI sensor technology,
- The GPS-based positioning system and attitude sensors,
- The 3-dimensional data analysis algorithms and software,
- The output graphics and GIS-compatible interfaces, and
- The provisions for remediation support documentation.

5.1 The Magnetometer Array

The marine magnetometer array specifically draws upon technology developments recently completed in the Airborne¹¹ *MTADS* program, which deploys a horizontal array of magnetometers on a helicopter that flies at 1-2 m above the ground. The marine application, in much the same way, will “fly” the magnetometer array between the water surface and the water-ground interface. The ideal standoff distance above the bottom is similar to that of the helicopter-supported sensor array. Because of constantly changing pitch, roll, and yaw motions of the helicopter we integrated a combination of GPS, fluxgate, and fiber optic ring gyro sensors to track the array attitude relative to the ground. Similar sensors will be used to map the motions of the marine array to provide a precise knowledge of the system attitude. This information is critical to placing each magnetometer sensor reading at a precisely known position in 3-dimensional space. In the helicopter-based system, radar, laser, and acoustic altimeters map the distance of the array above the ground surface. In the marine system a bottom-profiling sensor will provide sensor locations relative to the bottom and will also allow real-time vertical adjustments to maintain bottom clearance. All the airborne sensor data streams have been integrated into the *MTADS* Data Analysis System (DAS), which maps the magnetic and geophysical data. These components of the current *MTADS* DAS will be directly applicable to the marine platform and are not addressed as research issues in this project.

Other features developed for the Airborne *MTADS* are also directly applicable to the marine platform. The multi-component GPS data stream is used to create a real-time visual display for the helicopter pilot that allows him to set up and fly a survey grid without the aid of any ground crew or additional surface visual aids. The real-time pilot display is a feature that will be adapted for the marine system. Its incorporation will significantly reduce survey costs because we will not have to deploy other vessels to support a marine survey.

The airborne array is deployed at an altitude of 1.5-2.0 meters; it has a horizontal sensor spacing of 1.5-m. This is an increase from the 0.25-m spacing on the vehicular *MTADS* array. We anticipate that the marine array will also be deployed at a height of ~1 m above the bottom. At a first approximation, this would indicate a similar sensor separation should be deployed on the marine horizontal array. The 1.5 m spacing in the airborne array provides sufficient coverage to both detect and analyze most larger targets. However, the cross-track sampling is much less dense than the down-the-track data. When flying near the low altitude limit of the system, a decreased cross-track sampling would allow for more comprehensive detection of small targets and for more detail in the modeling of complex signatures. For this reason, we have narrowed the magnetometer sensor spacing on the marine array over that used in the airborne *MTADS*.

Because of variations in the ground level and because of the constantly changing attitude of the airborne platform we developed a new analysis approach for the airborne sensor data. Currently, the airborne DAS applies a full 3-dimensional fitting algorithm for each selected target using the sensor data for each sensor at its computed height above the ellipsoid. This new algorithm subsequently also replaced the two-dimensional fitting routine used for the vehicular survey data. The Airborne DAS fitting routines will be directly applicable for the marine system. We have deferred the analysis software adaptation for the marine system to take place in parallel with the follow-on ESTCP system development project.

5.2 The EM Array

A “marine version” of the EM61 time-domain sensor is commercially available. Although it has been deployed¹⁰ in limited tests, its performance is relatively poorly characterized. In this project, we have developed a new EM sensor in the tradition of the EM sensors that we developed for use on the *MTADS*

man-portable¹² and vehicular arrays. The vehicular *MTADS* uses an overlapping array of three 1-meter square coils. The capabilities of this EM array are complementary to the magnetometer array. The vehicular *MTADS* EM array allows detection of small UXO (20 mm - 60 mm targets) buried at 1 - 3 ft. Some of these small, shallow objects may go undetected by the magnetometer array. Additionally, the EM sensor signal contains some shape information that under ideal circumstances can be used to aid classification decisions. The ability to successfully exploit this information is an important component of this project (and other ongoing and pending UXO projects in SERDP and ESTCP). Directly mapping the vehicular *MTADS* EM array onto a marine system is not appropriate because the marine system has a substantially different design.

While the EM array has exquisite sensitivity on land for small shallow buried objects, it cannot be depended upon to detect any ordnance at depths greater than about 1.75 m. Large projectile and GP bomb duds are routinely found at depths of 2 meters or greater. Hence while one array or the other may be appropriate for many ranges, mixed use ranges with both small and large UXO duds require a multi-sensor approach to assure detection of all UXO.

5.3 The Program Plan and Milestones

There were several significant research issues associated with this project. The successful resolution of some of them involved some program risk. The primary program tasks reflect our approach to the evaluation and resolution of these issues. The time line for the **original** Program Plan is shown in Table 1. Because of delays in arrival of funding, the effective project start up was in July 2002. Therefore, the actual beginning timelines (Table 1) for the project started in the 4th quarter of 2002.

The technical approach for dealing with each of the research issues is detailed in the Program Project Plan that formed the basis for the program kick-off. This document is included as one of the appendices to this report. The program objectives were modified based upon an ESTCP Guidance Letter of 18 November 2002 and verbal guidance provided by the Program Office accompanying the Guidance Letter. As a result the program was modified in accordance with an Addendum to the original proposal. This was submitted to the Program Office on 15 December 2002 and incorporated into the Project Plan. A copy of this addendum is also included as an appendix to this report.

Table 1. Program plan for the Marine MTADS system development.

| Task | Performer | FY-2002 | | FY-2003 | | | |
|---|--------------|---------|---------|---------|------|---------|---------|
| | | 3rd Qtr | 4th Qtr | 1st Qtr | 2Qtr | 3rd Qtr | 4th Qtr |
| 1. Sensor Platform Dynamics | AETC/VCT | | | | | | |
| Engineering Feasibility | AETC/VCT | | | | | | |
| Mag Platform Preliminary Design | AETC/VCT | | | | | | |
| EM Platform Preliminary Design | AETC/VCT | | | | | | |
| 2. EM Sensor Performance Modeling | AETC | | | | | | |
| 3. Time-Domain EMI Instrument Design | AETC/Geonics | | | | | | |
| 4. Bottom-Penetrating Sonar Feasibility Study | AETC | | | | | | |
| 5. Optical Adjunct Feasibility Study | | | | | | | |
| Quarterly Web Reporting | | | | | | | |
| Annual & Final Report | | | | | | | |

6. Summary

The final product deliverables for this effort included a special Program Design Review presented to the Program Office on 18 July 2003 and this Program Final Report. The purpose of the special Design Review was to apprise the Program Office of progress made, to allow for feedback from the COR and the advisors, and to present information that the Program Office could use to make a GO/NO GO decision for proceeding with the preliminary tasks in the ESTCP 200324 project. To accomplish this effort we have drawn on the engineering and theoretical modeling resources of our organization and on engineering and design support from our subcontractors Vehicle Control Technologies, Inc., and Geonics, Ltd. Each of these studies has culminated in internal reports documenting the developments. The following reports, included as appendices to this report, document these efforts:

- Modeling of Electromagnetic Response of EMI Sensors Employed in a Salt Water Environment, AETC Report, 01/04,
- Concept Design for a Marine UXO Sensor Platform, VCT Tech Memo 02-06,
- Concept Design for a Marine UXO Sensor Platform – Autopilot for 2-m and 4-m Concept Vehicles, VCT Tech Memo 03-01, and VCT Tech Memo 03-02,
- EM68 – Marine EMI UXO Detector Project Development Interim Report, Geonics Report, April 2003,
- Report of Overlapping Receiver Coil Study, Geonics Report, 29 August 2003,
- EM68 – Marine EMI UXO Detector Project Development Report, Geonics Report, September 2003,
- EM68 Instructions for Control & Logging Program, Geonics Report, September 2003, and
- Evaluation of Performance and Capabilities of the DIDSON Imaging Sonar, AETC Report, 12/03.

In the following section we summarize the UX-1322 development effort, by drawing on these documents for illustration. The reader is referred to the reports for details of the studies.

7. Project Accomplishments

7.1 The Sensor Platform

7.1.1 Array Platform Design Concepts: At the beginning of their effort VCT was provided with a list of Top Level Design/Performance Requirements for the sensor platforms. They were provided information on the previously developed MTADS array systems. Additionally, they were provided with documents describing the design and performance of underwater systems demonstrated at Mare Island and with the description of underwater UXO survey systems that had recently been developed and demonstrated in Europe.¹³ While the original proposal for this project featured a concept based upon an array hard-mounted on a low magnetic signature vessel, neither we nor VCT were confident that this design was feasible for deploying a wide array. VCT considered a wide range of platform design concepts (Figure 1), and evaluated their potential performance against the top-level requirements. Design concepts included bottom-following platforms (sleds or roller designs), towed submerged platforms (with solid booms or flexible cables), and hybrid platforms dynamically suspended from a towed pontoon platform.

VCT translated the list of Top Level Requirements that we provided into a list of Second Level Performance Requirements. These were modeled both statically and dynamically against performance limitations of the various deployment concepts and a set of design implications were generated, which

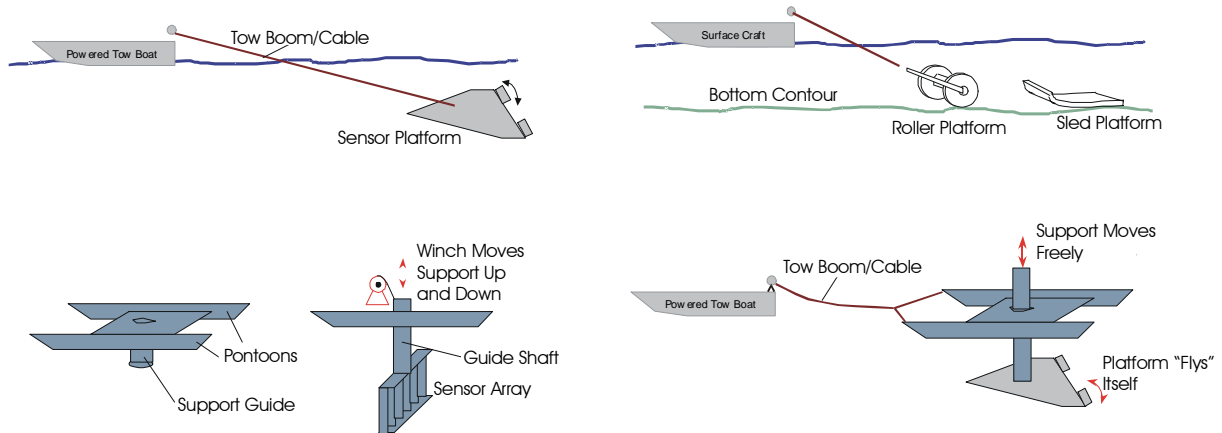


Figure 1. Sensor platform design concept feasibility study.

were called Design Decisions. These are summarized in Table 2. These design decisions ultimately effectively constrained the system concept to a submerged towed sensor platform tethered to the tow vessel by a flexible cable as the best performing concept. This concept had the least development risk associated with its implementation.

The preliminary design resulting from the concept feasibility study is shown in two perspectives in Figure 2. It is a wing-shaped fiberglass structure designed to be towed from a position well forward of the wing. Pitch stability is provided by the (yellow) wing extensions. Weighted skids on the bottom provide stability to ward off inevitable bottom collisions. Roll and depth control are provided by the elevators (red) on the trailing edge of the wing extensions. Elevators are controlled by two actuators (grey).

It was ultimately concluded that both the magnetometers and the EM sensor arrays can be mounted in a single platform. The EM array is embedded in the structure; the magnetometers are in bottles (blue) that extend through the top of the wing surface. The most difficult aspect of the design specifications to address was the very precise X, Y (0.05m), and Z (0.1m) sensor positioning (Requirement 5, Table 2). The coordinate system (see Figure 2) is set up with X and Y in the plane of the platform. X is positive in the forward (down-the-track) direction; y is positive to port; and Z points upward. VCT concluded that the best way to assure accurate sensor locations was to hard-mount the GPS antennas on the sensor platform. This led to the complex boom structure shown in Figure 2, which we considered to be risky and cumbersome to deploy.

We extended the concept study to evaluate the components of the vertical and horizontal sensor position error budget if the GPS antennas were moved forward to the tow vessel, and assuming use

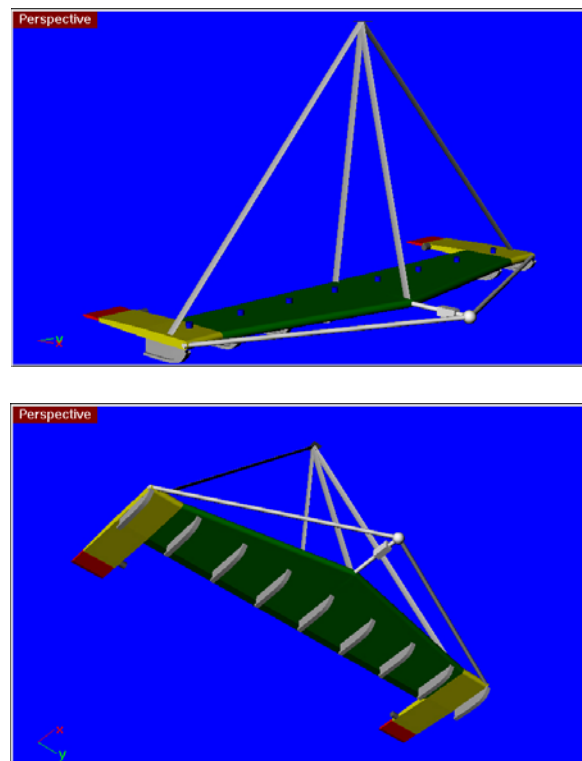


Figure 2. Preliminary concept design for the sensor platform.

Table 2. Marine MTADS survey platform, requirements and design decisions.

| | Top Level Requirement | 2nd Level Requirements | Design Decisions |
|----|---|--|--|
| 1 | House 7 magnetometer sensor array to nominally cover a 9 meter swath. | Sensor mounts spaced at 1.5m increments, perpendicular to direction of travel. | Goal to use one platform to house both magnetometers and EM sensors. EM may have to be removed for magnetometer surveys. |
| | House 8 electro-magnetic sensor array. | EM sensor has one coil 8mx1m and 8 coils 1m x 0.5m. | |
| 2 | Sensor orientation must be adjustable and securable | Mounting gimble provides tilt adjustment, with locking mechanism | |
| 3 | Provision for mounting of sensor electronic packages | Electronic packages must be mounted 2.5 to 3.5m from the sensors. Cables running between the sensor and the electronic packages will be secured, as will cables running from the electronic package to the vessel cabin. | |
| 4 | Sensors must be mounted in a magnetically clean environment | No electrically conductive or magnetic material is to be used within 1m of the sensor. The use of metal and conductive material will be avoided completely where possible, no carbon composites. | Central sensor platform constructed of fiber glass. Some aluminum frame components on extremities, if possible. |
| 5 | GPS technology allows position measurements to 0.05 m horizontal and 0.1 m vertical accuracy. Measurements of the platform position and attitude, relative to surface GPS antennae must minimize the additional errors involved in translating these positions to the sensor positions. | Angles used to position center of platform, relative to the master GPS antenna, assuming a 30 m arm must be accurate to 0.05° [sensor platform position uncertainty wrt master GPS antenna less than 3cm]. Angles used to translate platform position to sensor positions (i.e. platform attitude sensors) must be accurate to 0.1° [sensor position uncertainty due to platform orientation errors less than 3cm]. | Achieving angle measurement accuracy on rigid towing bar impractical. Extend platform-mounted GPS antennae above the water surface. Rigid towing bar not required for platform positioning accuracy. Therefore can use tow cable to minimize towing vehicle modifications. Heading accuracy of 0.1° impractical for magnetic compass. Extend platform-mounted GPS antennae above the water surface. Require AHRS-quality IMU for pitch and roll angle accuracy. Could eliminate platform-mounted GPS antennae if lesser accuracy can be accepted. |
| 6 | The magnetic signature of DC electrical currents necessary for platform control devices must be recognizable and removable for the measured total magnetic field data. | The 'on-time' of these currents must be: <than 0.1 sec duration, limited to 10% duty cycle, and easily demarcated in the data using the A/D logging functionality of the existing data acquisition system (single pole, 0 to 10v dc). | Place control surface actuators in far aft location. Manage actuator motor operating duty cycle as required to avoid excessive degradation of sensor performance. |
| 7 | Platform must be operable at speeds sufficient to allow efficient survey coverage rates | Survey speeds of 3 to 10 kts are considered reasonable, depending on sea and bottom conditions | Design to 5 kts maximum speed. |
| 8 | Platform must 'fly' nominally 1 m above the sea floor at survey speed. | The platform height above the sea floor must be monitored and used as input to for a vertical position control system. The vertical position control system must maintain sensor height to within 0.2 m | Echo-sounder needed on sensor platform. Depth sensor on sensor platform and towing craft echo-sounder too corrupted by wave motion. Two actuator/control surface arrangements to control depth and roll using fractional horsepower motors. |
| 9 | Platform should ride to surface at very slow speeds or when survey vessel is stopped. Platform design should consider the need to operate in minimal water depths | Platform buoyancy must allow for control of platform at normal survey speeds while maintaining positive buoyancy over a suitable range of water density conditions | Design for W-B < 0 for depth range (0 to 4m). There will be some minimum forward speed to produce the necessary down force to reach maximum depth. Skids and rugged surfaces on bottom of the sensor platform. Minimize snag junctures for fouling. |
| 10 | Platform accelerations must avoid our magnetic target response periodicity | Target response signatures occur from 2 to 10.0m along track. At 10 kts this equates to periods of 0.4 to 1.9 sec, and at 5 kts 0.8 to 3.9 sec. Altitude and attitude changes should avoid this periodicity if possible. | Desirable depth and roll motion characteristics designed into autopilot. Fixed vertical fins designed to provide desired lateral stability and turning characteristics. |
| 11 | Platform must have provision for mounting of auxiliary sensors | Echo-sounder, fluxgate magnetometer, tilt-meter. | Use same echo-sounder as on towing craft. Interlace pings. Use AHRS for combined compass and tilt measurements. |
| 12 | Platform must be deployable and recoverable from standard boat launch ramps | | Trailer stowage may require disassembly of GPS antenna mounts and perhaps towing bridle. Goal to keep sensor platform/control surface unit as one. Vertical fins on either side of control surface provide protection to prevent control surface damage. |
| 13 | Platform must be transportable on or in a trailer designed for towing | | Note: Over-road vibration requirements will dominate much of the instrument mounting design unless all instruments are removed for transit. |

of the best available (COTS) location and positioning sensors. The resulting concept design is shown in Figure 3. Here we have included general descriptions of the positioning sensors that are required to, as precisely as possible; derive the coordinates of the individual sensors in real time. The precise descriptions of the various positioning sensors are discussed in Appendix C. The most sensitive measurement that must be made is the angle that the tow cable forms relative to the long dimension of the

tow vessel. The contributions to the complete positioning error budget have been treated in a separate study, which has been continually refined as final choices are made for the individual components. It is currently our prediction that we will be able to locate the sensors in the horizontal plane to <15 cm and in the vertical plane to <20 cm using this design.

As a result of guidance provided by the Program Office (see Section 5.3 and the Appendix) we developed performance models for multiple sensor platforms, including horizontal arrays of 2, 4, and 10 meters. These models are described in Table 3 and shown in Figure 4 as wire frame diagrams and as perspective images. The general platform features remained constant among the models. A primary difference is that the number of the skids on the bottom surface is reduced for the smaller platforms. The 2-meter platform was modeled with the vertical stabilizers shown in Figure 4 because of its relative dynamic instability, which is described in Section 7.1.3. The 4-meter platform was modeled both with and without the vertical stabilizers. The 10-meter platform was modeled only without the vertical stabilizers. The size, weight, and specific gravity of the system components are detailed in Table 3. The total projected platform weight is calculated, as are the system center of gravity (X_{CG}) and the distance to the center of buoyancy (Z_{CG}).

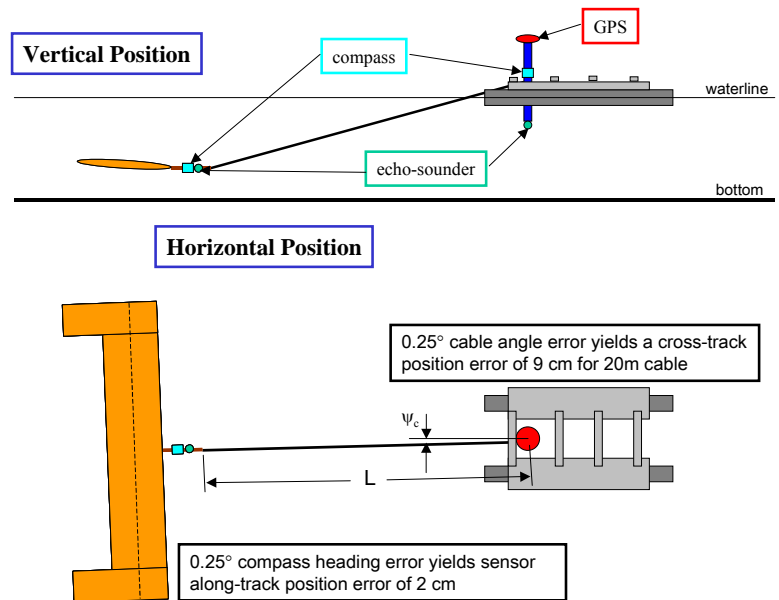


Figure 3. Concept diagram for the sensor platform and the tow vessel showing the identities of the positioning sensors.

Table 3. Comparison of the features of the 2-meter, 4-meter, and 10-meter sensor platforms.

| Component | 10m Platform | | 4m Platform | | 2m Platform | | Specific Gravity |
|-----------------------|--------------------|--------------|--------------------|--------------|--------------------|--------------|------------------|
| | Size (in) | Weight (lbs) | Size (in) | Weight (lbs) | Size (in) | Weight (lbs) | |
| Upper Wing Surface | 0.188 thick | 196 | 0.188 thick | 91 | 0.188 thick | 45 | 1.5 |
| Lower Wing Surface | 0.250 thick | 261 | 0.250 thick | 121 | 0.250 thick | 60 | 1.5 |
| Wing Ribs (7, 5, 5) | 0.375 thick | 63 | 0.375 thick | 33 | 0.375 thick | 26 | 2.0 |
| Upper Tip Surfaces | 0.188 thick | 59 | 0.188 thick | 43 | 0.188 thick | 42 | 1.5 |
| Lower Tip Surfaces | 0.250 thick | 78 | 0.250 thick | 57 | 0.250 thick | 56 | 1.5 |
| Tip Ribs (4) | 0.375 thick | 41 | 0.375 thick | 35 | 0.375 thick | 31 | 2.0 |
| Wing Spars (4) | 300" span, 1.8" | 152 | 125" span, 1.8" | 58 | 70" span, 1.8" | 36 | 2.0 |
| Skid Struts (9, 5, 3) | 0.5" x 4.0" x 2.0" | 380 | 0.5" x 4.0" x 1.3" | 158 | 0.5" x 4.0" x 1.3" | 84 | 2.0 |
| Floatation (8, 4, 2) | 20" x 36" x 2.5" | 151 | 20" x 30" x 2.5" | 1-Jan | 20" x 30" x 2.5" | 60 | 0.2 |
| Electronic Pod | 6" diam x 25" | 26 | 6" diam x 25" | 26 | 6" diam x 25" | 26 | 1.0 |
| Actuators (2) | | 15 | | 15 | | 15 | 4.0 |
| Dry Weight | | 1354 | | 874 | | 597 | |
| Wt-Buoyancy | | -6.5 | | -10 | | -6.7 | |
| X_{CG} , Z_{CG} | 0.014, 0.379 | | 0.008, 0.423 | | 0.007, 0.353 | | |
| Trim Angle | -2.1° | | -1.1° | | -1.2° | | |

The VCT sensor platform was designed employing a CAD system, assuming conservative engineering materials and design parameters. The structure is a fiberglass shell with internal spar and rib structural members. The skids have a specific gravity of 2, based upon a heavy fill material. The interior of the platform is designed to be flooded; it contains sufficient structural and non-structural foam to maintain the appropriate center of gravity, a nominal neutral pitch, and a slight buoyancy. The design studies were repeated for all three platforms. The basic component design platform parameters (Table 3) were used in the hydrodynamic modeling studies. The VCT sensor platform performance hydrodynamic modeling studies were carried out at two levels, static and dynamic platform modeling.

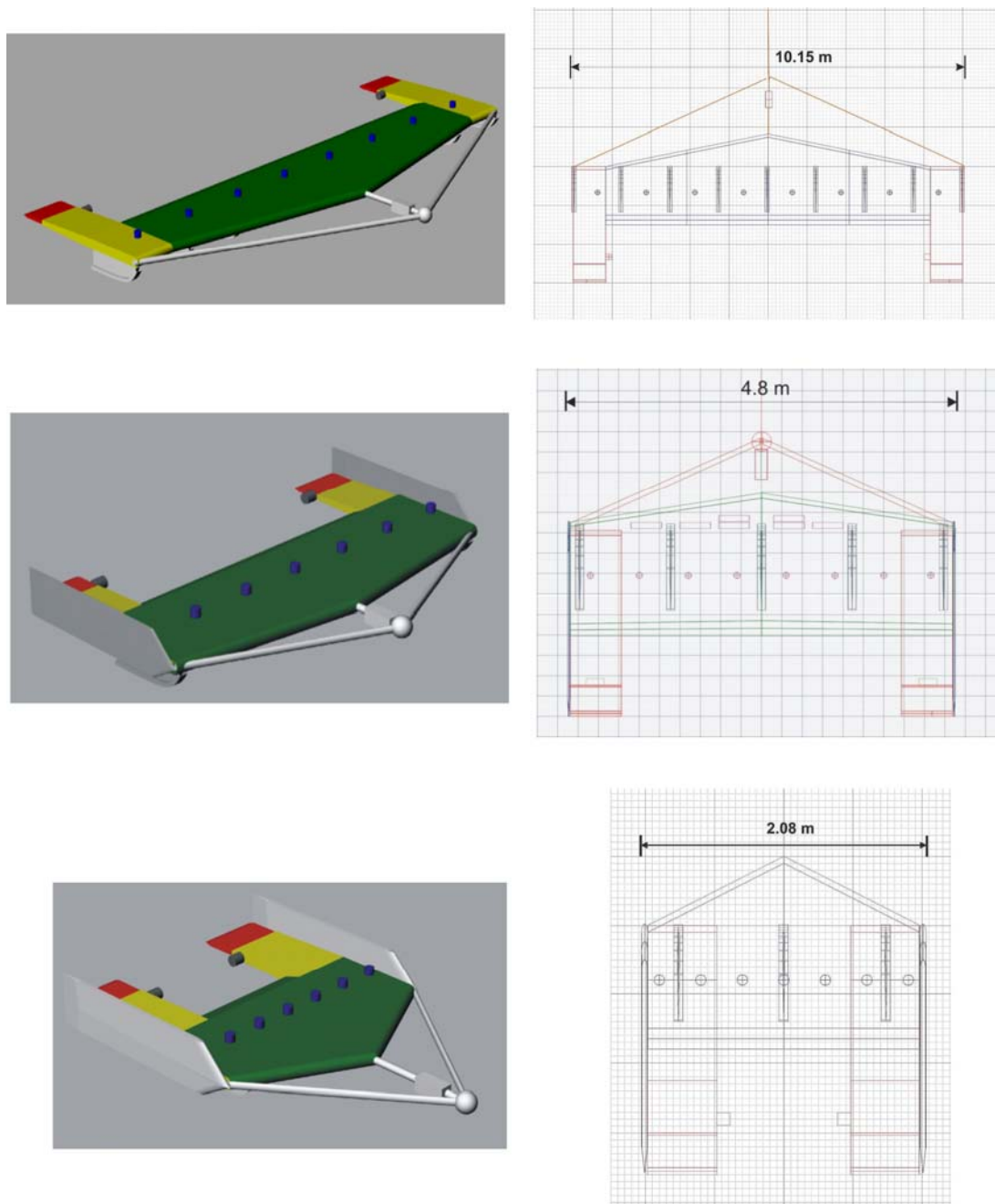


Figure 4. Wire frame and perspective renderings of the sensor platforms; 10-meters at the top, 4-meters in the center, and 2-meters at the bottom.

7.1.2 Static Platform Modeling: The static hydrodynamic modeling specifically treated issues including platform geometry, and weight and balance. The forward tow point location, the cable length, and the vehicle speed are all interrelated and affect the platform stability and motion control. The longitudinal position of the X_{cg} and the Z_{cg} (Z_{cg} is the difference between the vertical center of buoyancy and the vertical distance to the CG) establish the resting platform trim angle. The center panel in Figure 5 shows the relation of the platform pitch angle and the elevator (stern plane) pitch required to maintain the desired platform pitch. At 5 knots, a platform pitch of -2° is required to maintain 15 ft. depth. The upper panel in Figure 5 shows the catenary shape of the tow cable as a function of platform pitch (depth) and vessel speed (varying between 2 and 5 knots). The tow cable was assumed to have a diameter of 1 inch. Knowledge of the cable shape is important in calculating the distance that the tow point of the sensor platform trails the GPS antenna on the tow vessel. The bottom panel in Figure 5 shows the tension in the tow cable as a function of platform depth and vessel speed. At a speed 5 knots and depth of 15 feet, the the towing load of the platform and cable assembly is slightly less than 350 lbs. Towing this load is calculated to require ~ 10 horsepower, assuming that we are using a propeller with a 50% efficiency.

7.1.3 Dynamic Platform Modeling: The sensor platform design is open-loop stable providing passive stability, which is necessary for easy operation. However, the system performance modeling suggests that continuous altitude control during surveying can only be achieved by incorporating an autopilot to control the platform. The autopilot, which operates in a Windows™ environment will provide depth/altitude and roll control over the entire platform operating envelope. We originally constrained the actuator duty cycle to operate only during 0.25 seconds of each 1-second interval. This was done because we assumed the electrical currents associated with the actuator operation would swamp the magnetometers. The autopilot was designed under these constraints.

Subsequently, we have learned from laboratory experiments using both magnetometer and EMI sensors, in conjunction with the SeaNet actuator, that fully torque-loaded operation of the actuator provides no detectible signal at the EM receive coils

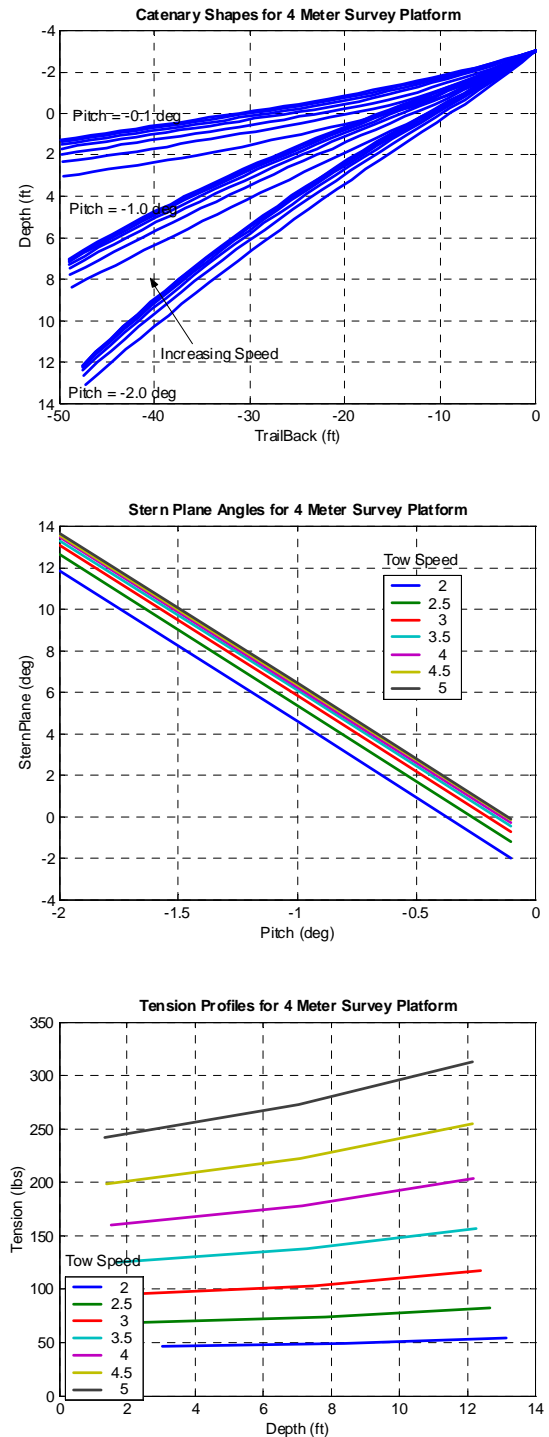


Figure 5. Static hydrodynamic modeling predictions for the 4-meter sensor platform.

and induced signals at the closest magnetometer that are less than 1 nT. The autopilot control software will be rewritten to allow continuous duty cycle operation of the actuators. The autopilot design and operational software are described in the VCT Tech Memo 03-02 in the Appendix. The dynamic platform modeling allowed us to track the platform system responses to autopilot commands and the ability of the system to tolerate and correct for tow point motions from surface wave action and heave and surge currents impacting the platform at depth. Figure 6 shows an autopilot modeling run for the 4-meter platform in response to a series of depth change command instructions (green line). The system response is shown for vessel speeds of 2 knots (red) and 5 knots (blue). The system response to an assumed 1° bottom slope change was modeled. An altitude of 3-ft above the bottom was maintained within 1 foot for the 4-meter platform, and within 2 feet for the 2-meter platform.

To simulate the tow point motion due to response of the boat to wave action, we assumed a frequency spectral response based upon sinusoids from $\frac{1}{4}$ to 2 rad/sec (by octaves). The result (Figure 7) was scaled to yield a total energy having ~ 2.5 times the energy of the sea state 1 spectra because motions at lower frequencies generally have more energy.

Figure 8 shows the platform depth response to the complex assumed multi-frequency surface wave structure. The depth response of the sensor platform at a vessel speed of 5 knots is no more than a few inches. Additionally, models were run for both 2-meter and 4-meter platforms operating at various speeds and for a variety of sea state conditions. Both platforms are more stable at 5 knot than at 2 knots, and the 4-meter platform is significantly more stable than the 2-meter platform.

Additional dynamic studies were done to consider the platform response to specific seaway motions. Such pressure surges might arise, for instance, during a survey if the platform encountered a bottom cross-current. Table 4 shows the modeled results for what we believe to be a worst-case orientation, i.e. a surge arriving from the rear quarter. Modest surges are not predicted to significantly affect platform orientation, and should be easily controllable. This study is treated in detail in the Addendum to VCT Tech Memo 03-02 included in Appendix C of this document.

7.1.4 Remaining Platform Issues: The platform concept design has been firmly established. Both sensor arrays will be housed in the same platform at the same time. Only one will be active during a survey. The platform dimensions have been established and a preliminary design has been developed that

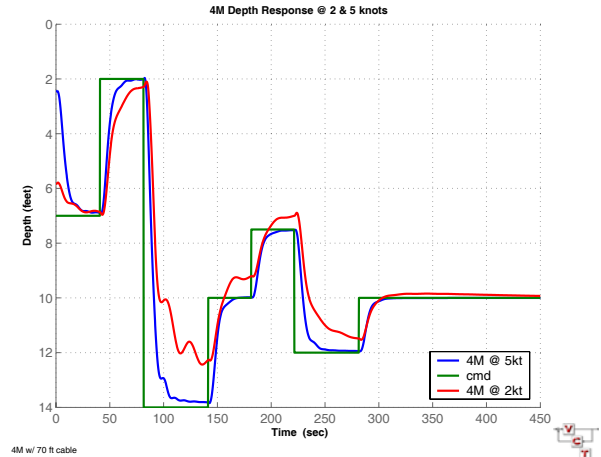


Figure 6. Four meter platform depth keeping response at 2 and 5 knots.

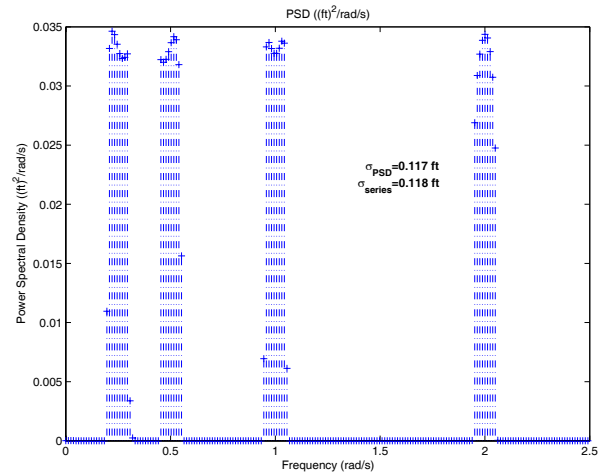


Figure 7. Frequency components from the boat contributing to the sensor platform tow point motion.

will accommodate the actuators and the magnetometer and EMI interface bottles. The location and motion sensors will be contained in a waterproof housing that will be accessed by marine connectors and will mate with the tow cable via marine connectors. One tow cable will accommodate all electronic and power conduits, 48 conductors in twisted pairs, and the Kevlar towing member. A second waterproof box will house the EMI interface electronics and will mate with connectors provided at the tow cable interface. The tow cable will have a shear pin connector at the vessel end and all the electronic and electrical cable connections will be made via breakaway connectors that can be easily re-mated if the platform hangs up and the shear pin parts.

A subcontract has been let to Structural Composites, Inc. (Melbourne Florida) to build the sensor platform. The platform preliminary design will not be fixed until Structural Composites has completed their design study and prepared “build-to” engineering drawings. At this point, they will conduct a Finite Element Analysis modeling study of their platform design and we will submit the analysis and drawings to VCT. VCT will again run the proposed design through their static and dynamic platform modeling hydrodynamic studies. At this point the preliminary design review for the platform will take place. All the actions described in this paragraph are taking place within the context of the follow-on ESTCP program. This was necessary because all component purchasing was required to take place in the ESTCP program and some component studies had to be conducted before design decisions could be finalized.

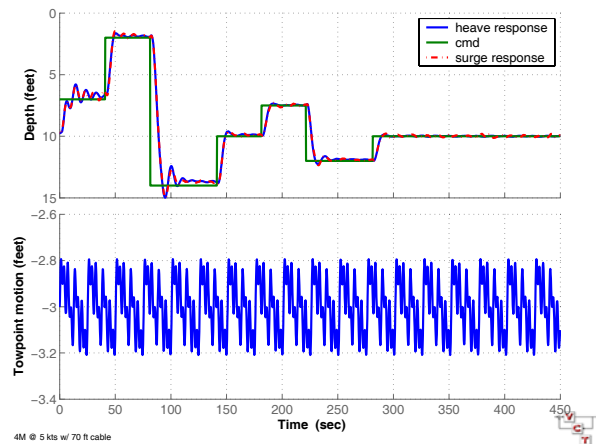


Figure 8. Four meter platform tow point depth response to heave and surge input.

Table 4. Platform response to a seaway surge surveying at 4 knots at a depth of 4 ft.

| Sea State | Standard Deviation | | |
|-----------|--------------------|--------------------|----------------------|
| | Depth Change (ft) | Pitch Change (deg) | Pitch Rate (deg/sec) |
| 1 | 0.03 | 0.22 | 0.31 |
| 2 | 0.31 | 2.37 | 3.31 |

7.2 EMI Sensor Response in Seawater

7.2.1 The Modeling Approach: Recently questions have been posed about the importance in seawater of the induced eddy currents and current channeling effects in the presence of a target when using EMI sensors. We have conducted an in depth study of these effects. The results are contained in a report “Modeling of Electromagnetic Response of EMI Sensors Employed in a Salt Water Environment,” which is in Appendix C of this report. The results are summarized below. The following assumptions define the context of the study.

- The transmitter and receive coils are co-located and lie in the horizontal plane,
- The sensor system is modeled as a magnetic dipole source,
- All model calculations were made in the frequency domain assuming a wide band sensor, frequencies (1-50,000Hz),
- The coils and the targets were assumed to be either in air, or embedded in sea water, and appropriate values for the conductivities, permeabilities, and permittivities were chosen.
- Spherical ferrous targets were chosen with 10, 20, and 80 cm radii, and
- We considered responses from targets at various distances below the coils and at various horizontal displacements from the coils.

Our forward model predicts the fields in air and seawater. As shown in Figure 9, the differences between seawater and air are significant only at relatively high frequencies ($>1\text{kHz}$). The relative increase of the signal in seawater (over air) is larger for targets displaced horizontally from the coils. It also increases with distance between the coils and the target and increases with increasing target size. The relative high frequency response is smaller for targets vertically displaced from the sensor.

7.2.2 Time Domain Instruments: The EMI sensor planned for the Marine MTADS (described later) will have numerous (and adjustable) time gates. The turn-on time of the earliest time gate following the end of the transmitter pulse will determine the high frequency response of the system. The actual delay of the initial gate is not yet determined. For the purpose of this modeling study we assumed the time gates of the Geonics EM-61, Mark II. The signal measured by these sensors is the time derivative of the vertical flux through the receiver coil. In this modeling study we approximated this flux by the magnitude of the time derivative of the vertical magnetic field at the center of the receive coil.

To consider the responses of the time domain instrument we proceeded as follows:

- Calculate the response fields (in phase and quadrature) for frequencies $<20\text{ kHz}$,

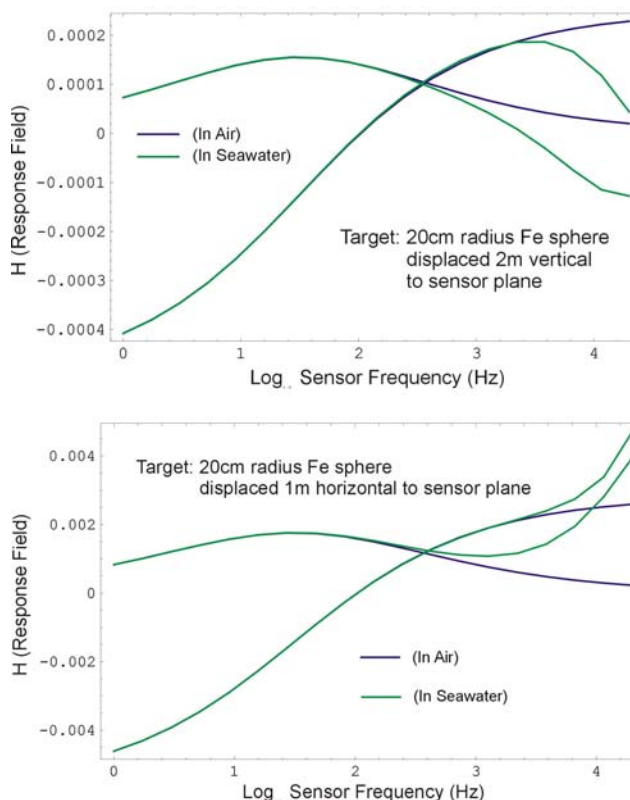


Figure 9. Response fields (inphase and quadrature) as a function of frequency for a 20-cm ferrous target.

- Fourier transform the transmit waveform,
- Convolve the response fields with the transmit waveform FFT and inverse FFT to obtain the response fields as a function of time,
- Take the time derivative of the response fields, and
- Integrate the time derivative of the response field over the assumed time gate to produce the predicted signal.

Figure 10 shows the predicted signal as a function of time for the intermediate sized target displaced horizontally from the coil. To determine the relative air and seawater signals one would then integrate over the appropriate time period corresponding to the measurement time gate. The earliest possible time gate for our instrument will likely open ~ 100 microseconds after the end of the transmit pulse. We expect little or no difference in measured signals for the Marine MTADS whether the targets are in open air, embedded in the earth, or at the ground interface in either fresh or salt water.

This modeling study (Appendix C) does, however, have implications for time domain systems that may have very early time gates (or be able to make measurements during the transmit pulse). Likewise, frequency domain EMI sensors with good high frequency response may detect differences in signals for targets in fresh and salt water. However, these differences will likely only require corrections to ground or fresh water measurement libraries. Because the enhancement in seawater signals occurs primarily only when the target is horizontally displaced from the sensor and for only the largest targets, it is unlikely that enhancement of seawater signals will prove particularly beneficial from a detection point of view.

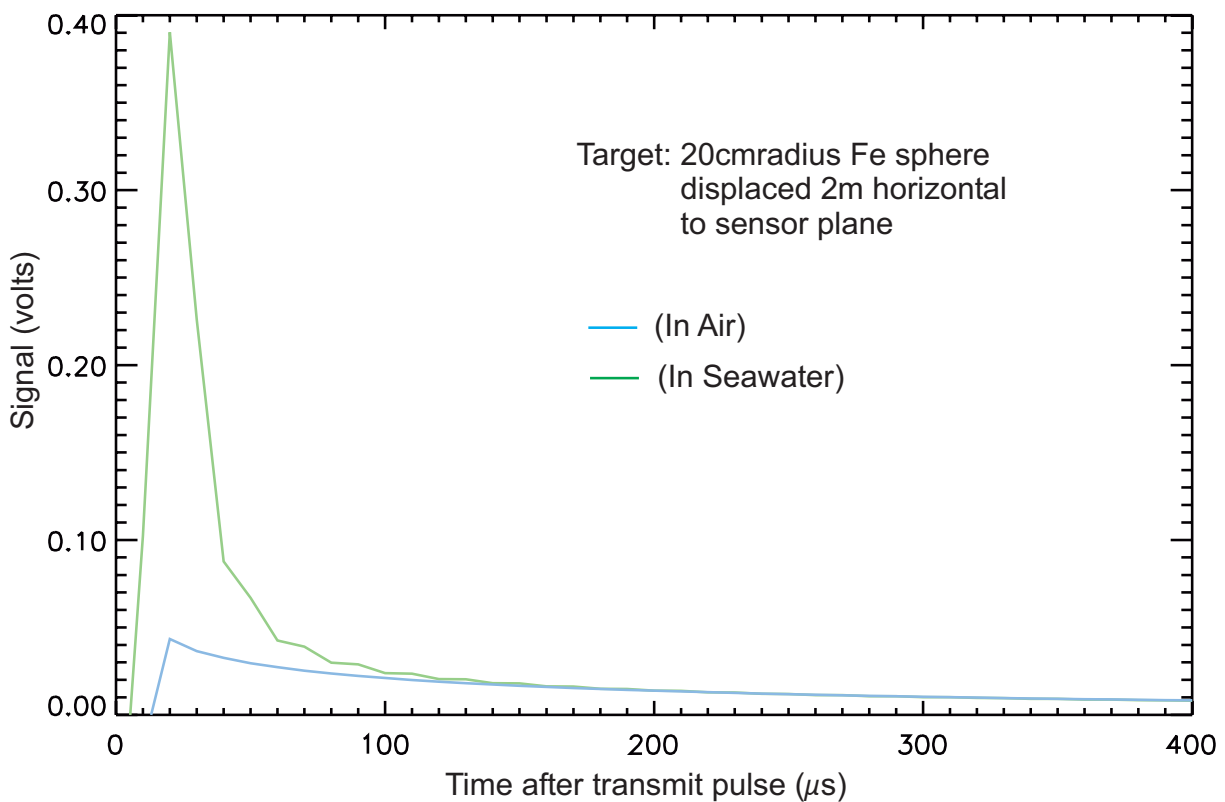


Figure 10. Time domain comparison of air and seawater sensor returns.

7.3 The EMI Array Design

We conducted a modeling study to evaluate the most efficient and effective design for a widely extended time-domain EMI sensor system. The efforts combined both a parametric modeling study and an experimental project to evaluate some breadboard designs prepared by using existing system components. These studies are described in the Geonics Reports included in Appendix C of this report. We briefly summarize the studies below.

7.3.1 Coil Designs: Assuming the dimensions of the EM array would be confined to a 1 meter by 4 meter mechanical footprint, sensor performance models were developed based upon all possible combinations of 3 different transmit coil designs and 3 different receive coil designs. The plots in Figure 11 show the projected receiver signal response as a function of target depth below the transmit coil for 2 different sized transmitter coils. All coils are normalized to have equal dipole moments (Coil Area X Number of Turns). The coil combinations considered are show below.

| Transmit Coils: | Receive Coils: |
|-----------------|----------------|
| 1.0 X 4.2 m | 0.5 X 0.5 m |
| 1.0 X 2.0 m | 0.5 X 1.0 m |
| 1.0 X 1.0 m | 1.0 X 1.0 m |

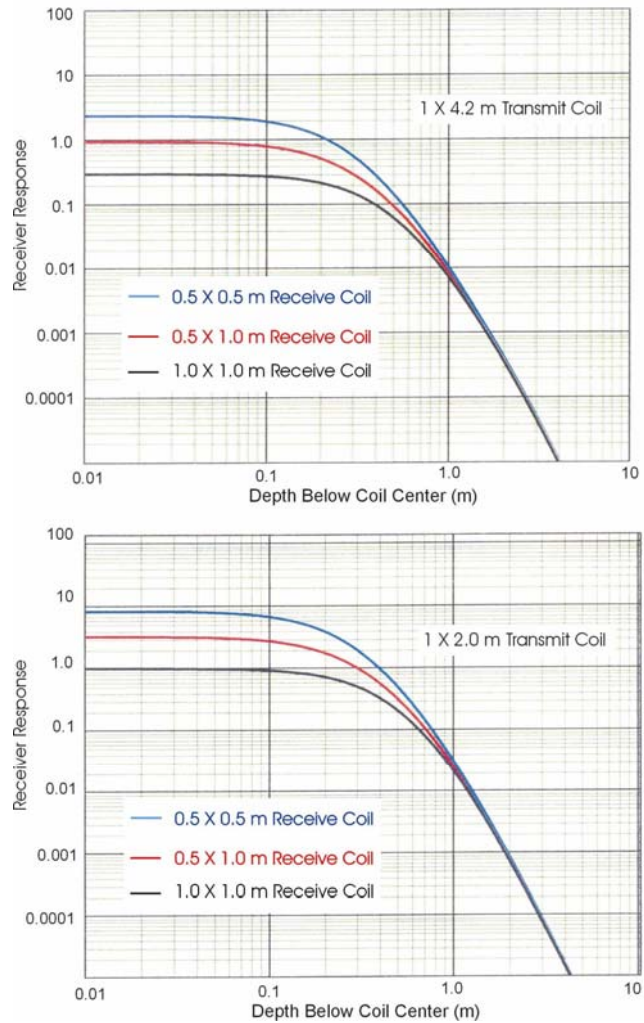


Figure 11. Receiver response as a function of depth below the coils for several different coil combinations.

The larger transmitter coil provides the most uniform radiation pattern below the coil and is the simplest design. The smaller receive coils have the highest sensitivity directly below the coils and provide better spatial resolution than larger coils. While the combination of smaller transmit and receive coils have the better detection sensitivity for small shallow objects, the fall-off in sensitivity is significantly greater for the smaller coils. This information is treated in greater detail in the reports.

7.3.2 Signal Distortion Effects: The design characteristics of time domain sensors naturally lead to distortions in the measured signals. These are of three primary types:

- Run-on Effect (or Turn-on Effect). This is the effect on a measured target response resulting from prior transmitter pulses.
- Turn-off Time Effect. This results from the finite turn-off time of the transmitter pulse, effectively limiting the bandwidth or frequency response of the sensor.
- Gate Width Effects. The number, width, and location of the detection time gates create signal distortions and affect the S/N of the measured signal.

As an example, in Figure 12 the time-decaying signal ($B_h(t)$) from the induced magnetic field of a horizontal 60-mm mortar is plotted. The measured signal decay ($F_h(t)$) of the mortar is plotted, as is the distortion ($|Sh(t)|-1$) due to a finite transmitter turn-off time of 0.1 msec. The predicted error ($\sim 30\%$ at 0.1 msec) decreases to a negligible level at 1 msec. The magnitude of the other signal distortion effects cited above varies from a few tenths of a percent to several percent, depending upon the target size and orientation and the time scale for the measurement. All the effects are predictable and can be corrected. Perhaps the greatest limitation on the time domain instruments results from the finite turn-off time of the transmitter pulse (typically $\sim 100\mu\text{sec}$).

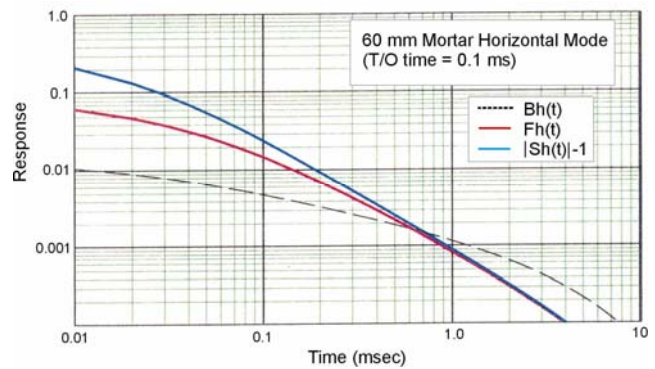


Figure 12. Distortion of the receiver signal due to the turn-off effect.

This limits sensitivity for very small objects whose signals decay very quickly. This is the primary reason that these instruments are not used in mine detection.

7.3.3 Testing Breadboard Arrays: A 1 meter \times 4 meter transmit coil (four turns) was setup as shown in Figure 13. It was driven by a Geonics Protem 57 transmitter. The detector was a modified Protem 47 (0.6 m, 700 kHz bandwidth) receiver coil. It was placed in two different positions (A and B), and ordnance was moved in 20 cm increments along Lines 1, 2, and 3. Measurements were made for a 60-mm mortar and a 105-mm projectile in various orientations. The results are summarized graphically in Figure 14. In the upper panel, the nearly-identical signal pairs were made by the Protem 47 and 57 receivers, see Appendix C for details.

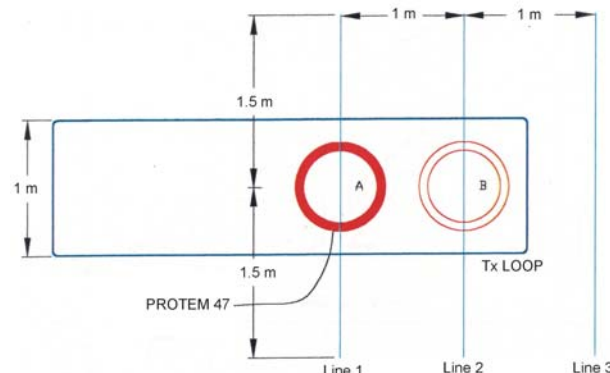


Figure 13. Test setup to evaluate a 4-meter transmitter with a small receive coil.

Data from these measurements provide information necessary to establish the preliminary requirements for both the transmitter coil and the receiver coil designs. We can confidently use the modeling predictions to develop a preliminary system design.

7.3.4 The EMI Array: Based upon the information from the EMI modeling program and the breadboard parametric measurements, the EMI array concept has been established, Figure 15. We will use a single transmitter coil, approximately 1 \times 4 meters. Four identical receive coils 0.5 \times 1.0 meters will be fit inside the loop of the transmitter coil. Preliminary designs have been developed for the coils and

for the driver, including the power transmitter, the transmission pulse sequence, and the detection gate designs. We currently plan to have up to 26 detection gates. These can be programmed into several different smaller groupings depending upon the size and depth of the ordnance in the ranges that need to be characterized. This will allow us to maximize both our detection efficiency (S/N considerations) and our ability to make classification decisions based upon shape and decay characteristics of the target signals. The larger targets (projectiles and bombs) have more slowly decaying signals that can be effectively exploited using the later time gate information.

Preliminary dimensions and weights for the coils, connectors, cables, and interface box are being used as design input for the sensor platform. Once the sensor platform design has been firmly established, the design has again been hydrodynamically modeled by VCT, and the preliminary design review for the platform is approved, we will proceed to the preliminary design review for the EMI array in preparation for its construction.

7.4 Marine Sonars

At the beginning of this project we proposed to consider both bottom penetrating and imaging sonar as classification adjuncts to the magnetic and EMI sensors. A study conducted early in the program revealed that the sophistication of low frequency sonars suitable for shallow bottom-penetration into the sediment layer was not suitable for this project. The level of development of these systems and their ability to confidently detect and classify objects even partially buried in the sediment, was still a very researchy endeavor. We decided that the program risk of trying to incorporate bottom-penetrating sonar was too high for this program.

Conversely, with ONR and DoD support an excellent hand-held high-frequency imaging sonar has been developed by the Applied Physics Laboratory at the University of Washington, working in conjunction with the Naval Explosive Ordnance Detection Technology Center. The system was designed for use as a handheld diver instrument for searching ship hulls for antiship mines. The instrument is just beginning to find its way into commerce and is being built, one unit at a time (as ordered) and vended through Sound Metrics, Inc. We conducted a product search for similar instruments, and identified several potentially

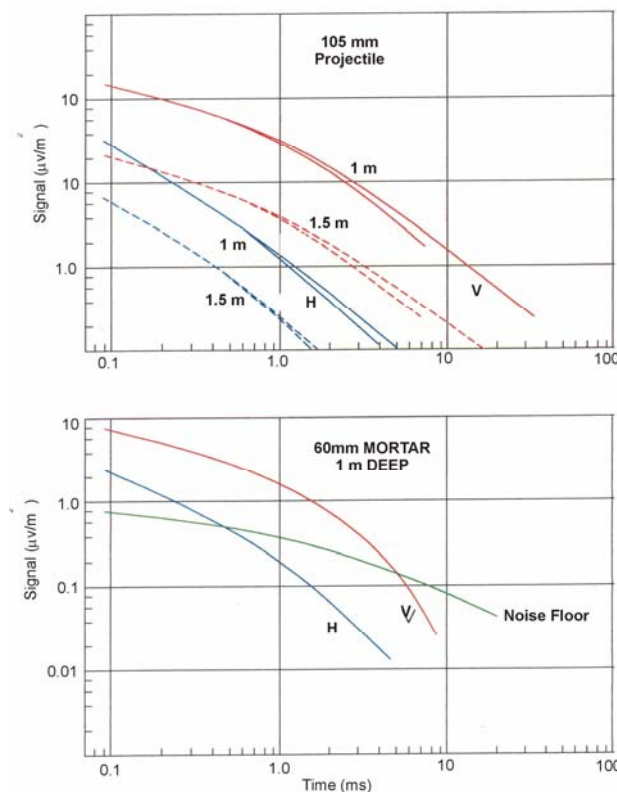


Figure 14. Signal response for two ordnance items in the test rig. Each is shown in both vertical and horizontal orientations. The 105-mm is shown at two "depths" below the coil.

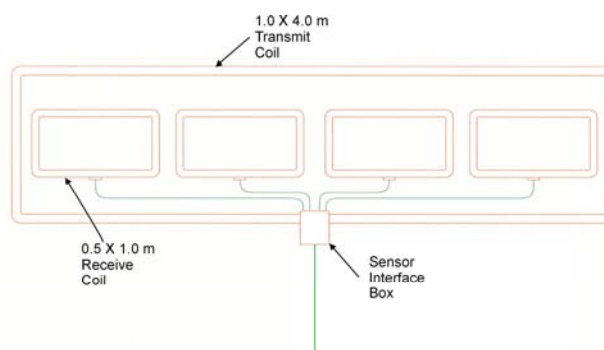


Figure 15. Final concept layout for the EM array.

competitive systems. Their attributes are described in the Imaging Sonar Report in Appendix C. The DIDSON unit from Sound Metrics appeared to be more technically appropriate for this application.

We envision using the DIDSON unit for two purposes. It will be mounted on the tow vessel as a forward-looking imaging sonar. The real time image will be available to the pilot and will be used as an obstacle avoidance tool. By adjusting the tilt of the unit we can image the full swath width of the sensor platform to image obstacles. Since it is looking well forward of the sensor platform, sufficient warning will be provided to allow the platform to be raised to miss pending obstructions.

The second use of the system will be as a classification tool. Because the sonar is provided with its own data interface and recording system, a permanent record can be kept of the bottom image. This data system records images with a time stamp, which can be correlated with the GPS time stamp that serves as a registration for all the other data streams being recorded. We will develop a data analysis utility that will allow us to clip and view the sonar image corresponding to a magnetic or EMI anomaly that is being analyzed.

During this program we visited the APL lab and conducted an evaluation of the DIDSON unit on Puget Sound. Its is easy to operate and we verified that it can be effectively used in a 30° forward looking orientation. Additionally, we used the system mounted on a specially designed fixture, which was also developed with DoD support. This mounting system, shown in Figure 16, allows the unit to be easily panned and tilted. This process can be automated for our use by correlating these functions with the depth finder output from the unit that is also mounted on the tow vessel.

The DIDSON unit was ordered as soon as our access to the ESTCP project was cleared. It has been delivered.



Figure 16. A specially develop sonar mounting system is shown in the left panel. The right panel shows the adjustment feature of the mounting system.

8. Conclusions

The primary decision point for this program resulted from the Special Design Review presented to the Program Office on 18 July 2003. No major impediments were identified that would compromise either the success of, or the proposed development schedule for the follow-on program. Following this presentation, the Program Office issued approval for initiating startup of UX2003-24.

Electronic and hardware components are being procured. They are being evaluated to establish the operating characteristics and possible interactions with other components. General component and system integration will begin in the spring of 2004 when the fiberglass sensor platform is delivered. We plan a series of integration and shakedown tests for the summer. These will take place on Pamlico Sound near Moorehead City, NC. Test operations will be staged from a private pier at a private resort property.

The locations and dates for the Final Demonstrations have not been established at this time. However, the originally-proposed sites at The Former Duck Test Range (Duck, NC) and at the Aberdeen Proving Ground remain viable options. We have had several other inquiries from potential demonstrations sites including Vieques, PR, Ostrich Bay in Pudget Sound, and additional sites in Aberdeen, MD.

9. Transition Plan

The transition path for this technology would logically be to license it to a private firm that provides UXO services to the US government. Historically, this path has not been effective (e.g. the Airborne MTADS) because of the way that UXO services are contracted. For a commercial firm to commit to a major equipment development they have to be able to identify sufficient probable business to allow them to recover their investment costs and potentially make a profit. Typically, UXO services are contracted by the Corps of Engineers in such small increments that UXO service provider firms are unwilling to make significant investments in a new technology.

A possible alternative transition plan would be to take advantage of the as-built Marine MTADS hardware, which will be owned by the government (ESTCP). Working with the Corps of Engineers (or one of the regional offices of the Corps) use of the equipment could be made available as Government Furnished Equipment (GFE) to the winning contractor on a substantial underwater UXO operation. AETC could effectively act as a consultant or subcontractor in the operation of the equipment that we have developed. A more fully developed transition plan can be drafted during the ESTCP demonstration phase of this program.

10. REFERENCES

1. “*MTADS* Unexploded Ordnance Operations at the Badlands Bombing Range, Pine Ridge Reservation,” NRL/PU/6110-98-353 (1998)
2. “Multi-sensor Towed Array Detection System for UXO Detection,” H.H. Nelson, and J.R. McDonald, *IEEE Transactions on Geoscience and Remote Sensing*, **39**, 1279 (2001)
3. “Electromagnetic Induction and Magnetic Sensor Fusion for Enhanced UXO Target Classification,” H.H. Nelson and B. Barrow, NRL/PU/6110-00-423 (2000)
4. “Analysis of Magnetic and EMI Signatures from Impacted Intact Ordnance and Exploded Fragments,” B. Barrow and H.H. Nelson, Proceedings of the UXO/Countermining Forum, Anaheim, CA, 2-4 May 2000
5. “Probabilistic Neural Networks for Unexploded Ordnance (UXO) Classification Using Data Fusion of Magnetometry and EM Physics-Derived Parameters,” S.J. Hart, H.H. Nelson, B. Grimm, S.R. Rose-Pehrsson, and J.R. McDonald, Proceedings of the UXO Countermining Forum, Anaheim, CA, 2-4 May 2000
6. “Using Physics-Based Modeler Outputs to Train Probabilistic Neural Networks for Unexploded Ordnance Classification in Magnetometry Surveys,” S.J. Hart, R.E. Shaffer, S. R. Rose-Pehrsson, and J.R. McDonald, *IEEE Trans. on Geoscience and Remote Sensing*, **39**, 797 (2001)
7. “Results of the *MTADS* Technology Demonstration #3, Jefferson Proving Ground, Madison, IN,” J.R. McDonald, H.H. Nelson, J. Russell, and R. Robertson, NRL/PU/6110-99-375 (1999)
8. “*MTADS* Magnetometer and EM Surveys at Ft. Ord, 5 March 2001,” J.R. McDonald and H.H. Nelson, NRL/PU/6110-01-439 (2001)
9. “Location and Characterization of Underwater UXO,” D. DeProspero, E. Cleary, and R.D. Lewis, Proceedings of the UXO FORUM, Nashville, TN, 28-30 May 1997
10. “Validation of Detection Systems (VDS) Test Program Final Report, Mare Island Naval Shipyard (MINS), Vallejo, CA,” Environmental Chemical Corp., for Pacific Division, Naval Facilities Engineering Command, Contract No. N 62742-98-D-1809
11. “Airborne UXO Surveys,” J.R. McDonald, ESTCP Project 2000311
12. “Man-Portable Adjuncts for the *MTADS*,” J.R. McDonald, H.H. Nelson, Thomas H. Bell and Bernard Puc, NRL/PU/6110-01-434
13. “A Review of Underwater UXO Systems in Europe,” Richard J. Wold and Valli Tuire, Proceedings of The UXO FORUM 2002, 3-6 September 2002, Orlando, FL
14. “Acoustic, Near-Video-Quality Images for Work in Turbid Water,” E.O. Belcher and Dana C. Lynn, Proceedings of the Underwater Intervention 2000 Conference, Houston, TX, January 2000

11. **APPENDICES**

Appendix A. UX-1322 Program Documents

Program Project Plan
ESTCP Guidance Letter of 18 November 2002
AETC Addendum to Original Proposal

Appendix B. UX-1322 Program Design Review

Appendix C. “Modeling of the Electromagnetic Response of EMI Sensors Employed in a Salt Water Environment,” Judy Soukup, AETC Incorporated, January 2004

“Concept Design for a Marine UXO Sensor Platform, Thomas F. Tureaud and Kenneth W. Watkinson, VCT Tech Memo 02-06

“Concept Design for a Marine UXO Sensor Platform – Autopilot for 2-m and 4-m Concept Vehicles,” Stacy J. Hills and Thomas F. Tureaud, VCT Tech Memo 03-02

“EM68 Marine EMI UXO Detector Project Development Interim Report,” Miro Bosnar, Geonics Report, April 2003

“Report of Overlapping Receiver Coil Study,” Miro Bosnar, Geonics Report, 29 August 2003

“EM68 – Marine EMI UXO Detector Project Development Report,” Miro Bosnar, Geonics Report, September 2003

“EM68 Instructions for Control & Logging Program,” Miro Bosnar, September 2003

“Evaluation of Performance and Capabilities of the DIDSON Imaging Sonar,” Chet Bassani, AETC Incorporated, December 2003

19 December 2002

Dr. Jeffrey Marqusee
ESTCP Program Office
901 North Stuart Street, Suite 303
Arlington, VA 22203

ESTCP Project No. UX-0324
Title: UXO Detection and Characterization in the Marine Environment

Dear Dr. Marqusee,

Based upon your ESTCP Guidance Letter of 18 November 2002 directing us to revise our proposal for the project cited above and the FY-2003 funding guidance provided by the Program Office, we have revised our Program Plan. Rather than redrafting the whole proposal (No 03 EB-UX1-008P), we have prepared an addendum to the proposal incorporating the requested changes and information. The addendum is attached to this letter. The addendum also incorporates new Tables of Project Milestones, Deliverables, and Reports, and a new 3-year Program budget. A draft version of this addendum has been reviewed by Dr. Andrews.

Thank you very much for your continued interest and support of our MTADS development programs. Please advise if further changes or modifications are needed for this effort.

Sincerely yours,

Jim R. McDonald
jmcdonald@va.aetc.com

Attached: Addendum to Proposal 03 EB-UX1-008P

ESTCP Marine MTADS

Addendum to:

AETC Proposal No. VA-02-007

ESTCP Proposal No. 03 EB-UX1-008P

ESTCP Project No. UX-0324

Based upon ESTCP Guidance Letter of 18 November 2002 and FY-2003 funding guidance provided (verbally) by the program office this Addendum establishes the following modifications to Proposal 03 EB-UX1-008P. The original content of the proposal is assumed to form the basis of Project UX-0324 except as detailed below.

1. Project No UX-0324 will be authorized to begin work contingent on the successful completion of SERDP Project 1322. SERDP Project 1322 funding for 2002 was received in July 2002. The Project was designed to be completed in one year, with a contingency to extend to 15 months in case of delays. Based upon progress made during the first 4 months of the SERDP Project, we anticipate completion of the SERDP tasks within the designed 12-month plan. We therefore anticipate beginning work on ESTCP Project UX-0324 at the beginning of the 4th quarter of FY-2003. Based upon Program Office guidance we understand that FY-2003 funding available to support the project will be at the level of \$0.9M. Table 1 in our proposal (03 EB-UX1-008P) is understood to be modified by slipping all entries by 5 months to begin on 1 July 2003. This makes the project final report deliverable in the 3rd quarter of 2006. This information is reflected in the Table of Milestones and Deliverables included below. The revised project milestones and deliverables are documented in separate tables attached to this document.

2. The second instruction in the guidance letter directs us to: *“Plan for a design goal of not more than 4 meters, with 2 meters as a lower risk option. Revise the budget to reflect a scoped-down system. Please ensure that the report at the conclusion of the SERDP project describes a system concept consistent with the system that will be supported.”* The major task currently underway in the SERDP program that is effected by this guidance is our study subcontracted with VCT to:

- (1) down-select among platform deployment design options,
- (2) complete a static platform engineering concept design for the 8-meter array, and
- (3) carry out a dynamic study of the hydrodynamic performance and control of the designed system. After completion of the hydrodynamic study, a C-code software routine will be written by VCT to allow an operator to fly the array platform using a “joystick.”

Tasks (1) and (2) were completed by VCT prior to the arrival of the 18 November ESTCP Guidance Letter. AETC issued a stop work order to VCT at that point and modified our subcontract effort with them to begin step (2) again assuming sensor arrays of both 4 meters and 2 meters and to carry each system through the static design and hydrodynamic modeling studies. This change order resulted in a delay of about one month and about \$25K additional costs. The delay does not affect the overall SERDP Project schedule.

Changing the horizontal dimensions of the array platforms will not result in a significant decrease in the cost of designing and building the platforms. Small savings (2 or 3% of the total program costs) could be realized if the number of magnetometer sensors was reduced. We

would prefer to forgo these small savings by reducing the inter-sensor spacing, thus increasing system performance. There are effectively no savings to be had in reducing the dimensions of the time-domain EM transmitter.

Significant program cost savings can be achieved only by deleting significant program capabilities (e.g. the time-domain EM array), decreasing labor costs associated with system development, or decreasing subcontracting costs associated with developing improved EM sensor concepts. As the Program Office stated that they preferred that we not delete the EM array from the system design, cost savings must result from the second two options. It is our opinion that the system integration and shakedown tests have been critical to the prior MTADS platform successes. Therefore, we propose to achieve cost savings by:

- (1) deleting the mechanical engineer from the labor mix
- (2) decreasing the labor commitment to software code development for analysis, and
- (3) decreasing the development subcontract with Geonics by ~50%.

Step (3) will not increase program risk, but will integrate EM sensors with essentially current design capabilities, i.e. similar to those of the EM 61 Mark II. Concurrently, we will truncate our ongoing (SERDP) EM modeling studies defining the effect of channeling in the saltwater environment. The results will not be able to be factored into the EM system design.

Decreasing the software labor support will not be allowed to affect the program risk. The reduced commitment will likely mean that we forgo developing a joint (or cooperative) analysis of electromagnetic and sonar imaging data, and that we limit development to implementing the positioning requirements imposed by the new platform attitude sensor data streams. We envision that the Marine MTADS DAS will otherwise be a direct mapping of the MTADS Airborne DAS capability. In addition, future efforts to incorporate the current DAS capabilities into commercial software would be leveraged by this program.

Deleting the mechanical engineering support from the labor mix does carry a limited increase in program risk. It means that we will rely on engineering consulting services and use overkill in materials decisions. We will mitigate this risk by carefully recruiting the new “technician” staff member, hiring only a person with significant electronics and hardware integration experience. This hire may be at a level higher than indicated by the job category in the revised budget.

3. *“Update milestones to include...shakedown tests, demonstration plans...and a cost and performance report....”* Separate tables are included in this document updating milestones and deliverables.

4. The enclosed budget spreadsheet reflects revised program costs consistent with the written and verbal guidance provided by the ESTCP Program Office. In part, anticipating the program start in the 4th quarter of FY-2003 mitigates the significantly decreased first year available funding. We have slid only about half of these deferred costs into 2004. Overall, we are proposing a total program cost about \$700K less than that documented in ESTCP Proposal No. 03 EB-UX1-008P. This reflects decreasing the level of our labor commitment by about 1.5 persons, and about a \$100K reduction in subcontracted EM development work. This decrease in program costs will be reflected in our demonstrating a system with reduced innovation, a reduced system production rate, and an increased (per acre) survey production cost. However, we anticipate only a slight increase in risk to the overall program goals.

Table 1. Marine MTADS Project Milestones

| Task | Milestone | Date |
|----------------------------------|-----------------------|-----------------------|
| Sensor Platform/Vessel Interface | Acquire Components | 2003-Q4 |
| | Complete Integration | 2004-Q2 |
| Tow Vessel | Procurement | 2003-Q4 |
| | Customize | 2004-Q2 |
| | Delivery | 2004-Q3 |
| 4-Meter Sensor Platform | Let Contract | 2003-Q4 |
| | Take Delivery | 2004-Q1 |
| | Procure Mag Sensors | 2003-Q4 |
| | Procure EM Sensor | 2004-Q2 |
| 2-Meter Sensor Platform | Take Delivery | 2004-Q3 (If Required) |
| | Acquire New EM Sensor | 2004-Q3 |
| DAQ | Procure Components | 2003-Q4 |
| Imaging Sonar | Procure | 2004-Q2 |
| | Integrate | 2004-Q3 |
| DAS | Complete Integration | 2005-Q3 |
| Complete Component Integration | | 2004-Q4 |
| System Shakedown #1 | | 2005-Q1 |
| System Shakedown #2 | | 2005-Q2 |
| Complete System Integration | | 2005-Q3 |
| System Demonstration #1 | | 2005-Q4 |
| System Demonstration #2 | | 2006-Q2 |

Table 2. Marine MTADS Deliverables/Reports

| Task | Deliverable | Date |
|------------------------|----------------------|---------------|
| Sensor Platform Design | Interim Report | 2003-Q4 |
| System Shakedown | Interim Report | 2005-Q3 |
| Demonstration #1 | Test Plan | 60 days< Demo |
| | Demonstration Report | 2006-Q1 |
| Demonstration #2 | Test Plan | 60 days< Demo |
| | Demonstration Report | 2006-Q2 |
| Program | Annual Report | 2004-Q4 |
| | Annual Report | 2005-Q4 |
| | Final Report | 2006-Q3 |
| | C&P Report | 2006-Q4 |

For the time being we have left the production of a second sensor platform in the budget for year 2. This is consistent with our carrying the 2-meter platform through static and hydrodynamic engineering design per the Program Office direction. In the event that a larger array cannot be successfully deployed, all the preparation design work for the 2-meter platform will have been completed.

Table 3. ESTCP Marine MTADS, Proposal No. 03 EB-UX1-008P, Project No UX-0324

DATE: Revised 12/10/02

Rates are fully burdened using DCAA approved rates

AETC

PROPOSAL# VA-02-007

POP: Jan 01, 2003 - Sep 30, 2006

Lbr Benefits @ 42.5% Overhead @ 54.25% G&A @ 18.8% Computing @ \$4.50 hr

| LABOR CATEGORY | RATE | YEAR 1 | | RATE | YEAR 2 | | RATE | YEAR 3 | | TOTAL - 36 MONTHS | |
|--------------------------------------|----------------------------|--------|-----------|-----------|--------|-------------|-----------|--------|-----------|-------------------|-----------|
| | | HOURS | COSTS | | HOURS | COSTS | | HOURS | COSTS | HOURS | COSTS |
| Principal Investigator | \$150.50 | 400 | 60,200 | \$156.52 | 600 | 93,912 | \$162.78 | 800 | 130,224 | 1,800 | 284,336 |
| Senior Geophysicist | \$98.16 | 400 | 39,264 | \$102.08 | 600 | 61,248 | \$106.17 | 800 | 84,936 | 1,800 | 185,448 |
| Mechanical Engineer | MTS 3 \$93.80 | 0 | 0 | \$97.55 | 0 | 0 | \$101.45 | 0 | 0 | 0 | 0 |
| Computer Scientist | MTS 4 \$83.76 | 600 | 50,256 | \$87.11 | 1,040 | 90,594 | \$90.59 | 1,040 | 94,214 | 2,680 | 235,064 |
| Technician | MTS ? \$55.00 | 2080 | 114,400 | \$57.20 | 2,080 | 118,976 | \$59.49 | 2,080 | 123,739 | 6,240 | 357,115 |
| DIRECT CONTRACT LABOR | | 3,480 | \$264,120 | | 4,320 | \$364,730 | | 4,720 | \$433,113 | 12,520 | 1,061,963 |
| TRAVEL COSTS | Trip Rate | #Trips | | Trip Rate | #Trips | | Trip Rate | #Trips | | #Trips | |
| Wash DC - Raleigh NC | 2 nights \$1,276 | 4 | 5,104 | \$1,276 | 6 | 7,656 | \$1,276 | 6 | 7,656 | 14 | 20,416 |
| Wash DC - Toronto CAN | 2 nights \$1,822 | 2 | 3,644 | \$1,822 | 2 | 3,644 | | | | 4 | 7,288 |
| Wash DC - S.Diego CA | 2 nights \$3,396 | 1 | 3,396 | \$3,396 | 1 | 3,396 | \$3,396 | 2 | 6,792 | 4 | 13,584 |
| Wash DC - Pan.City FL | 2 nights \$1,370 | | 0 | \$1,370 | 1 | 1,370 | | | | 1 | 1,370 |
| Wash DC - West Coast | | | 0 | | | | | | | | |
| Est. Los Angeles Area | 2 nights \$3,403 | 2 | 6,806 | \$3,403 | 2 | 6,806 | | | | 5 | 13,612 |
| Wash DC - East Coast | | | | | | | | | | | |
| Demo Support - 8 People | 10 nights \$3,607 | | | | | | \$3,607 | 8 | 28,856 | 8 | 28,856 |
| MAJOR EQUIPMENT | Unit Rate | #Units | | Unit Rate | #Units | | Unit Rate | #Units | | #Units | |
| Magnetometer Array Platform | \$110,000 | 0 | \$0 | | 1 | \$110,000 | | | | 1 | 110,000 |
| Magnetometer/Geometrics | #822ROV \$33,260 | 8 | \$266,080 | | 0 | \$0 | | | | 9 | 266,080 |
| GPS Hardware/Trimble | \$100,000 | 0 | \$0 | | 1 | \$100,000 | | | | 1 | 100,000 |
| Attitude Sensors (Various) | \$59,400 | 0 | \$0 | | 1 | \$59,400 | | | | 1 | 59,400 |
| EM Platform | \$89,100 | 0 | \$0 | | 1 | \$89,100 | | | | 1 | 89,100 |
| Sonar Hardware | \$80,000 | 0 | \$0 | | 1 | \$80,000 | | | | 1 | 80,000 |
| DAQ Electronics | \$59,400 | 1 | \$59,400 | | 0 | \$0 | | | | 1 | 59,400 |
| DAS Hardware | \$29,800 | 1 | \$29,800 | | 0 | \$0 | | | | 1 | 29,800 |
| Vessel Purchase/Customize | \$71,300 | 1 | \$71,300 | | 0 | \$0 | | | | 2 | 71,300 |
| Hardware/Electronics Spares | \$59,400 | 0 | \$0 | | 1 | \$59,400 | | | | 2 | 59,400 |
| Boat Trailer | \$15,000 | 1 | \$15,000 | | 0 | \$0 | | | | 1 | 15,000 |
| Sensor Platform Trailer | \$17,000 | 1 | \$17,000 | | | \$0 | | | | 1 | 17,000 |
| Mag Sensor Replacements | | | | \$33,267 | 0 | \$0 | \$14,851 | 2 | \$29,702 | 1 | 29,702 |
| Support for Demo #1 | | | | | | | \$142,571 | 1 | \$142,571 | | 142,571 |
| Support for Demo #2 | | | | | | | \$118,802 | 1 | \$118,802 | | 118,802 |
| OTHER DIRECT COSTS | Unit Rate | #Units | | Unit Rate | #Units | | Unit Rate | #Units | | #Units | |
| Computing Costs | \$5.35 | 3,480 | 18,618 | \$5.35 | 4,320 | 23,112 | \$5.35 | 4,720 | 12,520 | 11,620 | 62,167 |
| Consumable Mat'l & Supplies (Lot) | \$10,000 | 1 | 10,000 | \$11,880 | 1 | 11,880 | \$10,000 | 1 | 10,000 | 3 | 31,880 |
| Publications & Reporting (Lot Price) | \$10,000 | 1 | 10,000 | \$14,256 | 1 | 14,256 | \$30,000 | 1 | 30,000 | 3 | 54,256 |
| SUBCONTRACTS | | | | | | | | | | | |
| GEONICS | Est Contract price + 2.12% | | 53,180 | | | 51,060 | | | | | 104,240 |
| TOTAL ESTIMATED COSTS | | | 833,448 | | | 1,350,541 | | | 820,012 | | 3,004,001 |
| FIXED FEE | 7.98% | | 66,509 | | | 107,773 | | | 65,437 | | 239,719 |
| PROPOSAL TOTAL | | | \$899,957 | | | \$1,458,314 | | | \$885,449 | | 3,243,720 |



November 18, 2002

Dr. J.R. McDonald
AETC Incorporated
1225 Jefferson Davis Highway, Suite 800
Arlington, Virginia 22202

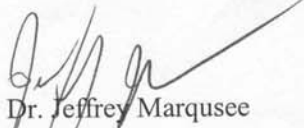
SUBJECT: UXO Detection and Characterization in the Marine Environment; ESTCP #UX-0324

Dear Dr. McDonald,

The Environmental Security Technology Certification Program (ESTCP) has completed its review of proposals for FY03 in response to the U.S. Army's Humphries Engineer Center Support Activity solicitation # BAA-02-0003. I am pleased to announce that your proposal was selected to participate in the FY 2003 ESTCP program.

During the evaluation process, members of the review committee or ESTCP staff may have identified minor deficiencies in the proposal and have accordingly made recommendations for improving the proposal to increase the likelihood of a successful technology demonstration and validation. If this situation applies to your proposal, an attachment lists these recommendations. Please review these and incorporate them into your proposal and submit this revised proposal to ESTCP as soon as possible, but no later than December 11, 2002. This document will become the foundation of the contract that will soon be developed. If you have any questions or concerns regarding these recommendations, please contact Dr. Anne Andrews, the ESTCP Unexploded Ordnance Program Manager, by e-mail at Anne.Andrews@osd.mil, telephone 703-696-3826, or fax 703-696-2114.

We appreciate your efforts to support ESTCP and look forward to working with you.


Dr. Jeffrey Marqusee
Director
Environmental Security
Technology Certification Program

Enclosure
Cc: Dr. John O. Curtis Contracting Officer's Representative

ESTCP Program Office
901 North Stuart Street, Suite 303
Arlington, Virginia 22203
Tel: (703) 696-2117 Fax: (703) 696-2114

ESTCP FY03 Proposal Modifications

Please include recommended proposal modification(s) in your revised proposal.

Proposal Number: 03 EB-UX1-008P

Project Title: UXO Detection and Characterization in the Marine Environment

Project #: UX-0324

Issues:

- Funding of this project is contingent on the successful outcome of the SERDP system design studies.
- The proposed 30-foot array presents more risk than the program office is prepared to undertake. Plan for a design goal of not more than 4 meters, with 2 meters as a lower risk option. Please revise the budget to reflect a scoped-down system. Please ensure that the report at the conclusion of the SERDP project describes a system concept consistent with the system that will be supported.
- Prior to hardware construction, plan to provide detailed plans for external engineering review.
- Update milestones to include an interim report following the system shakedown tests, demonstration plans 2 months prior to each field demonstration, and a cost and performance report upon completion of the project.
- Plan to consult with the program office regarding hardware ownership and technology transfer.

Technology Needs for Underwater UXO Search and Discrimination

SERDP UX-1322, PROJECT PLAN

Project Objective & Deliverables: The fraction of UXO contaminated area that is underwater and inaccessible to ground-based search technologies is poorly defined, but is likely over a million acres in the continental US. New techniques and new platforms to support integrated magnetometer/EM search arrays in a robust and versatile underwater system that will both detect and discriminate shallow-buried UXO are needed. Because underwater UXO clearance is difficult and expensive, the ability to differentiate between intact UXO and OE scrap during survey and analysis is very important. Many components of the Airborne *MTADS* UXO search system can be adapted for use in underwater search platforms. Other components, specific to the marine environment, must be developed for this application. This project addresses development issues that must be completed before construction and testing of underwater search systems can begin. Specifically, we will develop a concept for mounting and stabilizing underwater search arrays that will allow them to be dynamically suspended close to the bottom during surveys. Using EM modeling studies we will develop an engineering design for a new EMI array that will be specifically tailored for marine applications, assuming a 1-meter standoff between the array and the sediment surface. Both magnetometer and EMI array platform engineering designs are deliverables for this project. We will also address the development of a precisely-cued visualization system based upon a high frequency (>1 MHz) imaging sonar. Its potential value will be evaluated in tradeoff studies with optical visualization systems.

Technical Approach and Risks: Task 1 begins with a marine engineering study of both potential vessel parameters and platform designs. In this study the dynamic interactions of the sea state, the boat dimensions, its conformation, and potential marine hardware fixture platforms will be considered. The product of this effort is an engineering feasibility study that will bound the parameters for the boat and the platforms. We will determine whether the sensor array platforms can be hard-mounted on the support vessel. The design of the depth control system will be established, as will the attitude compensation system to decouple the pitch and roll motions of the vessel from the array. Of primary consideration in the design is the safety of personnel and equipment. Operationally, ease of use, survey production rates, economy and equipment ruggedness are important. Our approach will be based upon good engineering practices and will emphasize the use of COTS components, when feasible. At the culmination of the engineering feasibility study we will be in a position to begin development of the specifications for the marine vessel, the platform interface and motion control systems, and the engineering designs for the magnetometry and EMI array platforms.

The primary focus of Task 2 is an EMI modeling study. The goals of this effort are to assure the detectability of all small shallow-buried UXO while at the same time exploring strategies for extracting the necessary shape information from target signatures to support UXO classification decisions. Achieving these goals requires making measurements at both early and late times and devising strategies for providing the necessary illumination of each target from multiple directions. There will be tradeoffs among the number and dimensions of transmit and receive coils, their power levels, firing strategies, and placement of detection time gates. Factored into this also is an awareness of seawater effects on early-time signals and the vanishing of usable

signal to noise during late measurement times. We have learned from several years of trying to extend benchtop performance into field surveys, that precise control of timing, sensor positioning and externally induced noise sources is critical to performance. The deliverable for Task 2 is a design document with recommendations and alternatives for sensor design and deployment strategies. It is likely that bench top (in water) experiments will be required to support the effort.

In Task 3 we will implement the results of our design studies from Task 2. The ultimate products of Task 3 are sensor design specifications and a sensor design document. We have learned from the last couple of EM61 instruments that we have taken to the field, that more is not always better. More power driven into the ground, or more time gates to sample the return signal, can be overdone and result in no additional (or even degraded) performance. In our new design and deployment strategies we must emphasize creating a very clean transmit pulse (to allow clean early-time measurements to be made) while creating sufficient raw power to be able to make high signal-to-noise measurements at several milliseconds delay. Task 3 will also likely require both modeling studies and bench top and field measurements.

In Task 4 we will review all recent studies of low intermediate frequency sonar applications to study sub-bottom structures. This includes the efforts both of our company and others in support of marine mine countermeasures. Many of these efforts also incorporate optical (laser) imaging in shallow water (and surf zone) environments. The result of this task is a report evaluating the state of the technology with recommendations as to whether the science is mature enough to implement in a follow-on to this program.

In Task 5 we will explore the possibility of setting up company demonstrations of both a shallow water high-frequency sonar imaging system and a laser-based optical imaging system. We will demonstrate the systems side-by-side in turbid water to evaluate the relative strengths and weaknesses of each system in realistic marine settings.

Benefits/Payoffs: In the long term, the underwater search system that we wish to develop will provide DoD the capability to conduct comprehensive UXO surveys in a shallow water environment typical of most of our UXO contamination problems associated with CTT ranges and the harbors used by our military and in the manufacture and shipping of munitions. The combined sensor approach emphasizes both detection and discrimination capability. Our goal for detection limits for single isolated UXO targets are 60-mm mortars (or their equivalents) if they are buried shallow in the bottom sediments. The short-term goals for this SERDP project are to complete the platform concept study and develop the engineering design documents that can be used to manufacture and deploy the marine *MTADS* sensor platforms.

Technology Needs for Underwater
UXO Search and Discrimination
SERDP Project UX-1322

P.I. Jim R. McDonald
AETC, Inc.

Email: jmcdonald@nc.aetc.com














Jim McDonald
David Wright
Chet Bassani
AETC, Inc.

Miro Bosnar
Geonics, Ltd

Tom Tureaud
VCT, Inc.

Our objective is to develop a geophysical search platform to survey, detect, and classify potential UXO hazards in shallow water areas associated with DoD ranges

- Both passive sensors (magnetometers) and active (EMI) sensors will be incorporated into a single sensor platform
- This project addresses the research issues required to adapt successful land-based UXO technologies for shallow water

| Task | Performer | FY-2002 | | FY-2003 | | | |
|--------------------------------------|--------------|---|---|---|---|---|---|
| | | 3rd Qtr | 4th Qtr | 1st Qtr | 2Qtr | 3rd Qtr | 4th Qtr |
| 1. Sensor Platform Dynamics | AETC/VCT | | | | | | |
| Engineering Feasibility | AETC/VCT |  | | | | | |
| Mag Platform Preliminary Design | AETC/VCT | | |  | | | |
| EM Platform Preliminary Design | AETC/VCT | | |  | | | |
| 2. EM Sensor Performance Modeling | AETC/Geonics |  | | | | | |
| 3. Time-Domain EMI Instrument Design | AETC/Geonics | |  | | | | |
| 4. Sonar Target Characterization | AETC | | | | | | |
| High Frequency Sonar Imaging | AETC | | | | | | |
| Bottom-Penetrating Sonars | AETC | | | |  | | |
| 5. Optical Adjunct Feasibility Study | AETC | | | |  | | |
| Quarterly Web Reporting | |  |  |  |  |  | |
| Annual & Final Report | | | | | | |  |

We are transferring the Airborne *MTADS* UXO search and analysis technology to the marine shallow water environment

Many system components will adapt directly (or indirectly) to the Marine System. These include:

- Data acquisition and pilot guidance systems,
- Magnetometer sensors,
- EMI sensor technology (but not the sensor design),
- Positioning system and attitude sensors,
- The data analysis algorithms and software,
- Output graphics and interfaces, and
- Remediation support documentation.



The R&D issues that we have addressed in preparing to build a prototype include:

- What is the most practical design for the sensor platform?
An “airfoil wing” towed by a cable.
- Can both magnetometer and EMI arrays be fielded on one platform?
Yes, current design incorporates both arrays.
- Are there restricting positioning and control issues?
Yes, current design requires degraded, but acceptable, position accuracy.
- How do we best incorporate new marine depth, distance, and direction sensors?
Current plan calls for 3 compasses, a dual GPS system, and IMU sensors.
- Are acoustic or optical imaging sensors useful adjuncts to the magnetometer and EMI sensors?
Probably. High Resolution Sonar will be incorporated.
Laser imagers have been deselected. Probably replaced by TV.

The R&D issues, Continued

- What is the best approach for upgrading and integrating the DAS?
Decision deferred to watch Geosoft Integration with DAS.
 - How can we best use an EMI sensor?
As an adjunct to the Mag Array.
 - How does seawater affect the EMI sensor performance?
Seawater is not an issue for our Time-Domain Array.
 - Can we use the EMI sensor to detect small-shallow objects AND for classification?
We will see.
- What kind of measurements does this require us to make?
Careful common registration of Mag and EM is most important.
- What are the constraints on the EMI sensor design?
Most difficult is likely to be detection of the smallest UXO.

Sensor Platform Engineering Study
Task 1

- Carried out in conjunction with Vehicle Control Technologies, Inc.
Tom Tureaud, Kenneth Watkinson, Stacey Hills
- They were provided a set of operational requirements, performance conditions, platform dimensions, and sensor restrictions, including range of water depths, wave & wind conditions, sensor hold-off and stability requirements, and limitations on vessel speed, size & weight.
- Their work began with an engineering feasibility study to define the support vessel, establish the sensor deployment concept, and determine the hardware constraints.

Perform Design Tradeoffs, Evaluate System Design Options

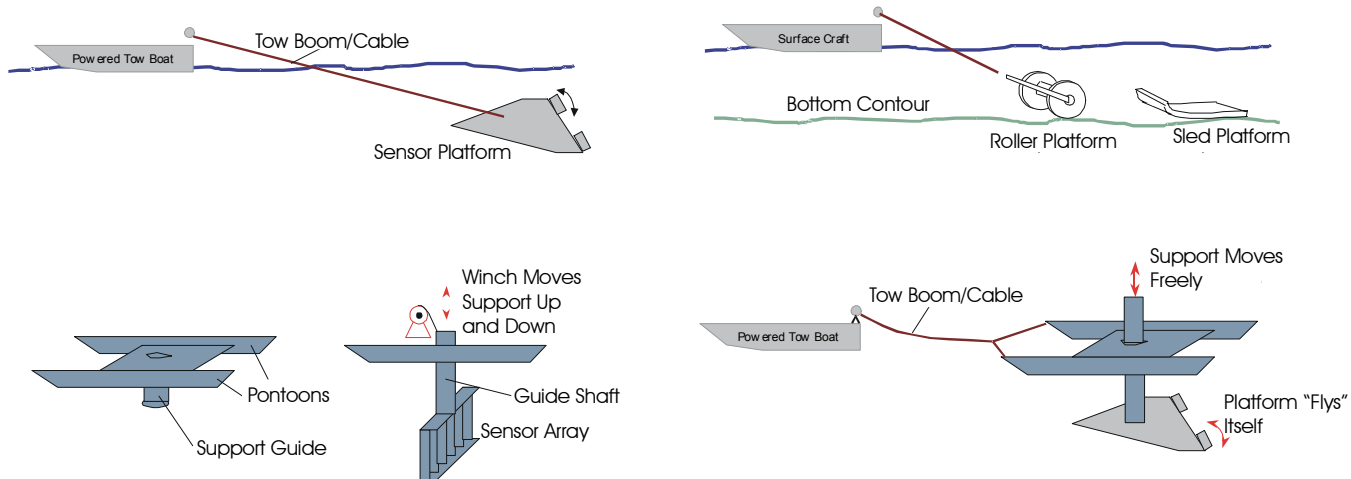
Sensor Platform

control effectors in sensor body
 winch/boom motion control
 combination topside/sensor body control

Establish Flow-Down Requirements

actuation systems, weight & trim, motion measurement
 instrumentation, control algorithms

Maintain Compatibility with Commercially-Available Components

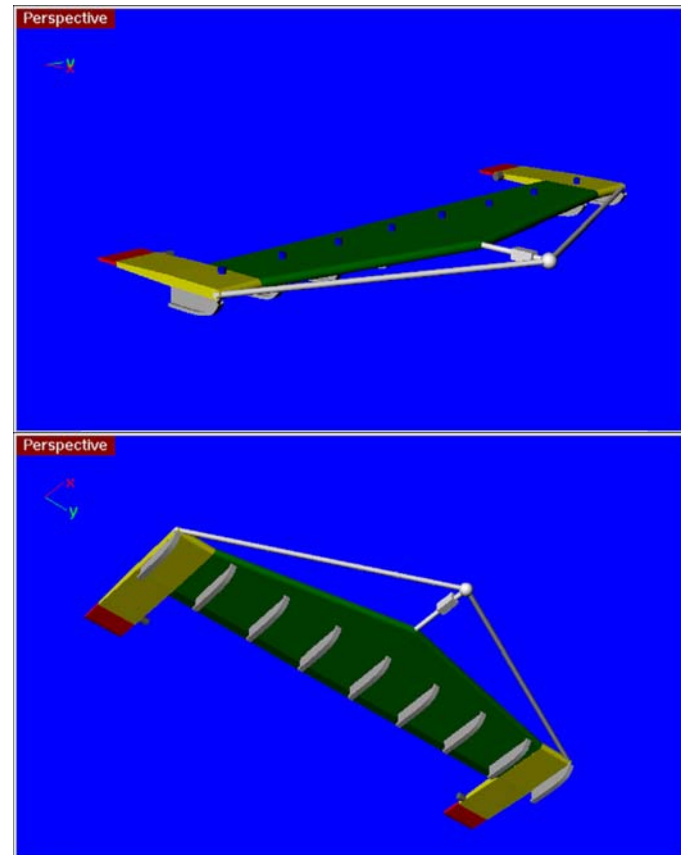


The tradeoff and down-select study converged on a cable-towed “flying” sensor platform, towed by a pontoon boat.

The platform is an airfoil, stabilized by weighted skids on the bottom, a fiberglass skin (flooded internally) with flotation to provide positive buoyancy.

Platform attitude is controlled by actuators operating two control surfaces.

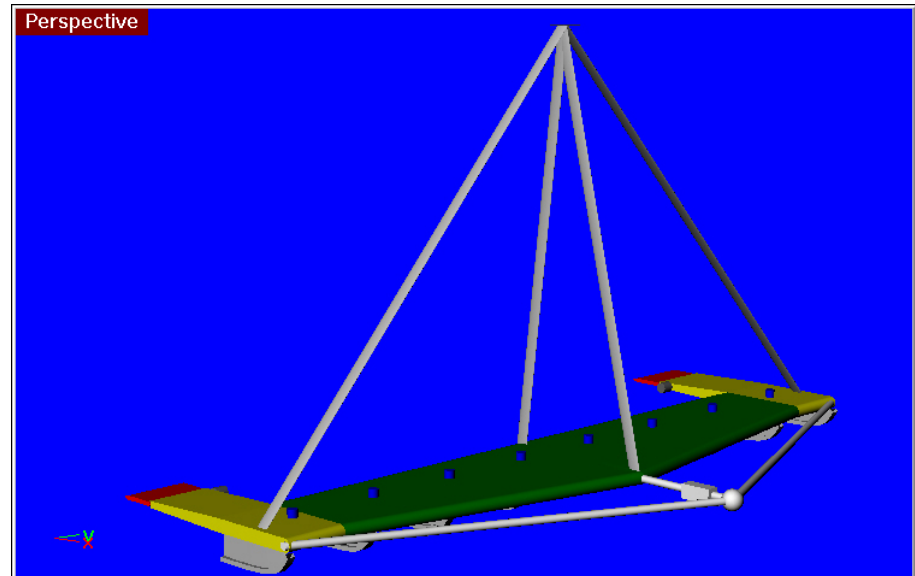
The design provides for both sensor arrays to be embedded in the airfoil.



Early versions of the sensor platform postulated using GPS, mounted on a superstructure for positioning the sensors.

This design was rejected because it was felt to be too cumbersome for operation in 15 ft of water.

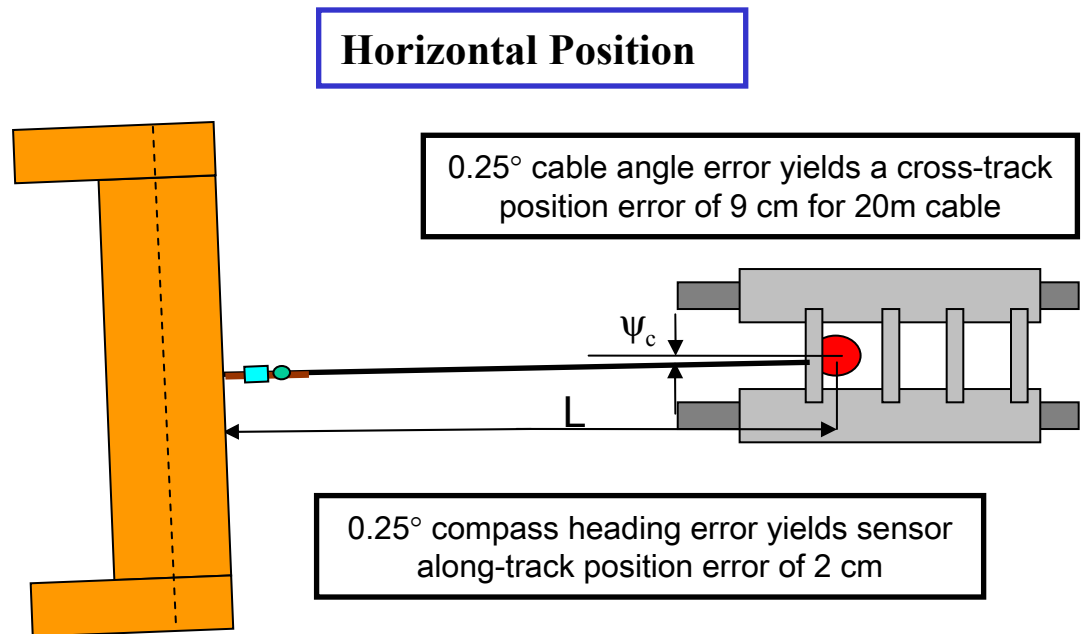
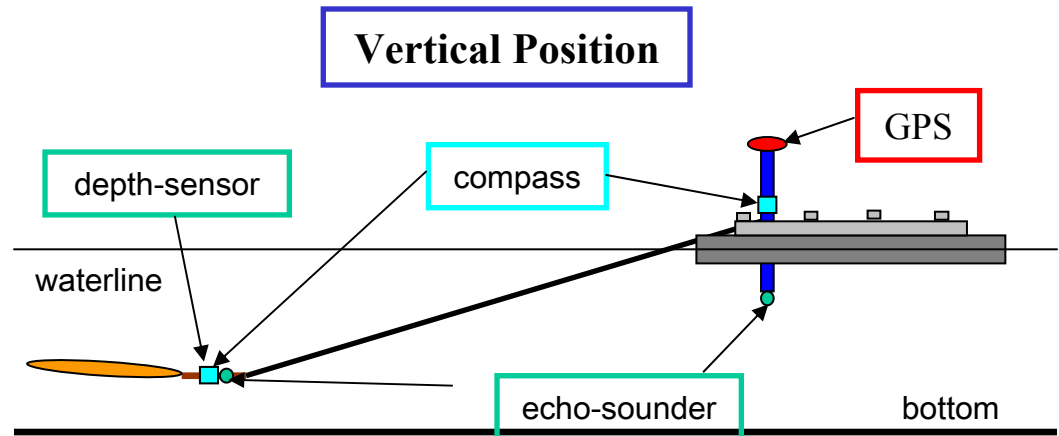
We may still choose to provide sockets for mounting poles for very shallow water surveys. Sensor location precision would be improved.



We opposed relying on GPS on the sensor platform with a super-structure that might cause instabilities and control problems.

Depth sensors, echo-sounders, digital compasses, and careful measurement of the cable angle at the boom on the boat will allow sensor positions to be referenced to the GPS antennas on the boat.

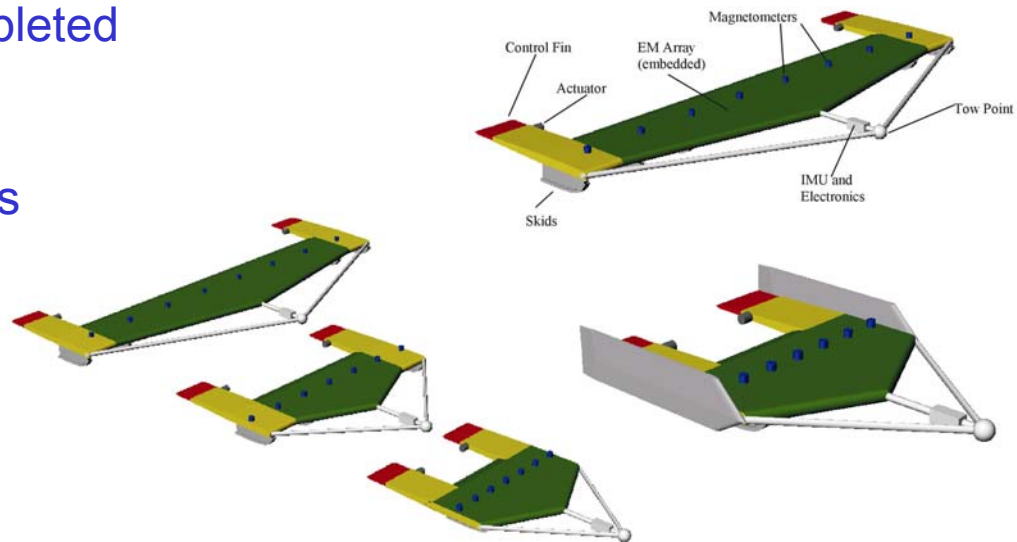
Sensor position accuracies of 10-15 cm should be possible.

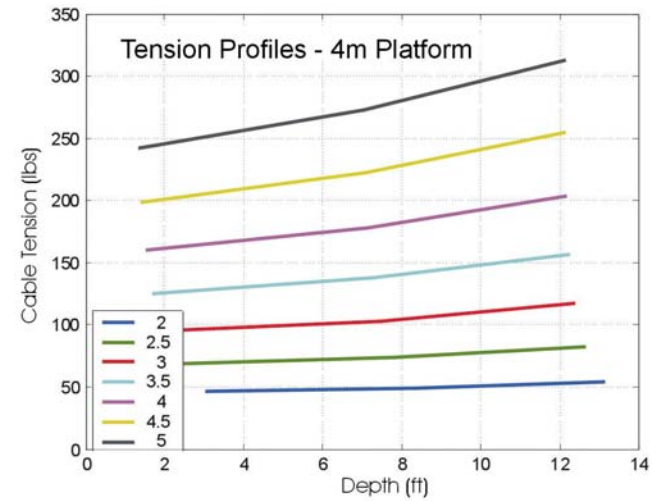
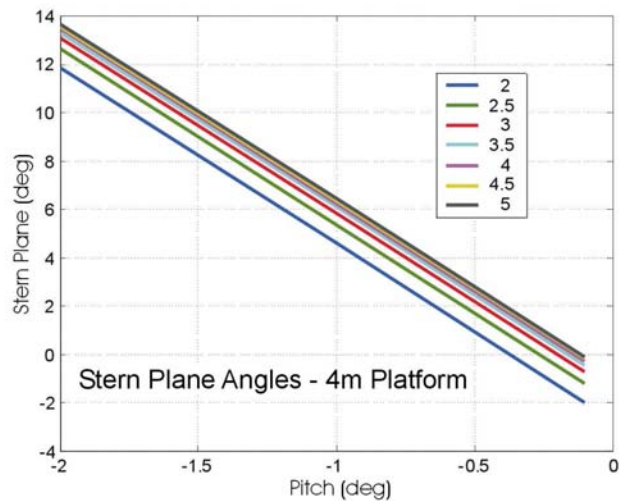
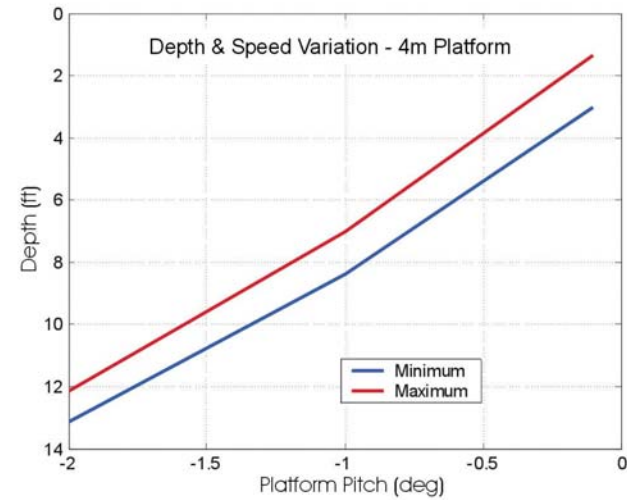
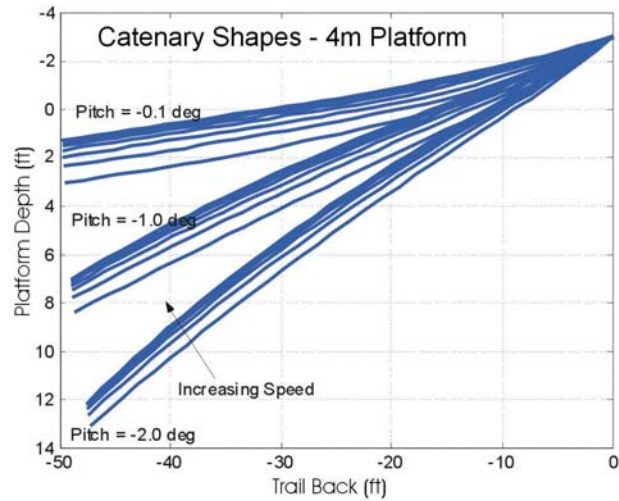


Program Office direction specified that the 10-m platform be downsized to a 4-m platform, and that provision be made to reduce to a 2-m array.

The VCT static engineering design study was redone on the two smaller platforms and the dynamic modeling study was completed for all three platforms.

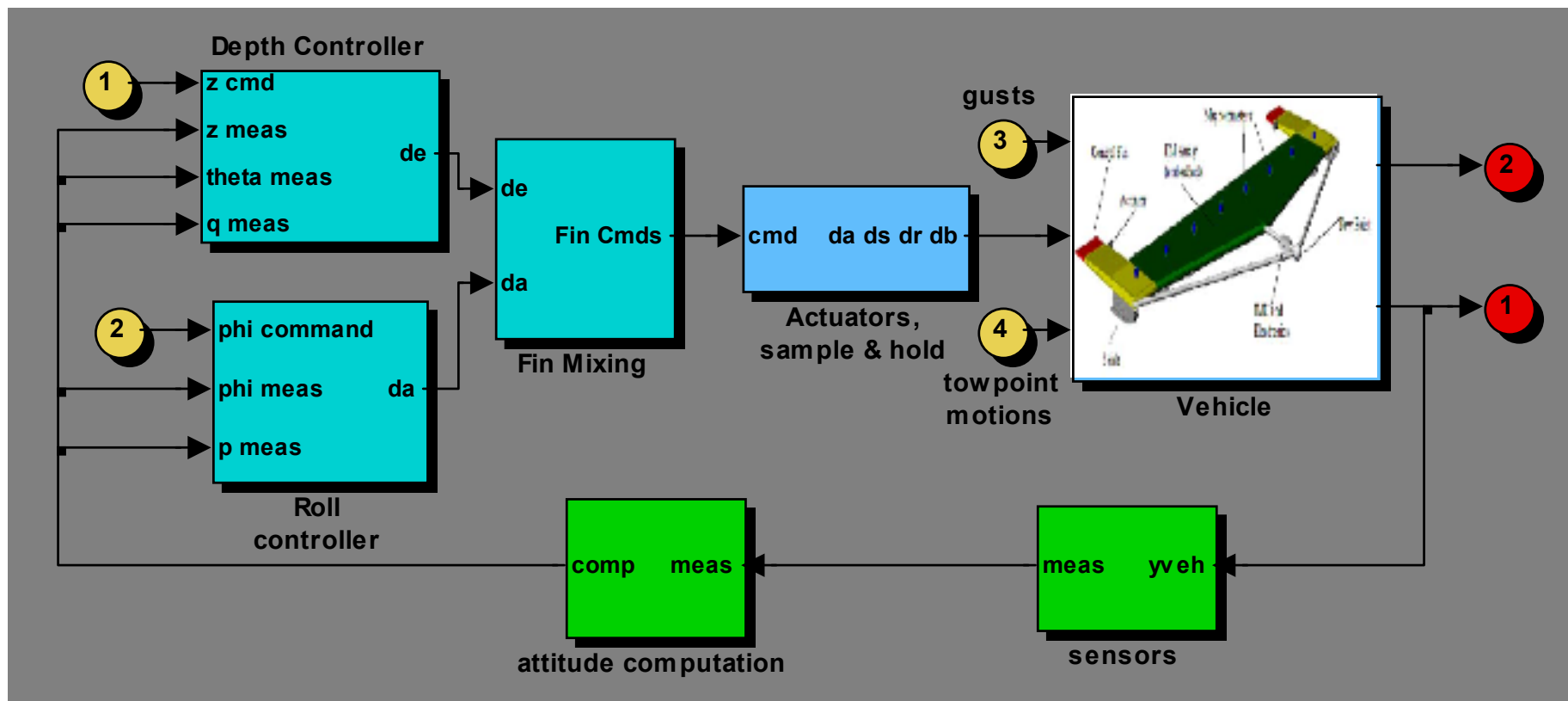
Major component features were retained. The horizontal array dimensions were shrunk.



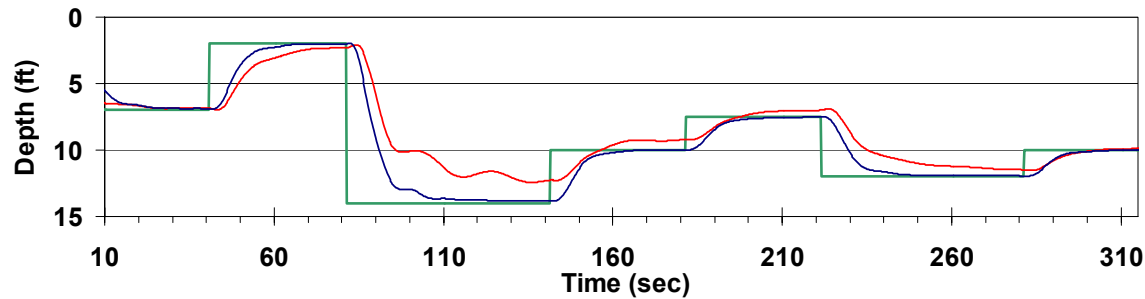


VCT Also Developed and Delivered an Autopilot

- Goals
 - Altitude (depth) & roll control
 - Water depths of 5 – 15 feet
 - Speeds from 2 – 5 knots
 - Cable lengths from 30 – 70 feet
 - Minimized the actuator duty cycle
 - Robust to seaway and tow-point motion
- Computation
 - 2 Hz update rate
 - 0.5 second sample & hold
0.1 second computational delay
 - 1 radian/second (~ 0.16 Hz) inner loop cross-over



4m Boom Depth Response (Time)

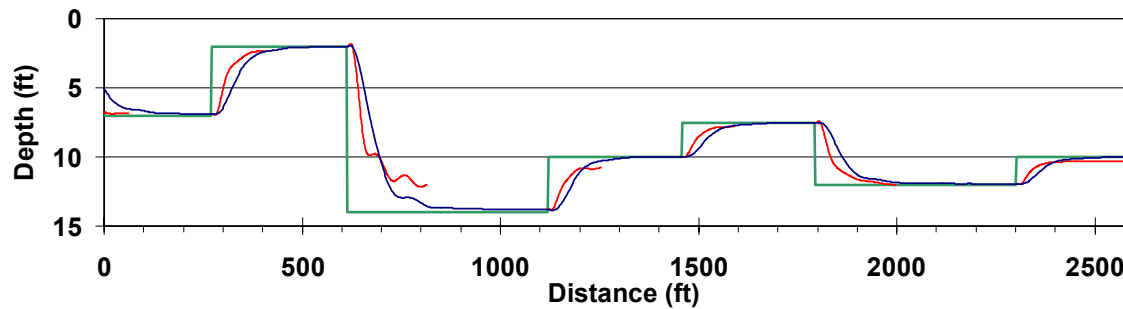


— Depth Command

— 2 kt Response

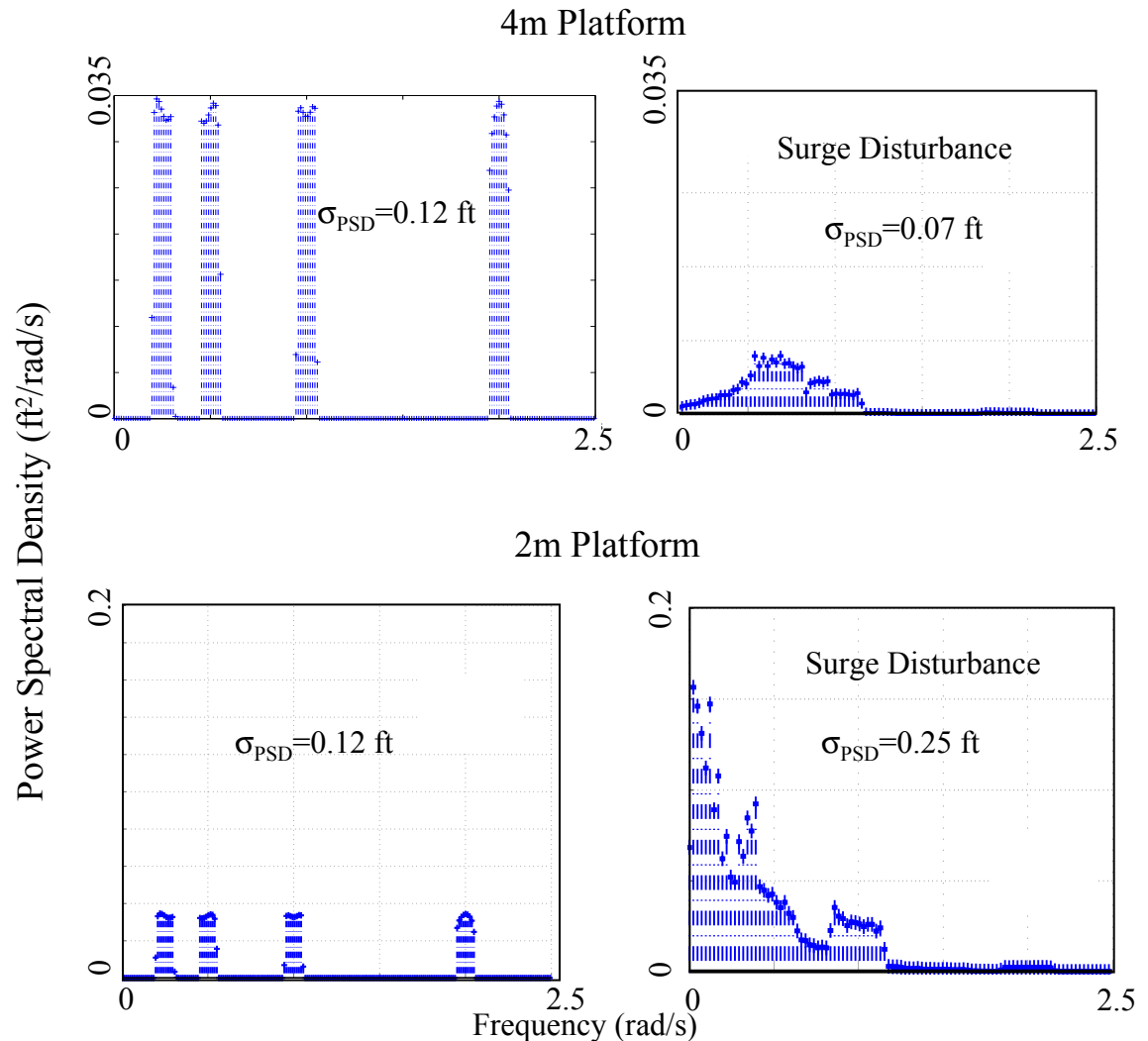
— 5 kt Response

4m Boom Depth Response (Distance)



Dynamic modeling was performed for both 4m and 2m wide platforms.

Results of the modeling show that the 2m platform is unstable using the down-selected towed-wing configuration.



Power Spectral Density (PSD) Plots :

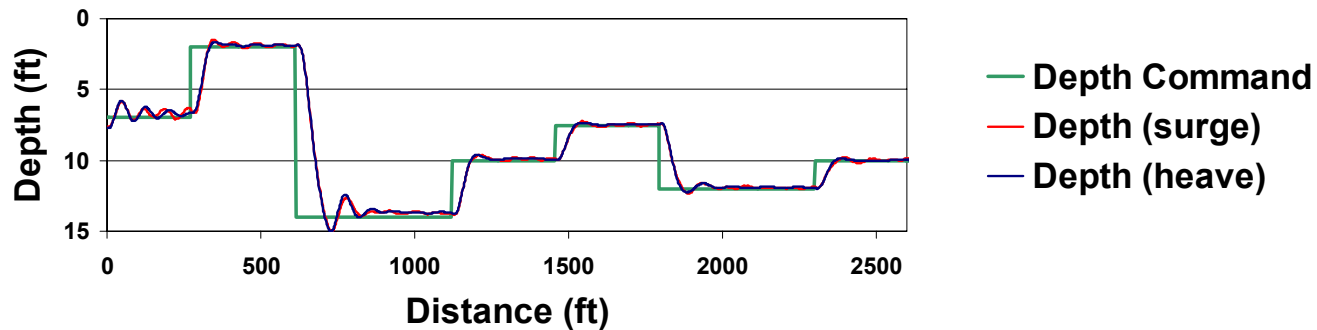
Towpoint Motion

Tow Body Motion

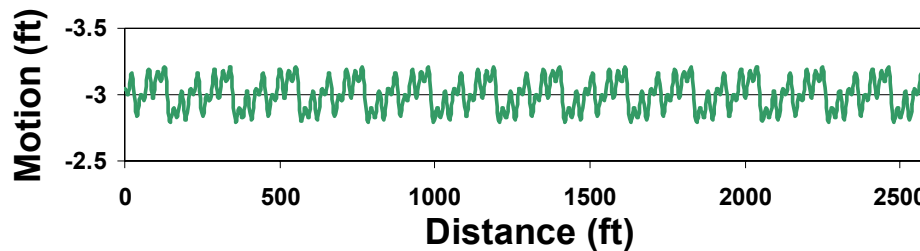
Energy = 3 x sea state 1

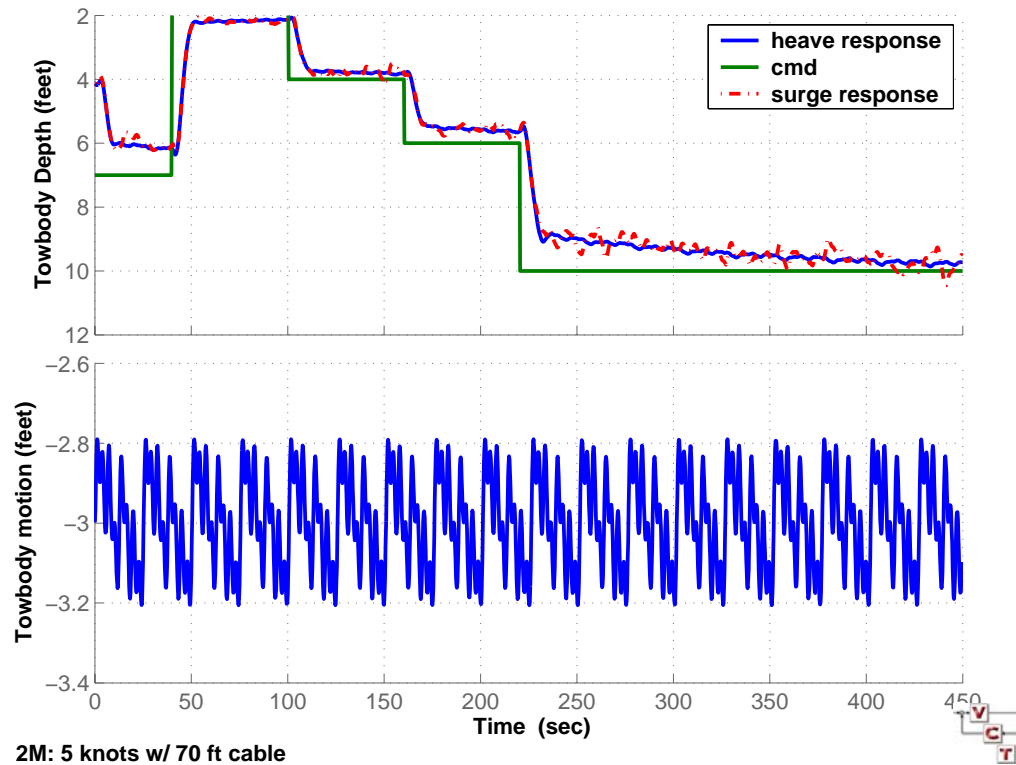
(Surge)

**4m Platform Depth Response
with Tow-point Motion (speed = 5 kt)**



Tow-point Heave/Surge Input



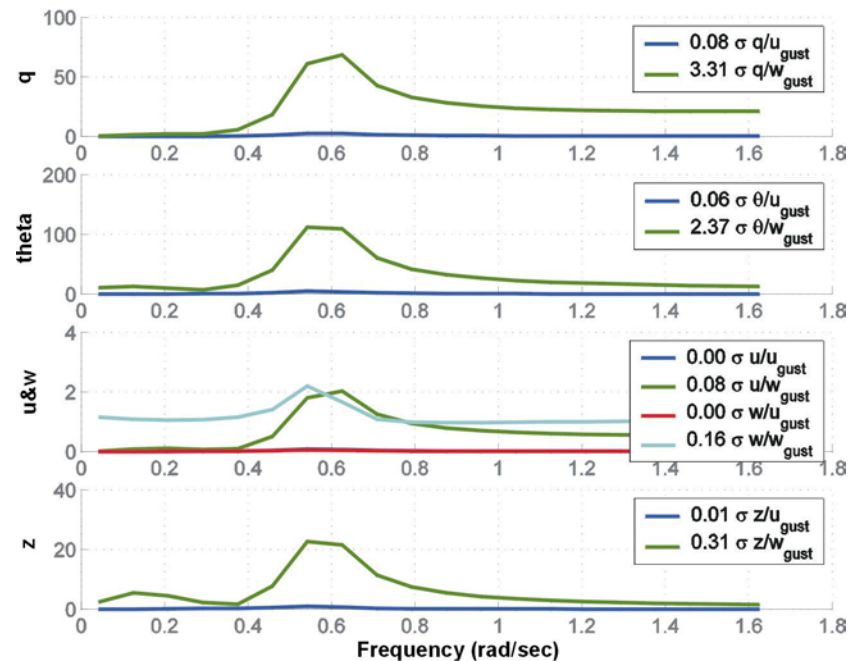


Towpoint depth response & towpoint heave/surge input 2M configuration @ 5 knots

An additional dynamic study was done to consider vertical platform response to specific seaway motions, i.e. a vertical pressure surge arriving from the rear quarter.

The conclusion is that there is no concern for surveys in sea state 1, and no concern for the system integrity in sea state 2.

Platform Depth = 4 ft, Bottom Depth = 7 ft, Sea State = 2



Vehicle Response to Seaway Motion at a Speed of 4 knots, and a Depth of 4 ft

| Sea State | Standard deviation | | |
|-----------|--------------------|-----------------|-----------------------------|
| | Depth (ft) | Pitch (degrees) | Pitch rate (degrees/second) |
| 1 | 0.03 | 0.22 | 0.31 |
| 2 | 0.31 | 2.37 | 3.31 |

w_{gust} = vertical component of the water velocity (ft/sec)

theta = platform pitch angle (deg)

q = platform pitch rate (deg/sec)

z = vehicle depth (ft)

u = forward velocity of platform (ft/sec)

w = vertical velocity of platform (ft/sec)

σ = standard deviation over a survey leg

- 4M design is more robust than 2M with respect to
 - Towpoint motions and altitude control
- Low speeds are less robust for both configurations
 - Recommend maintaining speeds close to 5 knots
- Slow update rate limits
 - altitude keeping ability
- Kiting is not a controllability issue
 - Vehicle predictably kites with cross current
- Roll control
 - Roll control is marginally stable at low speeds
 - Recommend permanently zeroing the roll command

- The EMI Sensor provides unique capabilities:

They are more sensitive to small shallowly-buried objects and non-ferrous targets, and less sensitive to geological interference.

The EMI target signature contains shape information that can potentially be used for classification decisions,

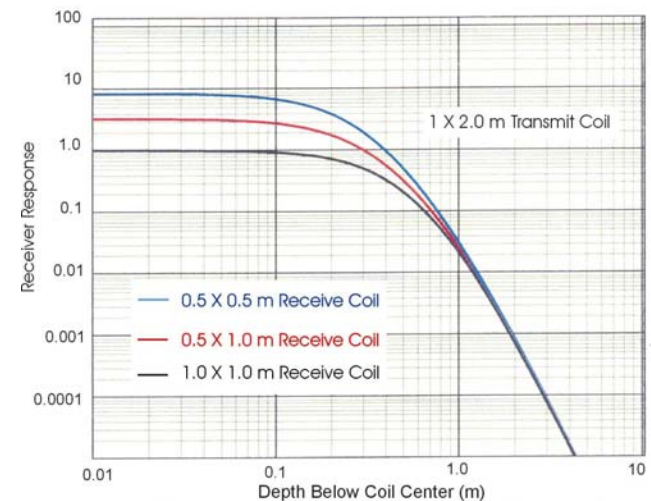
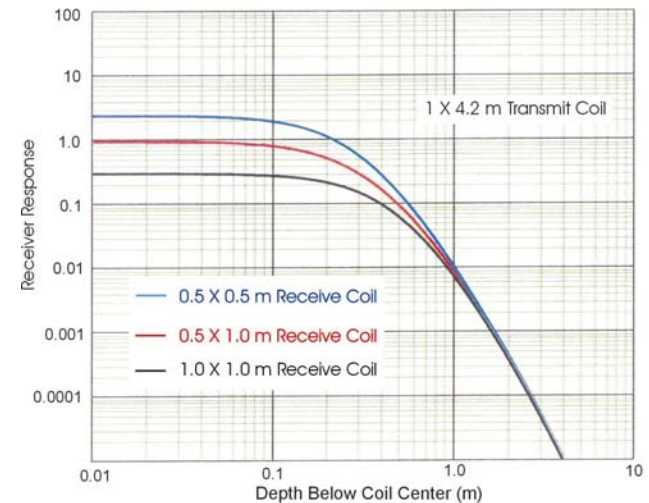
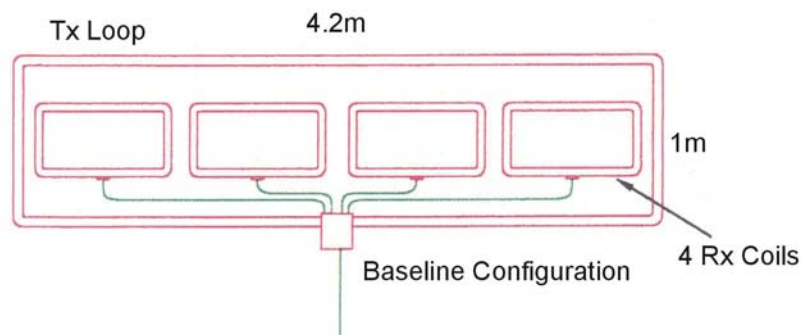
- AETC conducted EMI modeling studies to predict sensor performance in seawater relative to in air. **Reported at IPR.**
- Geonics/AETC conducted EMI modeling studies to consider sediment effects and the interaction of specific EMI design features with sensor performance. **Reported at IPR.**

Studies carried out with Miro Bosnar at Geonics addressed several issues:

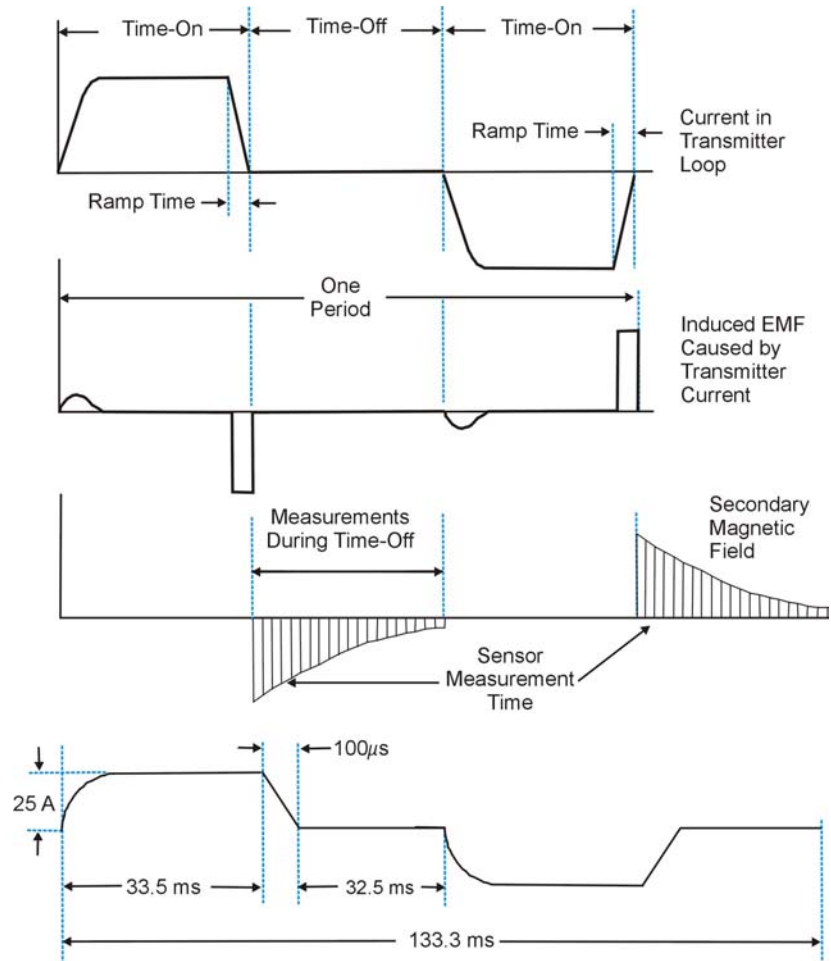
- ❖ EMI Array Design Concepts
 - Transmitter and Receiver Configurations
 - Sensor Performance Parametric Modeling
- ❖ Target Response
 - Numerical Modeling &
 - Experimental Modeling
- ❖ Mechanical Component Preliminary Design

Several different EMI array designs were considered.

Studies began by modeling the transmit energy and receiver coil sensitivity assuming a small plate-like target directly below the receive coil.



Assuming these waveforms, signal distortions were modeled for the “Run-on Effect” (Turn-on) & Turn-off time effects within the context of a Power Law Signal Decay, Exponential Signal Decay, and using an existing analytical model for the decay of a 60-mm mortar.



$$dbH(t) = k (t - \alpha)^{-\beta} e^{-\gamma t / \gamma}$$

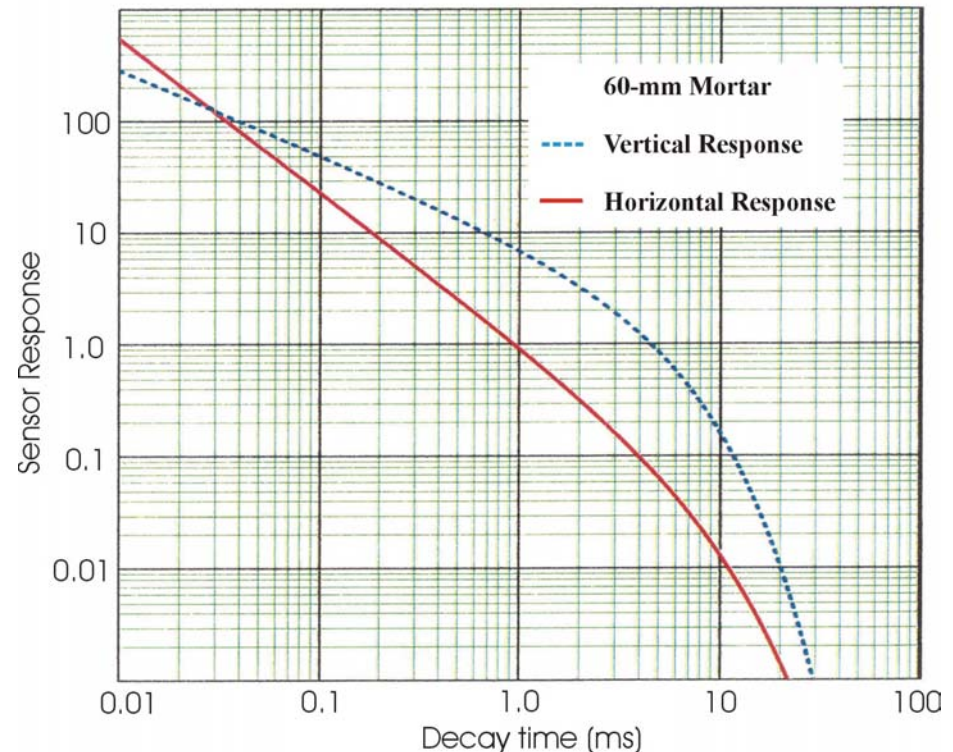
| Vertical: | Horizontal: |
|---------------------|----------------------------------|
| $k = 1.034$ | $k = 8.426$ |
| $\alpha = 0.000469$ | $\alpha = 2.127 \text{ e}^{-13}$ |
| $\beta = 1.348$ | $\beta = 0.76425$ |
| $\gamma = 7.787$ | $\gamma = 4.425$ |

The analytical expressions developed by Pasion and Oldenburg for the eddy current decay of a 60mm mortar are plotted.

All UXO signal decays begin following a power law response and slowly evolves to an exponential decay.

Behaviors are very complex, depending upon shape, orientation, wall thickness, component materials, fuzes, etc.

Small items decay faster.



Three types of signal distortions were considered in the analysis:

Run-On Effect (or Turn-On Effect)

This is a measure of the effect on a measured target response resulting from prior transmitter pulses.

Turn-Off Time Effect

This results from the finite time for the transmitter pulse to fully turn off. Turn-off time effects the bandwidth or frequency spectrum of the transmitter.

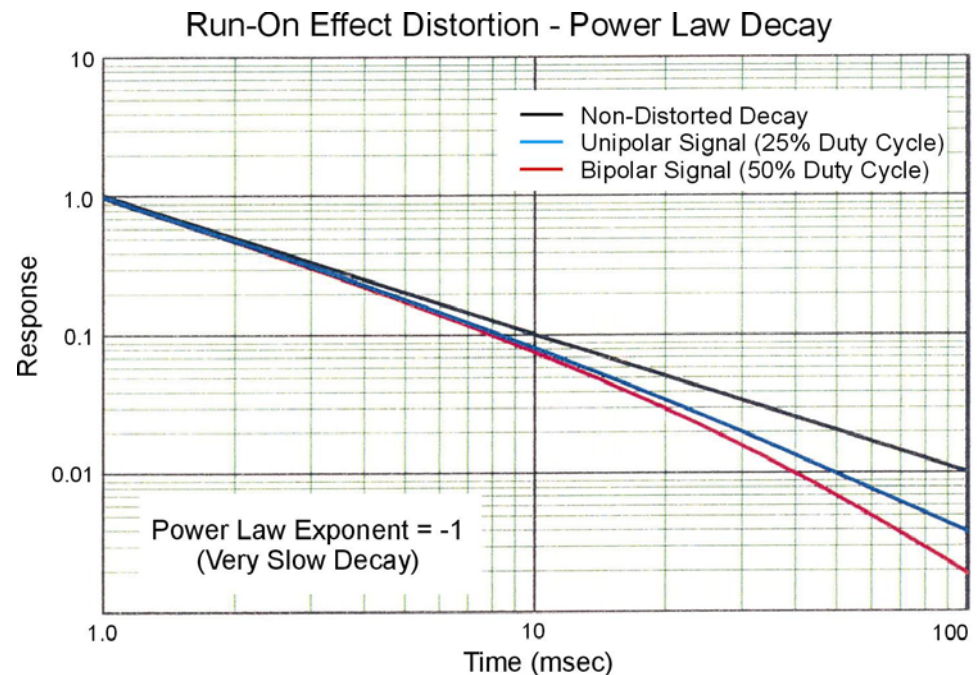
Gate Width Effects. The number and width of the detection time gate windows create signal distortions and affect the S/N of the measured signal.

All effects are predictable, requiring 2-20% (worst case) corrections.

The Run-on effect signal distortion is plotted for a very slowly decaying signal assuming a detector duty cycles of 25% and 50%.

The bipolar transmit case predicts a distortion of about 10% at 10 msec, which increases with time.

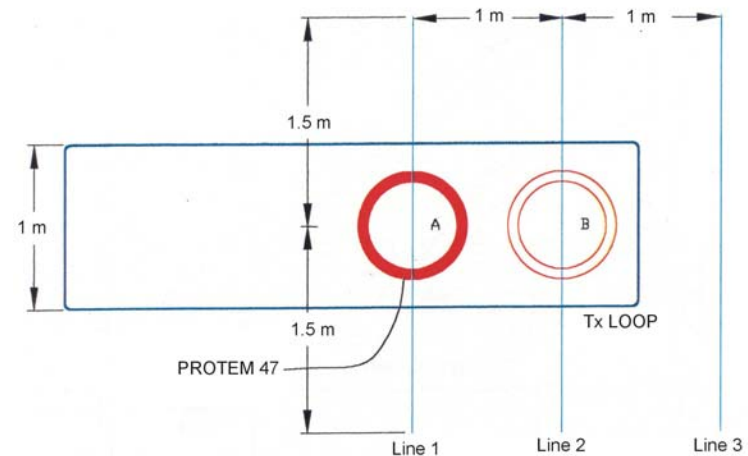
The exponential response model predicts ~20% signal distortion assuming a 20 msec decay constant, which is independent of the measurement time.



The 4-m (4-turn) loop was used, elevated 1.0 & 1.5 m above the test UXO placed on the surface. Two transmitters were used, Protem 47, battery operated, 300Hz; and Protem 57, medium power, 30 Hz .

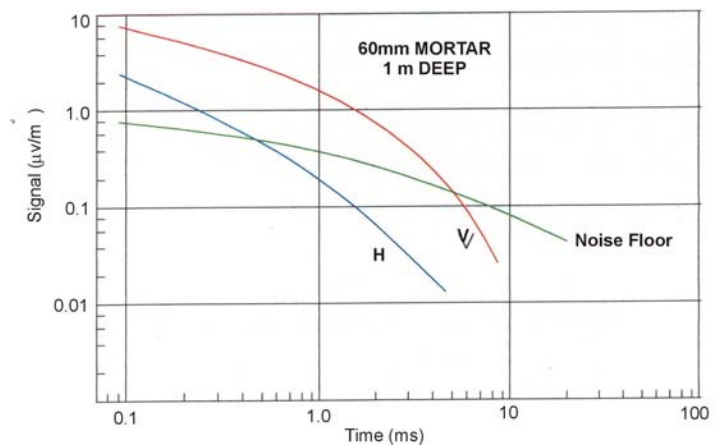
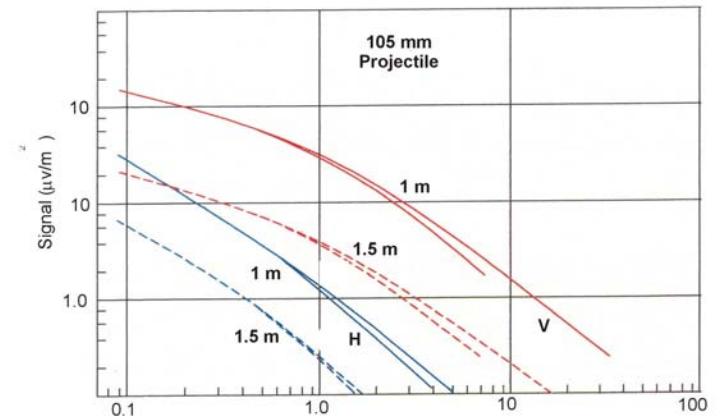
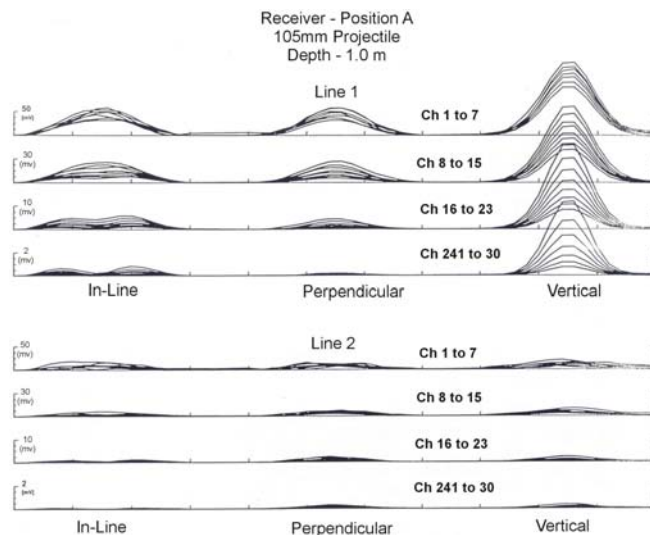
The modified PROTEM 47, (0.6 m, 700 kHz bandwidth) was used as a receiver in 2 different positions (A & B)

Measurements were made moving the UXO (in 20 cm increments) along Line 1, Line 2, & Line 3



Signals from the 60mm were too small to fully characterize the response.

Data from both UXO provide information necessary to establish the preliminary requirements for both the transmitter coil and the receiver coils designs and to confidently use the modeling predictions to develop a system design.



- The predictions from the EMI modeling programs correlated with the experimental measurements, will be used to develop the EMI system preliminary design.
- Geonics has begun Phase II of their development program.
- The results will form the basis for the EM system transitioning to the prototype construction phase in the follow-on program.

The final EMI design will not be frozen until after the design work is completed by the fabricator.

Magnetometers

Two Geometrics 822 Magnetometers in water-tight marine housings and a Maglog DAQ interface have been Ordered. They will be used to evaluate component performance and interfaces.

The sensors will be ultimately be incorporated into the Magnetometer Array.



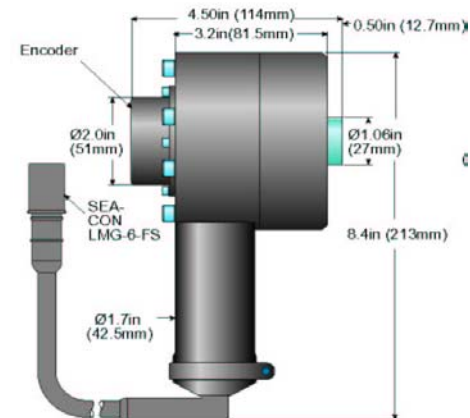
Actuators must:

- Generate 15 lb-ft torque,
- Operate on a 25% duty cycle,
- Generate minimal interference for the Magnetometers, and
- Operate from water-tight vessels.

SeaNet Electric Rotary Actuator



- Compact, lightweight & precise
- 6,500 meter depth rating
- High output-to-weight ratio (60 Nm, 45 lb-ft)
- Position, velocity and torque control
- Used in multiple applications, including camera pan & tilt unit, linear actuator assemblies, and ball valve actuation



Output
 60 ft-lbs (80nm)
 0-90° / sec @ 1.5A
 0-45° / sec @ 1.0A

Input
 150 VDC Power
 Power ground
 +/-5 V speed command
 12V instru. power
 Signal ground

Tecnadyne Model 60 Actuator

Based upon performance, the choice was clear, We have ordered these units.

We will build housings for them.



Precision Navigation, Inc
Model: PNI TCM 2-20

Accuracy = 0.5°
Resolution = 0.1°
Readout = 30 Hz

We have had mixed results with IMUs with both the hand-held sensors and the vehicular platforms.

It is important that we get it right this time.
An acceptable solution is likely to be expensive.



Grumman: Model IMU-200

| Inertial Measurement Units (IMU) | | | | | | | |
|----------------------------------|---------|-------------|------------|---------|---------|----------|-------------|
| MFG | MODEL | VSUPPLY | O/P TYPE | WT (kg) | TEMP | DRIFT/HR | PRICE (\$K) |
| HONEYWELL | HG1700 | +5,+/-15VDC | SDLC RS422 | 0.9 | -54+85C | 1 DEG | 18 |
| HONEYWELL | | | | | | 2 DEG | 13 |
| HONEYWELL | | | | | | 3 DEG | 11 |
| HONEYWELL | | | | | | 10 DEG | 8 |
| NRTHRP GRUMMAN | TRF 90 | 3.3,15,+/-5 | RS485 | 0.4 | -40+71C | 2.0 DEG | 10 |
| NRTHRP GRUMMAN | IMU 200 | 5,+/-15 | RS422 | 1.4 | 0+50C | 0.1 DEG | 65 |
| NRTHRP GRUMMAN | IMU 600 | +/-5,+/-15 | RS485 | 1.5 | -40+70C | 0.01 DEG | 120 |



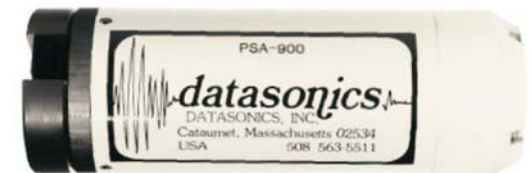
Honeywell: Model 1700 IMU

Depth sounders will be used to:

- Measure the sensor platform height above the bottom, and
- Measure the tow vessel (GPS) height above the bottom.



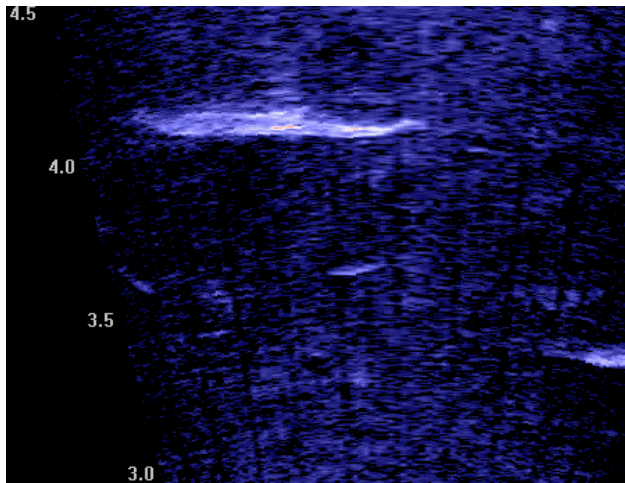
Bathy 1500MBLK



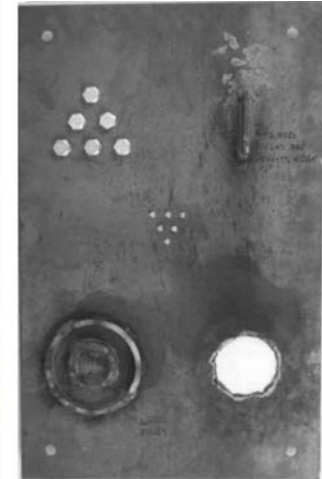
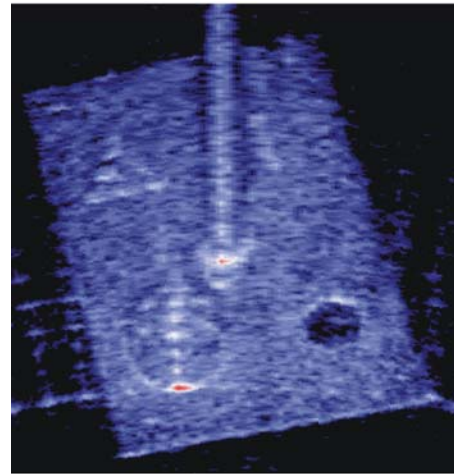
Datasonics PSA-900

| DEPTH SOUNDERS | | | | | | | | | | |
|----------------|-----------|---------------|-----------------|----------------|---------------|------------|-----------|----------|-----------|-------|
| MFG | MODEL | Accuracy (cm) | Resolution (cm) | Supply Voltage | Current (amp) | Beam (deg) | Rate (Hz) | Wt. (kg) | Range (m) | Price |
| O D E | BATHY1500 | +/-2.5 | 1 | 115 AC | 0.5 | 3 | 18 | 10.7 | 0-5 | |
| BENTHOS | PSA-900 | | 1 | 15-28 DC | 0.1 | 8 | 10 | 3.2 | 0.3-30 | |
| BENTHOS | PSA-916 | | 1 | 7-24 DC | 0.1 | 14 | 5 | 0.7 | 100 | |

- High-frequency imaging sonar will provide both classification information for proud objects and a bottom imaging.
- These instruments, which effectively operate as cameras are commercially available.
- **We will visit APL on 13 August** to learn more about the DIDSON instrument; its data logging capability, and system interface options.

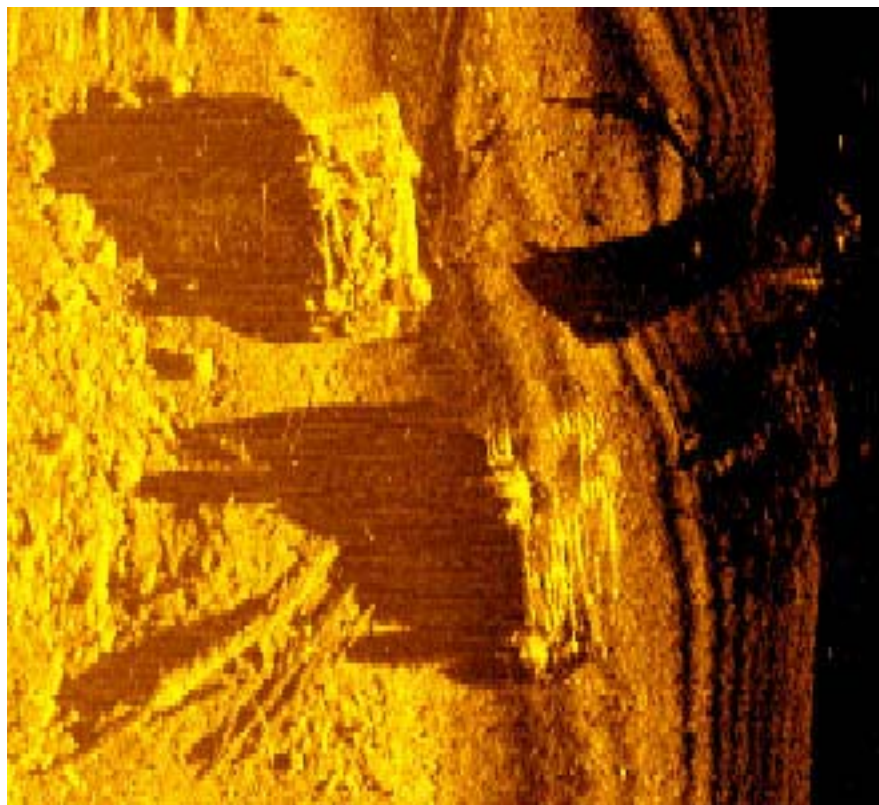


MPEG clip of a school of king salmon



DIDSON sonar (left) and photographic images of a 12X18" plate with buttons, rings and holes

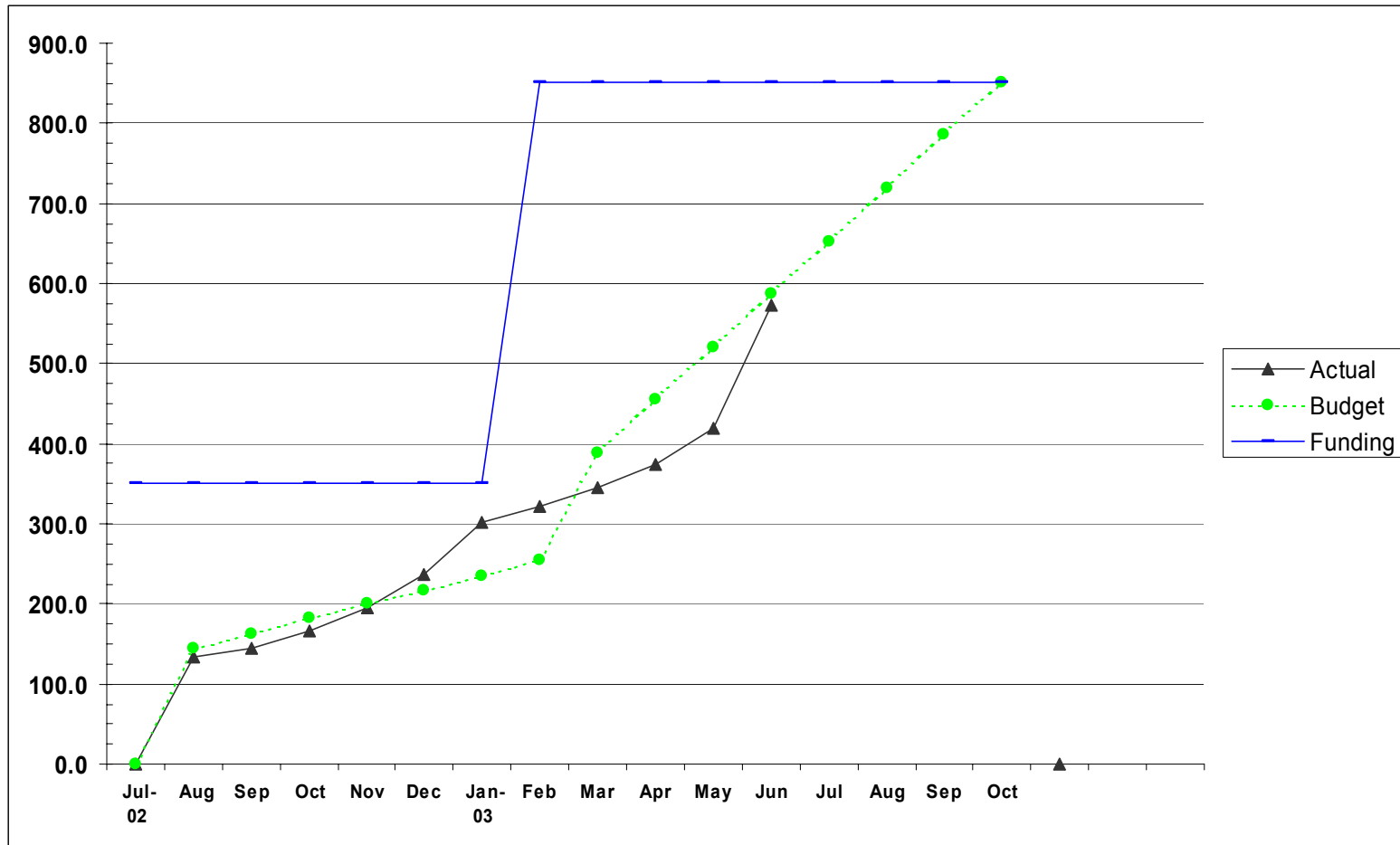
Marine Sonics, Inc.
Sea Scan
Side Scan Sonar



1200 kHz Image of two automobiles in
The Arkansas River.

| Marine Engineering and Fabrication Firms | | | | | | | | |
|---|------------------|------------------------------------|------------------------------------|-----------------------------------|------------------------|----------------------|----------------------|-------------|
| FIRM | Location | Materials Experience | Marine Experience | Customers | Hand Layup | In-House Engineering | COMMENTS | PRICE (ROM) |
| Advanced Technologies Inc. | Newport News, VA | KV,C,FG | YES | Boeing, NASA, Navy | YES | YES | Site Visit Completed | ~\$250K |
| Phoenix International | Annapolis, MD | Fiber Composites Matl. Development | YES | Navy & Marine Systems | NO | YES | Site Visit 7/24 | |
| Structural Composites Inc | Melborne, FL | KV,C,FG | YES | Navy DARPA/Maritech Race Boats | YES | YES | | ~\$121K |
| Advanced Composites Engineering | Temecula, CA | KV,C,FG | Aircraft & Auto Components | | YES | YES | | ~\$120K |
| Carbon Fiber Manufacturing | Charlston, SC | KV,C,FG | Auto Bodies Aircraft Components | | YES | YES | | |
| Mitech Systems | Columbus,OH | KV,C,FG | ROV Components | | Prototype & Model Shop | YES | Sketchy Info | |

| Task Number | FY-2002 | FY-2003 |
|---|---------|---------|
| | \$K | \$K |
| 1. Sensor Platforms | 161 | 176 |
| 2. EMI Sensor Modeling | 150 | 125 |
| 3. EMI Sensor Design | 40 | 135 |
| 4a. High-Frequency Sonar | 0 | 20 |
| 4b. Bottom Penetrating Sonar | 0 | 25 |
| 5. Optical System Demonstration | 0 | 20 |
| Total Budgeted | 351 | 501 |
| Total Expended (as of 6/30/2003) | 351 | 221.1 |



- Marine Platform Engineering Feasibility Study
Completed
- Magnetometer Array Preliminary Engineering Design Plan
- EM Array Platform Preliminary Engineering Design Plan
Single Platform - Completed
- EM Sensor Performance Modeling Study
AETC & Geonics Studies - Completed
- Sensor Platform Build-to Design
Follows Preliminary Component Design Review, and
Subcontract to Engineering Construction Firm
- Complete EMI Preliminary Design
- Specify High Frequency Sonar
- Specify An Optical Imaging Adjunct (**TV cameras and VCR**)

We anticipate that all major components of this program will be completed in early August.

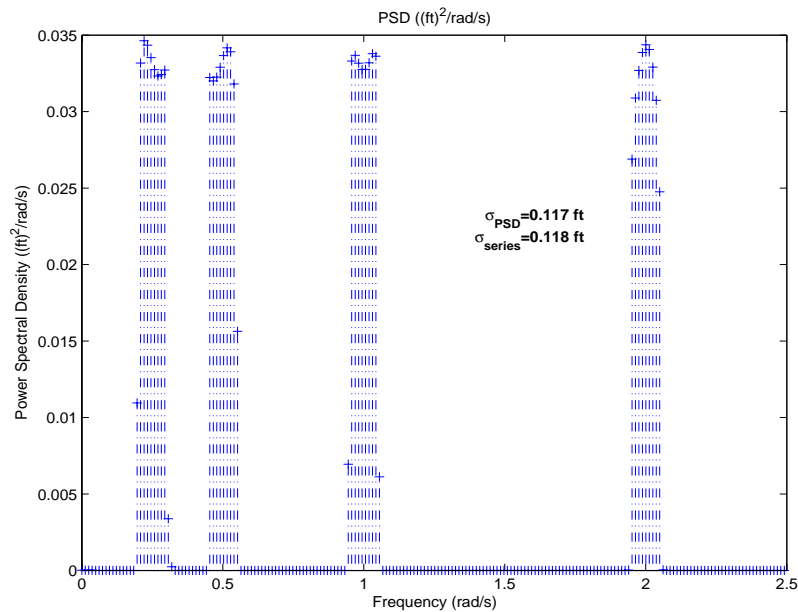
Successful completion will form the basis for transition to the ESTCP Demonstration/Validation Project.

The remaining funds in the SERDP program will be used to draft the final report and prepare for the Partners Symposium.

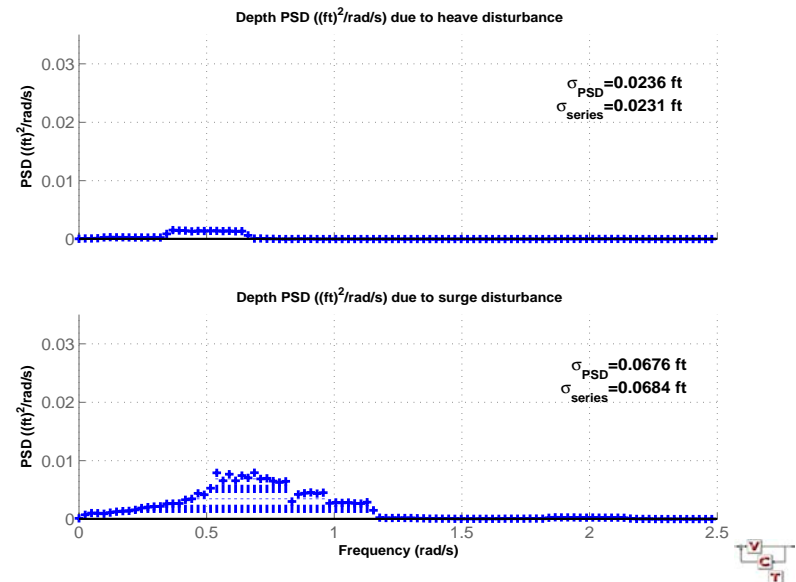
Backup Vugraphs

To create a stable survey system we must address sensor performance questions, platform engineering design approaches, and deployment issues

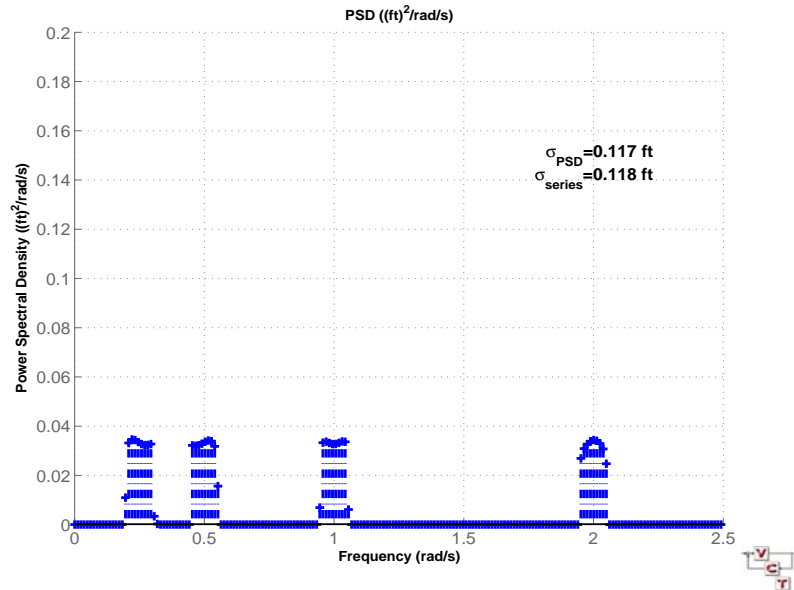
- The array platform must be stable and maneuverable to maintain a constant height above the bottom, decoupled from the vessel motions
- We must have sensitivity to detect all UXO, and
- To minimize recovery expenses, target classification is an important issue



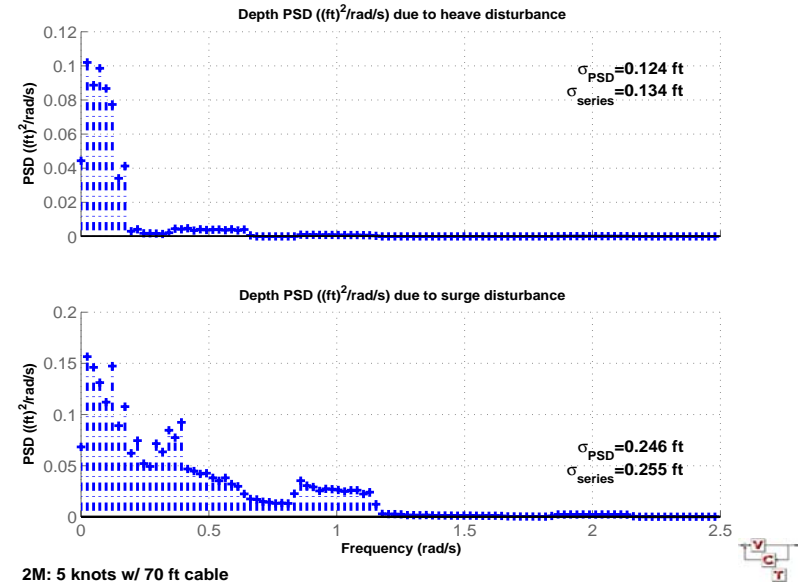
PSD of towpoint motion.
Energy is triple that of sea state 1



PSD of towbody depth @ 5 knots

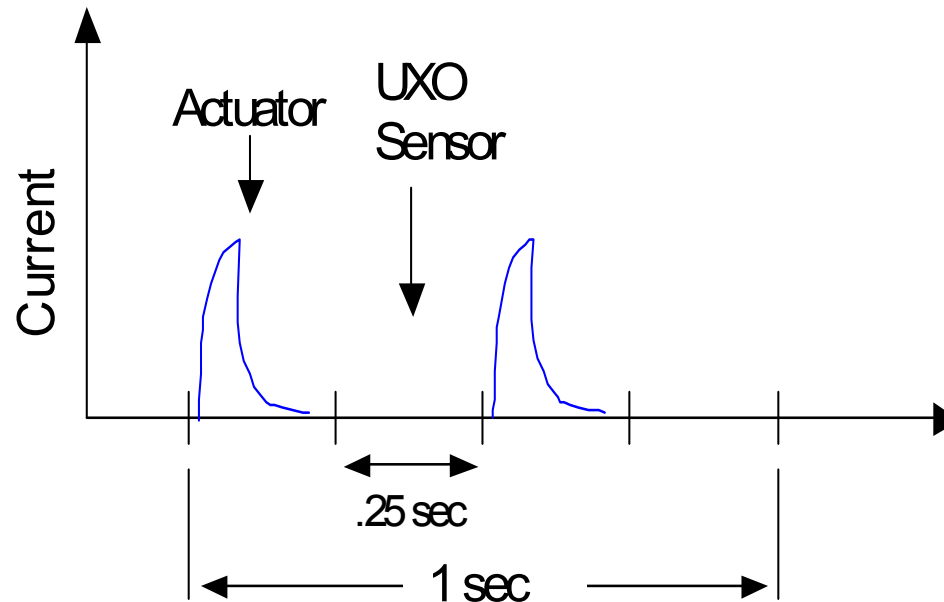


PSD of towpoint motion
Energy is triple that of sea state 1



PSD of towbody depth @ 5 knots

- Over a 1 second period the actuators will receive commands at a rate of 2 Hz, leaving a minimum of .25 seconds between commands for clean data acquisition
- Empirical testing of the magnetic and electromagnetic signature of the actuators is pending



| Gain name | Speed | | | | | |
|----------------|--|------------------------|-------------------------|------------------------|------------------------|-----------------------|
| | 1 | 2 | 3 | 4 | 5 | 6 |
| kq | 275 Gm: 6 dB Pm: 48 deg wc: 0.5 rad/s | 95 7.3 49 0.8 | 57 7.7 57 0.85 | 42 7.7 63 0.9 | 38 6.8 69 1.1 | 34 6 74 1.25 |
| kw_q_notch | 0.22 | 0.315 | 0.43 | 0.545 | 0.673 | 0.8 |
| ktheta | 110 8.8 46 | 86.45 8.6 46 | 57 10 46 | 42 12 51 | 38 12 50 | 34 12 53 |
| ktheta_i | 0 0.25 | 0 0.5 | 0 0.53 | 0 0.47 | 0 0.5 | 0 0.52 |
| zcomp | tf([1 .01],[1 .09]) | tf([1 .01],[1 .07]) | tf([1 .01],[1 .05]) | tf([1 .01],[1 .05]) | tf([1 .01],[1 .04]) | tf([1 .01],[1 .03]) |
| kz (deg/ft) | 11 8.7 45 | 4.323 11 46 | 2.4225 12 45 | 1.68 12 46 | 1.406 13 45 | 1.02 14 45 |
| kz_i | 0.22 0.1 | 0.1729 0.14 | 0.0969 0.18 | 0.0672 0.22 | 0.0562 0.25 | 0.0408 0.24 |
| kp | 66 13.8 51 1 | 19 13.4 62 1 | 10 13 70 1 | 7 13 78 1.1 | 4.6 12 58 1 | 3.8 12 61 1 |
| pcomp | 1 | 1 | 1 | 1 | tf([1 1],[1 .1]) | tf([1 1],[1 .1]) |
| kphi | 50.82 12.2 66 | 18.24 12.7 70 | 11 13 74 | 7.7 14 75 | 3.082 15 60 | 2.546 16 61 |
| kphi_i | 5.082 0.5 | 1.824 0.5 | 1.1 0.5 | 0.77 0.5 | 0.3082 0.5 | 0.2546 0.5 |

qcomp=notch*lag
lag=tf([1 .5],[1 .05])

2nd order actuators: wn=2 Hz, zeta=0.7

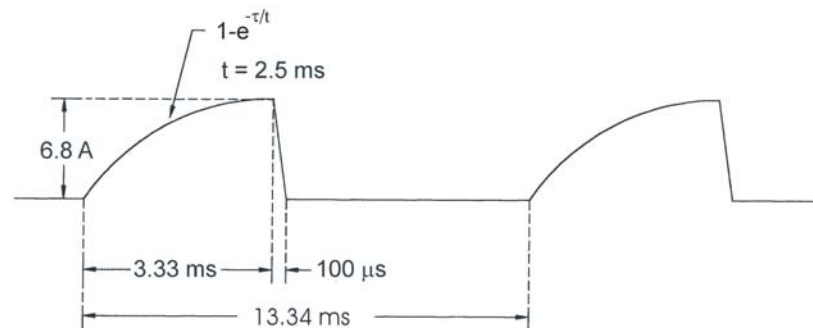
Sample rate = 2 Hz
1 dt S&H, 1/10 s delay(Pade)

Recently questions have been posed about the importance in seawater of the induced eddy currents and current channeling effects in the presence of a target when using EMI sensors.

Both in support of this project and others we have worked with Judy Soukup and Roy Jones (AETC) on the study described below.

Assumptions: The EM61-Mk2 transmit waveform, co-located transmit and receive sensors, seawater conductivity $\sigma=4.3$, permeability $\mu=\mu_0$, permittivity $\epsilon=81\epsilon_0$, targets are Fe spheres (radii=10, 20, & 80cm), $\sigma=10^7$, $\mu=100\mu_0$, $\epsilon=\epsilon_0$.

EM61-Mk2 TRANSMITTER CURRENT WAVEFORM

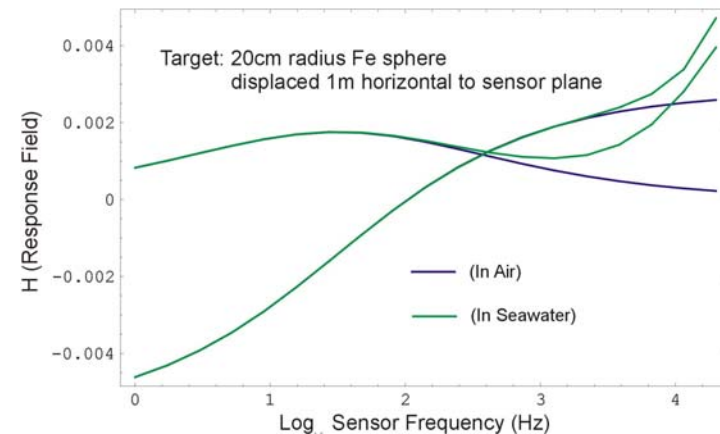
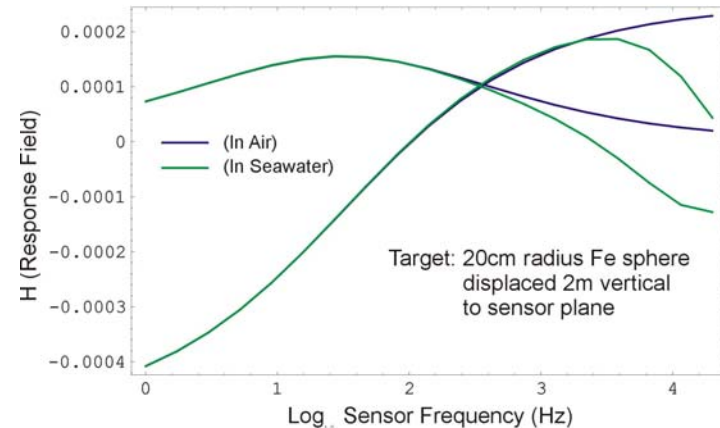


Our forward model predicts the fields in air and seawater.

The differences between seawater and air are significant only at high frequencies (>1kHz).

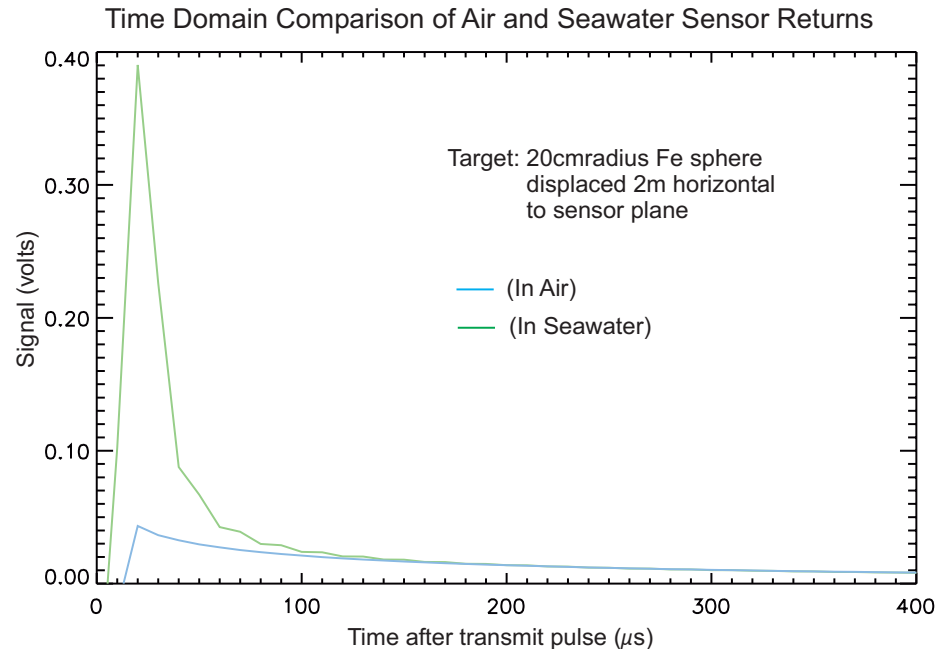
The relative increase of signal in seawater(over air) is larger for targets displaced horizontally. It also increases with distance and with target size. The high frequency response is smaller for targets vertically displaced from the sensor.

INPHASE AND QUADRATURE RESPONSE FIELDS



Convolving the transmit waveform with the response fields and taking the time derivative yields the signal versus time. The quantity measured by a time-domain instrument is the integral of the signal over a specific time gate.

The differences between seawater and air are significant only at very early times (corresponding to the high frequencies of the preceding slide). For the 80 cm sphere (2000 lb bomb), the signal in a time gate starting at 150 μs is 20% larger in seawater.



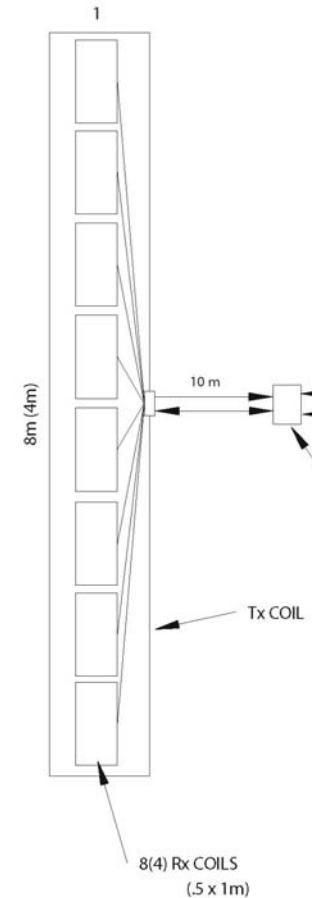
These effects may be exploitable in a frequency-domain instrument.

EMI Sensor Performance Modeling – Task 2

Priority Requirements:

The EMI Sensor Array Should

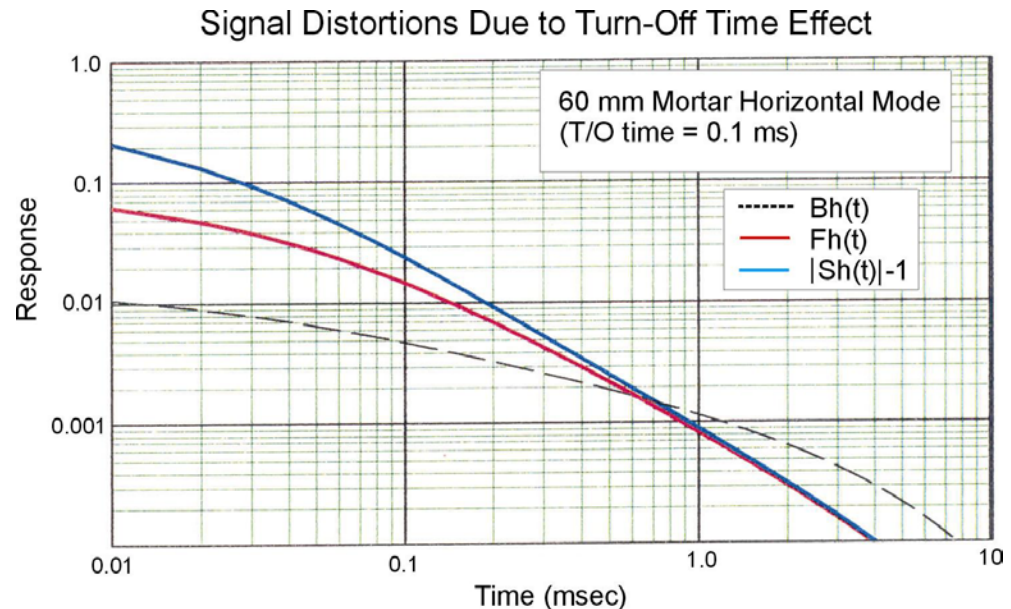
- Detect all small, shallow UXO
- Locate targets accurately
- Predict target size and depth
- Provide classification information



The signal decay of a horizontal 60mm mortar is plotted, as is the distortion due to a presumed transmitter turn-off of 0.1 msec.

The predicted error (~30% at 0.1 msec), decreases to a Negligible level at 1 msec.

The predicted errors are somewhat smaller For a vertically-oriented mortar.

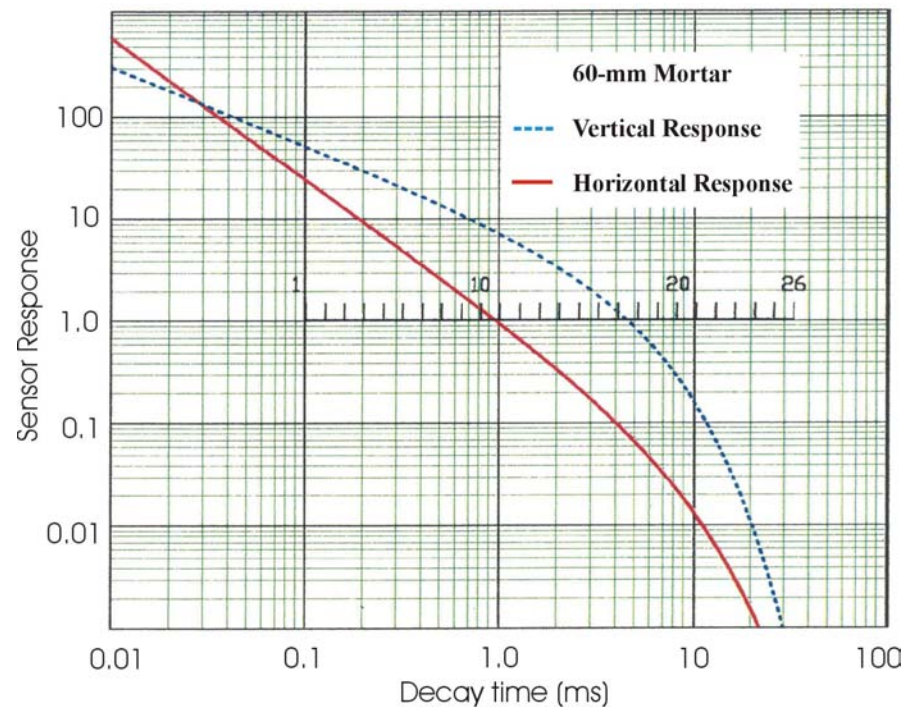


The model for the EM68 assumes 10 gates/decade of time with a gate width/gate location = 0.26.

One wants enough gates to sample the decay waveform without significantly affecting the signal/noise ratio.

This arrangement (geometric gate spacing) uniformly samples the initial power law decay.

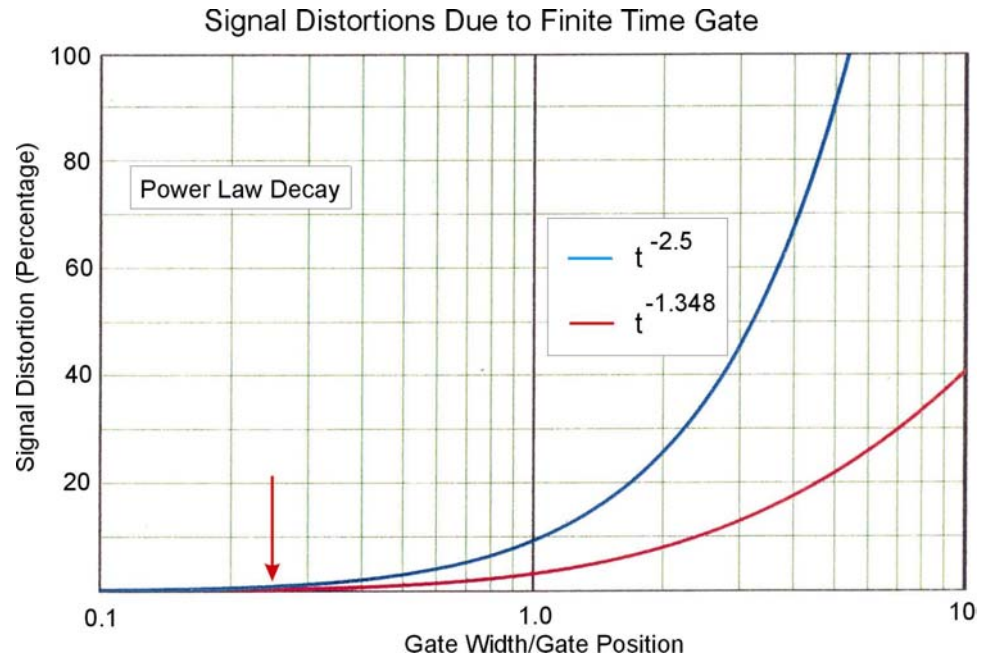
Earlier gates (narrower) have a higher noise level (but also have a higher signal level).



The model for the EM68 assumes 10 gates/decade of time with a gate width/gate location = 0.26.

The two curves in the power law presentation represent fast and slow decays

Using the proposed time gate arrangement, for even the -2.5 power law exponent, the distortion error is <2%.



Soil Conductivity Effects

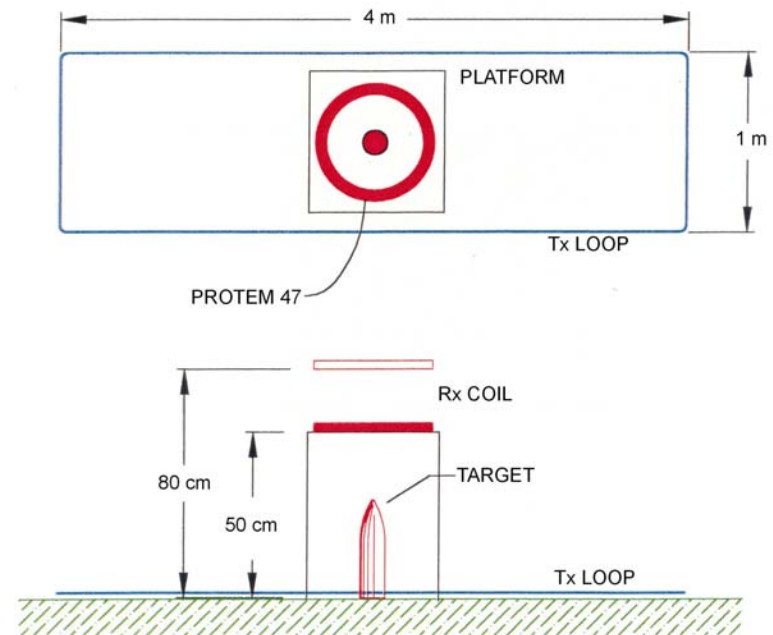
A 1 X 4 m transmit loop was set up on the ground with a modified Protem 47 coil above as a receiver.

Measurements were made 50 and 80 cm above a large and a small target.

The system was tested against widely differing soil types:

30 ohm-m

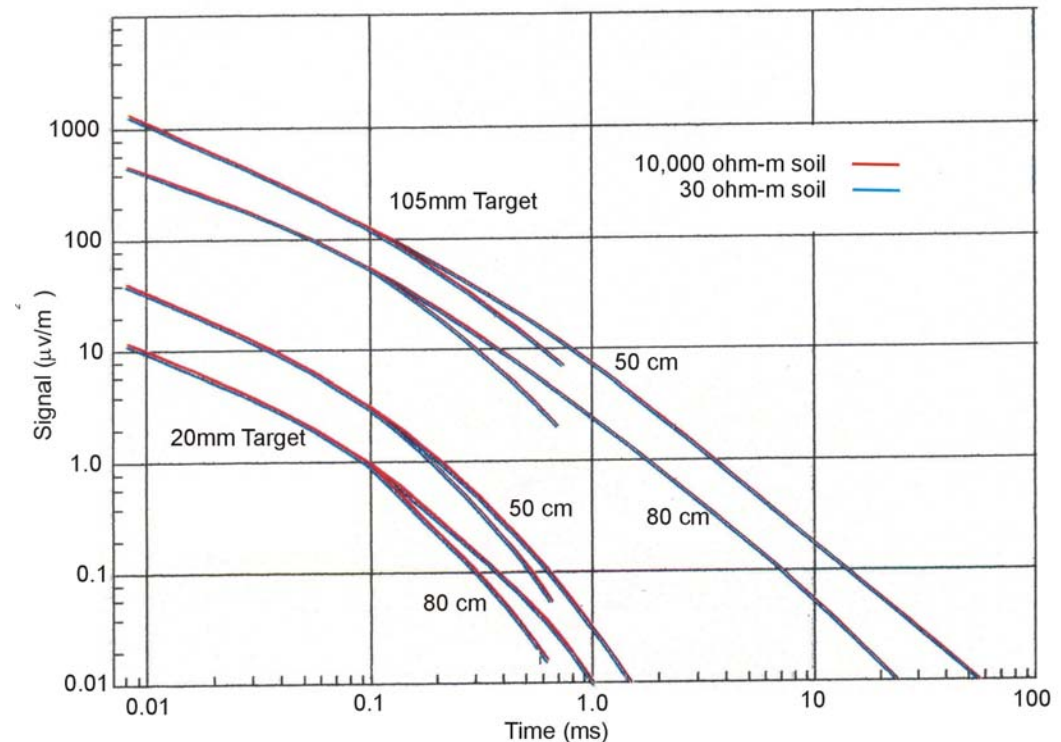
10,000 ohm-m



Soil Conductivity Effects

Measured signal returns were indistinguishable at both early and late times for both small and large targets

The shorter curves reveal run-on distortions at late times when using the 300Hz transmitter. The upper curve of each pair used a 30 Hz transmitter



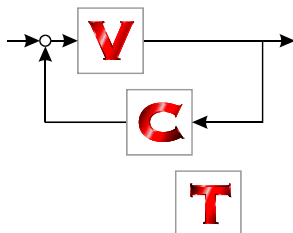
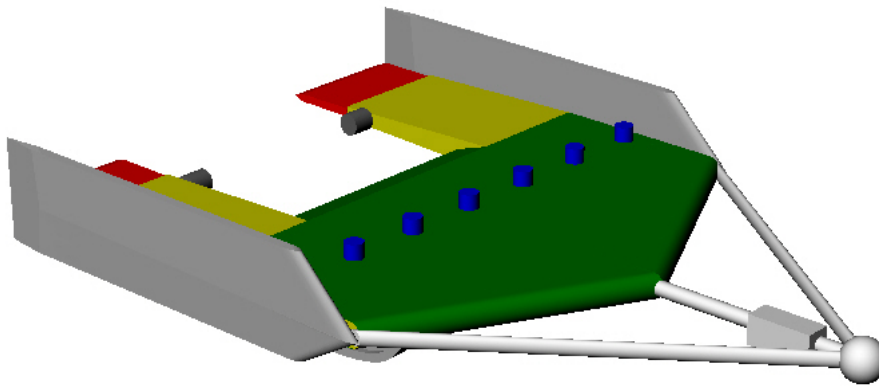
| Task | Performer | FY-2002 | | FY-2003 | | | |
|--------------------------------------|--------------|---------|---------|---------|------|---------|---------|
| | | 3rd Qtr | 4th Qtr | 1st Qtr | 2Qtr | 3rd Qtr | 4th Qtr |
| 1. Sensor Platform Dynamics | AETC/VCT | | | | | | |
| Engineering Feasibility | AETC/VCT | | | | | | |
| Mag Platform Preliminary Design | AETC/VCT | | | | | | |
| EM Platform Preliminary Design | AETC/VCT | | | | | | |
| 2. EM Sensor Performance Modeling | AETC/Geonics | | | | | | |
| 3. Time-Domain EMI Instrument Design | AETC/Geonics | | | | | | |
| 4. Sonar Target Characterization | AETC | | | | | | |
| High Frequency Sonar Imaging | AETC | | | | | | |
| Bottom-Penetrating Sonars | AETC | | | | | | |
| 5. Optical Adjunct Feasibility Study | AETC | | | | | | |
| Quarterly Web Reporting | | | | | | | |
| Annual & Final Report | | | | | | | |

VCT TECH MEMO 03-02

CONCEPT DESIGN FOR A MARINE UXO SENSOR PLATFORM AUTOPILOT FOR 2M & 4M CONCEPTS

STACY J. HILLS

THOMAS F. TUREAUD



Vehicle Control Technologies, Inc.

11180 SUNRISE VALLEY DRIVE · SUITE 350 · RESTON, VA
703-620-0703 FAX 703-620-1734 WWW.VCTINC.COM

Prepared for
AETC
Address
Address

February 2003

Under
P.O. #####

Table of Contents

| | |
|--|-----------|
| I· Introduction | I |
| 2· 2M and 4M Vehicles | 3 |
| Table 2-1 · UXO Sensors for the three platforms. | 3 |
| Geometry | 3 |
| Table 2-2 Component Comparison Chart | 4 |
| Figure 2-1 · CAPTION | 4 |
| Figure 2-2 · CAPTION | 5 |
| Figure 2-3 · CAPTION | 5 |
| Figure 2-4 · Side View of Platform | 5 |
| Figure 2-5 · CAPTION | 6 |
| Figure 2-6 · CAPTION | 6 |
| Hydrodynamics | 7 |
| 2-Meter Platform | 7 |
| 50 ft Tow Cable | 7 |
| 70 ft Tow Cable | 7 |
| Figure 2-7 · Pitch Angle, Stern Plane Angle and Tension Profile results for the 2 Meter Platform | 8 |
| Figure 2-8 · Pitch Angle, Stern Plane Angle and Tension Profile results for the 4 Meter Platform | 8 |
| Control Fin Torque | 9 |
| Wing Near-Surface Effect | 10 |
| Figure 2-9 · CAPTION | 10 |
| Figure 2-10 · CAPTION | 11 |
| 3· Autopilot Design | 13 |
| Goals | 13 |
| Characteristics | 14 |
| Duty Cycle | 14 |
| Figure 3-1 · Representation of the actuator duty cycle | 14 |
| Computational Rate | 14 |
| Hardware | 15 |
| Design | 15 |
| Figure 3-2 · Top-level autopilot block diagram | 16 |
| Figure 3-3 · Depth/pitch control loop block diagram | 16 |
| Design Challenges | 17 |
| Figure 3-4 · Change in maximum response frequency with speed | 17 |
| Figure 3-5 · Peak in pitch rate per elevator frequency response moves with speed | 18 |
| Figure 3-6 · Variable notch filter | 18 |
| Near-Surface Effects | 19 |
| Margins and Design Details | 19 |
| Figure 3-7 · 4M configuration design summary | 20 |
| Figure 3-8 · 2M configuration design summary | 20 |
| 4· Marine Vehicle Time Histories | 21 |
| Depth Profile | 21 |
| Figure 4-1 · 5 KTS (blue) and 2 KTS (red) depth keeping for configurations 4M (left) and 2M (right) | 21 |
| Altitude Profile | 22 |
| Figure 4-2 · Example of altitude profile | 22 |
| Figure 4-3 · 4M configuration altitude profile at 5 KTS (blue) and 2 KTS (red) diving (left) and climbing (right) | 23 |
| Figure 4-4 · 2M configuration altitude profile at 5 KTS (blue) and 2 KTS (red) diving (left) and climbing (right) | 23 |
| Response to Tow Point Motions | 24 |
| 4M configuration | 24 |
| Frequency Domain | 24 |
| Figure 4-5 · Open-loop vs. closed-loop depth response to tow point heave and surge, 4M configuration | 24 |
| Time Domain | 24 |
| Figure 4-6 · (a) Wave height PSD of sea state 1 at 5 KTS; (b) Boat tow point motion PSD | 25 |
| Figure 4-7 · Tow point depth response and tow point heave/surge input 4M configuration at 5 KTS | 25 |
| Figure 4-8 · (a) PSD of tow point motion; (b) PSD of towbody depth due to heave and surge, 4M configuration at 5 KTS | 26 |
| Figure 4-9 · Tow point depth response for 4M configuration at 2 KTS | 26 |
| 2M configuration | 27 |
| Frequency Domain | 27 |
| Figure 4-10 · Open-loop vs. closed-loop depth response to tow point (a) heave and (b) surge, 2M configuration | 27 |

| | |
|--|----|
| Time Domain | 27 |
| Figure 4-11 · Tow point depth response and tow point heave/surge input 2M configuration at 5 KTS | 28 |
| Figure 4-12 · (a) PSD of towpoint motion; (b) PSD of towbody depth 2M configuration at 5 KTS | 28 |
| Figure 4-13 · Towpoint depth response of 2M configuration at 2 KTS | 29 |
| Kiting | 30 |
| Figure 4-14 · Lateral response of 4M configuration at (a) 5 KTS to 0.5 knot cross current and at (b) 5 KTS to 10° roll command | 30 |
| 5· Autopilot Software..... | 32 |
| ap_if.h | 32 |
| 6· Summary & Conclusions | 36 |
| 4M configuration | 36 |
| 2M configuration | 36 |

I • Introduction

This document describes the concept design performed by Vehicle Control Technologies, Inc. (VCT) in support of the AETC effort to develop an Underwater UXO (Unexploded Ordinance) vehicle. The concept design study is for the development of an underwater vehicle (platform) to support UXO search technologies. The UXO search technologies are developed by AETC, and their design and function are not addressed herein.

This report is the second in a series of two describing the development of the marine vehicle concept design. The concept design examines several systems and performance options and then down-selects to a best candidate. In the concept, UXO sensor implementation and operation are the primary concerns, but additional sensors to operate, control and locate the marine vehicle are accounted for.

The first report described the UXO marine search requirements, the design alternatives and the resulting steady state hydrodynamic performance of the platform concept design.

This second report adds static hydrodynamic analysis for two additional vehicle sizes; a 2 meter (2M) length and a 4 meter (4M) length. The main portion of this report analyzes the dynamic response of these two vehicles and develops an autopilot for each. The autopilot is demonstrated through a series of time history simulations. Block diagrams and source code are also provided.

This marine platform is intended for operation in shallow environments. These initial concept design results are presented in terms of vehicle geometry, size, weight, component layout and basic hydrodynamic performance. Also discussed are launch and recovery operations, and concepts for the towing platform and connection device. The second report of this series will provide the development of the dynamics of the marine system, including the control system required to operate the vehicle.

2· 2M and 4M Vehicles

VCT TM02-06¹ documented the hydrodynamic results for the 10M vehicle. Those results showed the feasibility of that vehicle from the static design perspective. VCT TM02-06¹ included weight and balance design, basic vehicle and sensor layout, cable length and sizing, hydrodynamic performance of the main wing and the control surfaces, actuator sizing for the control surfaces, and a general discussion of the towing platform.

In this effort, we expand on the previous effort and develop similar results for a 2M and a 4M vehicle. The 2M and 4M designations refer to the number of receive arrays that are mounted in the vehicle; 2 and 4 respectively. These receive arrays are the original size described in the first report; 1.0M in length by 0.5M in width. The main transmit array is reduced in width only to fit into the two vehicles. By reducing the spacing between each magnetometer, both vehicles are able to accommodate all seven magnetometers.

The sensor suites for these vehicles are as defined for the 10M vehicle except for the electromagnetic sensors. The size of the transmit sensor is reduced with the size of each vehicle (Table 2-1). The other platform control sensors remain unchanged; echo sounder, inertial measurement unit (IMU), heading compass, depth gage and control fin actuator.

| Instrument | 10M | 4M | 2M |
|--------------|-------------|-------------|--------------|
| Magnetometer | 7 | 7 | 7 |
| - spacing | 1.5m | 0.8m | 0.5m |
| EM Rx Sensor | 8 | 4 | 2 |
| - size | 1.0m x 0.5m | 1.0m x 0.5m | 1.0m x 0.5m |
| EM Tx Sensor | 8.0 m x 1m | 4.0m x 1.0m | 2.0m x 1.0 m |

Table 2-1 · UXO Sensors for the three platforms.

Geometry

In order to accommodate the 1.0m x 0.5m receive sensors, the smaller sized vehicles are scaled only in width. In other words, the geometrically smaller 4M and 2M vehicles are generated by shortening only the main wing component. The basic dimensions of the smaller vehicles are the same, including the 24" wide wingtips that contain the control fins. In addition, the distance of the tow point ahead of the wing was kept constant at 2 FT.

Table 2-2 summarizes the basic component sizes and their associated weights. Notice that the dry weight of the vehicles does not decrease linearly with the vehicle size. This is partly due to the constant weight of the control sensors and the constant control tip section size. The platform buoyancy (6 to 10 LBS positive) is held constant along with the trim angle and the location of the center of gravity. Figure 2-1 presents the weight and balance details along with the vehicle dimensions in inches.

¹ Tureaud, T.F. and K.W. Watkinson, "Concept Design for a Marine UXO Sensor Platform", VCT Tech Memo 02-06, November 2002.

Figure 2-2 and Figure 2-3 present solid model views of the three sized UXO platforms. There are minor differences in the geometry of the control surface wings, the 2M has the main wing's leading edge extended to the full span. The tow point ball is held at a constant 2 FT in front of the main wing's nose with two strength member/guard rail bars extending back to the vehicle. Figure 2-4 presents a side view, which looks the same for all three vehicles.

Figure 2-5 and Figure 2-6 present a perspective and a side view of the 2M vehicle with the vertical stabilizing fins. These stabilizing fins are non-moveable and are approximately 1.5 FT tall, running the length of the main wing's edge. They are of sufficient size to make the marine platform hydrodynamically stable in the lateral (side) direction.

| Component | 10M | | 4M | | 2M | | Specific Gravity |
|-----------------------------------|-----------------------------|--------------|-----------------------------|--------------|-----------------------------|--------------|------------------|
| | Size (inches) | Weight (LBS) | Size (inches) | Weight (LBS) | Size (inches) | Weight (LBS) | |
| Upper wing Surface | 0.188 thick | 196 | 0.188 thick | 91 | 0.188 thick | 45 | 1.5 |
| Lower wing surface | 0.250 thick | 261 | 0.250 thick | 121 | 0.250 thick | 60 | 1.5 |
| Wing ribs (7, 5, 5) | 0.375 thick | 63 | 0.375 thick | 33 | 0.375 thick | 26 | 2.0 |
| Upper tip surfaces | 0.188 thick | 59 | 0.188 thick | 43 | 0.188 thick | 42 | 1.5 |
| Lower tip surfaces | 0.250 thick | 78 | 0.250 thick | 57 | 0.250 thick | 56 | 1.5 |
| Tip ribs (4) | 0.375 thick | 41 | 0.375 thick | 35 | 0.375 thick | 31 | 2.0 |
| Wing spars (4) | 300" span 1.8" ² | 152 | 300" span 1.8" ² | 58 | 300" span 1.8" ² | 36 | 2.0 |
| Skid struts (9, 5, 3) | 0.5" x 4.0" x 2.0" | 380 | 0.5" x 4.0" x 1.3" | 158 | 0.5" x 4.0" x 1.3" | 84 | 2.0 |
| Floatation (8, 4, 2) | 29" x 36" x 2.5" | 151 | 29" x 30" x 2.5" | 101 | 29" x 30" x 2.5" | 60 | 0.2 |
| Electronic pod | 6" dia x 25.0" | 26 | 6" dia x 25.0" | 26 | 6" dia x 25.0" | 26 | 1.0 |
| Actuators (2) | | 15 | | 15 | | 15 | 4.0 |
| Dry Weight | | 1354 | | 874 | | 597 | |
| Wt-Buoy | | -6.5 | | -10.0 | | -6.7 | |
| X _{CG} , Z _{CG} | 0.014, 0.379 | | 0.008, 0.423 | | 0.007, 0.353 | | |
| Trim Angle | -2.1° | | -1.1° | | -1.2° | | |

Table 2-2 Component Comparison Chart

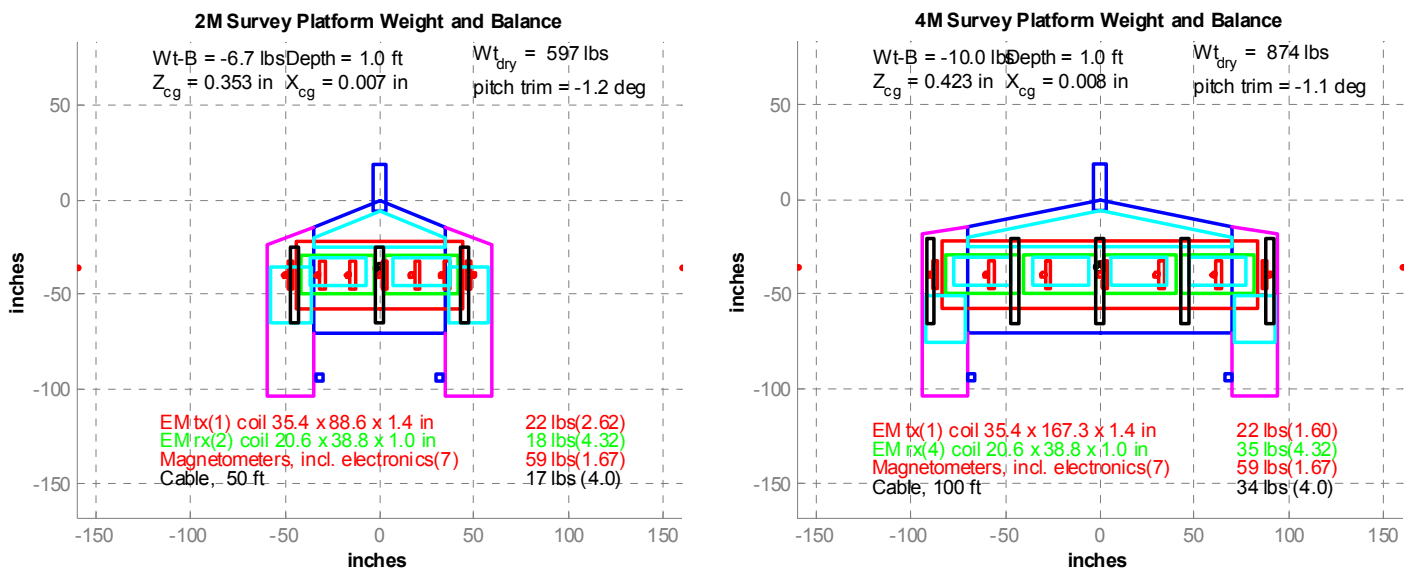


Figure 2-1 CAPTION

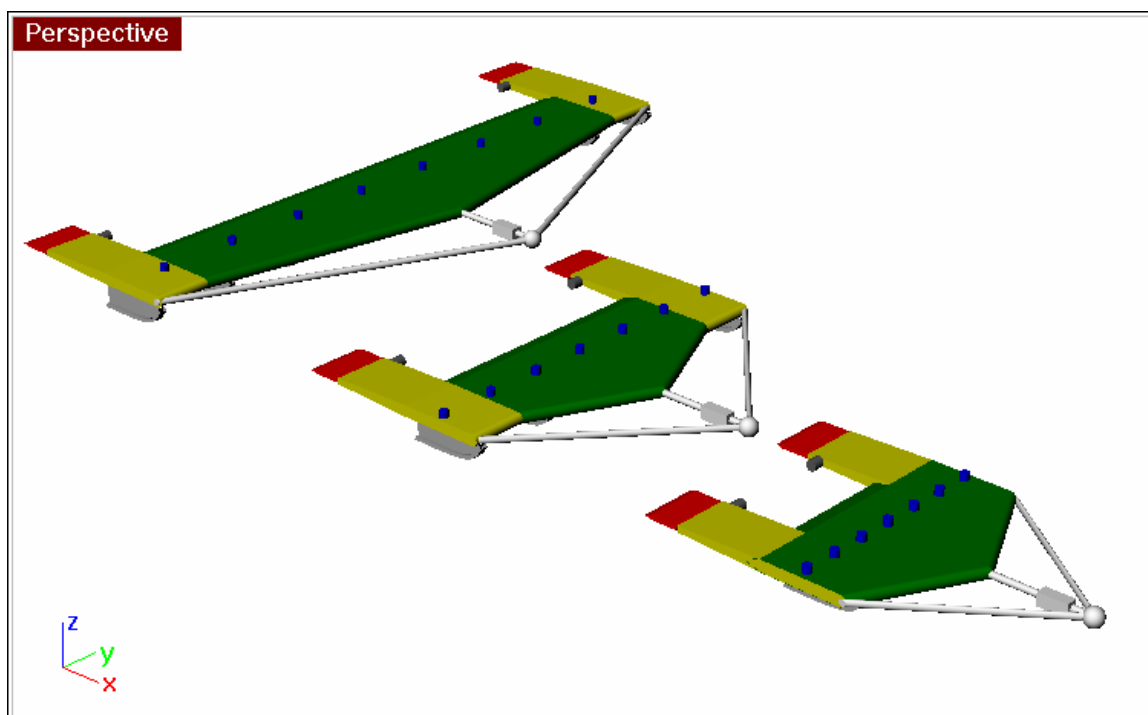


Figure 2-2 · CAPTION

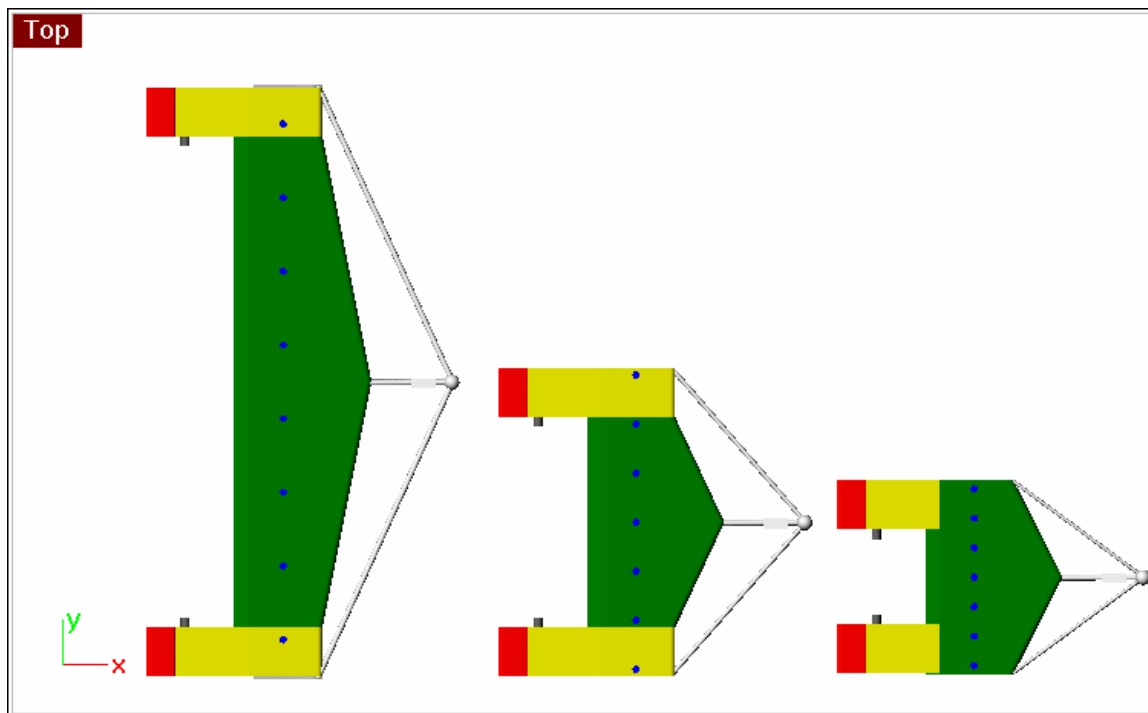


Figure 2-3 · CAPTION

Side View

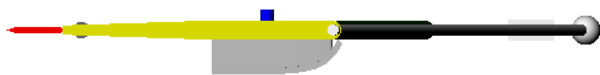


Figure 2-4 · Side View of Platform

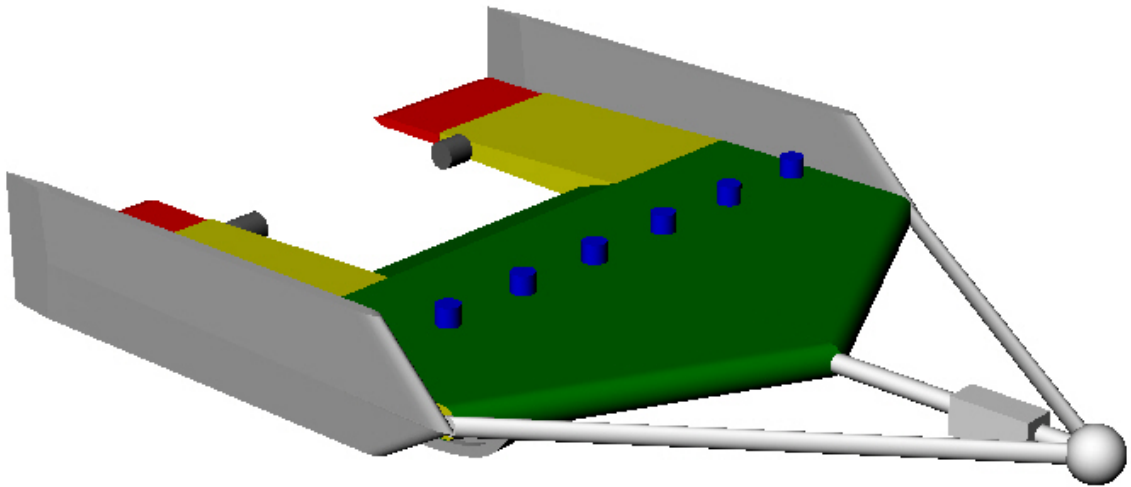


Figure 2-5 · CAPTION

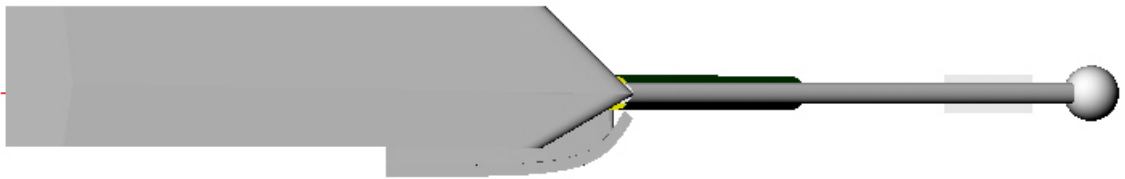


Figure 2-6 · CAPTION

Hydrodynamics

2-Meter Platform

A scale version of the 10-meter (10M) survey platform was developed and modeled. This was primarily developed by scaling the span of the 10M platform, as described above. The platform is called the 2-meter (2M) size because it accommodates two 1 meter EM receive arrays. Not scaled were the seven magnetometers, the cross sectional area of the EM sensors, the cabling (including the tow cable), the position measurement electronics and the actuators. The model was made to be slightly buoyant and it has a pitch trim angle of about 2° when on the surface.

50 ft Tow Cable

The 2M platform was first towed with the nominal 50 FT tow cable (Figure 2-7a-c). The pitch angle of the platform had to be increased to 8.0° in order to approach the 13 FT depth (Figure 2-7a). Along with this, the control fin angles range had to increase to over 25° deflection (Figure 2-7b). This large deflection angle is the likely cause for the fins stalling and lose of effectiveness. However, the results are presented for comparison. The reduced lifting area of the platform requires larger pitch angles to counter the cable tension (Figure 2-7c). In order to generate the extra pitch, the control fins **must deflect more**.

70 ft Tow Cable

Next the cable length was increased to 70 FT (Figure 2-8a-c). This value is within the parameters examined in detail in the previous report¹. The larger scope requires less vertical tension than shorter cables to achieve the same depth (Figure 2-8a). As seen, the 13 FT depth is obtained with 5° pitch angle and the stern plane needs only to deflect to just above 16° (Figure 2-8b). This is an acceptable maximum.

Cable tension at the surface vessel for the 2M with a 70 FT cable is presented in Figure 2-8c. The maximum value is similar to that of the 4M, and less than the 350 LBS of the 10M. **Thus a conservative estimate for towing horsepower is still on the order of 10 to 15 HP.**

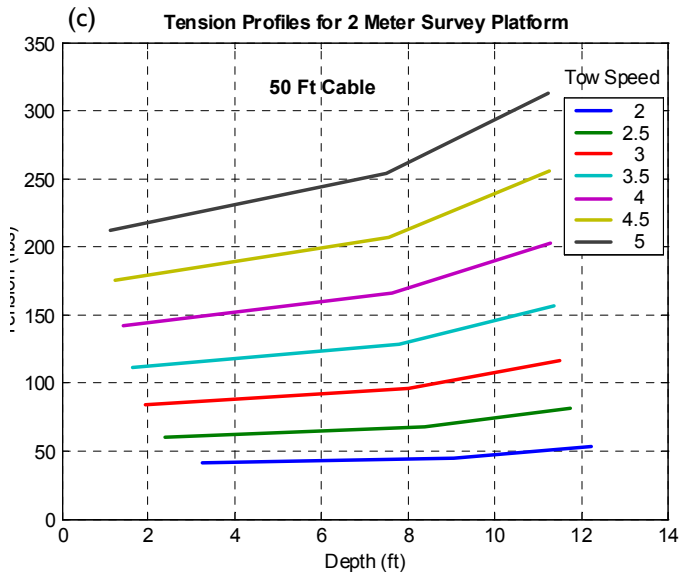
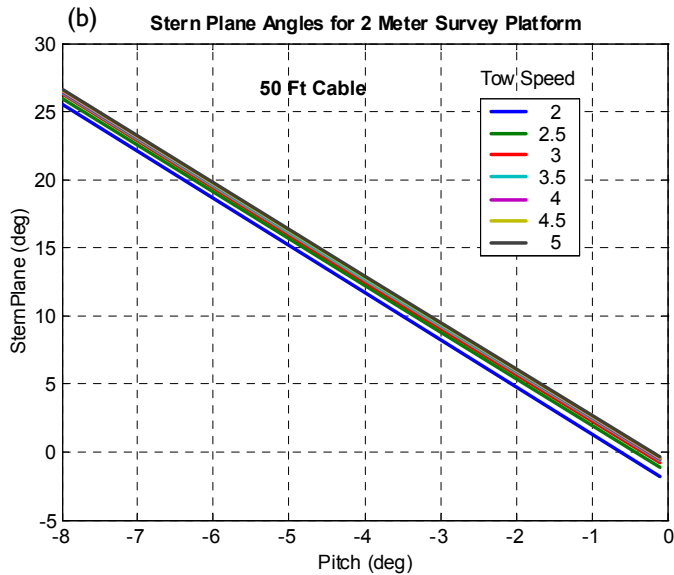
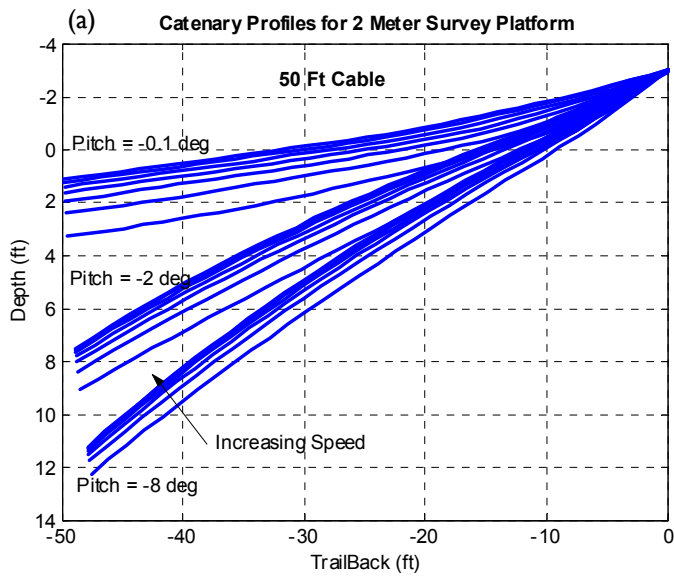


Figure 2-7 · Pitch Angle, Stern Plane Angle and Tension Profile results for the 2 Meter Platform

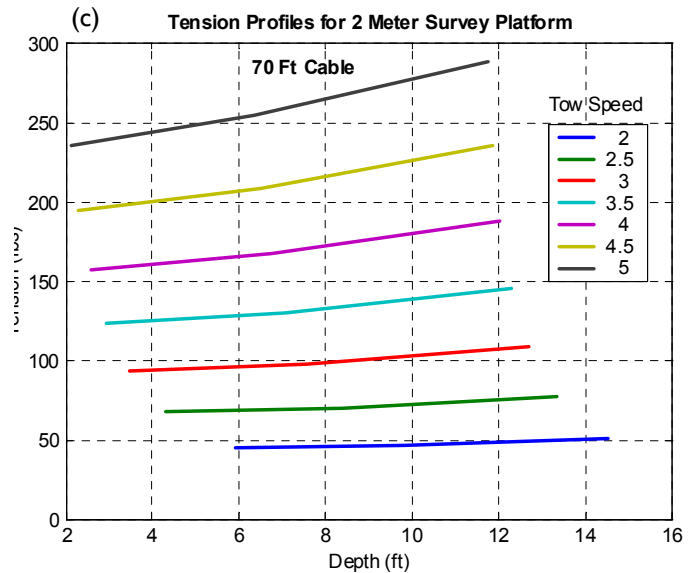
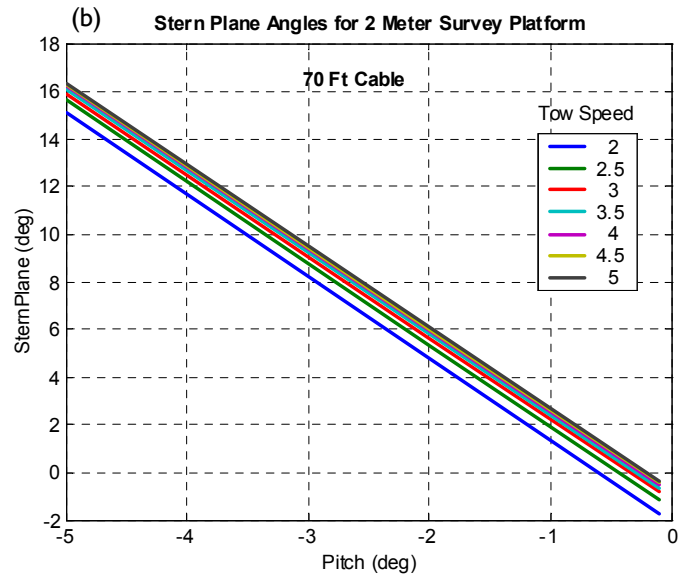
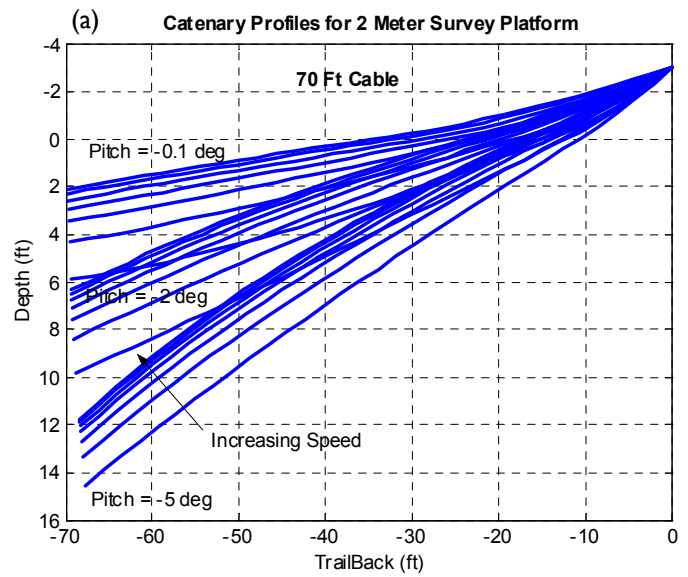


Figure 2-8 · Pitch Angle, Stern Plane Angle and Tension Profile results for the 4 Meter Platform

Control Fin Torque

The control fins for both the 4M and the 2M are the same physical size. When this fin is deflected as a stern plane or aileron for vehicle control, the control actuator must produce sufficient torque to counter the hydrodynamic loads. Here we estimate the required torque for the control surface deflection.

The moment generated by the control fin due to its deflection is a product of the lift of the fin and the distance from the axis of rotation. In this design, the control actuator is located forward, near the leading edge of the control fin. As a general estimate, the lift of a fin acts at approximately the $\frac{1}{4}$ chord of the fin.

The control fin for these vehicles has the following geometry

$$\begin{aligned} \text{CS span} &= 1.76 \text{ FT} \\ \text{CS chord} &= 1.12 \text{ FT} \\ \text{Area} &= 1.972 \text{ FT}^2 \\ \text{Distance to } \frac{1}{4} \text{ chord} &= 0.28 \text{ FT} \end{aligned}$$

We calculate the lift due to deflection to be $C_{L\delta} = 0.671$, defined as

$$C_{L\delta} = \frac{L}{\frac{1}{2} \rho U^2 A \delta_s}$$

So, for a maximum deflection of 15° with the vehicle operating at 5 KTS, we can estimate the required torque to be approximately 7 FT-LBS. Using a safety factor of two, we can say that the maximum torque required is 14 FT-LBS to deflect the control fins.

Both the Tecnadyne Model 60 and Model 20 should be sufficient for the control fin actuators. These are both off-the-self actuators, and the cost difference between the two is small; thus, choosing the larger of the two is suggested. However, these actuators are rate driven (not position controlled) and would need modification to become a servo type actuator. Contacts at Technadyne (858) 756-9660, suggest that these modifications can be incorporated into their actuators.

As an alternative, Raytheon Corp has developed an actuator for its underwater systems. This actuator is currently used on the Mk 30 torpedo, and it is able to produce approximately 15 FT-LBS maximum torque. This actuator is position controlled but does not include a sealed housing. It is typically mounted internal to an already sealed, dry hull. The cost of the Raytheon actuator would need to be obtained from the company.

Wing Near-Surface Effect

When a lifting surface like a wing approaches a boundary, the influence of the boundary is reflected in the hydrodynamic performance of the wing. In the case of a free surface boundary, the wings lift capability is reduced. Referring to the data and modeling in Waldin², the nominal lift of a wing in the presence of a free surface may be modified by the following equation,

$$\frac{C_{L2}}{C_{L1}} = 1 + \frac{\frac{A}{4\sqrt{\frac{1}{4} + 4(h/b)^2 + A^2/4}} \left[\frac{1}{\frac{1}{4} + 4(h/b)^2} + \frac{1}{A^2/4 + 4(h/b)^2} \right] + \frac{1}{\frac{A}{2} + \frac{8}{A}(h/b)^2}}{\frac{2(\sqrt{A^2 + 1} + 1)}{A}}$$

where,

- h = height from surface
- b = chord of airfoil
- A = airfoil's aspect ratio
- C_{L2} = lift slope of airfoil near surface
- C_{L1} = lift slope of airfoil with no surface effects

Figure 2-9 is a plot of the equation over a range of aspect ratio and depth-to-chord values. As a lifting airfoil approaches the free surface its ability to generate lift is reduced. Figure 2-10 presents open-loop time histories for the 4M vehicle operating within 2 FT of the surface. Here, the stern plane is set at a fixed deflection. At this depth, the near surface modeling shows a small effect on the vehicle performance. Depth changes approximately 0.2 FT, while the difference in vehicle pitch angle is less than 0.1°.

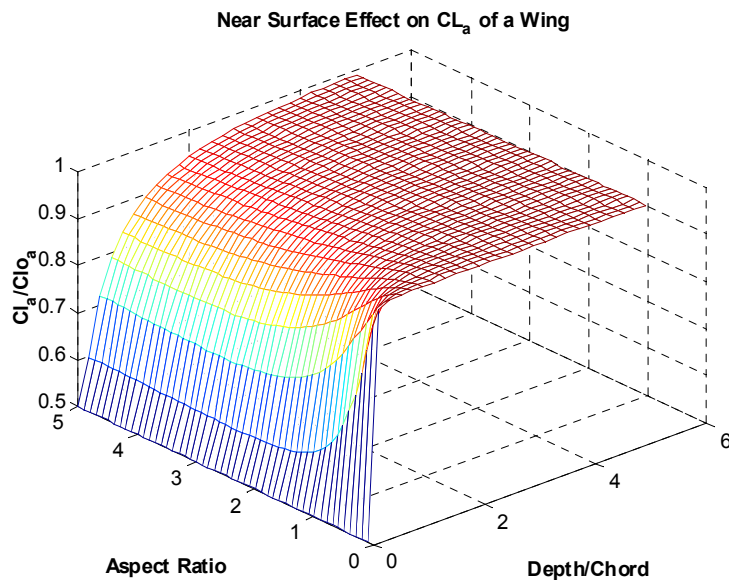


Figure 2-9 · **CAPTION**

² **naca tr 1232, 1955, pp671**

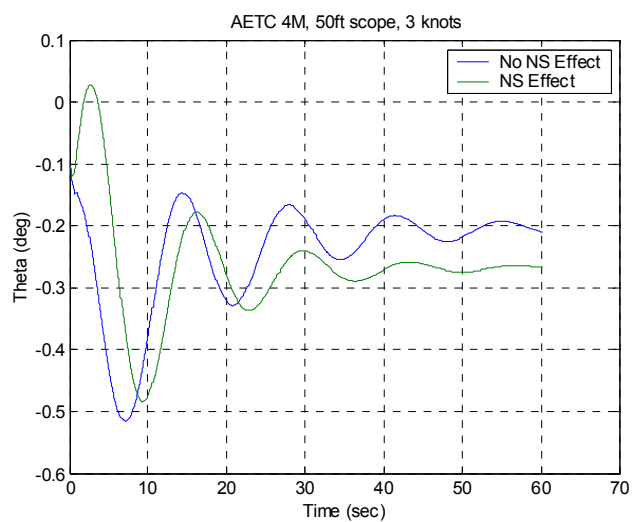
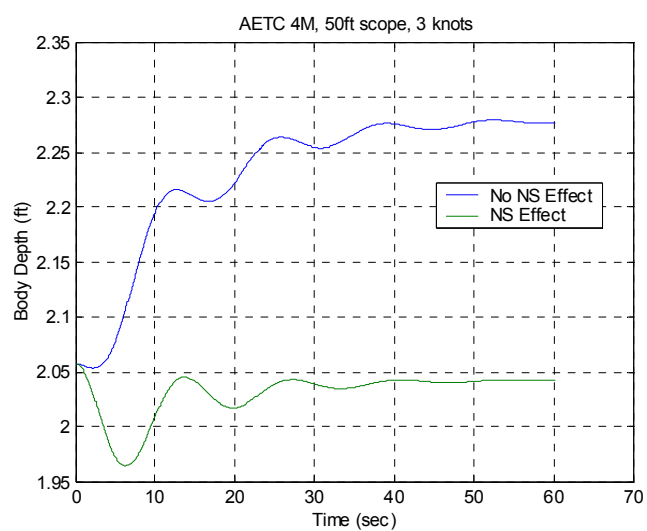


Figure 2-10 · CAPTION

3· Autopilot Design

Both vehicle designs are open-loop stable, but an autopilot is necessary to achieve continuous altitude control during UXO sweeps. Inherent, passive stability is useful and necessary for easy operation and safety. The full utility of the vehicle can only be realized with an autopilot to fly it in a controlled manner bringing the UXO sensors in proximity to their targets on the bottom.

Goals

Only four numerical requirements were given for the autopilot. One is the desired vehicle altitude, and the others describe the vehicle operating envelope. No steadiness or disturbance rejection requirements were stated. Disturbances are expected to be minimal since the intent is to only deploy the system on very calm days. Therefore, the overall goal of the autopilot design is to provide a stable sensor platform with reasonable steadiness performance and robustness to the disturbances expected under these calm conditions.

Nominally, the primary control mode will be altitude control with a commanded altitude of ~1 meter. However, a depth control mode is included for operations such as surfacing/submerging or obstacle avoidance. Vehicle roll angle command is available for small corrections to instrument or hydrodynamic bias.

The autopilot is to provide depth/altitude and roll control over the following operating range:

- Water depths of 5 to 15 FT
- Speeds from 2 to 5 KTS
- Cable lengths from 30 to 70 FT

The actuator duty cycle must be limited to minimize interference with UXO sensors. The actuators are DC motors that draw high current and cause a strong electromagnetic signal, which directly interferes with the UXO magnetometers. The amount of time the actuators draw current must be minimized, and this must be reconciled with the steadiness of the platform. There is no numerical steadiness requirement, but the vehicle must be stable and controlled to within reasonable bounds of the command.

There is no requirement for control in any environmental disturbances, such as waves or currents. However, even the calmest environments have some disturbance to which the autopilot must provide robustness. Therefore, the impact of some tow point motion and current will be explored.

Characteristics

Some basic control system characteristics must be chosen before the autopilot design can proceed. These selections hinge upon the estimated duty cycle of the actuator.

Duty Cycle

The actuator duty cycle is a function of the actuator rise/settling times and the rate at which new commands are sent to the actuator. The actuator dynamics may be estimated for these purposes but must be tested, once the hardware becomes available, to ensure all assumptions hold. An example of the actuator duty cycle is shown (Figure 3-1) with time along the abscissa and actuator current increasing with the ordinate. Over a one second period the actuators will receive a command two times (i.e., 2 Hz). The estimated time for the actuator to reach the commanded value, and for the actuator current to return to zero, is 0.25 SEC. This leaves an ~0.25 SEC period for the UXO sensors to operate within each 0.5 SEC autopilot cycle for the UXO sensors to operate.

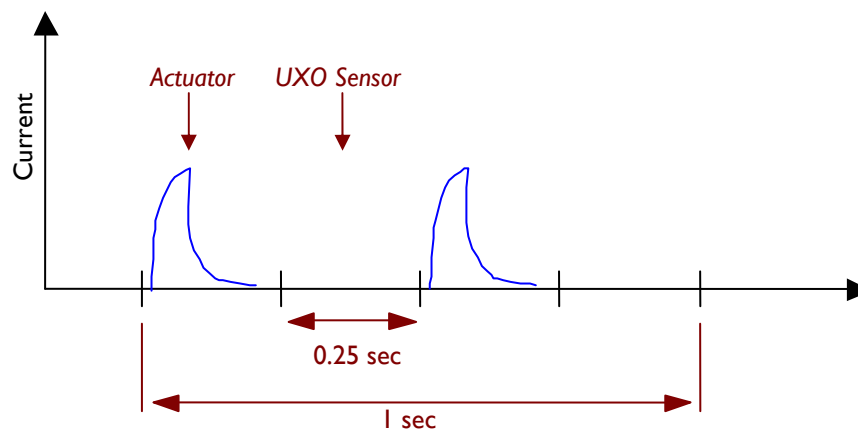


Figure 3-1 · Representation of the actuator duty cycle

Computational Rate

The selection of the actuator update rate also specifies the autopilot computational rate. The autopilot must operate at least as fast as commands are to be sent to the actuators (there is no reason for it to run faster). Therefore, the autopilot computational rate is 2 Hz. This leads to a measurement-to-command sample and hold of $\frac{1}{2}$ SEC. For the sake of robustness, an additional 0.1 SEC computational delay is added. Ultimately, this leads to the choice of an inner-loop cross-over frequency in the range of 1 RAD/SEC (~ 0.16 Hz). This is nominally the highest frequency input to which the autopilot responds.

Hardware

Hardware and instrumentation recommendations were provided in the initial report³. Additional details about hardware most closely linked to the performance of the autopilot are provided here.

An actuator must be able to follow (within $\sim\pm 10\%$) a small signal sinusoid ($\sim 1^\circ$ peak-to-peak) at a frequency of 2 Hz in order to achieve the desired duty cycle. Additional requirements on power (a function of the size of the control surfaces and the vehicle speed) and packaging are met by the Tecnam Model 60 rotary actuator (<http://www.tecnadyne.com/rotact.htm>). It consists of a high speed DC motor linked to a harmonic drive and is contained in an oil-filled pressure housing rated to 5,000 FT of ocean depth.

An Inertial Measurement Unit (IMU) is necessary to provide the feedback measurements for the control system. Many acceptable units are available but the recommended Honeywell HGI700 ring laser gyro package offers the most precision for the lowest cost.

Depth, altitude and speed measurements must be available to the control system. They must be reliable and stable, as they are the direct measurement of the desired control variable.

Design

The autopilot architecture is a cascaded feedback system similar to those used in missiles and torpedoes. Each feedback loop is designed with linear techniques standardized many decades ago. The overall block diagram (Figure 3-2) shows the **main autopilot components** highlighted in **cyan**. These are the depth and roll controllers and the fin mixing module.

The depth controller (Figure 3-3) consists of three cascaded feedback loops; depth, pitch angle and pitch rate. The outer loop (on the left) is the depth control loop. The depth error signal (the difference between the depth command and the depth measurement, or feedback) is passed through a compensator. The compensator is a digital filter network that conditions the error signal to achieve the desired feedback loop frequency domain characteristics. The compensated signal passes through proportional and integral gains, whose sum is the vehicle pitch angle command. The pitch angle feedback **loop is similar but for the integral** and its output is a vehicle pitch rate command. The output of the pitch rate feedback loop is the elevator command.

Altitude control will be achieved indirectly by computing a commanded depth. This serves to isolate the control system from signal drop-outs characteristic of echo sounders and results in a single vertical control loop.

The roll controller consists of a proportional/integral roll feedback loop and a proportional roll rate feedback loop producing an aileron command.

The fin mixing module is used to prioritize (in case control surface limits are exceeded) and combine the two commands (elevator and aileron) such that they are ready to be sent to the two actuators. This step is necessary because the two functions, roll and pitch control, are competing in this control surface design scheme.

The dynamics of the actuators, vehicle and sensors have all been simulated to best capture their impact on the control system design.

³ Tureaud, T.F. and K.W. Watkinson, "Concept Design for a Marine UXO Sensor Platform", VCT Tech Memo 02-06, November 2002.

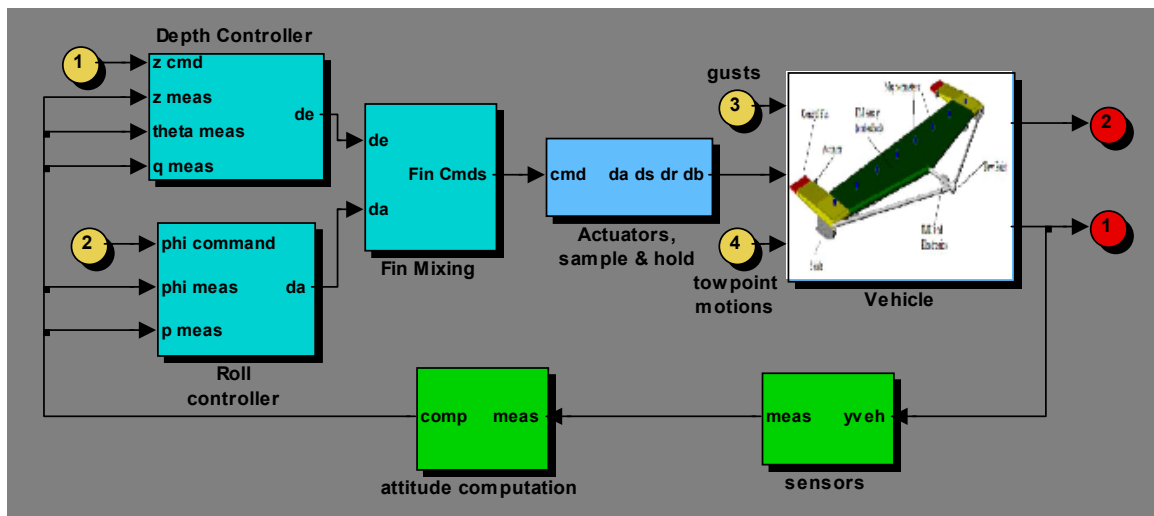


Figure 3-2 · Top-level autopilot block diagram

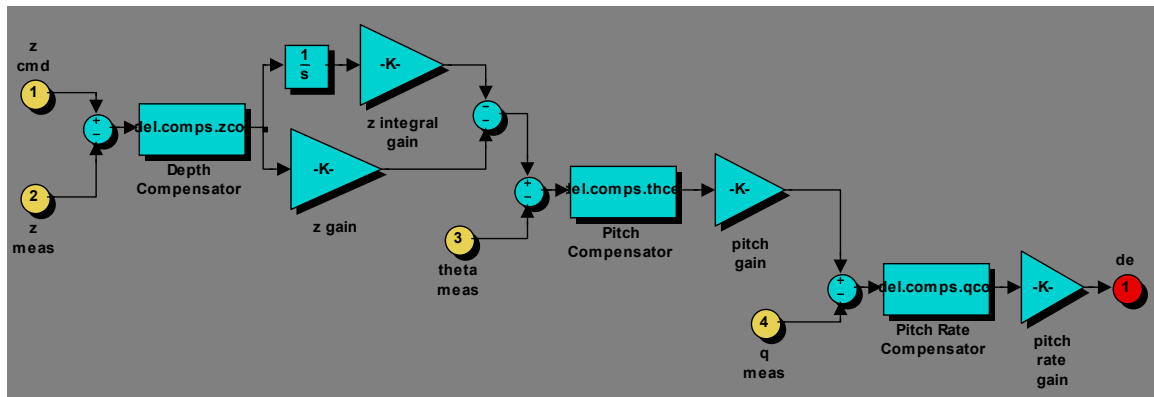


Figure 3-3 · Depth/pitch control loop block diagram

Design Challenges

The primary challenges for the design of the autopilot were the low minimum speed and a large peak in the pitch rate frequency response.

The minimum required speed (2 KTS) is problematic because the vehicle is controlled, like a winged aircraft, by pointing the lift of the wing. At low speeds wing lift is quite low. Furthermore, the maximum frequency at which the lift responds to control input reduces proportionally with speed. Figure 3-4 shows the frequency response of the vehicle pitch to elevator input at 2 and 5 KTS. For frequencies near DC, there is lift at both speeds. The available bandwidth is drastically reduced from 5 to 2 KTS. That is, at 2 KTS the vehicle will not respond to elevator motions much above $\frac{1}{2}$ RAD/SEC, while at 5 KTS it will respond to elevator motions over 1 RAD/SEC. At low speeds, the inner loop cross-over frequency will be well short of the target of 1 RAD/SEC. The conclusion here is the vehicle is less controllable at low speeds due to reduction in lift and is sluggish to respond due to the reduction in bandwidth.

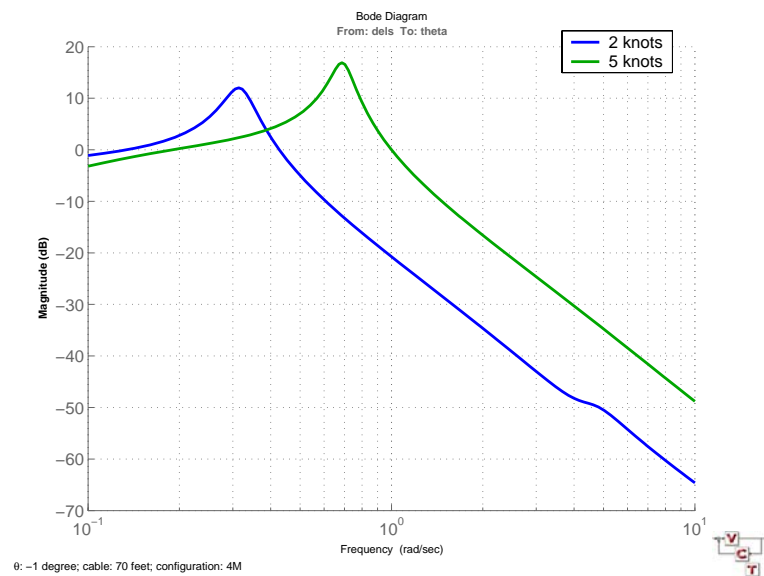


Figure 3-4 · Change in maximum response frequency with speed

The problematic peak, and associated 180° phase change, in the pitch rate per elevator frequency response is shown in Figure 3-5. The peak varies in magnitude and frequency in proportion to the speed of the vehicle. In fact, the peak tends to occur at or near the inner loop cross-over frequency at each speed (reduced from the goal of 1 RAD/SEC with speed as demonstrated above). The phase change of this peak is enough to create positive feedback at certain frequencies, thereby making the control system unstable. The solution is a notch filter for the pitch rate compensator that is variable with speed (Figure 3-6). The notch has been chosen with sides shallow enough to allow for variance in the peak frequency.

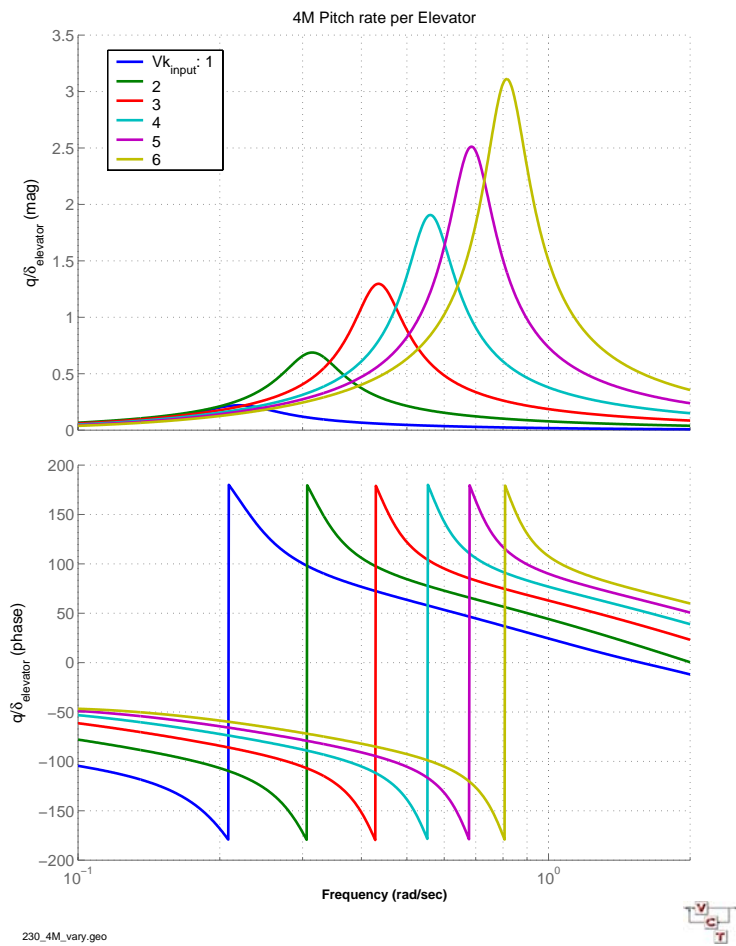


Figure 3-5 · Peak in pitch rate per elevator frequency response moves with speed

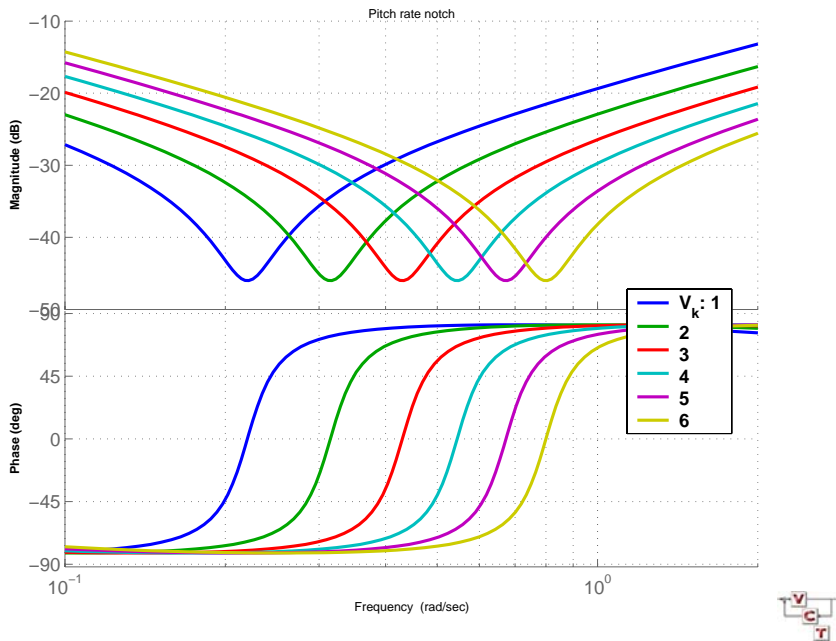


Figure 3-6 · Variable notch filter

Near-Surface Effects

The impact on the autopilot of the near surface effect was evaluated in the frequency domain only. That is, the margins were compared with and without the near surface effect enabled. The result was the gain margin was eroded ~ 0.3 dB, and the phase margin was bolstered $\sim 3^\circ$. The near surface effect has negligible impact on control.

Margins and Design Details

Gain and phase margins are a minimum 6 dB and 45° , respectively, for each feedback control loop over the entire operating envelope. This is standard practice for the design of linear feedback control systems to maintain robustness to modeling errors, additional delays, changes in hardware characteristics, etc. The selected gains and compensators and the resulting margins and cross-over frequencies are shown in Figure 3-7 and Figure 3-8 for the 4M configuration and 2M, respectively. The names of the gains or compensators are shown in the left column and the speed of the vehicle increases from left to right as shown in the top row. Each **gain value or compensator transfer function** is shown in **black**; the **gain margin** is shown in **green**; the **phase margin** in **blue**; and the **cross-over frequency** in **red**. Notice the reduction in the inner loop (kq) cross-over frequency with speed.

The studied operating speed ranges from 2 to 5 KTS. Gains have been chosen from 1 to 6 KTS in order to maximize robustness of the autopilot when running at the ends of the operating speed range. This does not mean the vehicle should be run on this extended speed range. In fact, the 2M configuration is not longitudinally controllable at 1 knot, as indicated by the lack of data at that speed (Figure 3-8). The smaller size of 2M yields very little lift, and that is available only at very low frequencies so that low speed control is difficult or impossible.

Numbers in the tables are for a cable length of 50 FT but margins were checked at cable lengths from 30 to 70 FT. Some towed vehicles have dynamics that require gains to be scheduled with both speed and cable length. These margins and cross-over frequencies were insensitive to cable length, so the gains vary only with speed.

black gain value or compensator transfer function
 green gain margin
 blue phase margin
 red cross-over frequency

Configuration: VCT AETC(230_4M.geo) model using AETC autopilot (AETC_att.mdl)

| Gain name | Speed | | | | | | | | | | | |
|------------|---------------------|---|---------------------|------------------|---------------------|-------------------|---------------------|------------------|---------------------|------------------|---------------------|-----------------|
| | 1 | | 2 | | 3 | | 4 | | 5 | | 6 | |
| kq | 275 | Gm: 6 dB Pm: 48 deg wc: 0.5 rad/s | 95 | 7.3 49 0.8 | 57 | 7.7 57 0.85 | 42 | 7.7 63 0.9 | 38 | 6.8 69 1.1 | 34 | 6 74 1.25 |
| kw_q_notch | 0.22 | | 0.315 | | 0.43 | | 0.545 | | 0.673 | | 0.8 | |
| ktheta | 110 | 8.8 46 | 86.45 | 8.6 46 | 57 | 10 46 | 42 | 12 51 | 38 | 12 50 | 34 | 12 53 |
| ktheta_i | 0 | 0.25 | 0 | 0.5 | 0 | 0.53 | 0 | 0.47 | 0 | 0.5 | 0 | 0.52 |
| zcomp | tf([1 .01],[1 .09]) | | tf([1 .01],[1 .07]) | | tf([1 .01],[1 .05]) | | tf([1 .01],[1 .05]) | | tf([1 .01],[1 .04]) | | tf([1 .01],[1 .03]) | |
| kz | 11 | 8.7 45 | 4.323 | 11 46 | 2.4225 | 12 45 | 1.68 | 12 46 | 1.406 | 13 45 | 1.02 | 14 45 |
| (deg/ft) | | | | | | | | | | | | |
| kz_i | 0.22 | 0.1 | 0.1729 | 0.14 | 0.0969 | 0.18 | 0.0672 | 0.22 | 0.0562 | 0.25 | 0.0408 | 0.24 |
| kp | 66 | 13.8 51 1 | 19 | 13.4 62 1 | 10 | 13 70 1 | 7 | 13 78 1.1 | 4.6 | 12 58 1 | 3.8 | 12 61 1 |
| pcomp | 1 | | 1 | | 1 | | 1 | | tf([1 1],[1 .1]) | | tf([1 1],[1 .1]) | |
| kphi | 50.82 | 12.2 66 | 18.24 | 12.7 70 | 11 | 13 74 | 7.7 | 14 75 | 3.082 | 15 60 | 2.546 | 16 61 |
| kphi_i | 5.082 | 0.5 | 1.824 | 0.5 | 1.1 | 0.5 | 0.77 | 0.5 | 0.3082 | 0.5 | 0.2546 | 0.5 |

qcomp=notch*lag
 lag=tf([1 .5],[1 .05]) 2nd order actuators: wn=2 Hz, zeta=0.7 Sample rate = 2 Hz
 1 dt S&H, 1/10 s delay(Pade)

Figure 3-7 · 4M configuration design summary

Configuration: VCT AETC(230_2M_case1.geo) model w/ 50 feet of cable & 11 nodes using AETC autopilot (AETC_att.mdl)

| Gain name | Speed | | | | | | | | | | | |
|------------|--------------------|--------------------------------|--------------------|-----------------|---------------------|-----------------|----------------------|-------------------|----------------------|-----------------|----------------------|-----------------|
| | 1 | | 2 | | 3 | | 4 | | 5 | | 6 | |
| kq | 25 | Gm: dB Pm: deg wc: rad/s | 25 | 6 46 0.48 | 21.6 | 6 47 0.66 | 17.6 | 6.1 47 0.83 | 15 | 6 49 0.98 | 14 | 7.3 45 1 |
| kw_q_notch | 0.24 | | 0.38 | | 0.55 | | 0.7 | | 0.85 | | 1.1 | |
| ktheta | 10 | | 10 | 7.5 54 | 9.72 | 9 59 | 10.56 | 9 59 | 11 | 9 54 | 8.4 | 11 54 |
| ktheta_i | 0 | | 0 | 0.23 | 0 | 0.28 | 0 | 0.36 | 0 | 0.43 | 0 | 0.41 |
| zcomp | tf([1 .01],[1 .1]) | | tf([1 .01],[1 .1]) | | tf([1 .01],[1 .06]) | | tf([1 .01],[1 .045]) | | tf([1 .01],[1 .045]) | | tf([1 .01],[1 .045]) | |
| kz | 0.6 | | 0.6 | 9.4 47 | 0.3888 | 11 45 | 0.3168 | 13 49 | 0.33 | 12 55 | 0.252 | 12 57 |
| (deg/ft) | | | | | | | | | | | | |
| kz_i | 0.024 | | 0.024 | 0.09 | 0.0156 | 0.11 | 0.0127 | 0.12 | 0.0132 | 0.15 | 0.0101 | 0.16 |
| kp | 30 | 14 46 1 | 7.2 | 14 45 1 | 3 | 14 46 1 | 1.9 | 14 50 1.1 | 1 | 15 57 1 | 0.83 | 14 58 1.2 |
| pcomp | 1 | | 1 | | 1 | | 1 | | 1 | | 1 | |
| kphi | 13.5 | 14 70 | 4.32 | 12 67 | 2.25 | 11 61 | 1.444 | 12 66 | 0.9 | 12 65 | 0.747 | 12 68 |
| kphi_i | 0.135 | 0.41 | 0.432 | 0.48 | 0.225 | 0.5 | 0.1444 | 0.5 | 0.09 | 0.5 | 0.0747 | 0.5 |

qcomp=notch*lag
 lag = tf([1 2],[1 .2]) 2nd order actuators: wn=2 Hz, zeta=0.7 Sample rate = 2 Hz
 1 dt S&H, 1/10 s delay(Pade)

Figure 3-8 · 2M configuration design summary

4• Marine Vehicle Time Histories

Upon completion of the linear design the autopilot was coded and integrated with the vehicle simulation. The following sections present the autopilot performance as tested in the VCT simulation.

Depth Profile

The ability to follow an extreme depth profile is shown in Figure 4-1. The left plot shows the 4M configuration and the right 2M with the response at **5 KTS** in blue and **2 KTS** in red.

Rise time (time to achieve commanded depth) decreases with higher speed for both configurations. Steady state depth error is not speed dependent. Each configuration will reach the same steady state error, regardless of speed, if given enough time. However, control at higher speeds is quicker and more predictable.

The smaller 2M configuration is less capable; as shown by its failure to follow the shallower depth profile. The **setting** time to the final commanded depth is over 200 seconds for both speeds.

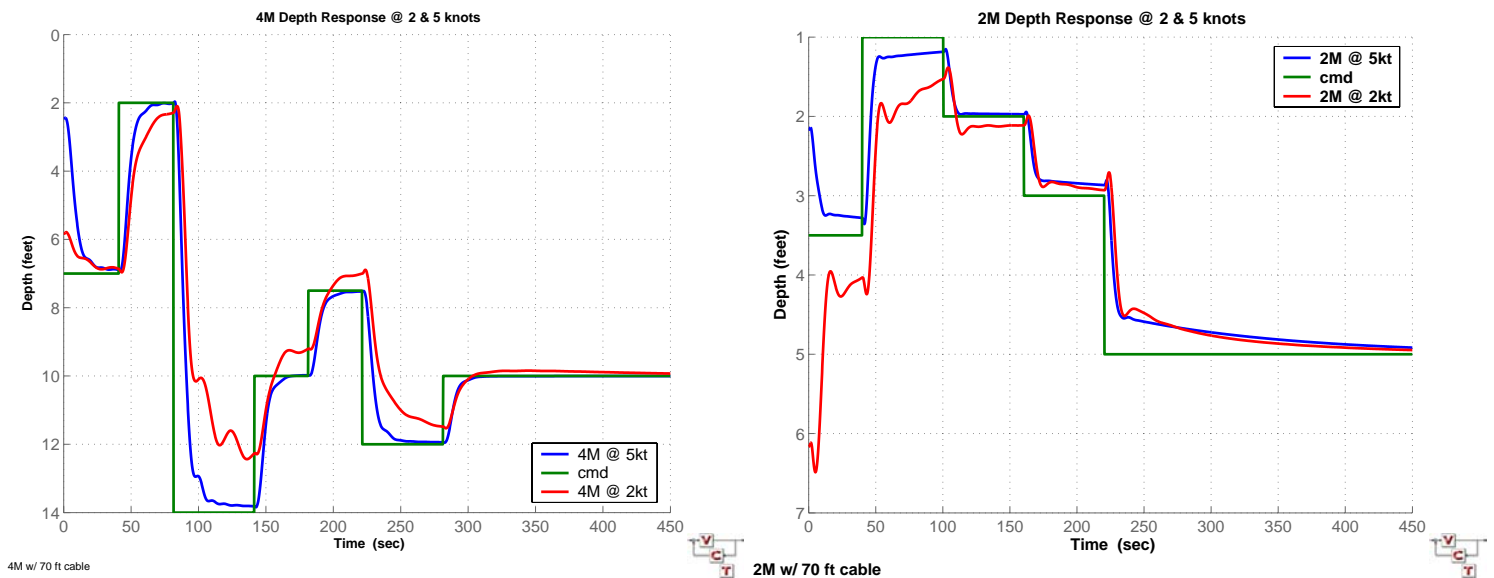


Figure 4-1 · 5 KTS (blue) and 2 KTS (red) depth keeping for configurations 4M (left) and 2M (right)

Altitude Profile

Altitude keeping is the primary control mode for this autopilot since it is desired that the UXO sensors be maintained at a constant distance from the bottom. An example bottom profile was constructed to test the performance of this control loop (Figure 4-2). Imagine the vehicle flying across the figure from left to right along the dotted line. The first minute of the profile is level after which the bottom slopes up or down at 1° until the water depth has changed by 11 FT. Finally, the profile is level again. The horizontal distance between the inception and culmination of the slope is 630 FT. The autopilot is commanded to hold an altitude of 3 FT throughout.

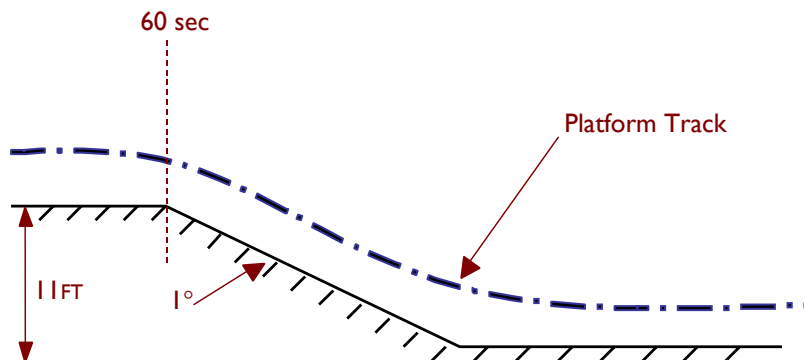


Figure 4-2 · Example of altitude profile

Both dives and climbs were tested (Figure 4-3 and Figure 4-4). The plot on the left is the response of the 4M configuration at speeds of 2 KTS (red) and 5 KTS (blue). The top half of the plot shows the depth of the vehicle and the bottom half shows the altitude. The 4M configuration maintains altitude within 1 FT, while the 2M configuration stays within 2 FT.

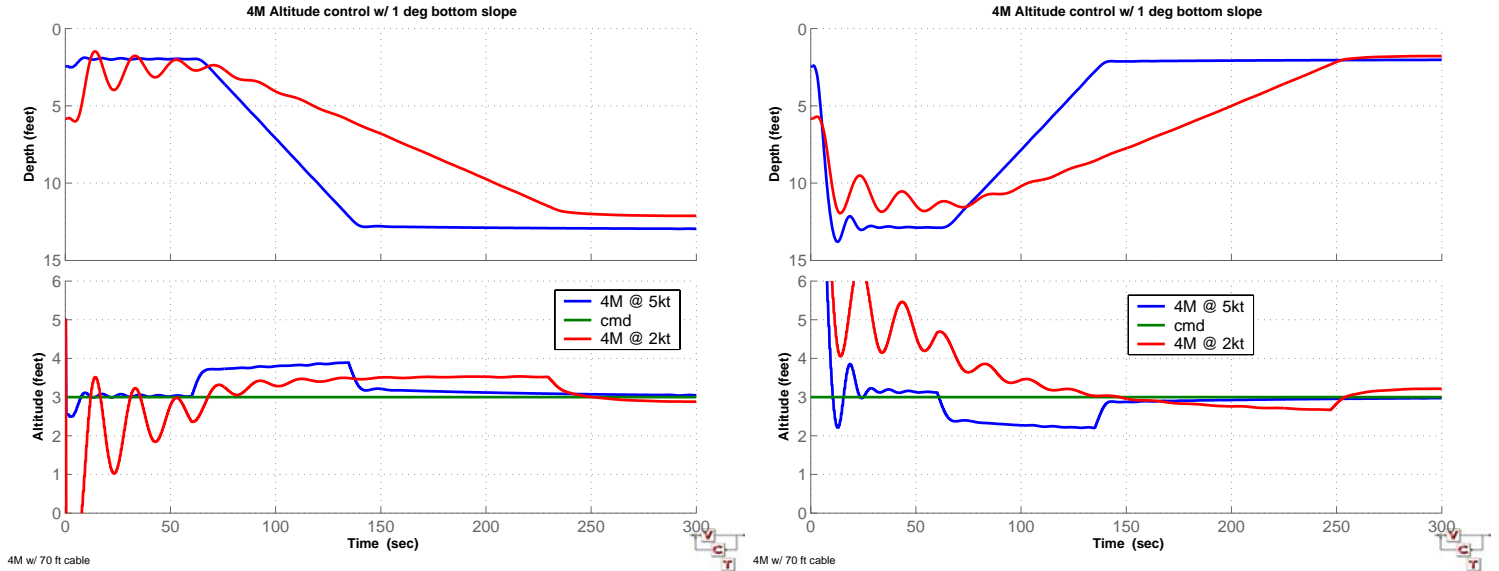


Figure 4-3 · 4M configuration altitude profile at 5 KTS (blue) and 2 KTS (red) diving (left) and climbing (right)

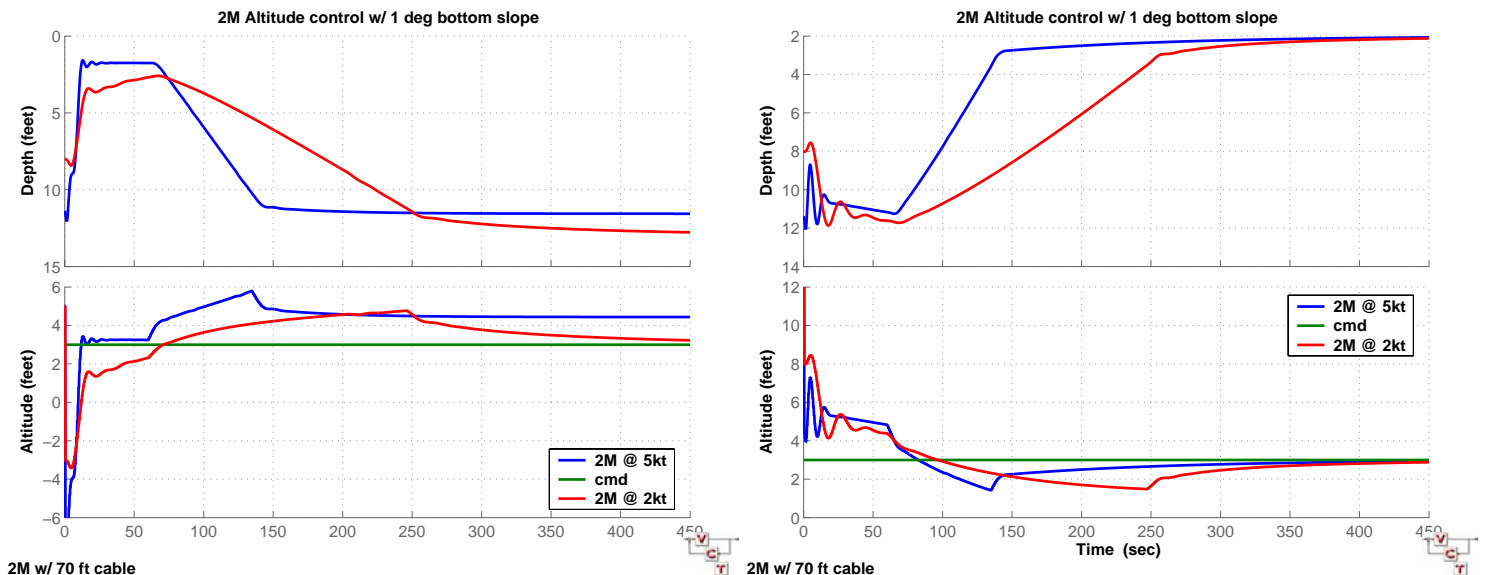


Figure 4-4 · 2M configuration altitude profile at 5 KTS (blue) and 2 KTS (red) diving (left) and climbing (right)

Response to Tow Point Motions

Disturbance rejection was not an autopilot design requirement, but robustness to potential disturbance is part of any good control system design. Therefore, an evaluation of the susceptibility of the vehicle to tow point motions was performed. Each configuration is presented singly.

4M configuration

An evaluation of both linear, frequency domain and non-linear, time domain is presented.

Frequency Domain

Open-loop (blue) and **closed-loop** (green) frequency response of vehicle depth to tow point heave (left) and surge (right) is shown in Figure 4-5. The autopilot satisfactorily quells tow point motions at frequencies below the inner loop cross-over frequency (~ 1 RAD/SEC). The closed-loop system has more susceptibility to motions in the range of 2 to 8 RAD/SEC, though these are **15 to 30 dB down**.

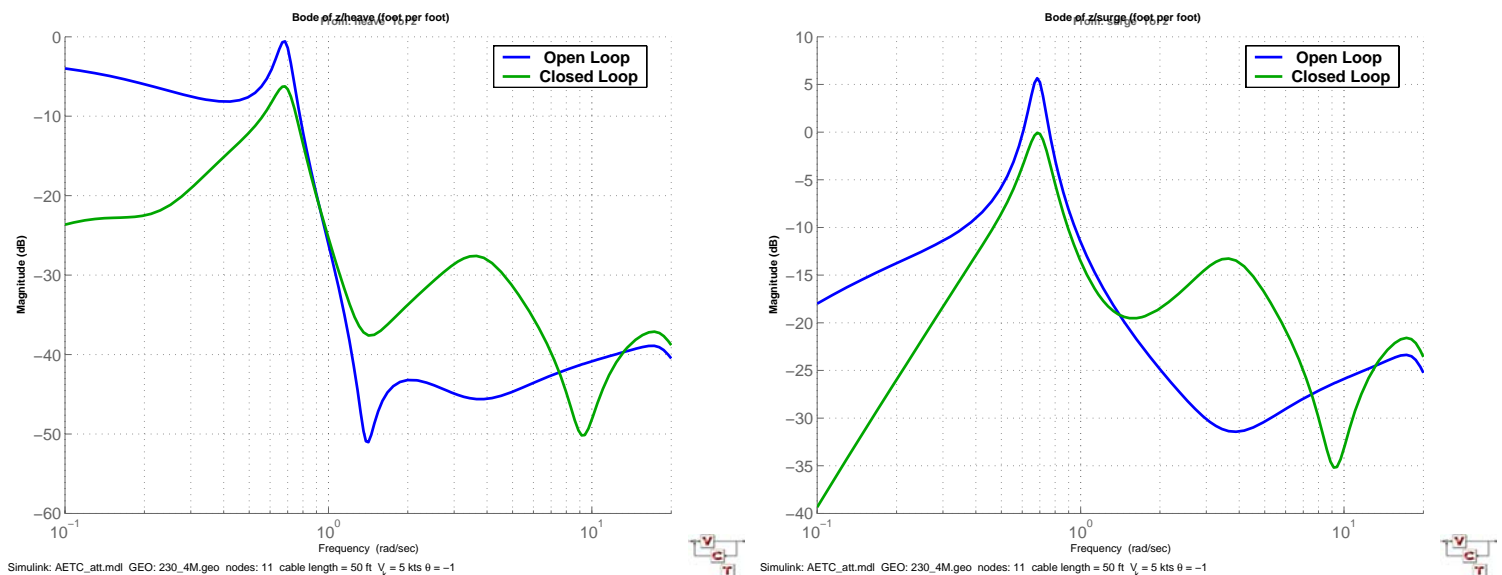


Figure 4-5 · Open-loop vs. closed-loop depth response to tow point heave and surge, 4M configuration

Time Domain

A Power Spectral Density (PSD) plot of the surface wave height of the open ocean at sea state I is shown in Figure 4-6a. This is commensurate with waves a few inches in height. Notice the energy is all in the frequency range from 5 to 16 RAD/SEC. The responding motion of a boat in this environment would be at significantly lower frequencies. To simulate the tow point motion, sinusoids from $\frac{1}{4}$ to 2 RAD/SEC (by octaves) were summed. The result (Figure 4-6b) was scaled to yield a total energy having ~ 2.5 times the energy of the sea state I spectra since motions at lower frequencies generally have more energy. It is conceivable to encounter heave motions of this magnitude, but it is quite unlikely for there to ever be equal energy in any other axis. However, for the sake of simplicity, the same spectrum was used for both heave and surge.

The lower plot of Figure 4-7 shows the time history of the simulated tow point motion in feet with a peak-to-peak magnitude of $\sim 4.8''$. The upper plot shows the depth response in feet (at 5 KTS) of the vehicle with this excitation on **tow point heave** (blue) and **surge** (red). The maximum depth motion is fractions of a foot.

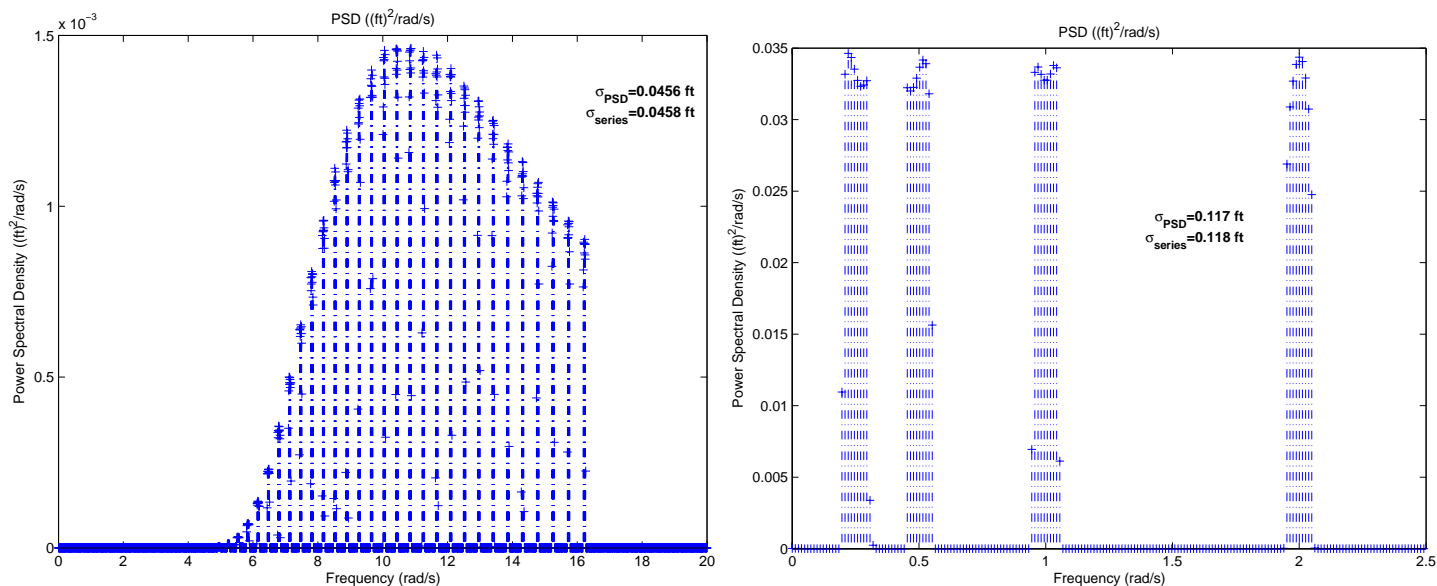


Figure 4-6 · (a) Wave height PSD of sea state 1 at 5 KTS; (b) Boat tow point motion PSD

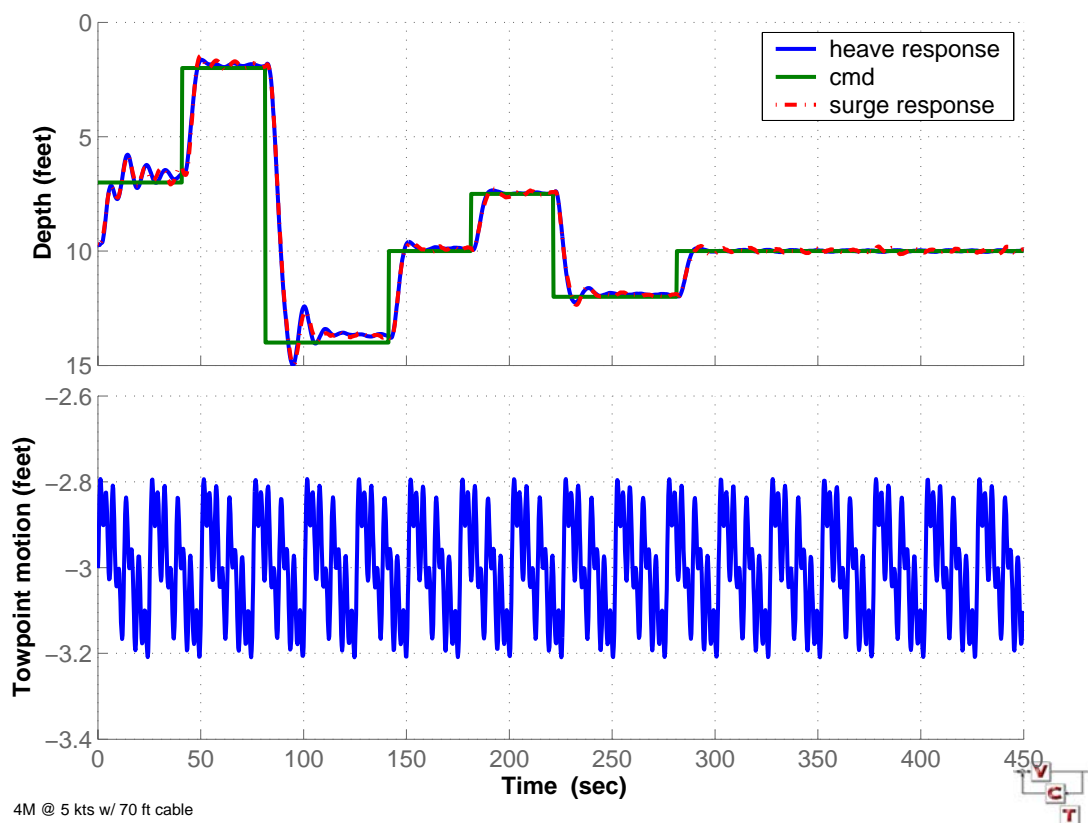


Figure 4-7 · Tow point depth response and tow point heave/surge input 4M configuration at 5 KTS

The PSD plots in Figure 4-8a present the input spectrum, while Figure 4-8b shows the amount of energy due to tow point heave (upper) and surge (lower). Very little energy makes its way through to the vehicle depth and almost nothing appears outside the autopilot frequency range of influence (<1 RAD/SEC).

The depth response to the same tow point motions (heave and surge) at 2 KTS is shown in Figure 4-9. The motion due to tow point heave is imperceptible and hidden behind that due to surge. However, the surge motion is still not more than $\frac{1}{4}$ FT.

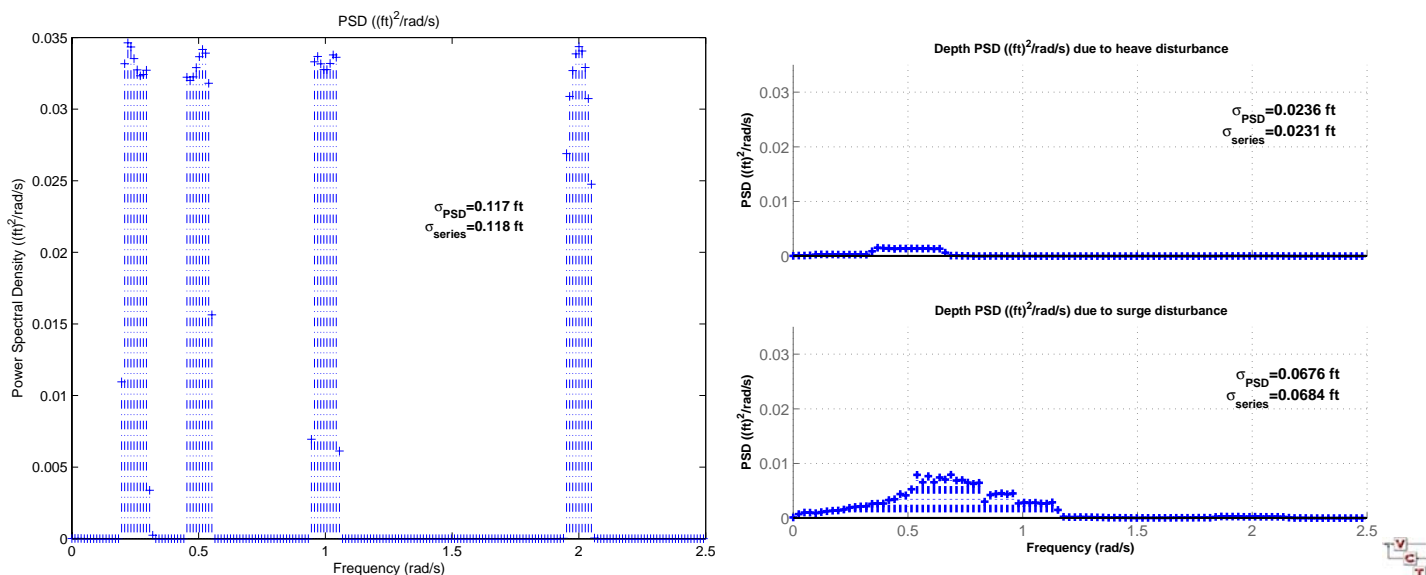
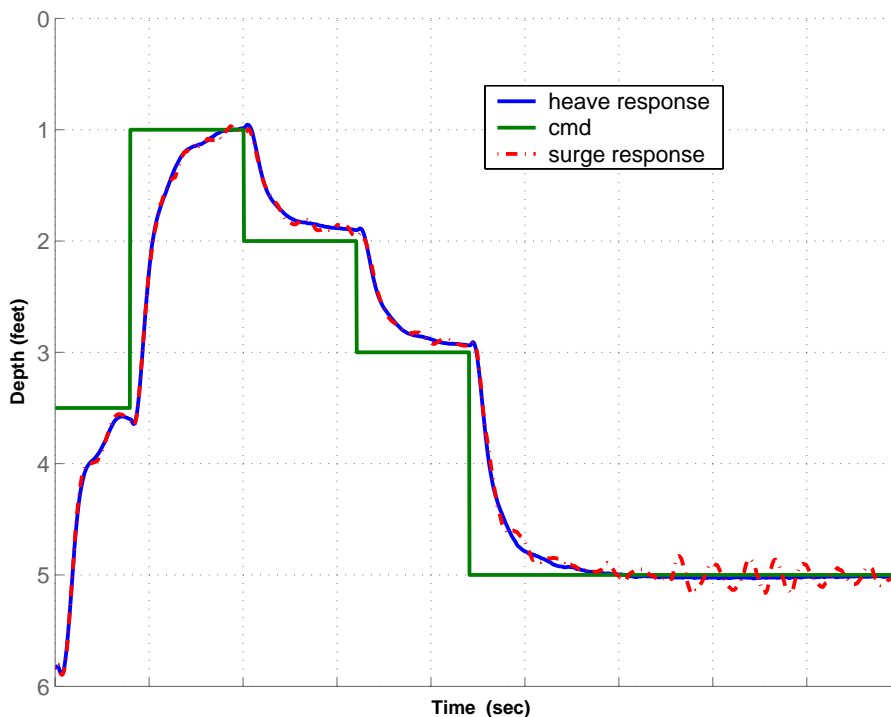


Figure 4-8 · (a) PSD of tow point motion; (b) PSD of towbody depth due to heave and surge, 4M configuration at 5 KTS



4M @ 2 kts w/ 70 ft cable

Figure 4-9 · Tow point depth response for 4M configuration at 2 KTS

2M configuration

Frequency Domain

Open-loop (blue) and **closed-loop** (green) frequency response of vehicle depth to tow point heave (left) and surge (right) is shown in Figure 4-10. The closed-loop system response to tow point disturbance is worse than the open-loop at frequencies greater than $\frac{1}{2}$ RAD/SEC. The inner loop cross-over for this speed (5 KTS) is 1 RAD/SEC, and the expectation of a well designed vehicle and autopilot would be for the closed-loop response to be lower than the open-loop for frequencies lower than the **cross-over**.

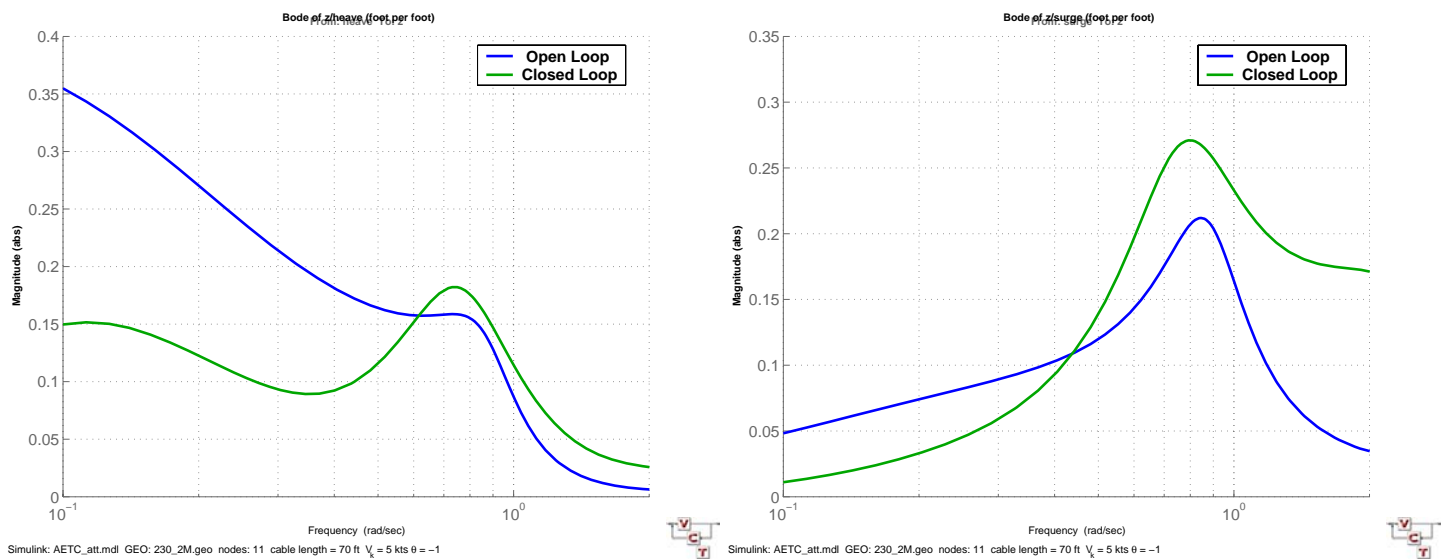


Figure 4-10 · Open-loop vs. closed-loop depth response to tow point (a) heave and (b) surge, 2M configuration

Time Domain **CHECK FIGURE REFs**

The depth response to tow point **heave** (blue) and **surge** (red) disturbance is shown in Figure 4-11. The motion due to surge is particularly large (0.5 to 0.75 FT). The PSD of the depth motion (right) is compared to the tow point motion (left) in Figure 4-12. The output motion scale dominates and the energy is greater by a factor of 1.06 for heave and 2.14 for surge. Though the input energy is overly large for typical tow point surge motion, the response is too sensitive to be considered a robust design. Further illustration is given in Figure 4-13 for the depth response to tow point motion at 2 KTS.

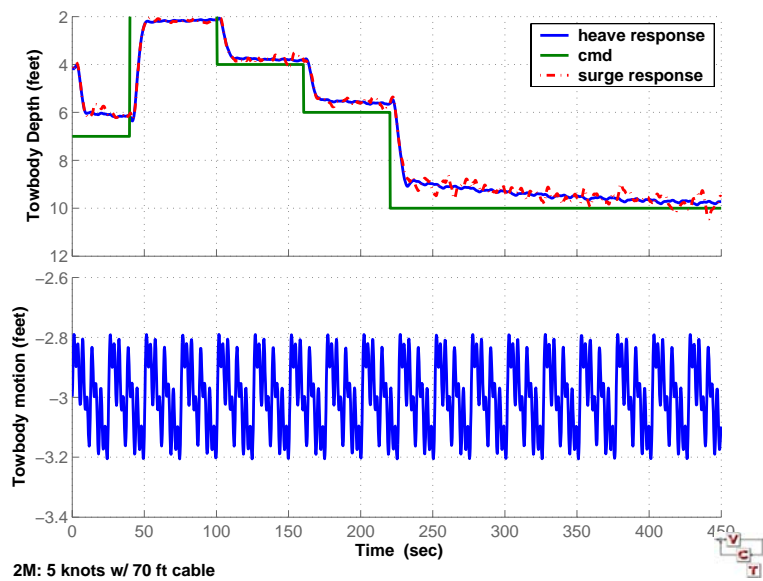


Figure 4-11 · Tow point depth response and tow point heave/surge input 2M configuration at 5 KTS

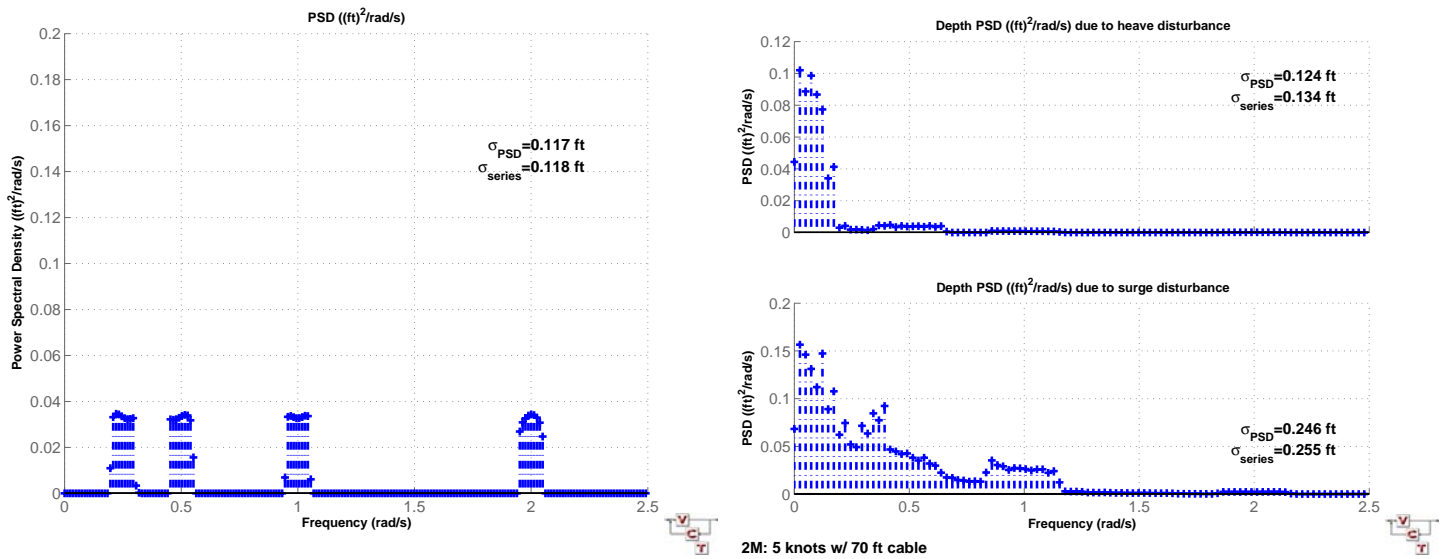
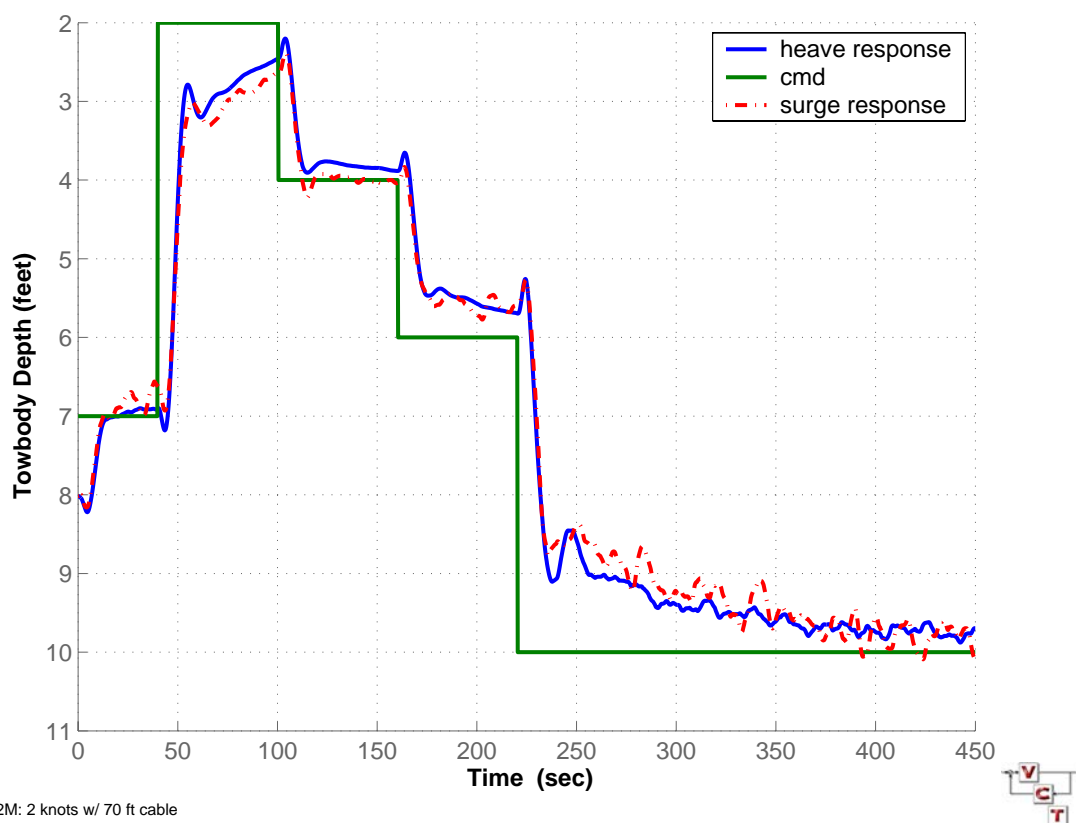


Figure 4-12 · (a) PSD of towpoint motion; (b) PSD of towbody depth 2M configuration at 5 KTS



Kiting

The lack of vertical control surfaces and the small size of the fixed vertical surfaces have led to an interest in lateral stability. Will asymmetries, water currents or sensor biases cause the vehicle to exhibit undesirable lateral motion described as kiting?

A cross current of 0.5 KTS on the 4M configuration traveling at 5 KTS produces ~ 7 FT lateral and $\sim 6^\circ$ heading offsets (Figure 4-14). Roll angle is presented in the top plot, while lateral offset is the middle plot and vehicle heading angle is the bottom. Though these offsets may be undesirable they are not unstable and they can be compensated by shifting the search track.

A 10° roll command while traveling at 5 KTS produces ~ 2.5 FT lateral and $\sim 0.2^\circ$ heading offsets (Figure 4-14). The impact on lateral stability of non-zero roll angles due to sensor bias or other asymmetries is minimal.

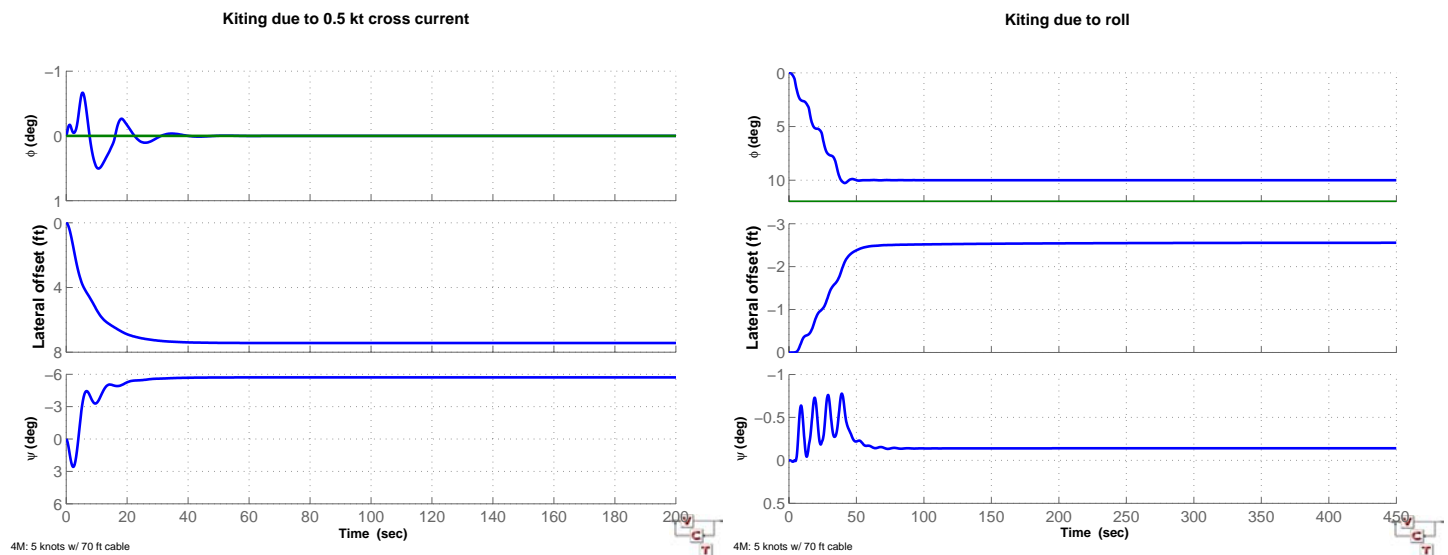


Figure 4-14 · Lateral response of 4M configuration at (a) 5 KTS to 0.5 knot cross current and at (b) 5 KTS to 10° roll command

5• Autopilot Software

The preliminary autopilot code is a modified copy of the autopilot used in the Large Scale Vehicle 2 (LSV2). This is preliminary code and will need revision, modification and complete testing during the detailed design phase.

The following are the preliminary C programming language header (.h) files for the autopilot interface. These contain all the interface information necessary to communicate with the autopilot.

ap_if.h

```

/*
 * AETC Autopilot CSC
 *
 * Filename: ap_if.h
 *
 * Description: This CSU provides the constant, structure, and
 *              interface definitions as well as global variable
 *              declarations for the AETC Autopilot CSC.
 *
 * Programmer: Stacy Hills
 *
 * Creation Date: 06/12/02
 *
 * $Log: /Autopilots/Bluefin/autopilot/ap_if.h $
 */
// 2      6/13/02 1:30p Kkueny
// Updated comments and removed references to other vehicles.
//
// 1      6/13/02 12:31p Kkueny
*/

#ifndef _VCT_APIF_H_
#define _VCT_APIF_H_

/*
 * Constant Definitions
 */
#define AP_DT 0.04

/*
 * Enumerated command modes
 */

/* Fin and rpm modes */
typedef enum {
    ZERO_CMD,          /* set output value to zero */
    AP_CMD,            /* use autopilot computed value */
    EXT_CMD,           /* use externally supplied value */
    SCRIPT_CMD

} OUT_MODE;

/* Depth control modes */
typedef enum {
    DEPTH,              /* track commanded depth */
    ALTITUDE            /* track commanded altitude */

} DEPTH_MODE;

/* Heading control modes */
typedef enum {
    HEADING_ANGLE,      /* track commanded heading angle */
    HEADING_RATE,       /* track commanded heading angle at commanded heading rate */
    OFFTRACK            /* track commanded track line */

} HEADING_MODE;

/* Speed control modes */
typedef enum {
    SPEED_CMD_HIGH,     /* Compute rpm command based on commanded speed */
    SPEED_CMD_LOW       /* Supplement commanded speed with computed boost */

} SPEED_MODE;

/* Mechanical stop modes */
typedef enum {
    LOW_SPEED,          /* High speed stops disengaged */
    HIGH_SPEED          /* High speed stops engaged */

} MECH_STOP_MODE;

/* Autopilot mode */
typedef enum {
    VCT,                /* Uses the VCT autopilot */
    OTHER               /* Uses external autopilot */

} AUTOPILOT_MODE;

/* Filter mode */

```

```

typedef enum {
    FILTER_RESET,          /* Reset autopilot filters */
    FILTER_UPDATE          /* Update autopilot filters */
} FILTER_MODE;

/* Autopilot Measurement Input & Control Output Data Structure */
typedef struct {
    double    aileron,          /* aileron angle (deg) */
    sternplane,          /* sternplane angle (deg) */
    rudder,          /* rudder angle (deg) */
    fin1,          /* port tab angle (deg) */
    fin2,          /* starboard tab angle (deg) */
    rpm;          /* motor rpm */

    MECH_STOP_MODE    mech_stop_mode;    /* mechanical stops position (enum) */
} AP_SET;

/* VCT Autopilot DOF (Degree Of Freedom) Structure */
typedef struct {
    /* Variables for each feedback control loop */
    double    cmd_unlimited,
    cmd_unlimited_last,
    cmd_limited,
    cmd_limit,
    cmd_filt,
    cmd_del,
    cmd_del_limit,
    cmd_limited_last,
    del,
    del_filt,
    del_last,
    del_limit,
    del_int,
    del_int_limit,
    dot_cmd,
    filt;

} DOF;

/*
 * Autopilot Data Structure Definitions
 */

/* Autopilot Navigation Input Data Structure */
typedef struct {
    double    depth,          /* vehicle depth (feet) */
    range_x,          /* x position on range (feet) */
    range_y,          /* y position on range (feet) */
    offtrack,          /* Distance from track (feet) */
    track_hdg,          /* Trackline heading (deg) */
    dircos[3][3],          /* direction cosine matrix[r][c] */
    roll,          /* vehicle roll angle (deg) */
    pitch,          /* vehicle pitch angle (deg) */
    heading,          /* vehicle heading angle (deg) */
    yaw_rate,          /* vehicle yaw rate (deg/sec) */
    roll_rate,          /* vehicle roll rate (deg/sec) */
    pitch_rate,          /* vehicle pitch rate (deg/sec) */
    north_velocity,          /* north velocity (ft/sec) */
    east_velocity,          /* east velocity (ft/sec) */
    down_velocity,          /* down velocity (ft/sec) */
    u,          /* axial velocity (ft/sec) */
    v,          /* lateral velocity (ft/sec) */
    w,          /* vertical velocity (ft/sec) */
    altitude;          /* altitude (feet) */
} AP_NAV;

/* VCT Autopilot Command Structure */
typedef struct {
    AUTOPILOT_MODE    autopilot_mode;

    /* Fin and rpm modes */
    OUT_MODE    log_aileron_mode,          /* The 1st 4 modes */
    log_sternplane_mode,          /* will remain regardless */
    log_rudder_mode,          /* of the fin */

    rpm_mode,          /* configuration on AETC */

    aileron_mode,          /*----The following modes are----*/
    sternplane_mode;          /*----specific to the given----*/
                                /*---fin

configuration on AETC---*/

    /* Depth control mode */
    DEPTH_MODE    depth_mode;

    /* Heading control mode */
    HEADING_MODE    heading_mode;

    /* Speed control mode */
    SPEED_MODE    speed_mode;

    /* Filter mode */
    FILTER_MODE    filter_mode;

    /* other commands */
    double    ext_log_aileron,          /* external logical aileron (deg) */

```

```

        ext_log_sternplane,          /* external logical sternplane (deg)*/
        ext_log_rudder,             /* external logical rudder (deg)    */
        ext_aileron,                /* external aileron (deg)           */
    */
        ext_sternplane,             /* external sternplane (deg)        */
        ext_rudder,                 /* external rudder (deg)            */
    */
        fin_rate,                   /* fin deflection rate (deg/s)      */
    */
    depth,                           /* depth (ft)                       */
    */
        depth_rate,                 /* depth rate (ft/sec)              */
    */
        depth_rate_limit,           /* depth rate limit (feet/second)   */
        pitch_cmd_limit,            /* pitch angle limit (deg)          */
        heading_angle,              /* heading angle (deg)              */
    */
        roll_angle,                 /* roll angle (deg)                 */
    */
        heading_rate,               /* heading rate (deg/sec)           */
        offtrack,                   /* offtrack (ft)                    */
    */
        speed,                      /* speed (feet/second)              */
    */
        ext_rpm,                    /* external rpm (rpm)               */
    */
        rpm_rate,                   /* rpm rate (rpm/sec)              */
    */
        altitude;                   /* altitude (feet)                  */
    */
} APCMD;

/* Autopilot ODR Data Structure */
typedef struct {
    double
        out_fin_cmd_d1,
        out_fin_cmd_d2,
        out_fin_cmd_d3,
        out_elevator_cmd,
        out_rudder_cmd,
        out_rpm,
        comp_q_del_filt,
        comp_q_del,
        comp_q_cmd,
        comp_theta_dot_cmd,
        comp_theta_del_filt,
        comp_theta_del_int,
        comp_theta_del,
        comp_theta_cmd_limited,
        comp_theta_cmd_unlimited,
        comp_z_del,
        comp_z_del_filt,
        comp_z_del_int,
        comp_z_cmd_limited,
        comp_z_cmd_filt,
        comp_r_del_filt,
        comp_r_del,
        comp_r_cmd,
        comp_psi_dot_cmd,
        comp_psi_del_int,
        comp_psi_del_filt,
        comp_psi_del,
        comp_psi_cmd_limited,
        comp_psi_cmd_unlimited,
        comp_y_del,
        comp_y_del_int,
        comp_y_cmd_limited,
        comp_rpm_cmd_unlimited,
        cmd_autopilot_mode,
        cmd_rpm_mode,
        cmd_aileron_mode,
        cmd_sternplane_mode,
        cmd_rudder_mode,
        cmd_heading_mode,
        cmd_speed_mode,
        cmd_mech_stop_mode,
        cmd_ext_aileron,
        cmd_ext_sternplane,
        cmd_ext_rudder,
        cmd_aileron_rate,
        cmd_sternplane_rate,
        cmd_rudder_rate,
        cmd_depth,
        cmd_depth_rate,
        cmd_pitch_cmd_limit,
        cmd_heading_angle,
        cmd_heading_rate,
        cmd_offtrack,
        cmd_speed,
        cmd_ext_rpm,
        cmd_rpm_rate,
        comp_kz,
        comp_kz_i,
        comp_ktheta,
        comp_ktheta_i,
        comp_kq,
        comp_ky,
        comp_ky_i,

```

```

        comp_kpsi,
        comp_kpsi_i,
        comp_kr,
        comp_u_est_limited,
        comp_u,
        comp_speed_cmd_boost,
        comp_ig,
        navout_p,
        navout_q,
        navout_r,
        navout_phi,
        navout_theta,
        navout_psi,
        navout_z,
        navout_u,
        navout_offtrack,
        navout_track_hdg;

    } AP_ODR;

/* Autopilot Input Data Structure */
typedef struct {

    APCMD cmd;                /* autopilot commands */

    AP_NAV nav;               /* vehicle nav info */

    AP_SET meas;              /* current fin positions, rpm */

} APIF_IN;

/* Autopilot Output Data Structure */
typedef struct {

    AP_SET cmd; /* next fin positions, rpm */

    AP_ODR drc; /* diagnostic values to record */

    int   sfw; /* software fault code */

} APIF_OUT;

/* AETC Autopilot I/F Subroutine */
int ap_if(APIF_IN *apin, APIF_OUT *apout);

#endif

```

6 Summary & Conclusions

4M configuration

The 4M configuration is a design with excellent stability, robustness and disturbance rejection. The wing is large enough to provide adequate lift and at sufficient bandwidth to allow for solid control over the entire desired operating speed range with room for measurement error. Control bandwidth does erode at lower speeds, so it is suggested that the vehicle be operated toward the middle and upper end of the speed range for best results.

The design displays sufficient robustness to boat tow point motions and currents. Any lateral motion due to currents is stable and gentle, such that it may be compensated by adjusting the search track.

Altitude control has the ability to follow gentle bottom trends typical of shallow water areas to be searched. Response to step command inputs is not rapid, but the performance of a rapid climb should be sufficient for use in avoiding obstacles identified by the tow boat mounted echo sounder.

The commanded roll angle should always be set to zero or should not exceed a couple of degrees as may be needed to compensate for sensor bias or vehicle asymmetry. Roll control should not be used to fly coordinated turns with the vehicle. At low speeds, roll angle commands more than a few degrees may be unstable.

This configuration provides a robust and stable UXO sensor platform.

2M configuration

The 2M configuration, by virtue of limited lift due to its small size, has significant stability and control issues. It may be unable to span the entire desired depth range as it takes over 3 minutes to converge on a depth command of only 5 FT. The lower end of the speed envelope would need to be raised in order to provide for enough margin in speed measurement to assure stable operation. The vehicle is uncontrollable at 1 knot of speed.

Finally, even small tow point disturbances create unacceptably large vehicle depth motions. The vehicle has better tow point disturbance rejection with the autopilot turned off.

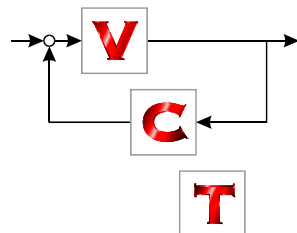
This configuration does not provide a robust and stable UXO sensor platform, and it should be eliminated as a candidate.

VCT TECH MEMO 02-06

CONCEPT DESIGN FOR A MARINE UXO SENSOR PLATFORM

THOMAS F. TUREAUD

KENNETH W. WATKINSON



Vehicle Control Technologies, Inc.

11180 SUNRISE VALLEY DRIVE · SUITE 350 · RESTON, VA
703-620-0703 FAX 703-620-1734 WWW.VCTINC.COM

Prepared for

AETC

1225 Jefferson Davis Hwy #800
Arlington, VA 22202

November 2002

Under
P.O. SD-949

Table of Contents

| | |
|---|----|
| 1· Introduction | 1 |
| 2· Requirements..... | 3 |
| Table 2-1 · Operational Requirements and Design Decisions | 5 |
| 3· Design Alternatives | 7 |
| Figure 3-1 · Surface Tow with Flyable Platform | 7 |
| Figure 3-2 · Winch Control with Vertical, Rigid Support Guide | 7 |
| Figure 3-3 · Combination Vertical Support with Flyable Platform | 8 |
| Figure 3-4 · Self-Propelled Platform | 8 |
| Figure 3-5 · Sled or Wheel Type | 8 |
| Sensor Platform Concepts | 9 |
| Table 3-1 · Concept Design Alternatives | 10 |
| 4· Other Systems & Lessons Learned..... | 11 |
| Table 4-1 · Existing Systems Summary | 12 |
| 5· Instrumentation..... | 13 |
| Figure 5-1 · Sensors for Vertical Position and Control | 14 |
| Figure 5-2 · Sensors for Horizontal Position and Control | 14 |
| Table 5-1 · IMU Sensor | 15 |
| Table 5-2 · Depth Sensor | 15 |
| Table 5-3 · Control Fin Actuators | 15 |
| Table 5-4 · Echo Sounders | 15 |
| 6· Down Select Platform..... | 17 |
| Geometry, Weight and Balance | 17 |
| Figure 6-1 · Perspective View of Survey Platform | 17 |
| Figure 6-2 · Side View of Platform | 17 |
| Figure 6-3 · Front View of Platform | 18 |
| Figure 6-4 · Platform with GPS Poles | 18 |
| Figure 6-5 · Top and Side View with GPS Poles | 18 |
| Figure 6-6 · Schematic of Structural Layouts | 19 |
| Table 6-1 · Component Weight and Size | 20 |
| Figure 6-7 · Survey Platform Layout red and green are the survey sensors, blue and magenta are the platform's structural components, cyan is the floatation elements | 20 |
| Towing Craft and Launch & Recovery | 21 |
| Figure 6-8 · Cable Drum and Clutch | 21 |
| Hydrodynamic Parametric Study | 21 |
| Nominal Design with Speed Variation: 2 to 5 KTS | 22 |
| Figure 6-9 · Nominal Design | 22 |
| Figure 6-10 · Nominal Design | 22 |
| Aerodynamic Center of Wing: 20% to 50% of Mean Aerodynamic Chord | 23 |
| Figure 6-11 · Wing A.C. Variation | 23 |
| Tow Point Location: 0, 2, 4 FT | 24 |
| Figure 6-12 · Towpoint Location Variation | 24 |
| Cable Length: 30, 50, 70 FT | 25 |
| Figure 6-13 · Cable Length Variation | 25 |
| Location of X_{CG} : -0.06" to 0.06" | 26 |
| Figure 6-14 · X_{CG} Variation | 26 |
| Location of Z_{CG} : 0.25" to 0.75" | 27 |
| Figure 6-15 · Z_{CG} Variation | 27 |
| 4 meter Platform | 28 |
| Figure 6-16 · 4 Meter Survey Platform Layout | 28 |
| Figure 6-17 Component Weights for 4 Meter Platform | 29 |
| Figure 6-18 · Catenary Shapes for the 4 meter Platform | 29 |
| Figure 6-19 · Depth Limits for the 4 meter Platform | 29 |
| Figure 6-20 · Stern Plane angle range for the 4 meter Platform | 29 |
| Figure 6-21 · Tension Map for the 4 meter Platform | 29 |
| 7· Summary | 31 |
| A· Memorandum | 33 |
| Sensor Vertical Position | 33 |
| Tow Body Depth Sensor or Fathometer | 33 |
| Tow Boom Pitch Measurement | 33 |
| Tow Body Attitude | 34 |
| Sensor Horizontal Position | 34 |
| Tow Body Heading | 34 |
| Summary | 34 |
| Marine MTADS Survey Platform Requirements Document | 35 |

I • Introduction

This document describes the concept design performed by Vehicle Control Technologies, Inc. (VCT) in support the AETC effort to develop an Underwater UXO (Unexploded Ordinance) vehicle. The concept design study is for the development of an underwater vehicle (platform) to support UXO search technologies. The UXO search technologies are those developed by AETC and their design and function are not addressed herein.

The present report is the first of a series of two reports describing the development of the marine vehicle concept design. The concept design examines several systems and performance options and then down-selects to a best candidate. In the concept, UXO sensor implementation and operation are the primary concerns, but additional sensors to operate, control and locate the marine vehicle are accounted for. This first report describes the UXO marine search requirements, the design alternatives and the resulting steady state hydrodynamic performance of the platform concept design.

The marine platform is intended for operation in shallow environments. These initial concept design results are presented in terms of vehicle geometry, size, weight, component layout and basic hydrodynamic performance. Also discussed are launch and recovery operations, and concepts for the towing platform and connection device. The second report of this series will develop the dynamics of the marine system including the control system required to operate the vehicle.

2· Requirements

The requirements for the operation and performance of the marine UXO vehicle are driven by the UXO search sensors. Not only does the sensor performance determine these requirements, but the geometry has as important a role, due to the large size of the sensors. AETC has specified the top-level requirements for the sensor operation and these are listed in Table 2-1.

The first column of Table 2-1 lists the top-level requirements describing the overall system, such as sensor number and size, speed and position accuracy. The second column lists the next level of requirements, adds detail to the first level, and supports them with additional components. The third column is a list of design decisions that stem from both levels of requirements. The design decisions apply directly to the marine system and, at this level, are mostly independent of the actual platform concept. For example, requirement 9 states that the sensor platform should rise to the surface when the survey vessel is stopped. This implies that the platform should be designed with positive buoyancy; that is, the weight of the platform is less than that of the amount of water it displaces.

Stated in general terms, the requirements state that the marine platform must transport the specified UXO sensors in a known, measurable manner through a shallow water environment. The speed of the traverse should be sufficient to support expected coverage rates. The UXO sensors must be positioned to within approximately 1 meter of the bottom, and the location of each sensor needs to be measured to within a prescribed accuracy. Construction of the sensor platform must be magnetically clean. Transport and launch of the system should be taken into account.

Derived from the requirements is a minimum set of sensors that will be used. One set will support the actual UXO search, and one set will support the operation of the platform. These are listed below. The platform control sensors are described in the Instrumentation section.

- › UXO sensors
 - Seven (7) magnetometers spaced at 1.0 to 1.5 meter increments perpendicular to the direction of travel.
 - Electro-Magnetic sensors: One coil 8m by 1m and 8 coils 1m by 0.5 m.
- › Platform Control Sensors
 - Echo sounder
 - Inertial Measurement Unit (IMU)
 - Heading Compass
 - Depth gage

Of all the requirements, two require especially close attention. These are requirements 5 and 11, which address the position and attitude accuracy of the platform sensors. The positions of the survey sensors must be accurately known with respect to the master GPS antenna. Nominal master GPS position errors are vertical 10 cm and horizontal 5cm. The error of the survey sensors must be small with respect to these base GPS errors. Measurements of the platform position and attitude, relative to the master, above-surface GPS antenna must minimize the additional errors involved in translating these positions to the sensor positions. To support this, angles used to translate platform position to sensor positions (i.e. platform attitude sensors) must be accurate to 0.1°. This requirement cannot be met with a COTS tow body heading sensor. To meet this requirement a GPS antenna on tall poles extending out from the water surface and high-quality IMU and attitude computation algorithms must be used.

The document in Appendix A discusses these accuracy issues in detail and presents the following summary

1. Position of the survey sensors must be known to within a few centimeters with respect to the master GPS antenna.
2. Rigid tow boom angle measurements of sufficient accuracy to support this are not practically attainable.
3. Tow body heading measurement with sufficient accuracy to support this is only attainable with extensive on-site compass compensation and calibration.
4. Rigid mounts of two GPS antennae extending from the sensor platform to above the water surface provides the required sensor position accuracy.

Or stated another way, if position errors from cable angle and tow body heading measurements are not acceptable, then rigid mounting of a GPS antenna extending from the sensor platform to above the water surface will provide the required sensor position accuracy. Two GPS antennae are required if the heading sensor accuracy for sensor along-track position errors is not acceptable. Error contributions from support deflections must be calculated.

| AETC Marine Platform Requirements and Design Decisions | | |
|---|--|--|
| Top Level Requirement | 2nd Level Requirements | Design Decisions |
| 1 House 7 magnetometer sensor array to nominally cover a 9 meter swath. | Sensor mounts spaced at 1.5m increments, perpendicular to direction of travel. | Goal to use one platform to house both magnetometers and EM sensors. EM will have to be removed for magnetometer surveys. |
| House 8 electro-magnetic sensor array. | EM sensor has one coil 8mx1m and 8 coils 1mx0.5m. | |
| 2 Sensor orientation must be adjustable and securable | Mounting gimble provides tilt adjustment, with locking mechanism | |
| 3 Provision for mounting of sensor electronic packages | Electronic packages must be mounted 2.5 to 3.5m from the sensors. Cables running between the sensor and the electronic packages will be secured, as will cables running from the electronic package to the vessel cabin. | |
| 4 Sensors must be mounted in a magnetically clean environment | No electrically conductive or magnetic material is to be used within 1m of the sensor. The use of metal and conductive material will be avoided completely where possible, no carbon composites. | Central sensor platform constructed of fiber glass. Some aluminum frame components on extremities, if possible. |
| 5 GPS technology allows position measurements to 0.05 m horizontal and 0.1 m vertical accuracy. Measurements of the platform position and attitude, relative to above surface GPS antennae must minimize the additional errors involved in translating these positions to the sensor positions. | Angles used to position center of platform, relative to the master GPS antenna, assuming a 30 m arm must be accurate to 0.05° [sensor platform position uncertainty wrt master GPS antenna less than 3cm]. Angles used to translate platform position to sensor positions (i.e. platform attitude sensors) must be accurate to 0.1° [sensor position uncertainty due to platform orientation errors less than 3cm]. | Achieving angle measurement accuracy on rigid towing bar impractical. Extend platform-mounted GPS antennae above the water surface. Rigid towing bar not required for platform positioning accuracy. Therefore can use tow cable to minimize towing vehicle modifications. Heading accuracy of 0.1° impractical for magnetic compass. Extend platform-mounted GPS antennae above the water surface. Require AHRS-quality IMU for pitch and roll angle accuracy. Could eliminate platform-mounted GPS antennae if lesser accuracy can be accepted. |
| 6 The magnetic signature of DC electrical currents necessary for platform control devices must be recognizable and removable for the measured total magnetic field data. | The 'on-time' of these currents must be: <than 0.1 sec duration, limited to 10% duty cycle, and easily demarcated in the data using the A/D logging functionality of the existing data acquisition system (single pole, 0 to 10v dc). | Place control surface actuators in far aft location. Manage actuator motor operating duty cycle as required to avoid excessive degradation of sensor performance. |
| 7 Platform must be operable at speeds sufficient to allow efficient survey coverage rates | Survey speeds of 3 to 10 kts are considered reasonable, depending on sea and bottom conditions | Design to 5 kts maximum speed. |
| 8 Platform must 'fly' nominally 1 m above the sea floor at survey speed. | The platform height above the sea floor must be monitored and used as input to for a vertical position control system. The vertical position control system must maintain sensor height to within 0.2 m | echo-sounder needed on sensor platform. Depth sensor on sensor platform and towing craft echo-sounder too corrupted by wave motion. Two actuator/control surface arrangements to control depth and roll using fractional horsepower motors. |
| 9 Platform should ride to surface at very slow speeds or when survey vessel is stopped. | Platform buoyancy must allow for control of platform at normal survey speeds while maintaining positive buoyancy over a suitable range of water density conditions | Design for W-B < 0 for depth range (0 to 4m). There will be some minimum forward speed to produce the necessary down force to reach maximum depth. |
| Platform design should consider the need to operate in minimal water depths | | Skids and rugged surfaces on bottom of the sensor platform. Minimize snag junctures for fouling. |
| 10 Platform accelerations must avoid our magnetic target response periodicity | Target response signatures occur from 2 to 10.0m along track. At 10 kts this equates to periods of 0.4 to 1.9 sec, and at 5 kts 0.8 to 3.9 sec. Altitude and attitude changes should avoid this periodicity if possible. | Desirable depth and roll motion characteristics designed into autopilot. Fixed vertical fins designed to provide desired lateral stability and turning characteristics. |
| 11 Platform must have provision for mounting of auxiliary sensors | echo-sounder, fluxgate magnetometer, tilt-meter. | Use same echo-sounder as on towing craft. Interlace pings. Use AHRS for combined compass and tilt measurements. |
| 12 Platform must be deployable and recoverable from standard boat launch ramps | | Trailer stowage may require disassembly of GPS antenna mounts and perhaps towing bridle. Goal to keep sensor platform/control surface unit as one. Vertical fins on either side of control surface provide protection to prevent control surface damage. |
| 13 Platform must be transportable on or in a trailer designed for towing | | Note: Over-road vibration requirements will dominate much of the instrument mounting design unless all instruments are removed for transit. |

Table 2-1 · Operational Requirements and Design Decisions

3• Design Alternatives

Several design concepts were conceived as general approaches to the marine UXO survey platform. The concepts generally are comprised of a combination of a sensor platform and a towing craft. The sensor platform contains the search sensors and is manipulated through the marine, shallow water environment by the towing craft. For positioning the sensors, the platform is either a passive unit controlled by external devices, or the platform controls its position with an active onboard system. The towing craft is generally a separate vehicle and provides the propulsion to move the sensor platform.

These concepts can be grouped into categories describing the overall operational characteristics. The groupings are shown below. With these groupings a list of advantages, disadvantages and design decisions have been developed. These results are shown in Table 3-1.

1. Surface Tow with Flyable Platform

Surface craft tows the sensor platform using rigid boom or flexible cable. The platform is close to neutrally buoyant and controls its depth via an on board control system.

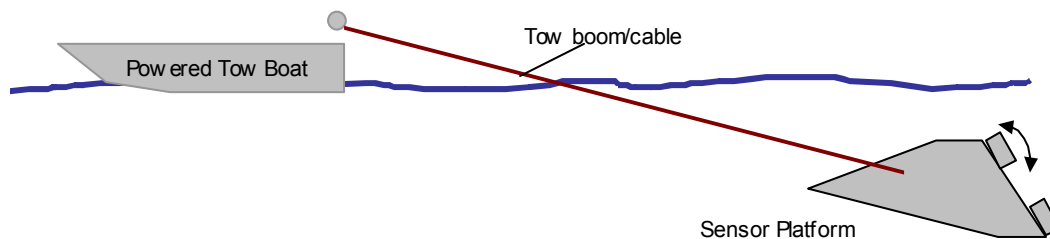


Figure 3-1 · Surface Tow with Flyable Platform

2. Winch Control with Vertical, Rigid Support Guide

Sensor array is supported by a guide shaft and is moved by winch control according to an onboard control system. The example surface craft is a Catamaran and is self-propelled; pontoons reduce roll motion due to waves.

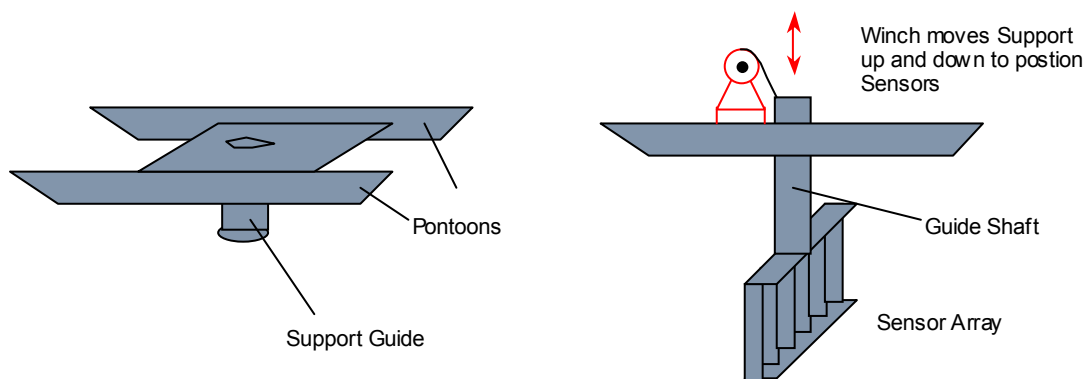


Figure 3-2 · Winch Control with Vertical, Rigid Support Guide

3. Combination Vertical Support with Flyable Platform

Sensor array is supported by a center shaft; the array platform controls sensor position by “flying” the platform. Support craft may be towed by another surface ship to distance metal from sensors.

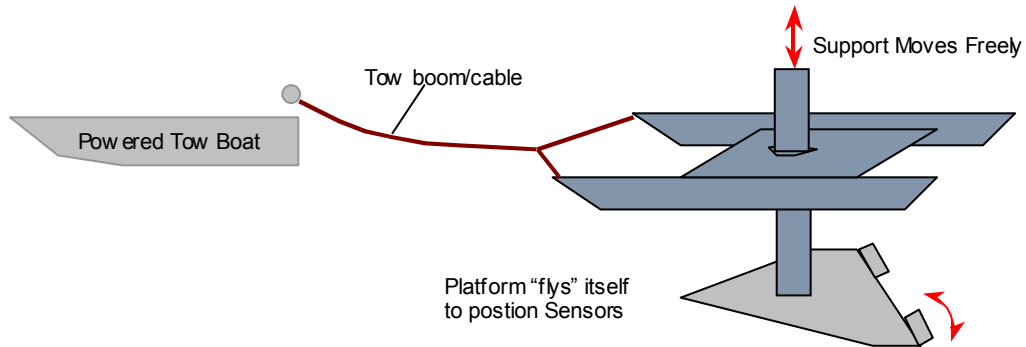


Figure 3-3 · Combination Vertical Support with Flyable Platform

4. Self-Propelled Platform

Sensor platform is self-propelled and is tethered to a surface craft for data and information transfer.

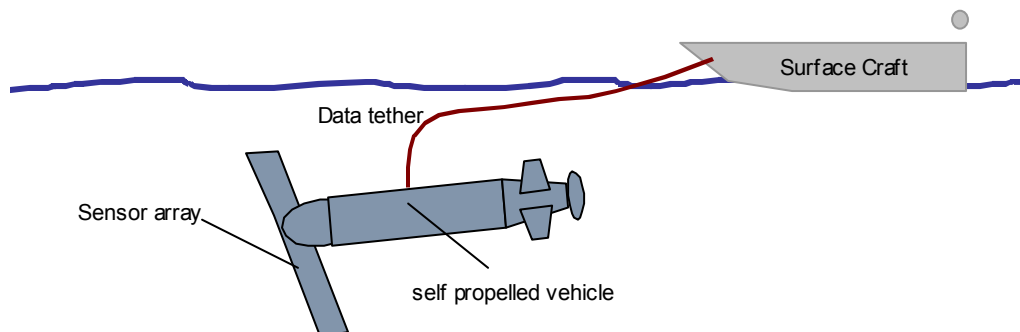


Figure 3-4 · Self-Propelled Platform

5. Sled or Wheel Type

Sensor platform is dragged or rolled across the bottom. No depth control required as platform follows the bottom contour.

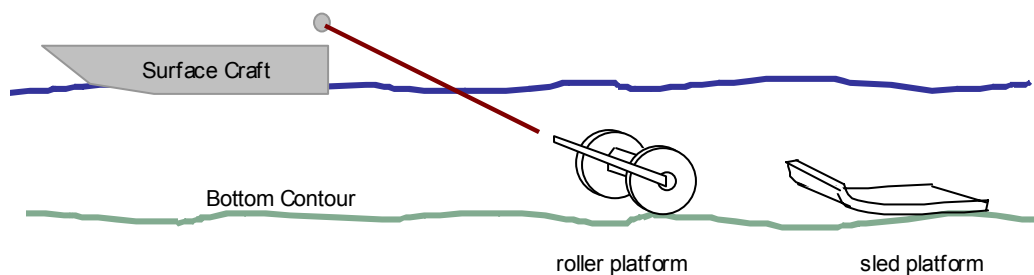


Figure 3-5 · Sled or Wheel Type

Sensor Platform Concepts

1. **Wing**

Aerodynamic shaped platform conforms around sensors. The platform is positioned by either a flyable configuration or by a winch control system.

2. **Segmented Grill**

Sensors are individually faired and assembled as a matrix. The platform is not aerodynamic and must be brute forced through the water. Platform is positioned as in 1.

3. **Sled**

The platform is just a large sled with either a flat bottom or runners. The system is dragged over the bottom.

4. **Roller**

Platform is rolled along bottom. Steam roller type configuration. Sensors are suspended with the rolling system.

| Concept Description | Advantages | Disadvantages | Design Decision |
|--|---|---|---|
| Wheel- or sled-supported sensor platform | Simple altitude-keeping mechanism. | Limited top speed, perhaps 2 to 3 KTS | Eliminate based on bottom type and speed limitations (requirement 7). |
| | Can be made to work in extremely shallow water. | Silt or mud bottom will pose significant bottom penetration, bog-down problems. | |
| | | Tall GPS masts are required to provide positioning accuracy. | |
| Vertical rigid support booms rigidly mounted sensor platform | | System must be very heavy and/or have dive planes for higher speed operation. | Eliminate based on inability to meet requirements 9, 12 & 13 due to topside equipment size, complexity, portability issues and problems for very shallow water. Also speed limits due to deflections and vibration (requirement 7) and probably requirement for a dedicated raft are significant. |
| | No submerged actuation systems. | Altitude control requires powerful topside motors and structurally robust mechanism to achieve sufficiently accurate altitude-keeping and rapid avoidance response. | |
| | Buoyancy precision not required. | Operation in very shallow water complicates towing craft structural support mechanism. | |
| | echo-sounder is the only submerged instrumentation required. | Potential for extensive damage to support booms and surface craft from running aground or hitting large objects. | |
| | GPS antennae can be placed on tops of booms to provide sensor position. | Portability difficulties due to size and complexity of topside equipment and sensor measurement corruption by the proximity of boat motors and generators may require dedicated raft. | |
| Vertical rigid support booms gimbal-connected to altitude- and roll-controlled sensor platform, sliding contact booms/surface craft. | | Deflection of booms due to thrust/drag loading problematic for attaining sensor position accuracy. | Eliminate based on complexity/portability/costs/speed/depth limitations; e.g. deflection and vibration, dedicated raft requirement, serious difficulties for use in very shallow water. Only reason to use this option is if the track-keeping control advantage is a deciding factor. |
| | | Limited top speed | |
| | No topside altitude-keeping motor/controller/mechanism. | Submerged control fin actuation system required. | |
| | GPS antennae can be placed on tops of booms to provide sensor position. | Potential for extensive damage to support booms and surface craft from running aground or hitting large objects. | |
| | Good sensor platform position control capability | Portability difficulties due to size and complexity of topside equipment and sensor measurement corruption by the proximity of boat motors and generators may require dedicated raft. | |
| Rigid tow bar connection to towed sensor platform | | Buoyancy precision required. | Eliminate based on complexity/costs for tow bar-topside connection. |
| | Relatively simple topside tow bar connection mechanism. | Submerged actuation system required. | |
| | Low damage potential for running aground or hitting large objects. | Buoyancy precision required. | |
| | Top speed limited mostly by obstructions and topography. | IMU tilt instrumentation required in submerged body. | |
| | No dedicated raft required to provide separation from boat motors and generators. | Tall GPS masts or acoustic positioning system on sensor platform are required to provide positioning accuracy. | |
| Tow cable to towed sensor platform | Simple topside tow cable connection. | Submerged actuation system required. | Possible configuration. Most simple and probably least cost and portable but has some position control and handling issues. |
| | Low damage potential for running aground or hitting large objects. | Buoyancy precision required. | |
| | Top speed limited mostly by obstructions and topography. | IMU tilt instrumentation required in submerged body. | |
| | No dedicated raft required to provide separation from boat motors and generators. | Tall GPS masts or acoustic positioning system on sensor platform are required to provide positioning accuracy. | |
| | | Must develop approach for stopping and turning the towed sensor platform. | |

Table 3-1 · Concept Design Alternatives

4 Other Systems & Lessons Learned

In addition to the Design Alternatives described in Section 3, several existing UXO marine platforms were examined. The source of the information describing these systems was originally provided to VCT by AETC.

At the Marine and Airborne UXO forum of 2002 several papers were included that presented either reviews of underwater UXO systems or descriptions of individual systems. This section presents a summary of the concepts and the described lessons learned ^{1, 2, 3}.

Selected papers discuss marine systems in the shallow water environment, usually 0 to 20 meters depth. The review focused on learning about the systems developed, how they were operated, and what issues were encountered. Table 4-1 lists a summary of the review along with a list of lessons learned from each system.

Several organizations have attempted to field a marine UXO system. Most consisted of a survey sensor suspended in the water by a rigid support structure. This sensor platform is adjusted for height and towed by a surface craft. A common problem with this type was array vibration – presumably due to the underwater structure. One system was towed as an underwater sled. Most of the described systems had trouble with accurate sensor position determination.

¹ Wold, R. and T. Vali, "A Review of Underwater UXO Systems in Europe", 2002 Marine and Airborne UXO Forum.

² Pehme, P., Q. Yarie, K. Penney, J. Greenhouse and D. Parker, "Adopting the Geonics EMGS for UXO Surveys in 0-20 meters of Water", 2002 Marine and Airborne UXO Forum.

³ Sontec, "System Data and Explanations Underwater Survey", www.sontec-gmbh.de

| Organization | System | Sensors | Description | Surface Craft | Lessons Learned |
|---|--|--|--|---|---|
| GTK (Geological Survey of Finland) | Underwater Cesium Magnetometer Array #1 | 4 Geometrics G-880, 1.8m spacing | light aluminum biplane-like wing 7m span | 3m x 4m raft, towed | Unable to determine sensor positions accurately enough to suit the client. System replaced with rigid boom system. Designed for 0 - 20m for silt or mud or depth varying significantly. |
| | Underwater Cesium Magnetometer Array #2 | | 7m sensor support spar, 2 vertical booms held in place by support lines between booms and boom-to-raft | 12m x 6m raft, powered | Vibration problems - presumably with increasing speed - and it only went 2 kts! Maximum depth 15m, minimum depth ? |
| Dredging Company German Subsidiary, Kokkola project | Flux-Gate Gradiometer Magnetometer Array | 8 flux-gate gradiometers, 0.5m spacing | 4.5m array, one vertical boom - 10m aluminum sail boat mast, raise and lower by hand winch | 4m x 6m raft, pushed | Underwater array was not as stable (as the GTK array) and was subject to considerable vibration. |
| BO.SCA, Venice, Italy | Bottom-towed Underwater Sled | 2 transverse cesium magnetic sensors, 3m apart | sled 3m x 3.5m, towed up to 4 kts, dive plane to keep down, compressed air to bring up | Craft of opportunity | Only works on sand or hard bottom. Requires pre-survey by sidescan for obstacles Requires post-survey by sidescan to verify coverage (sled makes line in sand during survey) |
| University of Hamburg | Towed sled Ordinance Clearance Authority of Hamburg project | 4 cesium magnetometers, 1.5m apart | 6m sensor spar, sled runners on ends, 1.8m altitude, positioning using acoustic transducers on ends to receiver on boat, also inclinometer and altimeter | towed from bridle to small boat, DGPS on boat | no lessons learned provided |
| GeoPro | flies at constant depth, array adapted from University of Hamburg system | 4 cesium magnetometers, 1.5m apart | 6m sensor spar, towed at constant depth, positioning using acoustic transducers on ends to receiver on boat, also inclinometer and altimeter | towed from bridle to small boat, DGPS on boat | no lessons learned provided |
| Sontec | Bottom-towed Underwater Sled, operated from a variety of craft | 4 to 8 cesium magnetometers | fixed frame set to be 0.25m to 2m off the bottom using sled runners | alloy-boats, canoes, zodiacs for very shallow water 0.2 to 4m, alloy survey boats for water to 10m, hovercraft for transition zone, swamps & tidal regions | no lessons learned provided |
| Geonics | surface or manually depth-controlled towed sensor for 0 to 20m of water | Geonics EM61 MK2 | depths <= 2m small surface raft with 1x1m transmitter coil and receiver all floated on surface, for depths > 2m surface raft for 4.8x8m transmitter coil and receiver on planing board whose maximum depth is limited by lines to the towing craft | small boat with tow line long enough to suitably reduce motor and generator interference, DGPS on raft, echo-sounder on tow craft - tow speed 2kts (4km/hr) | elevation of the transmitter and the receiver coil above the seabed could not be highly controlled - data sets suffer from a variable filtering by way of a changing distance from the seabed - towing mechanics should be improved |

Table 4-1 · Existing Systems Summary

5• Instrumentation

Concerning the operation of the marine platform, the types of measurements required are altitude, depth, UXO sensor X-Y position, heading angle, roll and pitch angles. These measurements will be used for both location of the positions of each UXO sensor with respect to the master GPS and for control of the platform.

There are five instruments that will be carried on board the towed platform. These are as follows:

- › IMU Table 5-1
- › Depth Sensor Table 5-2
- › Fin actuators (2) Table 5-3
- › Echo-Sounder Table 5-4

The **recommended units** are shown in green in the tables.

For vertical control (Figure 5-1), the echo sounders on the towing craft GPS antenna post and sensor tow body provide the needed vertical accuracy that is less than 2.5 CM. The echo sounder on the bottom of the GPS antenna post gives bottom depth with respect to the geoid, while the echo-sounder on the tow body gives tow body depth with respect to the bottom. The two signals can be correlated with recorded time shifted by delay in passage of tow body over the bottom point passed over previously by the towing craft echo sounder. Two additional sources may contribute to the vertical error. These are as follows:

- › Corruption by tow craft roll and pitch is probably acceptable but could be compensated for if desired ($\pm 10^\circ$ results in 8 CM error in 5m of water)
- › Corruption of sensor vertical position estimates due to tow body pitch and roll angle errors – up to 0.4° error acceptable – this is readily achievable

Horizontal sensor position errors with respect to the master GPS antenna need to be less than 3 or 4 CM. Survey sensor position (Figure 5-2) with respect to the tow body tow point can be estimated with sufficient accuracy with COTS magnetic compass hardware and software. A 0.25° accuracy can be achieved with standard compensation/calibration and would contribute less than 2 CM to sensor position error at a maximum span of 15 FT in either direction. Cable length calibration and tow point vertical separation measurements can be used to obtain horizontal range GPS-to-tow body tow point accurate to about 3 to 5 CM. A tow cable horizontal angle measurement for cross-track position estimation would be necessary to attain a 0.25° accuracy for a 20-meter length.

Vertical Position

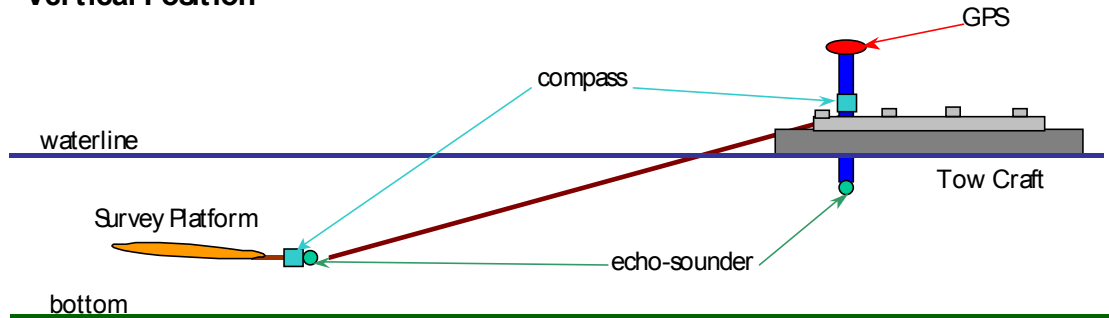


Figure 5-1 · Sensors for Vertical Position and Control

Horizontal Position

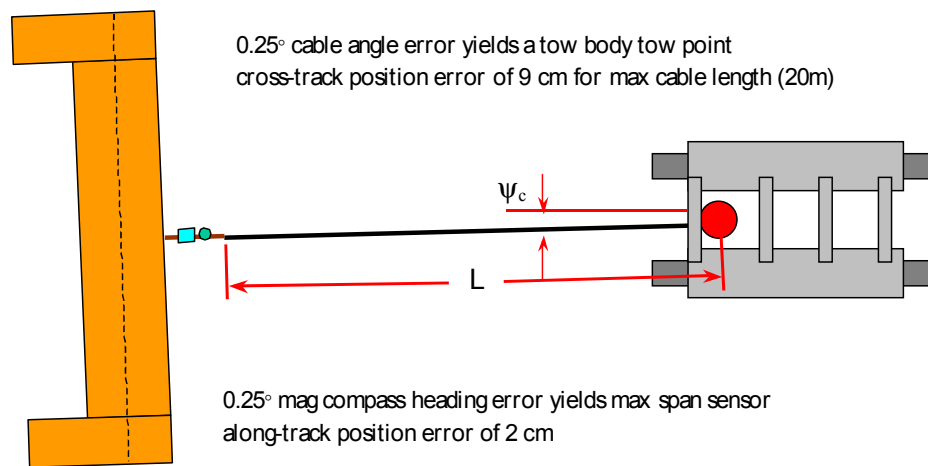


Figure 5-2 · Sensors for Horizontal Position and Control

Inertial Measurement Unit

| Manufacturer | Unit | Gyro Specs | | | | | | Accel Specs | | | | | Size | Weight | Price |
|-------------------|---------------|------------------|-----------------------------------|--------------------------------------|--|-------------------|-------------|--------------|--------------------------------|----------------------------------|---|-------------------|------------------------|--------|--------|
| | | Range (deg/s) | Random Walk (deg/root hour) | Bias Stability in run (deg/hr) | Bias Stability turn-on-to- turn-on (deg/hr) | Bandwidth (Hz) | Type | Range (g) | Random Walk (mg/root Hz) | Bias Stability in run (mg) | Bias Stability turn-on-to- turn-on (mg) | Bandwidth (Hz) | | | |
| Litton | LN-200 | 1000 | 0.04 - 0.1 | 0.35 | 1 - 10 | 500 | FOG | 40 | 0.05 | 0.05 | 0.2 - 1.0 | 100 | 3.5" dia X 3.35" h | | \$25k |
| Honeywell | HG1700 | 1000 | 0.125 - 0.3 | ? | 1 - 10 | 100 | RLG | 50 | ? | 1 | | 600 | 3.7" dia X 2.9" h | | \$11k |
| Systron Donner | DQI IMU | 1000 | 0.035 | 3 | 10 | 100 | Solid State | 70 | 0.06 | 0.2 | 1.5 | 600 | 3.189" X 3.53" X 3.84" | | \$15k |
| AGNC | 2000 cmlMU | 100 | 0.1 | 17 | 17 | 700 | Solid State | 2 | ? | 0.2 | ? | 500 | 3.235" X 1.7" X 1.1" | | \$8k |
| Crossbow | IMU 400CA-100 | 100 | 0.85 | 3600 | 3600 | 10 | Solid State | 2 | 10.2 | 8.5 | ? | 75 | 3" X 3.75" X 3.2" | <1.3 | \$3.5k |
| | IMU 300CB-100 | 100 | 0.85 | 3600 | 3600 | 10 | Solid State | 2 | 15.3 | 30 | ? | 75 | 3" X 3.75" X 3.2" | <1.3 | \$3k |
| | IMU600CA-200 | 200 | 1.25 | 108 | 108 | 100 | FOG | 2 | | 8.5 | ? | 100 | 5" X 6" X 4" | 3.5 | \$8.5k |

Table 5-1 · IMU Sensor

Depth Sensors

| Manufacturer | Sales # | URL | Type | Model | Price | Absolute Pressure | | | | Power | A/D Resolution |
|--------------|--------------|---|---------|----------|--------|-------------------|----------|------------------|--|---------------------|----------------|
| | | | | | | Range (psi) | Accuracy | Update Rate (ms) | | | |
| Heise | 251-473-1692 | http://www.heise.com/ | Digital | DXD | \$710 | 0-15 | ±0.02% | 15 to 50 | | 12 to 24 Vdc 15mA | 23 bits |
| Sensotec | | http://www.sensotec.com/index.html | Analog | FP2000 | \$505 | 0-15 | ±0.25% | | | 9 to 29 Vdc | - |
| Mensor | 800-984-4200 | http://www.mensor.com/Digital_Pressure_Transducer_6000.htm | Digital | CDS6000E | \$900 | 0-15 | ±0.02% | 20 | | 6-20 Vdc | Up to 1 PPM |
| TTI | | http://www.tti-global.com/Product.asp?Param1=DPM | Digital | DPM | >\$995 | 0-15 | ±0.025% | | | 9 Vdc 50mA | |
| Honeywell | 800-323-8295 | http://www.ssec.honeywell.com/pressure/ | Digital | PPTR | \$780 | 0-15 | ±0.10% | 8.33 | | 6 to 30 Vdc 19-27mA | Up to 10 PPM |

Table 5-2 · Depth Sensor

Actuators

| Type | Company | Model | Price | Depth | Torque | Max Angular Rate | Wt in | Wt in | Backlash | Casing Metal | | Power | Body | |
|--------------------------|------------------|-----------|---------|------------|----------|------------------------|----------|------------|----------------------------------|----------------------------------|---------------------|------------|---------|--------------------|
| | | | | Limit (ft) | (ft-lbs) | | Air (lb) | Water (lb) | | Type | Shaft | | Filling | Motor Type |
| Rotary Actuator | Tecnadyne | Model 60 | \$4,321 | 5000 | 60 | 0-90o/sec @ 1.5A | 5.5 | 4.2 | | 6061-T6 Al | passivated Type | 48-280 VDC | oil | DC Brushless |
| | | | | | | 0-45o/sec @ 1.0A | | | | | 303 stainless steel | | | Rotary, rare earth |
| | | Model 20 | \$3,621 | 5000? | 20 | | | | | | | | | |
| | | | \$3,521 | | | | | | | | | | | |
| Tilt & Pan (single axis) | ROS | R-10 | \$2,455 | 100 | 10 | 4.9 deg/sec (0.82 rpm) | 6.5 | 4.15 | 36 arcminutes | 6061-T6 Al | | | air | |
| | | R-10-FB | \$3,310 | 100 | 10 | 4.9 deg/sec (0.82 rpm) | 8.2 | 4.8 | 37 arcminutes | 6061-T6 Al | | | air | |
| | Kongsberg-Simrad | OE10-101 | \$5,775 | 10000 | 19 | (nominal) 3.6 rpm | 13 | 10 | <3 arcminutes | 6082-T6 Al caps, LM25 Al body | | 24 VDC | oil | |
| | | | | | | | | | harmonic gears for zero backlash | | | | | |
| | Tecnadyne | Model 100 | \$4,210 | 100 | 10 | 6 deg/sec | 7.5 | 5 | | 6061-T6 Al | | 110-120VAC | oil | |

Table 5-3 · Control Fin Actuators

Echo Sounders

| Seller | Model | URL | Depth Range | Frequency |
|----------------------------------|--------------------------------|---|-------------|-----------|
| Ocean Data Equipment Corporation | Bathy-1500 Survey Echo Sounder | http://www.oceandata.com/b1500.htm | 0.5 to 5m | 200kHz |
| Ocean Data Equipment Corporation | IES-10 Navigation Echo Sounder | http://www.oceandata.com/ies10/ies-10.htm | 0.5 to 5m | 200kHz |
| Marine Acoustics Limited | Small Boat Echo Sounders | http://www.marine-acoustics.co.uk/Products/Transducers/Echo-Sounders.html | ?? | 175kHz |

Table 5-4 · Echo Sounders

6· Down Select Platform

The vehicle concept design is a platform that is towed by a surface craft using a flexible cable. It was a goal of the study to design a single platform for UXO sensors, the EM sensors and the magnetometer suite. To operate each survey sensor suite individually, construction of two of the platforms is required. For a single platform design, mounting provisions for the two primary sensors will be made. This assumes that the magnetometers are able to operate in the presence of the large EM sensor as its size makes it integral with the platform construction.

Geometry, Weight and Balance

The platform will be constructed of a non-metallic or non-ferrous material, most probably fiberglass. The full-scale version will be approximately 30 FT long, 6 FT wide at its mid point, and 6 to 8" thick. The system will operate in a shallow water environment from approximately 2 FT down to 15 FT depth. Depth control will be provided by two independently actuated control flaps and an automatic control system. The actuators will be located approximately 1 meter from the main UXO sensors.

A perspective view of the survey platform is shown in Figure 6-1. Each of the major components is indicated. To get a sense of the platform thickness, side and front views are shown in Figure 6-2 and Figure 6-3. The magnetometers are shown with them being proud of the top surface by about 2". The EM sensors are not readily visible as they are embedded internal to the platform.

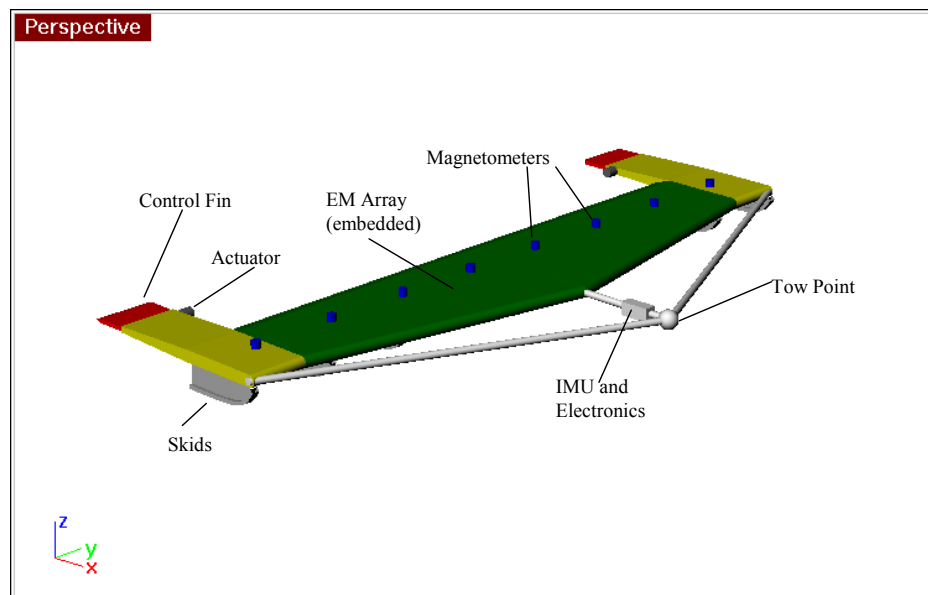


Figure 6-1 · Perspective View of Survey Platform

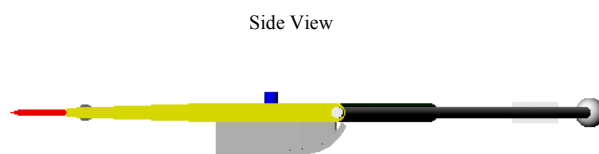


Figure 6-2 · Side View of Platform

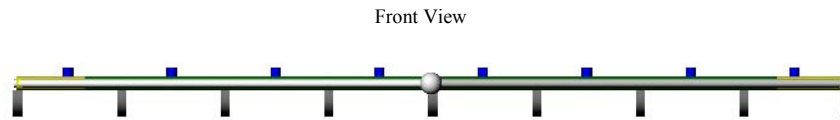


Figure 6-3 · Front View of Platform

In the next set of figures presents the same survey platform but with the GPS poles added. These poles are design in a truss arrangement and extend up 15 FT above the platform. The truss configuration can be clearly seen in Figure 6-4. If used, the poles would have an aerodynamic sheath over them that aligns with the local flow field. This would minimize any side lifting force due to the poles.

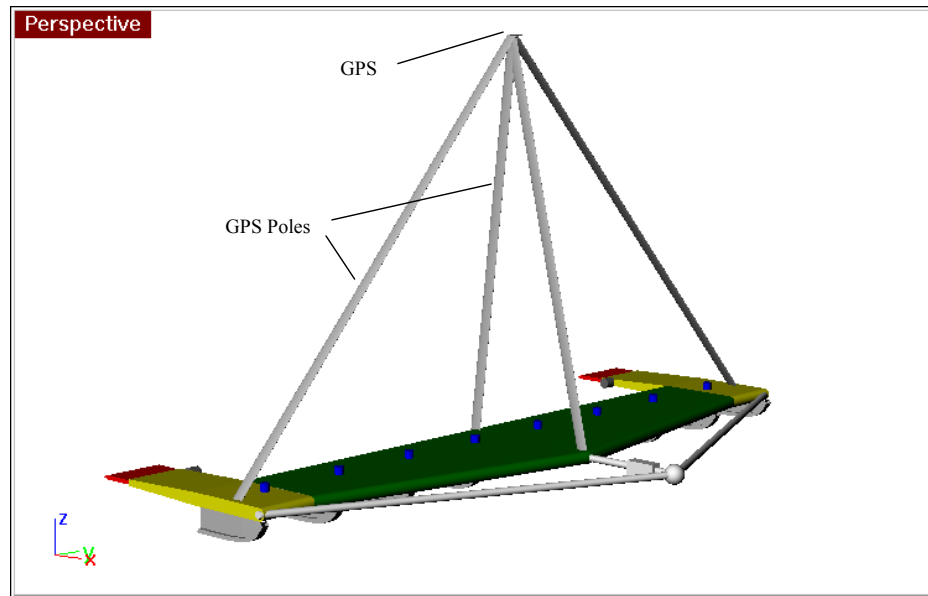


Figure 6-4 · Platform with GPS Poles

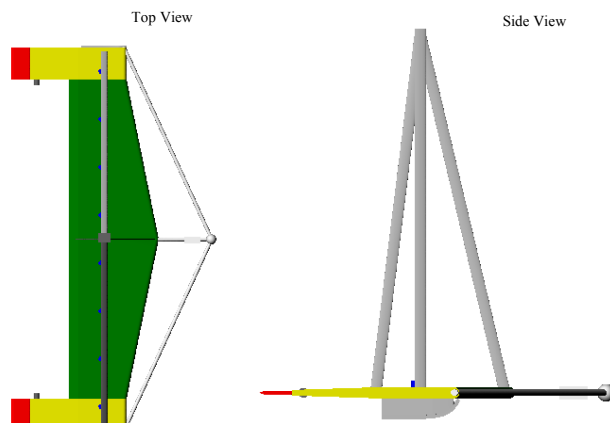


Figure 6-5 · Top and Side View with GPS Poles

Construction of the survey platform would use typical wing structural arrangements. This consists of an internal spar and rib configuration with a covering skin. The combination of the ribs and spars with the external skin has been a standard practice in aerodynamic wing design and allows for support of bending (lift) loads and for torsional stiffness. Figure 6-6 shows suggested arrangements of these components. The wing cross sectional shape does not have to be a strict airfoil shape. Our modeling uses a standard

NACA symmetrical airfoil. Final stress analysis requires formal structural loading calculations using a structural design code.

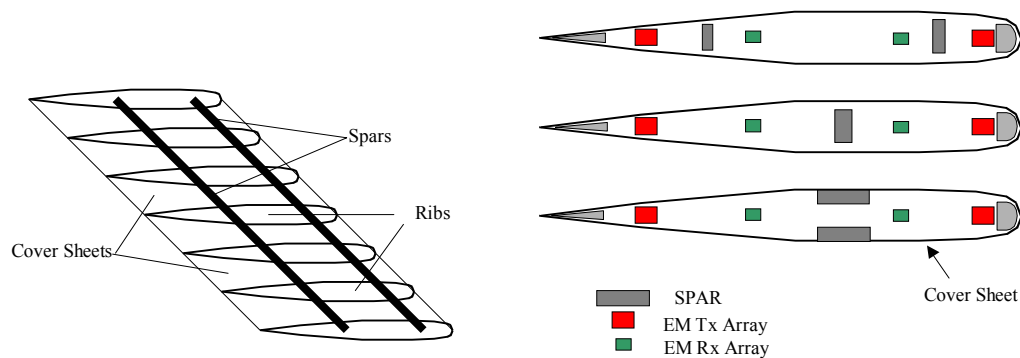


Figure 6-6 · Schematic of Structural Layouts

Assuming the use of standard fiberglass material in the construction of the survey platform, estimates were made of the platform's weight in air; that is its dry weight. This subtracted from the weight of displaced water determines the amount of total buoyancy. To produce positive buoyancy (having the platform float), foam floatation sections were required to counter some of the dry weight. In addition, these calculations lead to the determination of the platforms center of gravity (CG) defined from the nose. Figure 6-7 and Table 6-1 present a summary of the platforms weight along with schematics of the various components. Figure 6-7 is color coded:

red and **green** are the survey sensors,
blue and **magenta** are the platform's structural components,
cyan is the floatation elements.

This design has the following static properties

- › Net Buoyancy = 6.5 LBS (positive)
- › Weight, dry = 1354 LBS
- › Static Trim Pitch Angle = 2.1°
- › Location of the CG = (2.8331, 0.0, 0.0592) FT
- › Location of the CB = (2.8343, 0, 0.0277) FT

These properties are transferred and used in the hydrodynamic performance analysis.

| Component | Size inches | Weight lbs | Specific Gravity |
|--------------------|-----------------------------|------------|------------------|
| Upper wing Surface | 0.188 thick | 196 | 1.5 |
| Lower wing surface | 0.250 thick | 261 | 1.5 |
| Wing ribs (7) | 0.375 thick | 63 | 2.0 |
| Upper tip surfaces | 0.188 thick | 59 | 1.5 |
| Lower tip surfaces | 0.250 thick | 78 | 1.5 |
| Tip ribs (4) | 0.375 thick | 41 | 2.0 |
| Wing spars (4) | 300" span 1.8" ² | 152 | 2.0 |
| Skid struts (9) | 0.5" x 4.0" x 2.0" | 380 | 2.0 |
| Floatation (8) | 29" x 36" x 2.5" | 151 | 0.2 |
| Electronic pod | 6" dia x 25.0" | 26 | 1.0 |

| | | |
|---------------|----|-----|
| Actuators (2) | 15 | 4.0 |
|---------------|----|-----|

Table 6-1 · Component Weight and Size

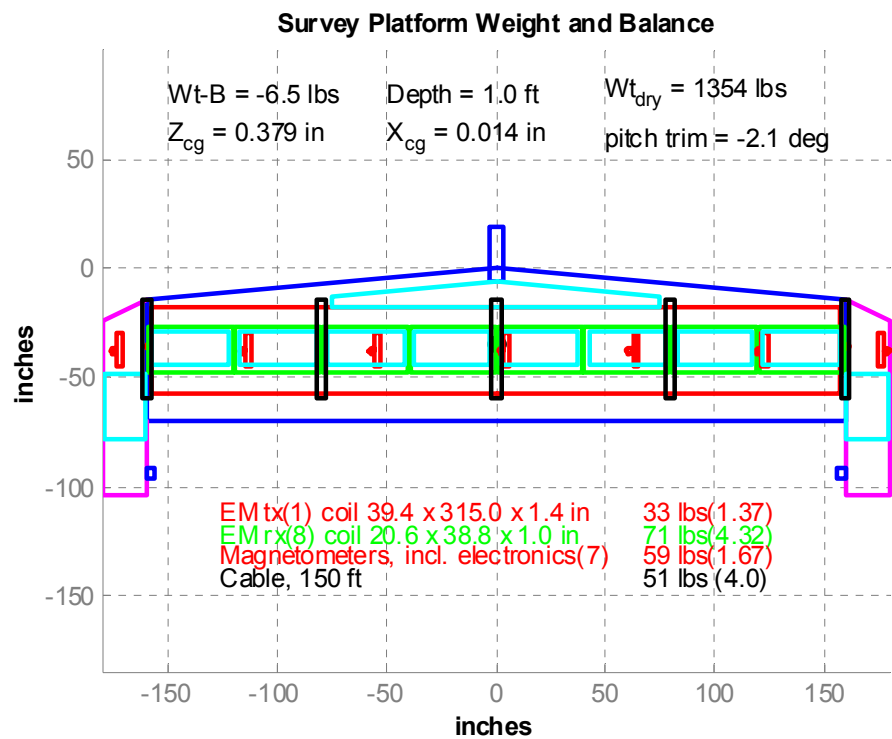


Figure 6-7 · Survey Platform Layout

red and green are the survey sensors,
blue and magenta are the platform's structural components,
cyan is the flotation elements

Towing Craft and Launch & Recovery

The overall size of the survey platform is approximately 30 FT long by less than 8 FT wide. The platform will be constructed as a single unit and must be transported to a survey site. A custom trailer will be required for the transport. This trailer must be able to support the approximately 1500 LBS vehicle and provide for launching at standard launch ramps. A roller and tilt mechanism to facilitate the transition into the water will be required. Since the platform is basically a large wing, windbreaks are needed while the trailer is in motion.

Attachment to the towing craft will be made using a winch and drum/clutch arrangement. The drum should be designed to hold the tow cable, and the clutch should be designed to support the towing load but allow release in the event of an underwater collision. Figure 6-8 shows a schematic.

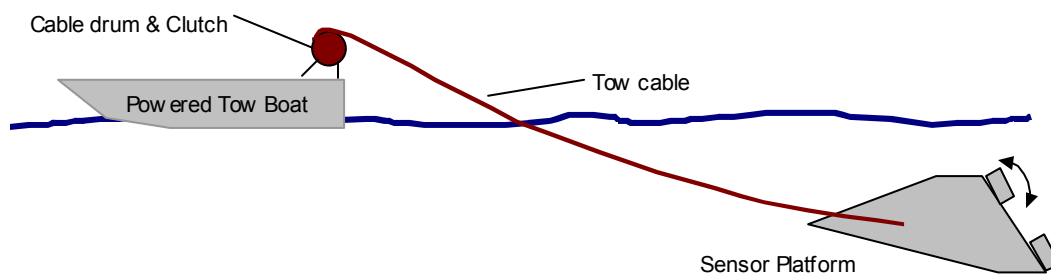


Figure 6-8 · Cable Drum and Clutch

Hydrodynamic Parametric Study

In order to examine the sensitivity and thus robustness of a towed underwater vehicle, it is standard practice to perform a parameter variation study. The parameters chosen are the principle design parameters of the study; in this case, speed, cable length, tow point location, location of the center of gravity, and location of the aerodynamic center.

In the figures presented, we use the nominal design values as the baseline case and move off this point by high and low values. For example the nominal cable length is 50 FT, the high and low values are 30 and 70 FT respectively. In each plot this high-low-nominal range is shown along with the speed range of 2 to 5 KTS. The speed is indicated in the variation studies as red for the high speed of 5 KTS and blue for the low speed of 2 KTS.

| Nominal Design Parameters | |
|-----------------------------|-----------|
| Tow Height above water line | 3 FT |
| Cable | 50 FT |
| Tow Point | 2 FT |
| Aerodynamic Center | 35% |
| X_{CG} | 0.0012 FT |
| Z_{CG} | 0.0316 FT |

Nominal Design with Speed Variation: 2 to 5 KTS

Figure 6-9 presents the tow body performance with the nominal design parameters. The left plot shows the cable's catenary shapes for three pitch angles across the speed range. This is the basic performance of the vehicle as it is being towed. The depth ranges from less than 2 FT to approximately 15 FT with a vehicle pitch angle of 1° . The right plot shows this in the form of two curves, the blue line is the lower speed of 2 KTS and the red line represents 5 KTS speed. The left plot of Figure 6-10 shows the corresponding required stern plane (control surface) angles. These range from -5° to 15° deflection – an acceptable range. The tension required to tow the system is shown in the right plot. The maximum of about 400 LBS in a very reasonable value in terms the tow cable and surface ship limits. This 400 LBS translates to approximately 12 HP, taking into account efficiency losses and safety factors.

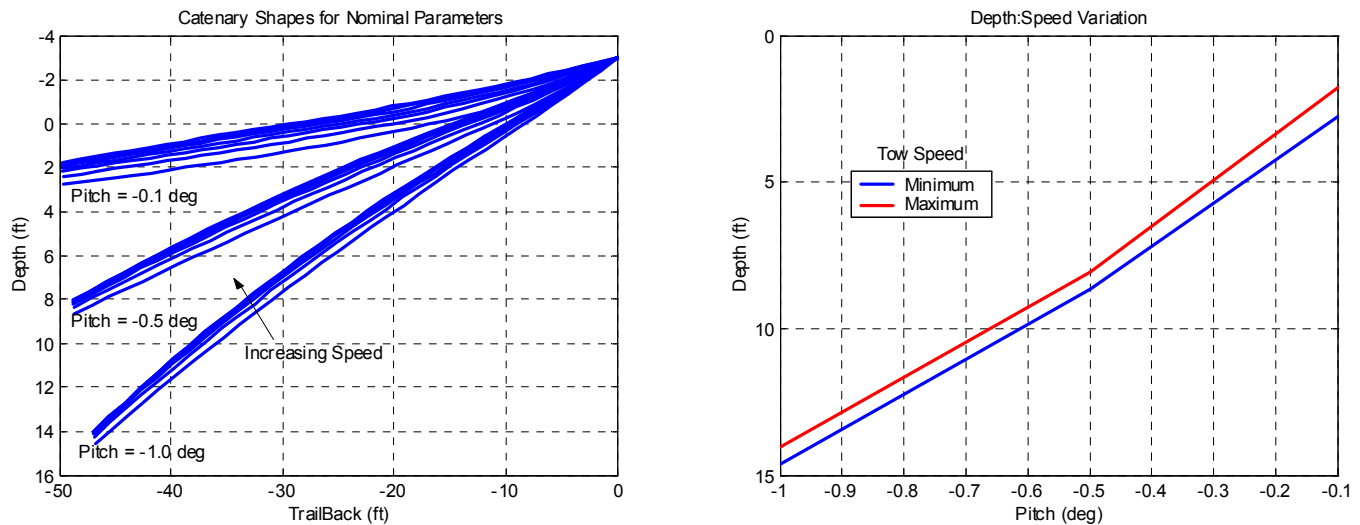


Figure 6-9 · Nominal Design

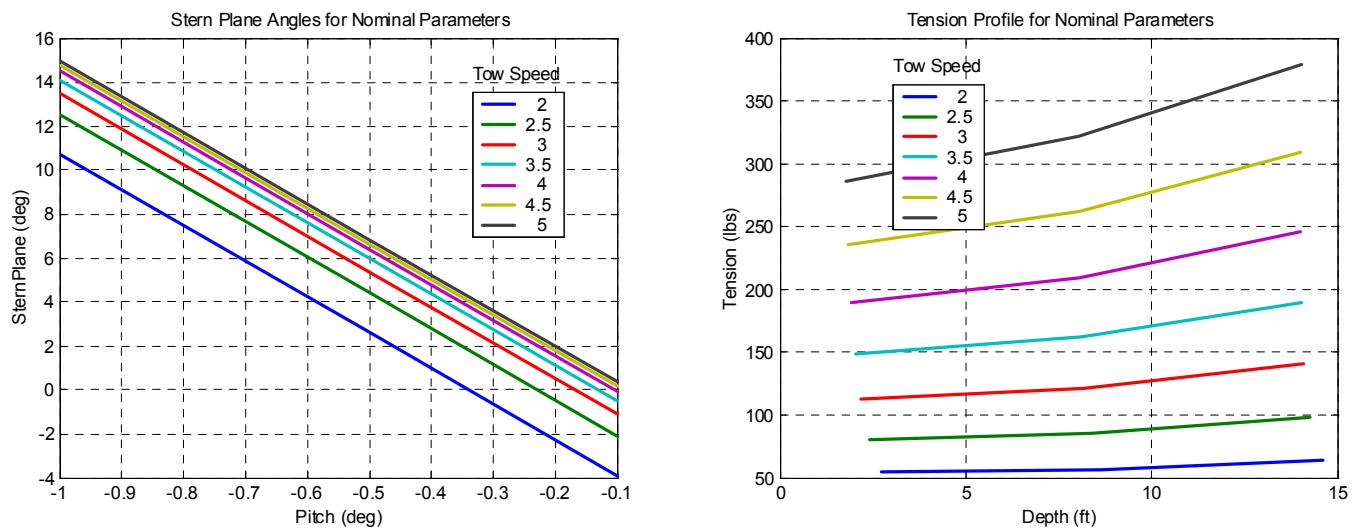


Figure 6-10 · Nominal Design

Aerodynamic Center of Wing: 20% to 50% of Mean Aerodynamic Chord

The aerodynamic center (AC) of the wing is the point at which the vehicle's lift force is applied. For a new vehicle of this type, mostly a flying wing, this precise location will probably not be known until the vehicle is tested in the water. Past experience has shown that the AC location does move with pitch angle and thus changes the pitch moment as the vehicle's angle of attack changes. Our calculations show that the nominal AC location is at a point 35% from the leading edge along the mean aerodynamic chord. To examine the effect of it's movement and precise location, we vary this value by $\pm 15\%$. This value of 15% is an extreme amount but we are using it to measure of the robustness of the design. From Figure 6-11 we see that the depth can vary by ± 6 FT and the stern plane angle by $\pm 5^\circ$ due to the AC location. So even with a large change in the location of the AC, using the nominal design parameters, the tow body is still able to meet its depth requirements within an acceptable stern plane range of deflection.

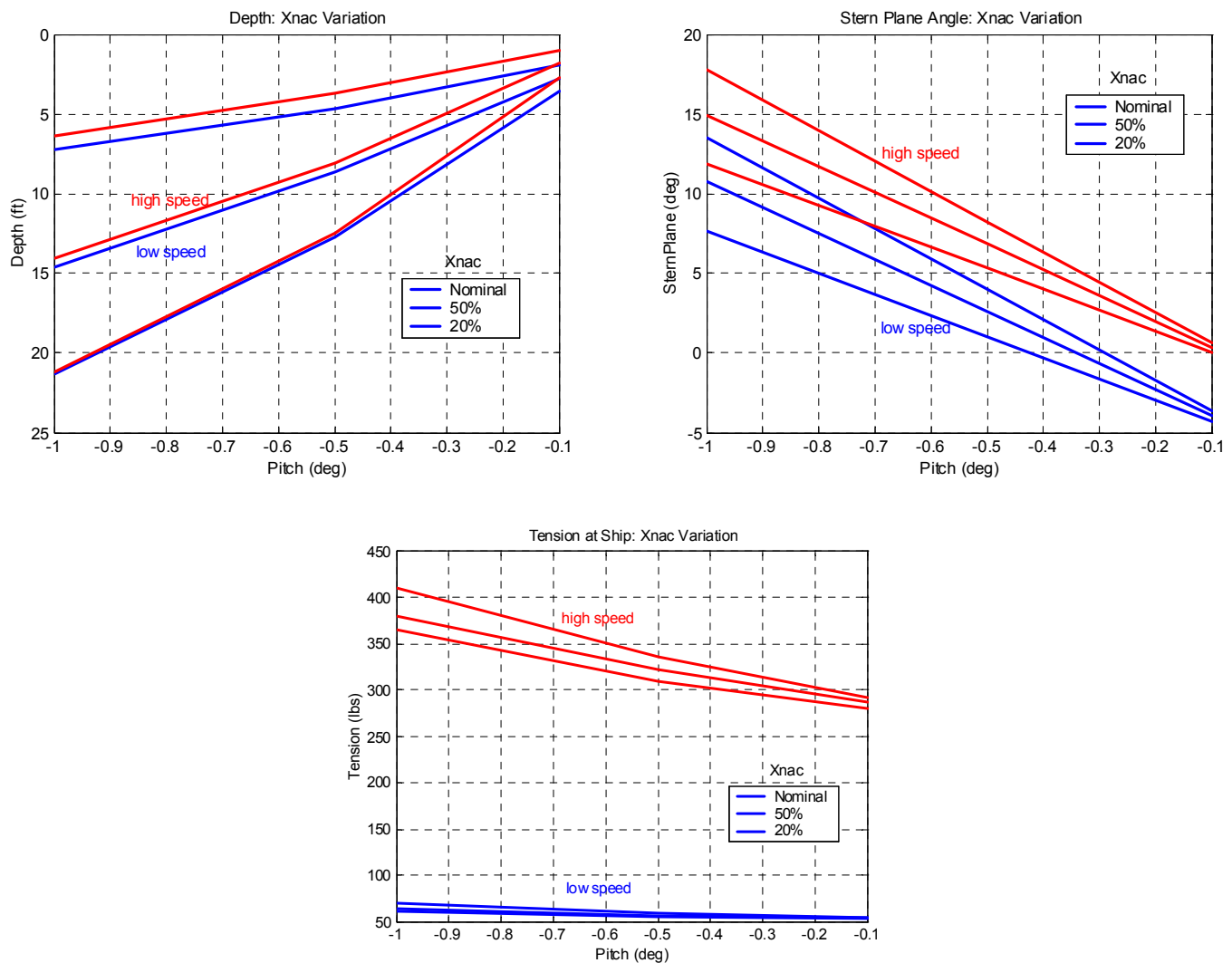


Figure 6-11 · Wing A.C. Variation

Tow Point Location: 0, 2, 4 FT

The tow point is where the tow cable attaches to the tow body. Nominally, this was set at 2 FT in front of the nose of the tow body; total distance from the EM array is over 3 FT due to the leading edge angle. The low value was set at 0 FT, or attached at the vehicle's nose, and the high value was set at 4 FT. Figure 6-12 presents these results. Other design factors will probably drive the location of the tow point more than the vehicle's pitch and stern plane performance. Those factors include the location of the IMU, consideration of tow point load distribution, among others.

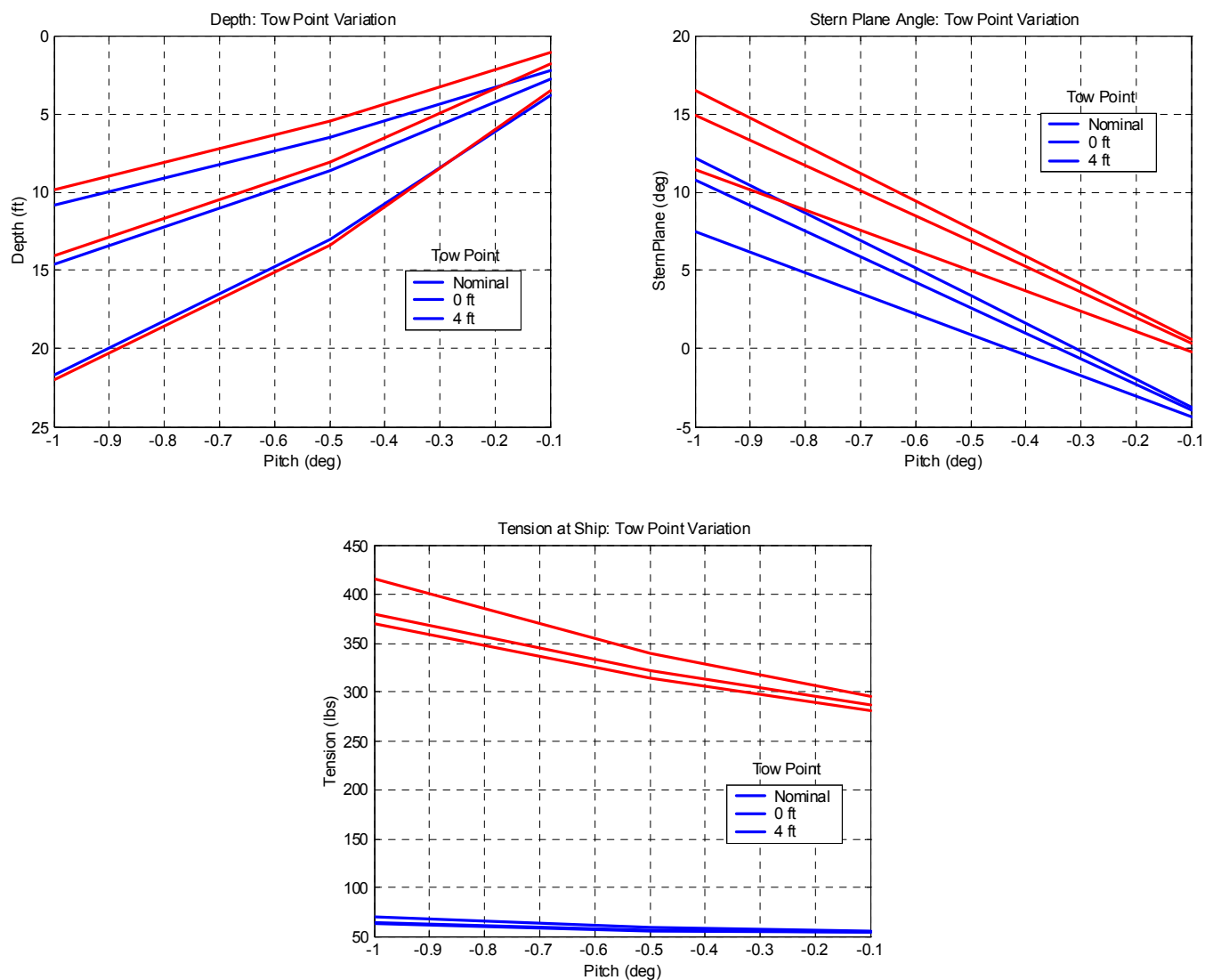


Figure 6-12 · Towpoint Location Variation

Cable Length: 30, 50, 70 FT

The nominal value for cable length is 50 FT with chosen values of 30 FT and 70 FT for the minimum and maximum. Figure 6-13 presents these results, and we see that by simply controlling the length of the cable there is a strong effect on the steady-state depth of the vehicle. The pitch angle and the stern plane angles are not directly affected by the cable length. The vehicle's force and moment balance are independent of the cable length, and thus the vehicle trims to the same angles. The depth of the tow body can be strongly affected by changing the tow cable length.

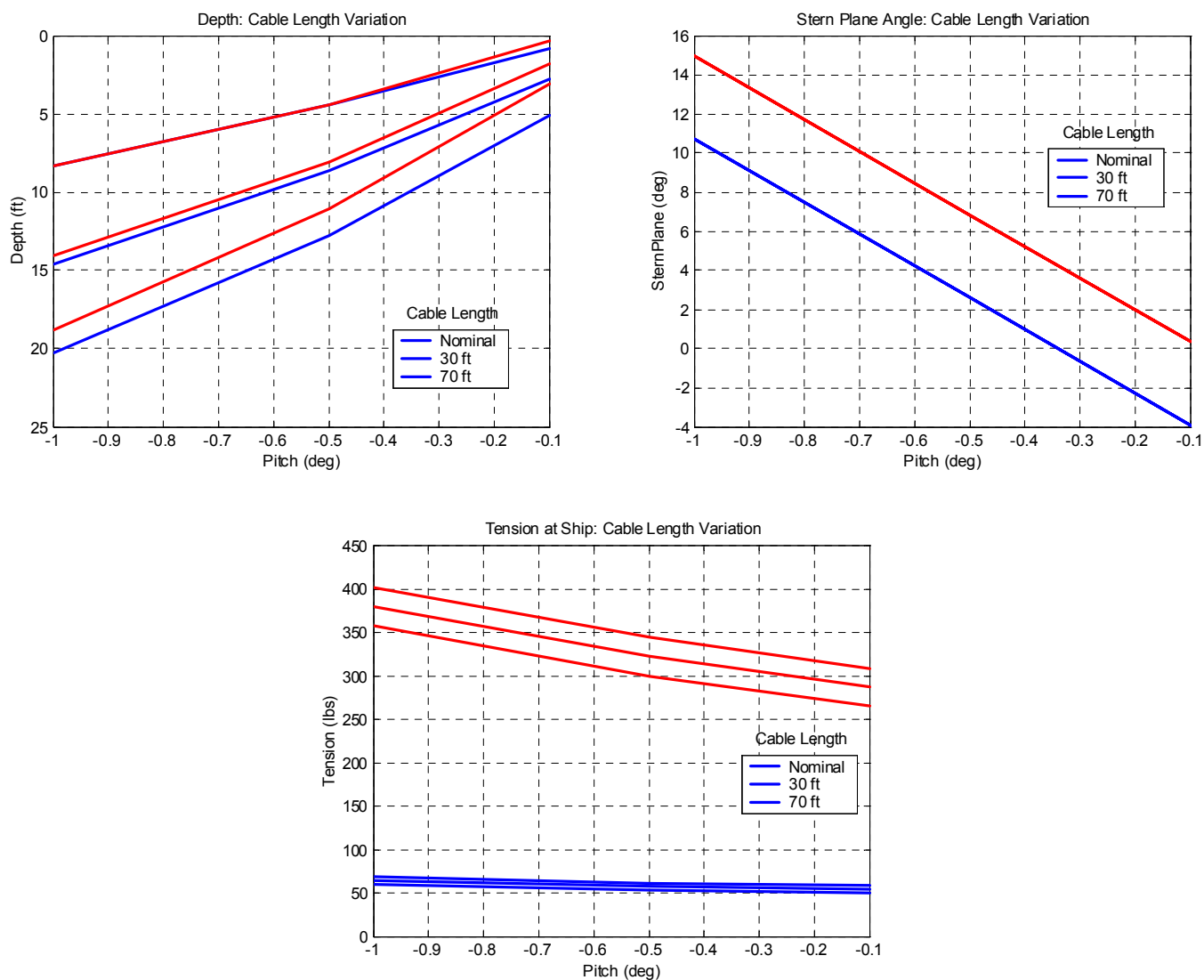


Figure 6-13 · Cable Length Variation

Location of X_{CG} : -0.06" to 0.06"

As can be seen in Figure 6-14, the longitudinal location of the CG with respect to the origin does not have a strong effect on the static performance of the tow body. More important is the effect that the X_{CG} has on the trim pitch angle when the vehicle is on the surface. This is calculated by including the vertical distance Z_{CG} . With a X_{CG} variation of -0.06" to +0.06" and a minimum Z_{CG} of 0.25", the trim pitch angle of the tow body will range between $\pm 13^\circ$. Larger X_{CG} values will lead to larger trim pitch angles when the vehicle is on the surface.

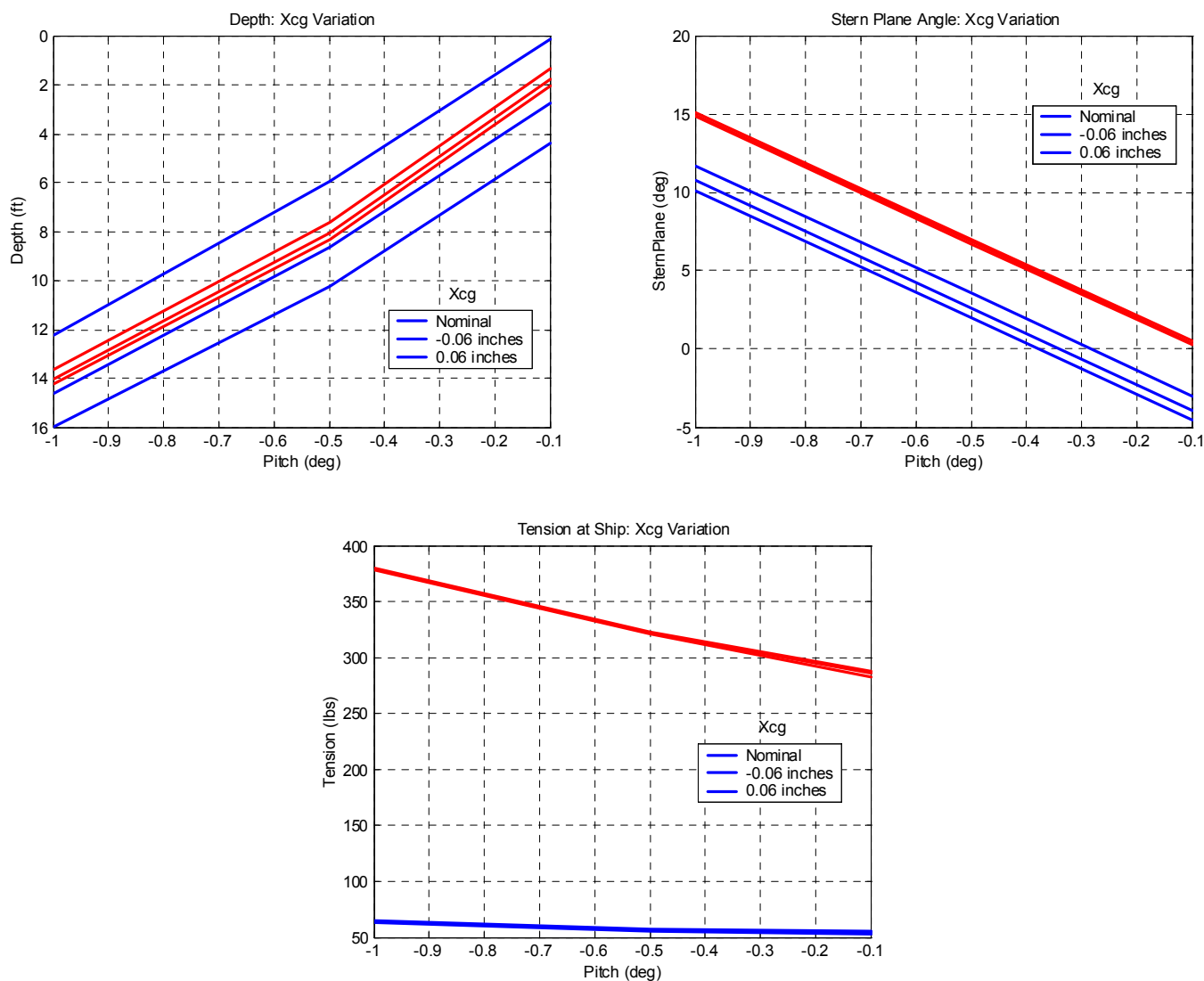


Figure 6-14 · X_{CG} Variation

Location of Z_{CG} : 0.25” to 0.75”

Z_{CG} is the difference between the vertical center of buoyancy (Z_{CB}) and the vertical distance to the CG. The nominal Z_{CG} is 0.0316 FT, or 0.379” below the center of buoyancy. We vary this parameter from 0.25” to 0.75” by moving the vehicles vertical CG. As with the X_{CG} , the Z_{CG} acts as a restoring moment and is more prominent at lower speeds. In the present design, this parameter must be constrained along with the X_{CG} to determine the trim pitch angles when the vehicle is at zero speed on the surface.

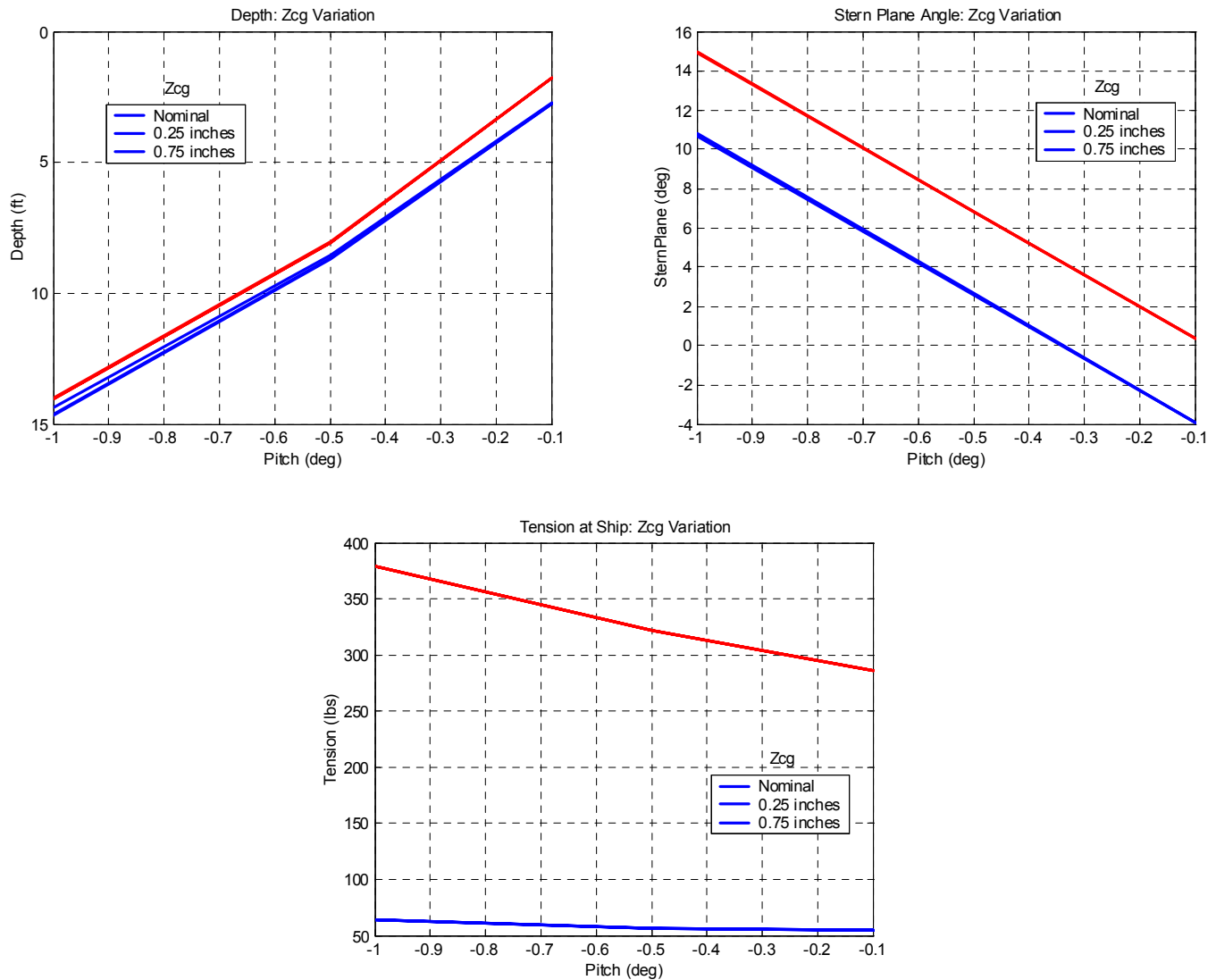


Figure 6-15 · Z_{CG} Variation

4 meter Platform

A scale version of the 10 meter survey platform was developed and modeled. This was developed by scaling in primarily the span direction of the full-sized platform described above. The platform is called the 4 meter size because it accommodates four 1 meter EM receive arrays. Not scaled were the seven magnetometers, the cross sectional area of the EM sensors, the cabling (including the tow cable), the position measurement electronics and the actuators. The layout and weight and balance are shown in Figure 6-16. The 4 meter platform was made to be slightly buoyant. Component weights and size are listed in Table 6-1.

Figure 6-18 through Figure 6-21 shows the nominal case results for the 4 meter scale model. The pitch angle of the platform had to be increased to 2.0° in order to approach the 13 ft depth. Along with this, the control fin angles range to about 14° . The reduced lifting area of the platform results in a reduction in the towing tension – from about 350 to about 300 LBS. The overall dry weight of the platform did not scale linearly with the reduction in span. The 4 meter platform has a dry weight of about 875 LBS, not quite half of the approximately 1400 LBS 10 meter vehicle. Compared to the 1355 LBS dry weight of the 10 meter vehicle, this is a reduction of only 35%. We see from this that the weight reduction with respect to width of the platform is not one to one. This is due to the fact that some of the components are the same – sensors, actuators, etc. – but also because the wing tips have not been scaled in order to keep the Control fins the same width (24”) and distance from the survey sensors.

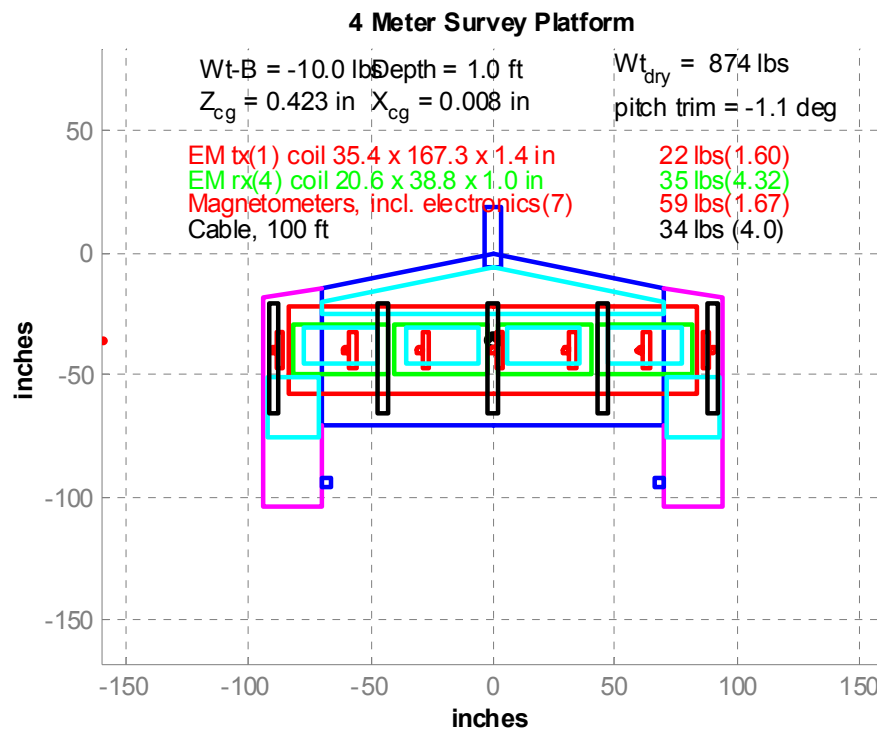


Figure 6-16 · 4 Meter Survey Platform Layout

| Component | Size inches | Weight lbs | Specific Gravity |
|--------------------|--------------------|------------|------------------|
| Upper wing Surface | 0.188 thick | 91 | 1.5 |
| Lower wing surface | 0.250 thick | 121 | 1.5 |
| Wing ribs (5) | 0.375 thick | 33 | 2.0 |
| Upper tip surfaces | 0.188 thick | 43 | 1.5 |
| Lower tip surfaces | 0.250 thick | 57 | 1.5 |
| Tip ribs (4) | 0.375 thick | 35 | 2.0 |
| Wing spars (4) | 300" span 1.8"² | 58 | 2.0 |
| Skid struts (5) | 0.5" x 4.0" x 1.3" | 158 | 2.0 |
| Floatation (4) | 15" x 30" x 3.0" | 101 | 0.2 |
| Electronic pod | 6" dia x 25.0" | 26 | 1.0 |
| Actuators (2) | | 15 | 4.0 |

Figure 6-17 Component Weights for 4 Meter Platform

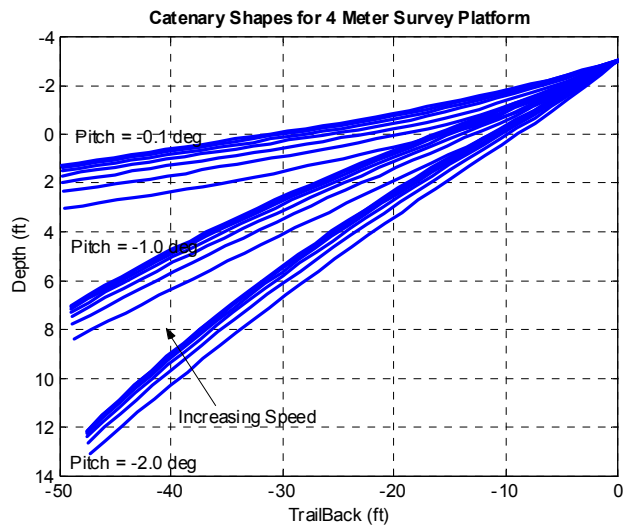


Figure 6-18 · Catenary Shapes for the 4 meter Platform

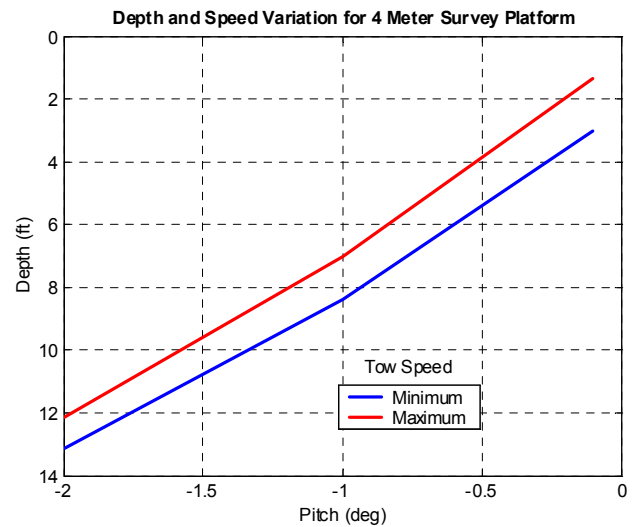


Figure 6-19 · Depth Limits for the 4 meter Platform

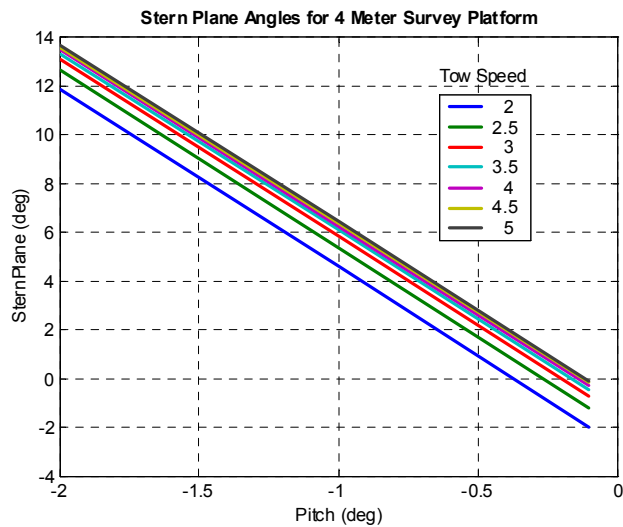


Figure 6-20 · Stern Plane angle range for the 4 meter Platform

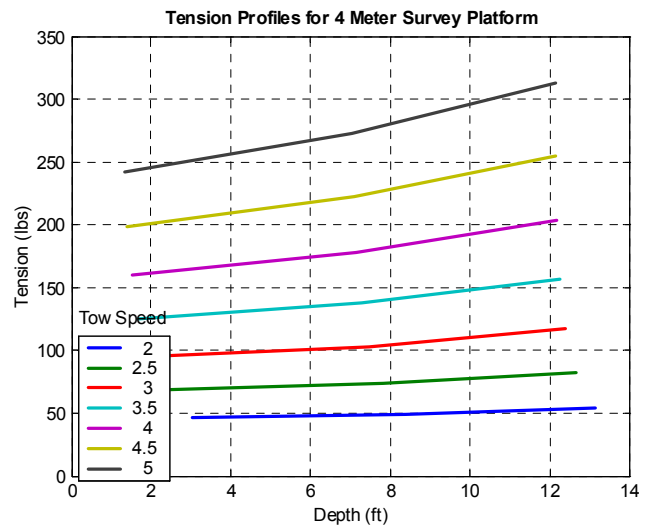


Figure 6-21 · Tension Map for the 4 meter Platform

7• Summary

This interim report is the first of two reports describing the concept design of a UXO sensor marine vehicle concept design. This report describes the UXO marine search requirements, the design alternatives, and the resulting hydrodynamics of the platform concept design. The concept design examines several system options. UXO sensor implementation and operation are the primary concerns, but additional sensors to operate, control and locate the marine vehicle are accounted for here. Initial results of the candidate vehicle's design in terms of its general geometry, size, weight, component layout, and basic hydrodynamic performance are presented. Also discussed are launch and recovery operations, and concepts for the towing platform and connection device.

There are two survey platform designs reported. The first is a 10 meter survey platform. This contains 8 Rx EM loops along with a Tx EM loop. The second design contains only 4 of the Rx EM loops and is included as a smaller scale version. This design is termed the 4 meter system and is approximately 5 meters in width. While being half the width, the 4 meter vehicle has a dry weight only 35% less than the 10 meter vehicle.

The construction of a platform will probably require that the EM sensors be embedded within the vehicle. This determines whether one or two survey platforms will be built. The answer depends on operation of the magnetometers in the presence of the EM sensor.

The second part of the concept design will address the vehicle dynamic performance analysis, the control algorithms development, and simulations of the platform operation.

This effort shows that, at the current analysis stage, both of the concept design UXO sensor marine platforms are feasible. No insurmountable issues were identified. The primary concern to date is whether the accuracy of the survey sensors position calculations is sufficient without a body mounted GPS. That is, whether or not the GPS support poles are required.

A•Memorandum

September 26, 2002

To: Jack McDonald, AETC

From: Ken Watkinson, VCT

Subject: position and attitude measurement requirements

In the attached table, requirements 5 and 11 are specified for position and attitude measurement accuracy for the **Marine MTADS Survey Platform**. The purpose of this memorandum is to clarify these requirements and offer some potential measurement approaches. The submerged sensor platform is referred to as the tow body and surface vessel that pulls the tow body is referred to as the towing craft. The tow boom is a rigid rod from the towing craft to the tow body. Use of a tow boom or a tow cable is being investigated.

Sensor Vertical Position

The vertical position of the master GPS antenna will be known to approximately 0.1m with respect to the reference earth geoid. Error in the knowledge of the sensors with respect to the master GPS antenna needs to be less than 0.1m so as to not contribute significantly to the sensor-to-geoid error. If the GPS antenna is on the towing craft, one approach to determining sensor vertical position is to measure the GPS antenna-to-waterline vertical distance and the fathometer-to-waterline vertical distance so that both the surface of the water and the fathometer bottom depth measurement can be related to the geoid. Then the tow body vertical position can be determined using the pressure depth measurement since it is with respect to the water surface. Alternatively, a tow body Fathometer can be used to measure the height above the bottom. Either of these measurements would provide the vertical position of the tow body origin with respect to the geoid. The sensors could then be related to the origin through measured body-axis positions and tow body attitude angles.

Tow Body Depth Sensor or Fathometer

Depth sensor errors are typically stated in % of full scale. For a nominal 15m full-scale water depth range sensor, the accuracy would need to be approximately 0.25% to provide measurement accuracy of 0.04m. Accuracies of 0.1%, and even 0.05%, are also available. Correction for barometric pressure will be required to obtain accuracy of a few centimeters. Wave action will cause errors since that changes the height of the surface of the water. This error source is a zero mean process. Post processing may be able to remove some of the tow body vertical position error due to wave action. If this cannot be done satisfactorily, then a tow body fathometer will be required. This seems likely to achieve vertical position accuracies of a few centimeters.

Tow Boom Pitch Measurement

It does not appear to be feasible to use a measurement of a rigid tow boom pitch angle to determine tow body vertical position. Obtaining a tow body origin vertical position accuracy of a few centimeters for a 10m tow boom length would require measurement of the tow boom pitch angle to an accuracy of approximately 0.1° . Such accuracy is not attainable using two GPS measurements without very large separation distances between the units – like 6 to 12m. Measuring the tow boom angle with respect to

the towing craft and then measuring the towing craft pitch angle would not yield accuracies on the order of 0.1° with any practical measurement instrumentation.

Tow Body Attitude

Measurement of tow body attitude for computation of individual sensor vertical positions can be done within the required 0.1° accuracy using a good quality IMU or AHRS and tailoring the attitude computation algorithms for the motion characteristics of the tow body (i.e. appropriate selection of blending filter characteristics).

Sensor Horizontal Position

Determination of the horizontal tow body origin position with respect to the master GPS antenna suffers from problems similar to the vertical position measurement – only there is no fixed reference like the bottom that can be used. As mentioned above, measurement inaccuracies of the tow boom angle and towing craft heading are greater than the 0.1° accuracy requirement. To achieve horizontal position accuracies of a few centimeters with respect to the master GPS antenna, the antenna must be rigidly mounted to tow body. Given the 4m maximum submergence requirement, this results in a structure that extends 5 to 6m above the tow body.

Tow Body Heading

Determination of the sensors' along-track position requires measurement of the tow body heading with respect to the track – to translate the master GPS antenna position to the sensors. The accuracy of a magnetic compass heading measurement is quite dependent on the compensation and calibration procedures. Obtaining accuracies of 0.1° is very demanding – requiring compensation at each operating site. Another approach could be to have two GPS antennae, one on each end of the tow body sensor platform (port and starboard). These two antennae would have to be mounted 5 to 6m above the tow body.

Summary

1. Position of the survey sensors must be known to within a few centimeters with respect to the master GPS antenna.
2. Rigid tow boom angle measurements of sufficient accuracy to support this are not practically attainable.
3. Tow body heading measurement with sufficient accuracy to support this is only attainable with extensive on-site compass compensation and calibration.
4. Rigid mounts of two GPS antennae extending from the sensor platform to above the water surface provides the required sensor position accuracy.

If you agree with the statement of accuracy requirements provided here and the conclusions drawn, or if further clarification or reassessment is required, please indicate such in your response. Major tow body configuration and instrumentation selection decisions depend on this analysis of measurement requirements. Thank you for your efforts toward laying the basis for a design.

Marine MTADS Survey Platform Requirements Document

Legend

Blue = Control Requirements

Red = Motion Measurement Requirements

| | |
|---|--|
| 1. House 7 magnetometer sensor array to nominally cover a 9 meter swath. | Sensor mounts spaced at 1.5m increments, perpendicular to direction of travel. |
| 2. Sensor orientation must be adjustable and securable | mounting gimble provides tilt adjustment, with locking mechanism |
| 3. Provision for mounting of sensor electronic packages | Electronic packages must be mounted 2.5 to 3.5m from the sensors. Cables running between the sensor and the electronic packages will be secured, as will cables running from the electronic package to the vessel cabin. |
| 4. Sensors must be mounted in a magnetically clean environment | No electrically conductive or magnetic material is to be used within 1m of the sensor. The use of metal and conductive material will be avoided completely where possible, no carbon composites |
| 5. GPS technology allows position measurements to 0.05 m horizontal and 0.1 m vertical accuracy. Measurements of the platform position and attitude, relative to above surface GPS antennae must minimize the additional errors involved in translating these positions to the sensor positions. | Angles used to position center of platform, relative to the master GPS antenna, assuming a 30 m arm must be accurate to 0.05°. Angles used to translate platform position to sensor positions (i.e. platform attitude sensors) must be accurate to 0.1° |
| 6. The magnetic signature of DC electrical currents necessary for platform control devices must be recognizable and removable for the measured total magnetic field data. | The 'on-time' of these currents must be < 0.1 sec duration, limited to 10% duty cycle, and easily demarcated in the data using the A/D logging functionality of the existing data acquisition system (single pole, 0 to 10v dc) |
| 7. Platform must be operable at speeds sufficient to allow efficient survey coverage rates | Survey speeds of 3 to 10 kts are considered reasonable, depending on sea and bottom conditions |
| 8. Platform must 'fly' nominally 1 m above the sea floor at survey speed. | The platform height above the sea floor must be monitored and used as input to for a vertical position control system. The vertical position control system must maintain sensor height to within 0.2 m |
| 9. Platform should ride to surface at very slow speeds or when survey vessel is stopped. Platform design should consider the need to operate in minimal water depths | Platform buoyancy must allow for control of platform at normal survey speeds while maintaining positive buoyancy over a suitable range of water density conditions |
| 10. Platform accelerations must avoid our magnetic target response periodicity | Target response signatures occur from 2 to 10.0m along track. At 10 kts this equates to periods of 0.4 to 1.9 sec, and at 5 kts 0.8 to 3.9 sec. Altitude and attitude changes should avoid this periodicity if possible. |
| 11. Platform must have provision for mounting of auxiliary sensors | Fathometer, fluxgate magnetometer, tilt-meter. |
| 12. Platform must be deployable and recoverable from standard boat launch ramps | |
| 13. Platform must be transportable on or in a trailer designed for towing | |

**Modeling of the Electromagnetic Response of
EMI Sensors Employed in a Salt Water Environment
Judy Soukup
AETC Incorporated**

1. Overview

Electromagnetic induction (EMI) occurs when a time-varying electromagnetic field is established over a conducting target. In response to this field, a secondary electromagnetic field is produced by the presence of a conducting target that can be detected at a distance, revealing the presence of the target and also, to some extent, its size and shape.

An example of a commercial EMI sensor is the GEM-3 from Geophex, Inc, which has a circular transmitter coil up to 90cm in diameter producing a primary (transmitted) field of about 0.5 Gauss at 50 cm, and operates in the range of 30 Hz to 30 kHz (frequency domain). Time domain instruments of similar size and power with multiple time gates are also available, such as the EM61 from Geonics. Both of these sensor types produce the primary field by a transmitter current loop and measure the secondary magnetic field with a receiver loop that is essentially co-located with the transmitter.

The primary magnetic field from the sensor induces, via Faraday's law, currents within a conducting target of interest, which are modeled here as an induced magnetic dipole. The primary electric field also produces currents within the conducting target, which can be modeled as an induced electric dipole. Both induced dipoles produce secondary electromagnetic fields. The contribution of the induced electric dipole can normally be neglected when the sensor and target are in air. This is not the case, however, when the medium is conducting, and the induced electric dipole in the target must be accounted for.

Such calculations are made in here for a system in both air and in seawater. The results show that, for a given spherical target, there is a range of target/sensor separation distances for which the secondary magnetic field from the target is larger in seawater than in air.

2. Phenomenology

The difference in signals in seawater and in air is due to the increased contribution of the induced electric dipole in the target to the measured magnetic field at the sensor. In air, the electric and magnetic fields from the source magnetic dipole are completely out of phase with each other, and therefore so are the induced dipoles in the target. In a conducting medium, however, the primary electric field has a component in phase with the primary magnetic field, and the dipoles induced in the target are also partially in phase. Thus, the secondary magnetic fields from the induced target dipoles are also partially in phase and can reinforce each other. This phase angle between the induced dipoles and between their secondary magnetic fields depends upon both the conductivity of the medium and the distance through which the fields travel. For a given conductivity and target, there is a range of distances for which the magnetic fields at the receiver from the two induced dipoles are in phase and reinforce each other.

Since the primary electric field from the source magnetic dipole decays as $1/R^2$ (compared to the primary magnetic field, which decays as $1/R^3$) and the secondary magnetic fields produced by the induced electric and magnetic dipoles decay as $1/R^2$ and $1/R^3$, respectively, it is possible for the contribution from the induced electric dipole in seawater to have, for the appropriate range of distances, a measurable effect.

3. Model Formulation

The sensor system modeled here is a vertical magnetic dipole source and a co-located receiver that measures the time derivative of the vertical magnetic field. The receiver is modeled as a point receiver with no area; we approximate the flux through the actual receiver by the field at the center.

The sensor and target are in an infinite medium with arbitrary conductivity (σ_1), permeability (μ_1) and permittivity (ϵ_1). The target is modeled as a sphere of radius R with arbitrary properties given by σ_2 , μ_2 and ϵ_2 .

We define, following Ward and Hohmann (1987), the following terms:

$$\begin{aligned}\hat{z} &= i\mu\omega \\ \hat{y} &= \sigma + i\epsilon\omega\end{aligned}\tag{1}$$

which yields

$$k^2 = -\hat{z}\hat{y}\tag{2}$$

The magnetic dipole source can be either a transverse dipole or a radial dipole. The spherical coordinate system for the calculations is shown in Figure 1, in which the dipole sources are located at $z = h$ in a right-hand coordinate system. The transverse dipole faces in the $+y$ direction and the radial dipole in the $+r$ direction. The target is located at the origin.

We formulate the general problem for a receiver located at (r, θ, ϕ) ; however, the calculations performed later will be for the specific case of a co-located source and receiver at $(r, 0, 0)$.

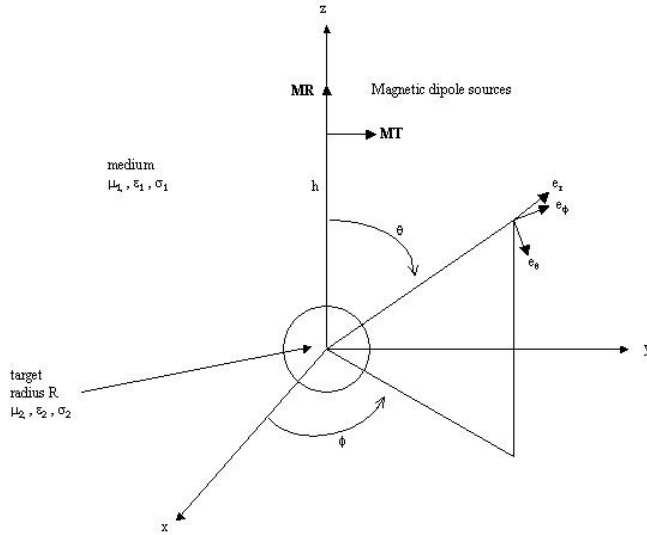


Figure 1. Spherical coordinate system showing transverse and radial magnetic dipole sources and the spherical target.

3.1 Transverse magnetic dipole potential

The fields are given in terms of potentials (Ward and Hohmann, p. 297). The transverse dipole potentials for the scattered field outside the sphere for a transverse magnetic dipole source are given by $\pi_a(MT)$ and $\pi_f(MT)$:

$$\pi_a(MT) = \sin \phi \sum_{n=1} a_{en} \frac{\hat{H}^{(2)}(k_1 r)}{r} P_n^1(\cos \theta) \quad (3)$$

$$\pi_f(MT) = \cos \phi \sum_{n=1} b_{en} \frac{\hat{H}^{(2)}(k_1 r)}{r} P_n^1(\cos \theta), \quad (4)$$

where $P_n^1(\cos \theta)$ is the associated Legendre function, and the function $\hat{H}_n^{(2)}(x)$ is given in terms of the spherical Bessel and Hankel functions j_n and $h_n^{(2)}$:

$$\hat{H}_n^{(2)}(x) = x h_n^{(2)}(x) = x[j_n(x) - i n_n(x)] . \quad (5)$$

The sums in equations 3 and 4 start at $n=1$ because $P_n^1(\cos \theta) = 0$ for $n=0$.

The magnetic field is derived from the potentials as follows:

$$\begin{aligned} H_r &= \frac{\partial^2(r\pi_f)}{\partial r^2} + k^2 r \pi_f \\ H_\theta &= \frac{\hat{y}}{r \sin \theta} \frac{\partial(r\pi_a)}{\partial \phi} + \frac{1}{r} \frac{\partial^2(r\pi_f)}{\partial r \partial \theta} \\ H_\phi &= -\frac{\hat{y}}{r} \frac{\partial(r\pi_a)}{\partial \theta} + \frac{1}{r \sin \theta} \frac{\partial^2(r\pi_f)}{\partial r \partial \phi} \end{aligned} \quad (6)$$

with similar equations for the electric field. [Note that Ward and Hohmann have an error in the equation for H_r on page 298.]

The coefficients a_{en} and b_{en} of equations 3 and 4 are found by matching boundary conditions (i.e., tangential E and H are continuous) on the surface of the target sphere.

$$a_{en} = - \left[\frac{k_2 \hat{y}_1 \hat{J}_n(k_1 R) \hat{J}'_n(k_2 R) - k_1 \hat{y}_2 \hat{J}'_n(k_1 R) \hat{J}_n(k_2 R)}{k_2 \hat{y}_1 \hat{H}_n^{(2)}(k_1 R) \hat{J}'_n(k_2 R) - k_1 \hat{y}_2 \hat{H}_n'^{(2)}(k_1 R) \hat{J}_n(k_2 R)} \right] \alpha_n \quad (7)$$

$$b_{en} = - \left[\frac{k_2 \hat{z}_1 \hat{J}_n(k_1 R) \hat{J}'_n(k_2 R) - k_1 \hat{z}_2 \hat{J}'_n(k_1 R) \hat{J}_n(k_2 R)}{k_2 \hat{z}_1 \hat{H}_n^{(2)}(k_1 R) \hat{J}'_n(k_2 R) - k_1 \hat{z}_2 \hat{H}_n'^{(2)}(k_1 R) \hat{J}_n(k_2 R)} \right] \beta_n \quad (8)$$

where

$$\alpha_n = \frac{i\hat{z}_1(2n+1)\hat{H}_n^{(2)}(k_1h)}{n(n+1)k_1h} \quad (9)$$

$$\beta_n = \frac{-i(2n+1)\hat{H}_n^{(2)}(k_1h)}{n(n+1)h}. \quad (10)$$

$\hat{J}_n(x)$ is given in terms of the spherical Bessel function

$$\hat{J}_n(x) = xj_n(x), \quad (11)$$

and the derivatives are defined as

$$\hat{J}'_n(k_2R) = \frac{\partial J_n(k_2R)}{\partial(k_2R)} \quad (12)$$

$$\hat{H}'^{(2)}_n(k_2R) = \frac{\partial \hat{H}_n^{(2)}(k_2R)}{\partial(k_2R)}. \quad (13)$$

[Note that Ward and Hohmann define this derivative incorrectly on page 297.]

3.2 Radial Magnetic Dipole Potential

The potentials for the scattered field outside the sphere for the radial dipole are given by $\pi_a(\text{MR})$ and $\pi_f(\text{MR})$, where

$$\pi_a(\text{MR}) = 0 \quad \text{by symmetry, and} \quad (14)$$

$$\pi_f(\text{MR}) = \frac{1}{h} \sum_{n=0} c_{en} \frac{\hat{H}^{(2)}_n(k_1r)}{r} P_n(\cos\theta) \quad (15)$$

Again, the coefficient c_{en} is found by matching boundary conditions at the surface of the target:

$$c_{en} = - \left[\frac{k_2 \hat{z}_1 \hat{J}_n(k_1R) \hat{J}'_n(k_2R) - k_1 \hat{z}_2 \hat{J}'_n(k_1R) \hat{J}_n(k_2R)}{k_2 \hat{z}_1 \hat{H}_n^{(2)}(k_1R) \hat{J}'_n(k_2R) - k_1 \hat{z}_2 \hat{H}'^{(2)}_n(k_1R) \hat{J}_n(k_2R)} \right] \gamma_n \quad (16)$$

where

$$\gamma_n = \frac{-i(2n+1)\hat{H}_n^{(2)}(k_1h)}{k_1h}. \quad (17)$$

The fields are obtained from equations 6, just as for the transverse dipole source, but this time using the appropriate potentials. Note that there is no field for the $n = 0$ term because $\pi_a = 0$ and π_f is independent of ϕ .

3.3 Magnetic fields

The first non-zero term for the magnetic field is $n = 1$ for both radial and transverse dipoles. The potentials for this term are:

$$\begin{aligned}\pi_a(MT) &= -\sin\theta \sin\phi \frac{a_{e1} \hat{H}_1^{(2)}(k_1 r)}{r} \\ \pi_f(MT) &= -\sin\theta \cos\phi \frac{b_{e1} \hat{H}_1^{(2)}(k_1 r)}{r} \\ \pi_f(MR) &= \cos\theta \frac{c_{e1} \hat{H}_1^{(2)}(k_1 r)}{hr}\end{aligned}\tag{18}$$

The transverse dipole magnetic fields are given by

$$\begin{aligned}H_r(MT) &= \frac{-2 \cos\phi \sin\theta}{r^2} b_{e1} \hat{H}_1^{(2)}(k_1 r) \\ H_\theta(MT) &= \frac{-\hat{y}_1 \cos\phi}{r} a_{e1} \hat{H}_1^{(2)}(k_1 r) - \frac{k_1 \cos\phi \cos\theta}{r} b_{e1} \frac{\partial \hat{H}_1^{(2)}(k_1 r)}{\partial r} \\ H_\phi(MT) &= \frac{\hat{y}_1 \sin\phi \cos\theta}{r} a_{e1} \hat{H}_1^{(2)}(k_1 r) + \frac{k_1 \sin\phi}{r} b_{e1} \frac{\partial \hat{H}_1^{(2)}(k_1 r)}{\partial r}\end{aligned}\tag{19}$$

and the radial dipole fields are given by

$$\begin{aligned}H_r(MR) &= \frac{2 \cos\theta}{hr^2} c_{e1} \hat{H}_1^{(2)}(k_1 r) \\ H_\theta(MR) &= \frac{-\sin\theta}{hr} c_{e1} \frac{\partial \hat{H}_1^{(2)}(k_1 r)}{\partial r}\end{aligned}\tag{20}$$

where $H_\phi(MR) = 0$ by symmetry. Also, note that the coefficients a_{e1} , b_{e1} and c_{e1} are functions of the properties of the two media and of the radius and location of the target, and have no r , θ , or ϕ dependence.

The explicit form of the Hankel function and its derivatives for $n = 1$ are:

$$\begin{aligned}\hat{H}_1^{(2)}(x) &= \frac{\sin x}{x} - \frac{\cos x}{x} + i \left[\frac{\cos x}{x} + \sin x \right] \\ \frac{\partial \hat{H}_1^{(2)}(x)}{\partial x} &= \left[\sin x + \frac{\cos x}{x} - \frac{\sin x}{x^2} \right] + i \left[\cos x - \frac{\sin x}{x} - \frac{\cos x}{x^2} \right] \\ \frac{\partial^2 \hat{H}_1^{(2)}(x)}{\partial x^2} &= \hat{H}_1^{(2)}(x) \left[-1 + \frac{2}{x^2} \right]\end{aligned}\tag{21}$$

4. Secondary magnetic fields from targets in air and seawater

Equations 21 were first evaluated using IDL (Interactive Data Language). However, the coefficients a_{en} , b_{en} and c_{en} are given by quotients of differences of extremely large and small numbers, reaching the machine limits of IDL accuracy. Therefore, the original form of the fields from equation 13 were input into Mathematica, which evaluates many of the expressions analytically and does not have the same machine accuracy limitations.

The calculations involve a sum over n (i.e., multipoles). For small targets at large sensor/target separations, when the source field is uniform over the target, only the first term was required. For larger targets, or for smaller separations, more terms were required. For the 20 cm radius targets, only the first term was required at all distances. The 80 cm target (roughly equivalent to a 2000 lb bomb), however, at least 3 terms were required.

Calculations were made of the secondary fields from a target in either air or seawater, separated by a distance D from a co-located vertical magnetic dipole transmitter and point receiver. Thus, for a target directly below the sensor, the dipole transmitter appears as a radial dipole (see Figure 1), and the measured field in this coordinate system is H_r . If the target is in the same horizontal plane as the sensor, the transmitter dipole is seen as a transverse dipole and, if we choose $\phi = 0$, the measured field is H_θ .

The assumptions for all calculations were:

- the sensor has co-located transmit and receive loops
- the transmit coil is horizontal and is modeled as a vertical magnetic dipole
- the receiver loop is horizontal, measures the time derivative of the vertical magnetic field flux, which is approximated by the value of the field's derivative at the center of the loop
- the target is a sphere with conductivity $\sigma = 10^7$, permeability $\mu = 100\mu_0$, and permittivity $\epsilon = \epsilon_0$
- the enclosing medium is either air or seawater
- for seawater, conductivity $s = 4.3$, permeability $\mu = \mu_0$ and permittivity $\epsilon = 81 \epsilon_0$,

All model calculations were made in the frequency domain (e.g., for a CW wideband sensor); these results were then transformed into the time domain (see section 3.2 below), using assumptions for the sensor transmitter waveform and time gates.

4.1 Frequency-domain signatures

The response fields were calculated for a CW source field; the range of source frequencies was from 1 Hz to 50,000 Hz. The sensor/target separation ranged from 0.2 m to 3 m and the targets were all spheres with radii of 20 or 80 cm.

Because the primary electric field created by a vertical magnetic dipole is zero directly underneath the source and is maximum in the horizontal plane of the source, we expect that the effect of the seawater on the response field will also be minimum below the sensor (it will not be zero due to the finite size of the target) and maximum in the horizontal plane.

Figure 2 shows the response fields as a function of target-sensor separation, for a 20 cm radius sphere in the horizontal plane of the sensor and a source frequency of 20,000 Hz. All blue curves are for the system and target in air; green curves are for seawater. The top graphs are the inphase and quadrature of the response field; the bottom graph is the magnitude. It is clear that the response in seawater is larger than that in air for a range of source-target horizontal separation distances. For this source frequency, size and

properties of target, and seawater parameters, the seawater response fields are larger than in air for horizontal separations of 1 to 8 meters.

Figure 3 shows the response fields for the same target and sensor system parameters, but for the target directly beneath the sensor. As expected, although the quadrature response fields are slightly larger in seawater at some distances (due to the phase changes from the conducting medium), the magnitude of the response is smaller in seawater for this geometry.

The response fields as a function of source frequency are shown in Figures 4 and 5 for the same 20 cm radius target, located in the horizontal plane and directly below the sensor, respectively. The source-target separation distance is 2 meters. The response fields in seawater differ from those in air for source frequencies greater than several hundred Hertz. Again, the difference between seawater and air is very small for targets directly below the sensor (Figure 5).

4.2 Time-domain signatures for the EM61

The sensor planned for the Marine *MTADS* system is a variant of the EM61-Mk2, a time-domain instrument. The signal measured by this sensor is the time derivative of the vertical flux through the receiver loop. For modeling purposes, we approximate this signal by the magnitude of the time derivative of the vertical magnetic field at the center of the receive coil.

However, the model results from the previous section cannot be used directly to predict the results of measurements with this instrument until the effects of the range of frequencies produced by the transmitter waveform and the specifics of the measurement time gates are accounted for. There are several different models of the EM61-Mk2; Figure 6 shows a typical EM61 transmit waveform and Table 1 lists several typical time gates.

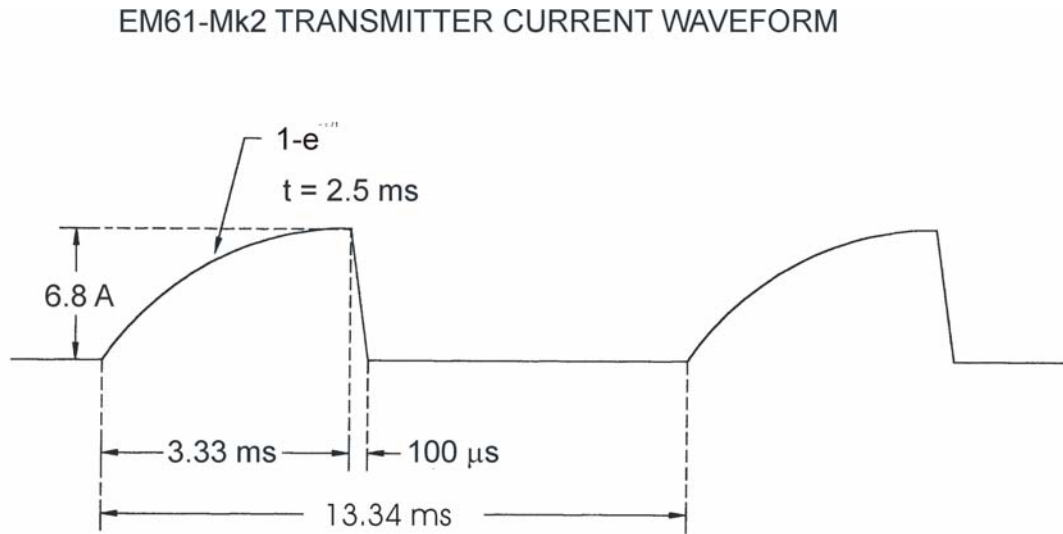


Figure 6. EM61-Mk2 transmitter current waveform used for model calculations

| time gate start (ms) | time gate end (ms) | time gate offset (μ s) |
|----------------------------|--------------------------|-----------------------------------|
| 3.430 | 3.830 | 0 |
| 3.455 | 3.830 | 25 |
| 3.580 | 3.765 | 150 |
| 3.670 | 3.853 | 240 |
| 3.830 | 4.045 | 400 |
| 4.290 | 4.570 | 860 |

Table 1. Typical time gates used by the EM61-Mk2 transmitter. The offset is with respect to the end of the transmit pulse, 3.43 ms after the start of the pulse.

The modeling procedure was the following:

- ♦ Calculate the response fields (in phase and quadrature) for frequencies $\leq 20,000$ Hz
- ♦ Fourier transform the transmit waveform
- ♦ Convolve the response fields with the transmit waveform FFT and inverse FFT to obtain the response fields as a function of time
- ♦ Take the time derivative of the response fields
- ♦ Integrate the time derivative over the assumed time gate to produce the predicted signal

Figure 7 shows the results of step 4: the time derivative of the response field for a 20 cm radius target at a source-target horizontal separation of 2 meters for both air and seawater. The signal is plotted as a function of time after the transmit waveform turnoff time. It is clear that the difference in signal when in seawater or in air is significant only at very early times (corresponding to high source frequencies). Whether this difference at early times is measurable depends upon the time gate of the sensor.

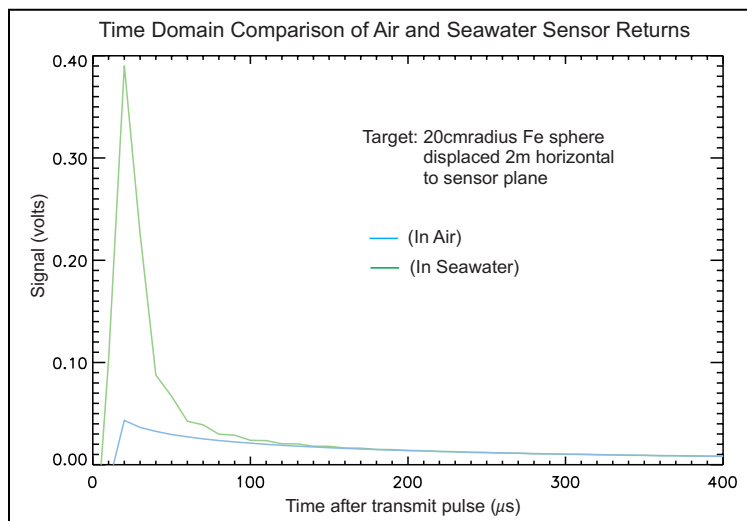


Figure 7. The time derivative of the response fields, in seawater (green) and air (blue) environment, for a 20 cm radius ferrous spherical target displaced 2 m horizontally from the sensor.

The actual measurement of the EM61-Mk2 is the signal, shown in Figure 7, integrated over the duration of the time gate. Table 2 shows the resulting percent difference between an air and seawater environment for several different targets, geometries and time gates.

| target radius | horizontal separation | vertical separation | time gate start | time gate end | time gate offset | air/sea difference |
|---------------|-----------------------|---------------------|-----------------|---------------|------------------|--------------------|
| (cm) | (m) | (m) | (ms) | (ms) | (μ s) | % |
| 20 | 1.0 | | 3.430 | 3.830 | 0 | 28 |
| | | | 3.455 | 3.830 | 25 | 0.76 |
| | | | 3.580 | 3.765 | 150 | -0.79 |
| | | | 3.670 | 3.853n | 240 | -0.73 |
| | | | 3.830 | 4.045 | 400 | -0.65 |
| 20 | 2.0 | | 3.430 | 3.830 | 0 | 130 |
| | | | 3.455 | 3.830 | 25 | 57 |
| | | | 3.580 | 3.765 | 150 | 1.2 |
| | | | 3.670 | 3.853 | 240 | -1.2 |
| | | | 3.830 | 4.045 | 400 | -1.9 |
| 20 | 3.0 | | 3.430 | 3.830 | 0 | 267 |
| | | | 3.455 | 3.830 | 25 | 234 |
| | | | 3.580 | 3.765 | 150 | 19 |
| | | | 3.670 | 3.853 | 240 | 5.0 |
| | | | 3.830 | 4.045 | 400 | -1.2 |
| 20 | | 2.0 | 3.430 | 3.830 | 0 | 30 |
| | | | 3.455 | 3.830 | 25 | 6.9 |
| | | | 3.580 | 3.765 | 150 | -3.3 |
| | | | 3.670 | 3.853 | 240 | -3.4 |
| | | | 3.830 | 4.045 | 400 | -2.9 |
| 80 | 2.0 | | 3.430 | 3.830 | 0 | 702 |
| | | | 3.455 | 3.830 | 25 | 221 |
| | | | 3.580 | 3.765 | 150 | 20.4 |
| | | | 3.670 | 3.853 | 240 | 8.8 |
| | | | 3.830 | 4.045 | 400 | 2.8 |
| 80 | | 2.0 | 3.430 | 3.830 | 0 | 175 |
| | | | 3.455 | 3.830 | 25 | 47 |
| | | | 3.580 | 3.765 | 150 | 6.6 |
| | | | 3.670 | 3.853 | 240 | 2.5 |
| | | | 3.830 | 4.045 | 400 | 0.21 |

Table 2. Percent difference in measured signals between seawater and air environment for various geometries and targets.

These results show that, while large differences are evident, they are only seen for time gates starting before 150 ms for the time gates of the envisioned sensor, the seawater effects are not very large. For example, for an 80 cm radius sphere (roughly equivalent to a 2000 lb bomb), the signal in a time gate starting at 150 ms is only 20% larger in seawater. In addition, the larger differences are for larger sensor-target separations, for which the magnitude of the fields is decreased and detection is more difficult.

5. General Conclusions

The largest effect of the seawater is when the target is in the horizontal plane of the sensor, and the smallest is when the target is directly below the sensor.

The difference between air and seawater fields increases with target size, sensor frequency and sensor/target separation. However, the magnitude of all signals decreases with distance from the sensor, and there is the additional skin depth effect in seawater, resulting in only a range of sensor/target separations for which the signal in seawater is larger than in air.

Because the effect increases with sensor frequency, it is sensitive to the frequency content of the transmit waveform. For the EM61-Mk2 waveform modeled here, the effect of the seawater is maximum immediately after the transmit waveform shuts off, so that exploiting it would require very early time gates. These time gates, however, are not optimum for discrimination.

For the 20 cm radius sphere, exploiting this effect will require time gates starting no later than 150 ms after the transmit pulse ends, and preferably within 25 ms. For the 80 cm radius sphere and the time gate that starts at 150 ms, there is a 20% increase in signal at 2 m horizontal separation.

The later starts are only useful for large standoff distances, where it is doubtful that detection can occur. (These model calculations looked only at the difference between seawater and air signals, and did not include sensor noise levels.)

In summary, it is possible that the effects of seawater might be exploitable with a frequency-domain instrument, but not with a time-domain instrument such as being built for this contract.

6. References

Stanley H. Ward and Gerald W. Hohmann, "Electromagnetic Theory for Geophysical Applications," pp. 131-311 in Electromagnetic Methods in Applied Geophysics, Volume 1. Theory, edited by Misac N. Nabighian. Society of Exploration Geophysicists, 1987.

Marine MTADS Sonar Imaging Requirements and Selection

Chester Bassani, AETC Incorporated

1 December 2003

It was decided that a forward looking sonar imager was required to complement the auxiliary sensors. This forward looking capability would increase the safety margin by allowing us to visually determine if any dangerous obstacles will interfere with our path. This safety margin will be most important when traveling at the upper limits of our specified velocity range of 1 to 5 knots. The investigation phase started by noting different side-scan and forward looking sonar systems. As side scan sonars are typically mounted in towed fish and we intend to mount our sonar on our surface vessel, this eliminated a lot of manufacturers. In sonar, higher frequencies yield better resolution while lower frequencies provide longer range. In our application the priority will be on resolution. Therefore we started by noting the different manufacturers and their highest operation frequencies. After much analyzing and down-selecting, the short list consisted of Marine Sonic Technology, Imagenex and Sound Metrics. The operating frequencies are noted below of each manufacturer and model:

1) Marine Sonic Technology Sea Scan:

600 kHz



2) Imagenex 881A:

1000kHz



3) Sound Metrics DIDSON:

1800kHz



DIDSON Selection and Visit:

As can be seen, the DIDSON provides us with the best resolution (highest operating frequency). Once our decision was made, a visit was arranged to see a DIDSON in operation. We visited Seattle, WA and met with Sound Metrics Corp. Mr. Ed Belcher and his associate, Mr. Bill Hanot demonstrated a DIDSON that was mounted on a University of Washington research vessel. The data from the DIDSON is accumulated by a topside laptop(Windows PC) and recorded with a VCR. The images are sent from the sonar head with a timestamp. This timestamp originates in the head and can be synchronized from the topside computer. This feature will be important as all our data will be linked via a common timestamp. We viewed the sonar images gathered from the bottom of the bay while instituting some situations that we expect while surveying, such as varying the tilt angle. This tilt angle will be changed for different operating depths and we had to confirm that the images are still adequate with a 30 degree tilt angle. Normally, forward looking sonars require to be basically horizontal to achieve a useable image.

Mounting:

Our system will be semi-rigidly fixed to our surface vessel with some adjustment capability, therefore any degradation of resolution due to non-ideal mounting characteristics were noted during our visit. We anticipate mounting the DIDSON similar to the mounting method shown in the following photographs.



This DIDSON mount was made by SPAWAR. The user can pan and tilt the sonar by panning and tilting the top plate.

**OVERLAPPING RECEIVER COIL STUDY
GEONICS REPORT
SUBMITTED 29 AUGUST 2003**



GEONICS LIMITED

1745 Meyerside Dr. Unit 8 Mississauga, Ontario Canada L5T 1C6

FAXED

Tel: (905) 670-9580
Fax: (905) 670-9204
E-mail: geonics@geonics.com
URL: <http://www.geonics.com>

FAX TRANSMISSION

PAGES: 1 + 6

DATE: August 29, 2003

TO: AETC

FAX#: 919 653 0219

ATTN: Jim McDonald

Dear Jim:

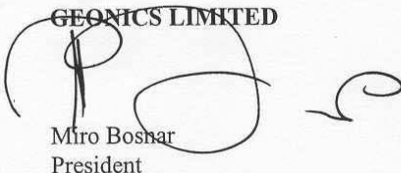
As per our conversation, please find attached results of the EM68 Sensor Resolution Test with two types of receiver coils, at the height of 1 metre above the target. Note that the calculated values, graphs, are response from a dipolar plate-like target and therefore the width of response is somewhat narrower than the measured response from 60 mm mortar, test target.

Note also that the smaller coils (1 x 0.5 m) have higher resolution and sensitivity, with about an equal amplitude in the "Dead Zone" in comparison with the larger Rx coil, and in my opinion, better sensors.

I look forward to your comments or questions regarding the above.

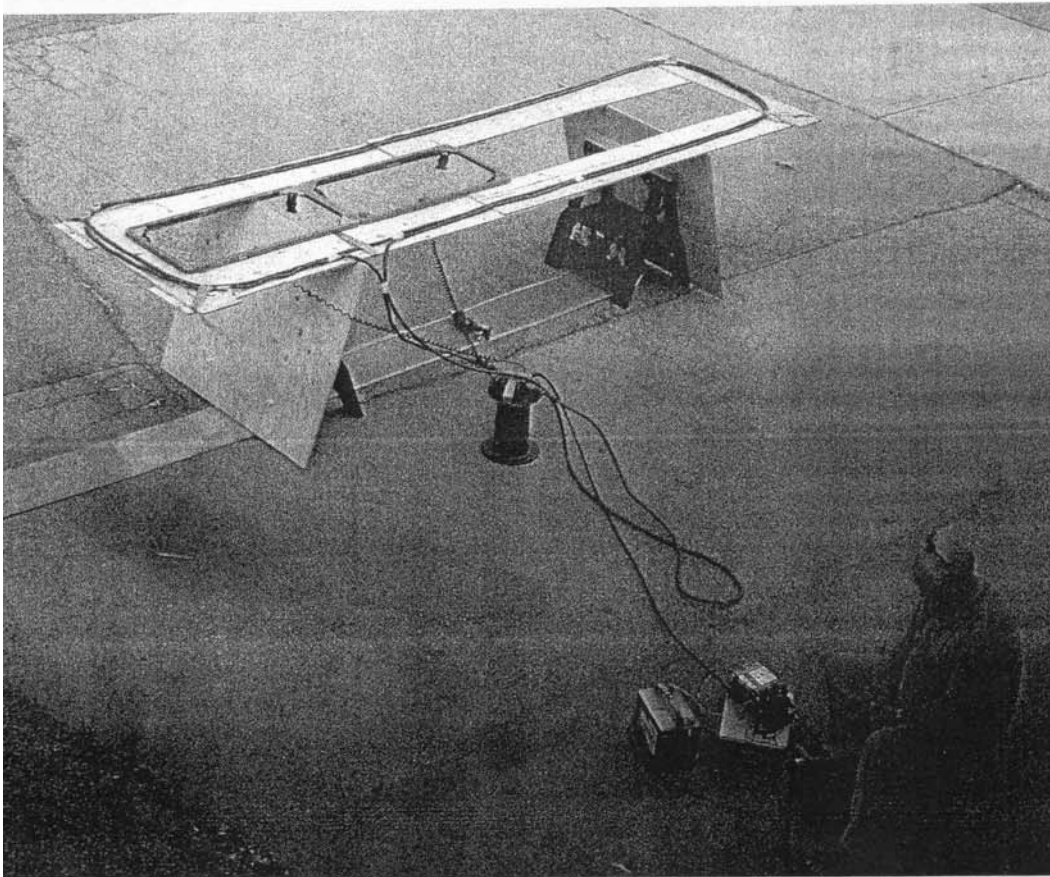
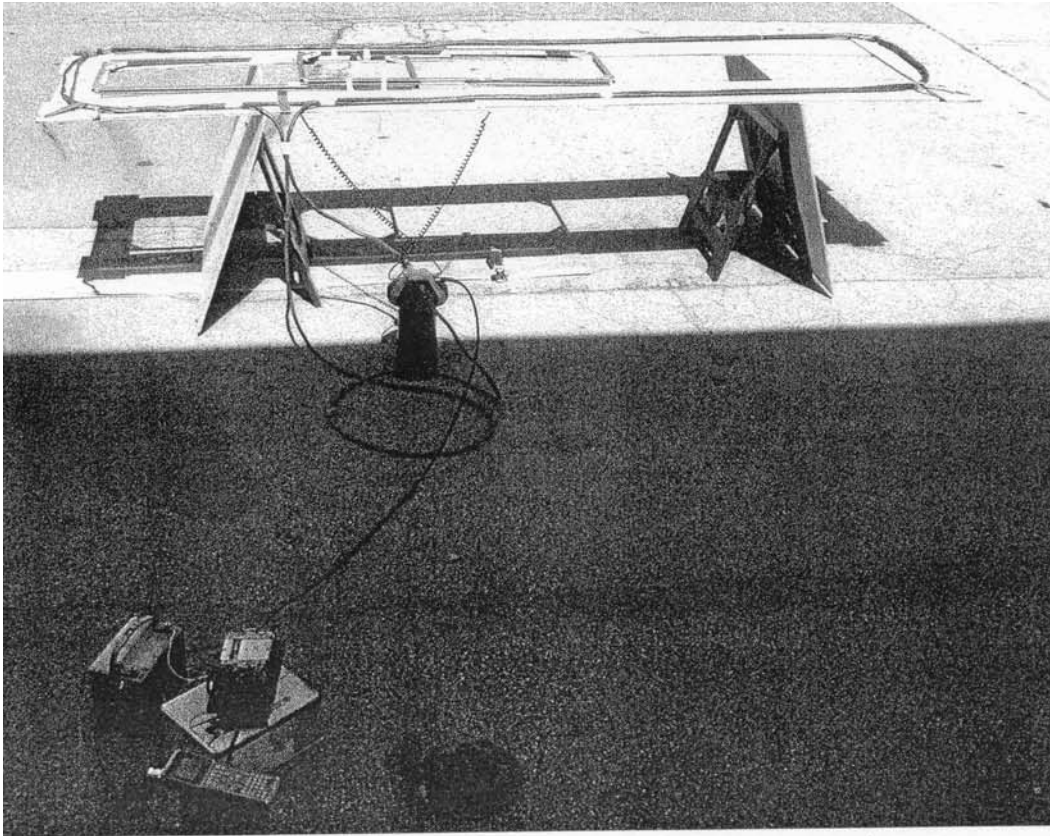
Best regards,

GEONICS LIMITED


Miro Boshar
President

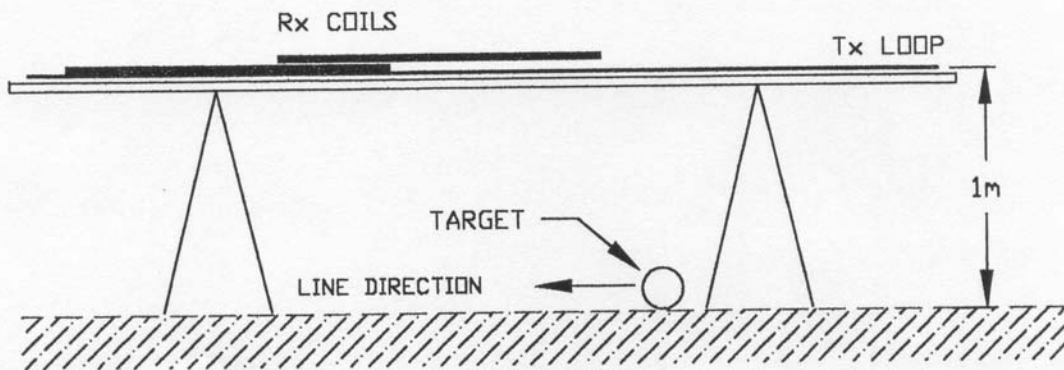
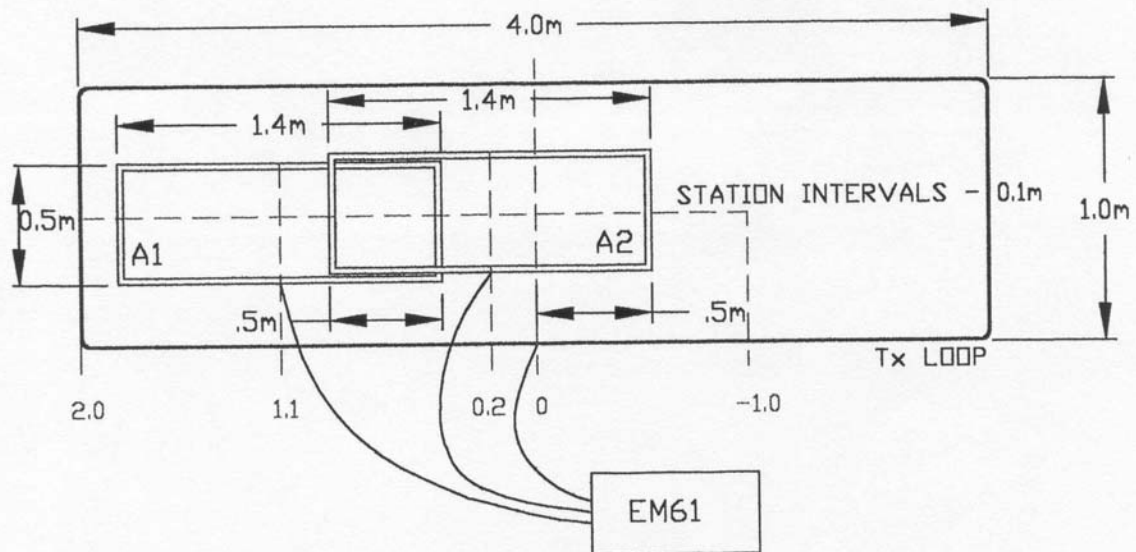
MB/nr
c:AETC EM68 test

PLEASE NOTIFY GEONICS IMMEDIATELY IF YOU DID NOT RECEIVE THE ENTIRE TRANSMISSION



EM68 EXPERIMENTAL MODELING

A. LATERAL RESOLUTION



EM68 EXPERIMENTAL MODELING

B. LATERAL RESOLUTION

